Universitat Autònoma de Barcelona

In vitro studies on the biological effects of cerium oxide nanoparticles

Laura Rubio Lorente

Universitat Autònoma de Barcelona

Facultat de Biociències

Departament de Genètica i de Microbiologia

Grup de Mutagènesi

In vitro studies on the biological effects of cerium oxide nanoparticles

DOCTORAL DISSERTATION

Laura Rubio Lorente

2017

Universitat Autònoma de Barcelona

Facultat de Biociències
Departament de Genètica i de Microbiologia
Grup de Mutagènesi

In vitro studies on the biological effects of cerium oxide nanoparticles

Dissertation respectfully submitted by

Laura Rubio Lorente

To Universitat Autònoma de Barcelona in partial fulfillment of the requirements for the degree of Doctor of Philosophy, as per the Doctorate Program in Genetics

Under the direction of Dr. Ricard Marcos Dauder and Dr. Alba Hernández Bonilla.

Dr. Ricard Marcos Dauder **Dr. Alba Hernández Bonilla** **Laura Rubio Lorente**

ABSTRACT

Rapid advances in nanotechnology promise to be of great benefit for many fields, including electronics, consumer products, alternative energy or medicinal uses among others. Despite the fact that good perspectives are predicted for the future of nanotechnology, there is increasing concern that human exposure to some engineered nanoparticles (NPs) may lead to significant adverse health effects.

Among the nanomaterials (NMs) most extensively used, cerium oxide NPs (nanoceria) has experienced a rapid increase in its production due to its novel industrial applications. More recently, nanoceria has been presented as a unique redox catalyst also for biological applications. Thus, nanoceria has emerged as a promising therapeutic agent, catalyzing reactive oxygen species (ROS)-detoxifying reactions, to be used in various diseases originated as a consequence of oxidative stress induction. Due to the potential of this NM and the lack of information regarding some toxicological aspects, in this Thesis we have performed extended *in vitro* studies on the biological effects of nanoceria.

From our first study we confirmed the ability of nanoceria to reduce the oxidative effects generated by a well-known oxidative compound in the epithelial BEAS-2B lung cell model. In our findings, nanoceria pre-treatment significantly reduced intracellular production of ROS, levels of DNA oxidative damage and cell death and it also induced the expression level of some genes involved in the oxidative *Nrf2* pathway. For our second study we assessed possible implications of nanoceria in cancer treatment. We made the assumption that the antioxidant properties that we found in our first study could be modulated by pH –as proposed by other authors-. Taking into account that tumoral cells are known to have a more acidic environment, nanoceria could have a pro-oxidative effect in these cells, while keeping its antioxidant properties in a non-tumoral environment. Although not proven yet, this idea has generated important scientific interest as it would meet the ideal standards of chemotherapy, where tumoral cells are selectively targeted, while non-tumoral cells are protected. However, our results do not support the hypothesis as we did not observe changes in the antioxidant properties of nanoceria in the tested tumoral cell lines and related environments.

To date, results obtained under short-term scenarios show controversy regarding the toxicological effects of nanoceria since harmful effects have been described in cancer and non-cancer cell lines using *in vitro* and *in vivo* models. Therefore, in our third study we attempted to overcome the limitations from short term approaches in studying the biological properties of nanoceria by introducing a long-term treatment design.

We evaluated the toxicological and carcinogenic potential of *in vitro* long-term low-dose exposure of nanoceria in lung epithelial BEAS-2B cells, along with the effects associated to a common plausible tobacco (CSC) co-exposure. We found that although nanoceria did not induce cell transformation on its own, it had a synergistic role on CSC transforming ability, as cells co-exposed to nanoceria-plus-CSC, showed more noticeable effects on all the hallmarks of cancer studied. Therefore, despite the antioxidant properties that were identified in the previous two studies, based on the results from this third study nanoceria cannot be considered safe as it may increase the oncogenic potential of other common environmental agents.

In our fourth and last study we presented a solution for the limitations associated to NP dispersion procedures in the field of nanotoxicology. Energetic dispersions are a source of variability between samples in the physico-chemical properties of NPs, potentially affecting the reliability of long-term experiments where several rounds of dispersions are required. In order to reduce this variability between samples, we proposed to aliquot and freeze NM stock dispersions. Thus, in this study we tested whether the physico-chemical properties (primary size, morphology, hydrodynamic size, zeta potential and ion release) and biological effects (viability, cellular uptake and induced ROS production) between fresh-prepared and frozen dispersions differed. In our results, we found that there were no differences between fresh and frozen preparations. Therefore, we concluded that store frozen NP storage is a convenient procedure to save time and increase reliability of long-term and high throughput methodologies.

Overall, we conclude with this Thesis work that nanoceria is a particle which despite showing antioxidant properties in short term treatments, it has the potential of modulating pro-oncogenic properties of other environmental compounds, and therefore its safety is questionable. Furthermore, we recommend long-term treatments for a better understanding of the possible effects of this NM, and that freezing NP storage of frozen NPs is a technique that will facilitate these studies by saving time while preserving reliability.

INDEX

1. INTRODUCTION

1. INTRODUCTION

1.1. Nanotechnology

1.1.1. General concepts

Nanotechnology is an emerging multidisciplinary science dealing with the manipulation and control of matter at dimensions between approximately 1 and 100 nanometers. At the nanoscale-range the properties of particles become determined by the quantum effects, instead of by physical effects as occurs in bigger scales. Accordingly, properties of nanoparticles (NPs) such as melting point, fluorescence, electrical conductivity, magnetic permeability, and chemical reactivity change as a function of the particle size; being these properties completely different from those of their bulk counterparts (Steigerwald and Brus, 1990; Wang, 1991; Weller, 1993; Stankic et al., 2016). This unique phenomenon has enabled the synthesis and production of desired size particles with novel properties and applications which has prompted a new industrial revolution.

Despite the fact that the concept of nanotechnology emerged the first time in 1959 with the physicist and Nobel Laureate Richard Feyman, it was not until the early 2000s when the use of nanotechnology was reflected in commercial products. Nowadays the number of nanotechnology products available in the market is dated to more than 1800 items used in many commercial products and processes (Vance et al, 2015). These nanoproducts are used in different fields like material science, electronics, fuel cells, biomedicine, food industry, cosmetics or textile among others (Yang et al., 2007; Liu and Gu, 2009; Epstein, 2011; Yen et al., 2011). Several estimates suggest that the use of nanomaterials (NMs) will continue experiencing an exponential increase, as substantial economic and technical resources are being dedicated to the study and design of new NMs with industrial applicability (Figure 1).

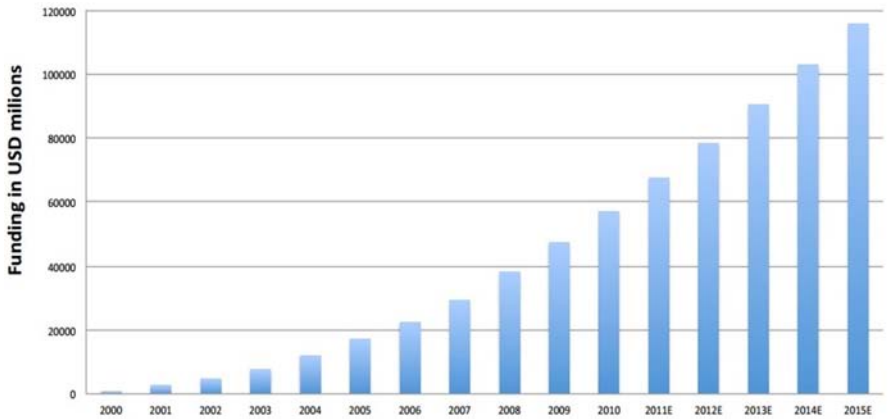

Figure 1. Cumulative global funding of nanotechnologies (source: Cientifica Ltd., 2011).

1.1.2. Potential health effects of NMs

The rapid development of the NMs industry and the exponential production of NPs of different natures has raised serious concerns about their potential harmful consequences on human health (Schmid and Riediker, 2008; Park and Grassian, 2010). The effects in occupationally and environmentally exposed populations are uncertain. Due to their small size NMs are able to penetrate into the cells and strongly react at the intracellular and nuclear level, unlike their macro counterparts. It is in this context where nanotoxicology emerges as a new field to study the potential risks associated specifically to NMs.

As previously described, the main characteristic of NMs is their nanoscale range size, which is in the transitional zone between individual atoms or molecules and the corresponding bulk materials. This can modify the physicochemical properties of the material as well as change their toxicological profiles. As the size of a particle decreases, its surface area/volume ratio increases allowing a greater proportion of its atoms or molecules to be displayed on the surface (Nel et al., 2009). This increases exponentially the number of reactive groups exposed on the particle surface (Figure 2). In general, the more reactive a particle is, greater is its toxicity. Thus, as the particle size shrinks, there is a tendency for toxicity to increase, even if the same material is relatively inert in bulkier form (Buzea et al., 2007).

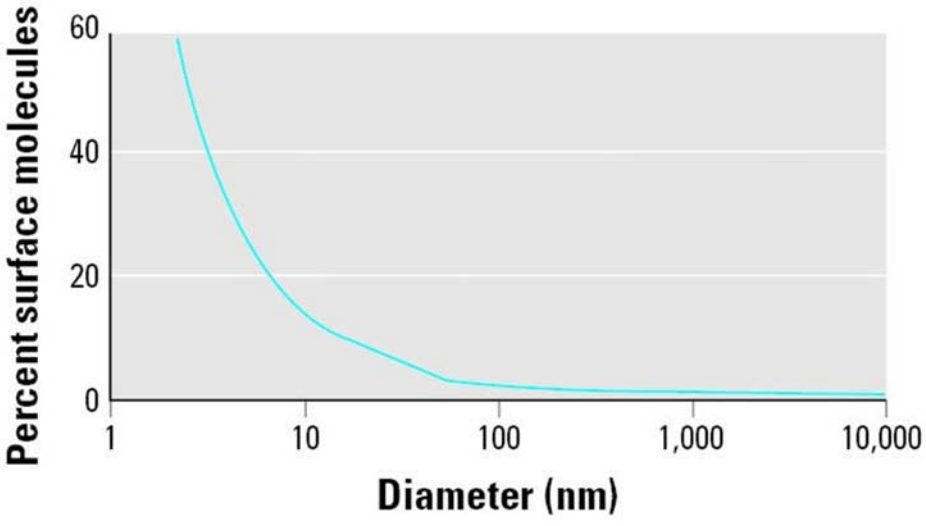

Figure 2. Inverse relationship between particle size and number of surface expressed molecules (adapted by Oberdörster et al., 2005)

Other NM properties such as solubility, shape, surface coating and aggregation could also affect the transport properties, with the possibility of modulating the toxic effects (Oberdörster et al., 2005).

Once inside cells, NPs may interact with proteins, membranes, DNA and different organelles to establish a series of NP/biological interfaces. These interactions lead to the formation of protein coronas, particle wrapping, intracellular uptake and biocatalytic processes that could have biocompatible or bioadverse outcomes. This wide range of cellular and intracellular responses strongly depend on NP physicochemical properties, concentration, duration of contact, subcellular distribution and interactions with biological molecules (Nel et al., 2009).

In this context, different i*n vitro* and *in vivo* studies have been performed in order to determine NM potential toxicity and their mechanisms in different biological scenarios (Hussain et al., 2005; Vevers et al., 2008; Xia et al., 2008; Poland et al., 2008) (Table1).

Nanomaterial	Cytotoxicity mechanism
TiO_2-NPs	- ROS production - Glutathione depletion and toxic oxidative stress as a result of photoactivity - Nanoparticle-mediated cell membrane disruption lead to cell death; protein fibrilation
ZnO-NPs	- ROS production - Dissolution and release of toxic cations - Lysosomal damage - Inflammation
Ag-NPs	- Ag^+ release inhibits respiratory enzymes and ATP production - ROS production - Disruption of membrane integrity and transport processes
Au-NPs	- Disruption of protein conformation
CdSe-NPs	- Dissolution and release of toxic Cd and Se ions
CeO_2-NPs	- Protein aggregation and fibrilation
Carbon Nanotubes (CNT)	- Frustrated phagocytosis causes chronic tissue inflammation and DNA oxidative injury

Table 1. Mechanisms of NM cytotoxicity (Adapted from Nel et al., 2009).

Despite the fact that nanotoxicology publications are increasing exponentcially, the comparison among studies is very difficult due to the high number of variables presented by a single NM (size, surface, electrical charge, morphology, concentration, and time of exposure, among others); all of them affecting their biointeracctions and effects. Thus, the European Agency for Safety and Health at Work (EU-OSHA) has quantified in 20 years the discrepancy between the knowledge of the commercially available NMs associated effects and their impact on human health and environment (Figure 3).

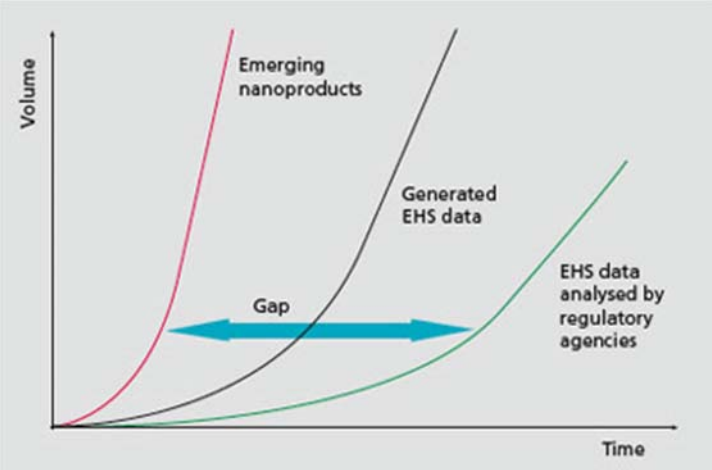

Figure 3. Gap between the emergence of products containing NMs in comparison to the generation of environmental health and safety data (EHS) and their subsequent use by regulatory agencies. (Source: "Novel Materials in the Environment: The case of nanotechnology", p.30. Royal Commision on Enviromental Pollution, 2008).

We are facing a new scenario of exposure that needs the development of new aproaches for the correct risk assessment determination, and the establishment of a regulatory framework where the exploitation of the new properties of NM is done guarantying the safety of the general population.

1.2. Cerium oxide NPs (Nanoceria)

Each of the unique physico-chemical properties acquired by compounds upon conversion to the nanoscale defines their applications in industry and technology. Nanoceria in particular has experienced a significant increase in its production and application in industry during the last few years due to its unique catalytic, magnetic and electronic properties and its abundancy in nature. This has led to nanoceria being considered among the NMs with higher growth projection (Ivanenko et al., 2013), as it

is reflected as well by the exponential increase in the number of publications about this compound in the last decade (Figure 4).

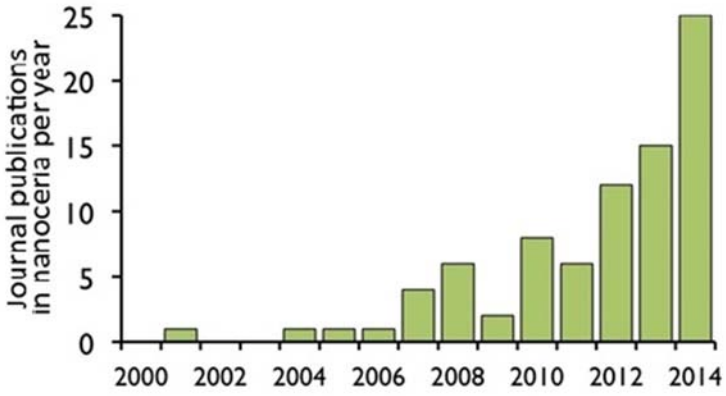

Figure 4. Journal publications in nanoceria per year. Environmental science: nanoblog; Nanoceria in our bodies, Palmero C. http://blogs.rsc.org/en/2014/12/01/nanoceria-in-our-bodies.

The unique properties of nanoceria are provided by the chemical structure of the crystal conformation of this rare earth element that belongs to the lanthanide series in the periodic table. Each cerium atom is bonded to eight oxygen atoms, while each oxygen atom is bonded to four cerium atoms (Figure 5). The complete unit cell, Ce_4O_8 measures 0.51 nm (5.1 Å) on an edge, and is a face-centred cubic fluorite lattice (Trovarelli, 1999). Crystallites are the elementary building blocks for NPs in general. Depending upon the synthesis conditions, crystallites can be comprised of several or many unit cells (Reed et al. 2014). For example, a 1.1 nm particle, the smallest ceria NP theoretically possible would contain 8 unit cells (2 × 2 × 2) (Hailstone et al., 2009). This fact entails the existence and synthesis of a huge variety of different nanoceria NPs with differences in particle size and morphology.

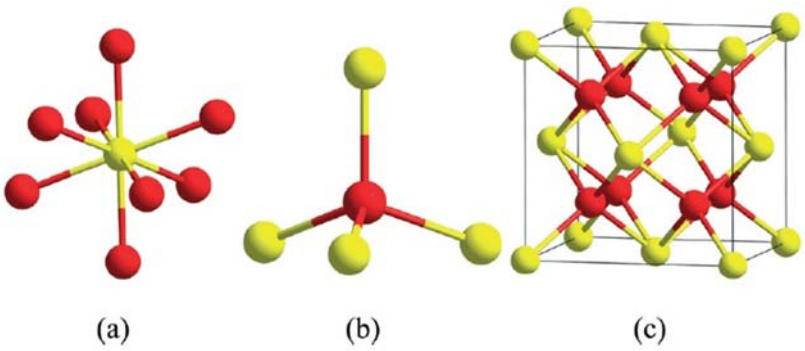

Figure 5. Structural analysis of ceria crystals and unit cells. Eight-fold coordinated cerium atoms (yellow) with four-fold coordinated oxygen atoms (red) in ceria crystals (a and b) and the primitive unit cell (c). (Figure adapted from Reed et al., 2014).

Ceria orbitals and electron configuration give it rare earth unique catalytic, magnetic and electronic properties (Xu and Qu., 2014). These properties make nanoceria an interesting material for industrial and commercial applications including catalysis (Lawrence et al., 2011) -as a diesel fuel additive to increase fuel combustion efficiency and decrease soot emissions (Park et al., 2008)-, in chemical mechanical planarization/polishing (Kosynkin et al., 2000), in semiconductors, in toner formulations (Bello et al., 2013), and as an additive in various nanocomposites, as reviewed by (Reed et al., 2014).

Regarding its biological applications, this NM has been presented as an interesting candidate for the treatment of diseases characterized by increased oxidative stress levels. However, its use as an antioxidant in therapeutics is still controversial due to both antioxidant and toxic observed effects (Yokel et al., 2014). Thus, the inevitable increase related to consumption and occupational exposures raises the need for a comprehensive, deep and reproducible toxicological characterization of nanoceria (Zhang et al., 2011). For instance, several companies and organizations have already identified nanoceria as a high priority material for toxicological evaluations (Integrated Laboratory Systems Inc., 2006; OECD, 2010).

1.2.1. Biological implications

1.2.1.1. Beneficial effects and applications of nanoceria

Despite the wide use of nanoceria in different industrial fields in the last decades, research on the biological applications of this rare earth oxide began around 2005 with some promising publications showing the antioxidant properties of nanoceria in cell culture models (Tarnuzzer et al*.,* 2005; Chen et al., 2006, 2013; Cohen et al., 2006; Rzigalinski, 2006; Schubert, 2006). Today, nanoceria is considered a promising therapeutic agent for dozens of diseases that are mediated through oxidative stress.

Reactive oxygen species (ROS) are generated by cells as by-products of their own aerobic metabolism, and they are essential to maintain the homeostasis of cells (Schieber and Chandel, 2014). Since ROS react with lipids, proteins, and DNA (Cross et al*.,* 1987), a wide range of different cytosolic antioxidant enzymes are responsible for counteracting ROS production, maintaining an oxidative redox balance. This balance between ROS production and antioxidant defences determines the degree of oxidative stress (Finkel and Holbrook, 2000). A majority of human disease conditions like atherosclerosis, hypertension, ischaemic diseases, Alzheimer's disease, Parkinson’s disease, cancer and inflammatory conditions are thought to be caused primarily due to

this imbalance between pro-oxidant and antioxidant homeostasis (Tiwari, 2001). Taking into account the relevance of ROS effects in many different oxidative diseases and the possibility to counteract them by using antioxidant compounds, a huge amount of literature about nanoceria properties has emerged in the recent years. These studies prompted an area of research engaged in the study of these NPs for biomedical applications. Specifically, nanoceria has emerged as a promising therapeutic agent to be used in various oxidative stress diseases/disorders, including neurodegenerative diseases, ischemic cardiomyopathy, ocular diseases, diabetes and cancer among others (Narayanan and Park, 2013).

From the chemical point of view, due to its unique redox properties, cerium can exist in two oxidation states, Ce^{3+} and Ce^{4+}. At the nanoscale level, the structure of nanoceria permits the coexistence of both oxidation states on the surface. This coexistence, along with its low reduction potential and high surface area to volume ratio, allows many surface cerium atoms switch between the two oxidation states. This way nanoceria acts catalyzing ROS-detoxifying reactions while simultaneously regenerating the reduced Ce^{3+} ions on its surface (Nelson et al., 2016). Thus, nanoceria consistently exhibits superoxide dismutase (SOD)-mimetic activity (Heckert et al., 2008) converting superoxide to hydrogen peroxide, as well as catalase (CAT)-mimetic activity (Pirmohamed et al., 2010) scavenging hydrogen peroxide molecules. This auto-regenerative potential of nanoceria is reflected in Figure 6.

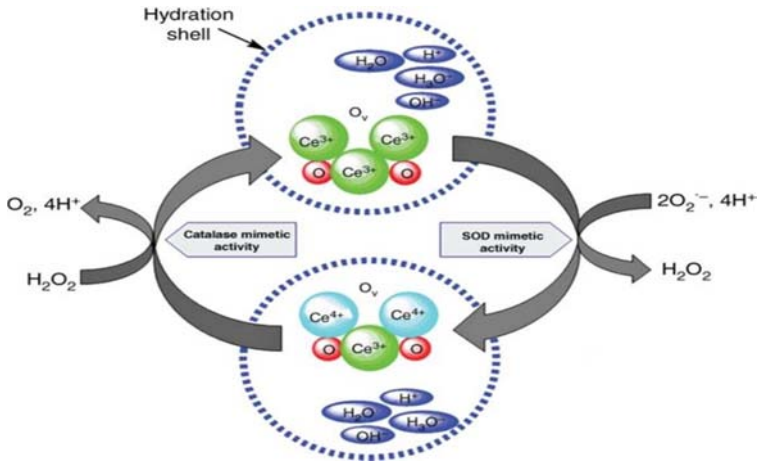

Figure 6. Reactive oxygen species scavenging and surface regeneration properties of nanoceria. (Adapted from Rzigalinski et al., 2016).

Nanoceria provides important advantages in comparison to other antioxidants. Free-radical scavengers such as vitamin E, ascorbate, carotenes or melatonin possess few active sites per molecule which implies that repeated dosing is required to replace

molecular species that were used in free radical reduction. Conversely, many active sites are available for free-radical scavenging in nanoceria as a consequence of the large surface to volume ratio presented by NPs. In addition, the auto regenerative reaction cycle of nanoceria ($Ce^{3+} \rightarrow Ce^{4+} \rightarrow Ce^{3+}$) is probably the mechanism by which this material gains an outstanding free-radical scavenging ability (Colon et al., 2009). Therefore, all these properties support nanoceria applicability in the treatment against diseases related with increasing levels of reactive oxygen species (ROS), even as an antitumoral agent, since it is known that ROS also contributes to cell transformation processes (Bach et al., 2016).

Different groups have shown *in vitro* protective effects of nanoceria using different cellular types including human colon and lung fibroblasts and breast epithelial cells acutely exposed to radiation (Tarnuzzer et al., 2005; Colon et al., 2009, 2010), neuronal rodent cells acutely exposed to glutamate (Schubert et al., 2006), and human umbilical vein cells submitted to acute doses of hydrogen peroxide (Chen et al., 2013). These antioxidant properties have also been observed in *in vivo* models. Thus, mice pre-treated with nanoceria showed an amelioration of the gastrointestinal radiation-induced damage by anti-oxidant mechanisms (Colon et al., 2010). Also, nanoceria treatment significantly reduced the free radical levels in the brain of mice with autoimmune encephalomyelitis of multiple sclerosis, preventing disease progression (Estevez and Erlichman, 2014). In addition, nanoceria was also able to reduce ROS levels and genotoxic effects induced by potassium bromate in an in vivo model such as *Drosophila* (Alaraby et al., 2016).

1.2.1.2. Harmful effects associated to nanoceria exposure

Despite the large number of studies supporting the antioxidant effects of nanoceria, some controversy exists regarding its beneficial impact, since different studies have also reported toxic effects of this NM (Yokel et al., 2014). Regarding *in vitro* studies, toxicity has been reported in human neuroblastoma cells (Kumari et al., 2014), lung adenocarcinoma A549 cells (Mittal and Pandey, 2014), in melanoma 518A2 and colorectal adenocarcinoma HT-29 cell lines (Pešić et al., 2015) and lung epithelial cells BEAS-2B (Park et al*.,* 2008 *;* Eom and Choi, 2009), among others.

Very few *in vivo* studies have been carried out so far, and most of them have focused on nanoceria toxicity following inhalation. Although limited data exist on nanoceria absorption by the gastro-intestinal tract, the assumption is that this uptake is extremely low. On the other hand, there is no evidence of nanoceria as a skin irritant or its uptake

through the skin (Yokel et al., 2014). With regard to *in vivo* inhalation experiments, some harmful effects have been observed. For example, several acute, sub-acute, sub-chronic and chronic nanoceria exposures via inhalation induced cytotoxicity through oxidative stress, leading towards a chronic inflammatory response and alveolar interstitial fibrosis (US.EPA, 2009; Staal et al., 2010; Srinivas et al., 2011; Demokritou et al., 2013; Keller et al., 2015). According to these results some authors conclude that nanoceria would be pro-inflammatory, and ultimately would induce pulmonary fibrosis (Ma et al., 2012).

It is assumed that toxic effects associated to nanoceria exposure could occur via two different mechanisms: (i) toxicity based on the chemical composition, or (ii) due to stress/mechanical irritation or stimuli caused by the surface, size, and/or shape of the particles (physical aspects) (Yokel et al., 2014). Although it is not simple to differentiate between these two mechanisms of cytotoxicity, most authors have pointed out its redox activity -associated to its chemical composition- as the main cause of nanoceria toxicity (Karakoti et al., 2012; Grulke et al., 2014). According to different studies, nanoceria would exert its toxicity through the oxidative stress pathway by increasing cellular ROS concentrations, what would lead to strong induction of the Heme oxygenase 1 (*HO-1)* gene via the *p38-Nrf-2* signalling pathway (Eom et al., 2009), also altering the expression of several other genes (Rothen-Rutishauser et al., 2009). In addition, ROS mediated DNA damage and cell cycle arrest have been suggested to play a major role in nanoceria-induced apoptotic cell death in A549 cells (Mittal and Pandey, 2014). These proposed mechanisms are indicated in Figure 7.

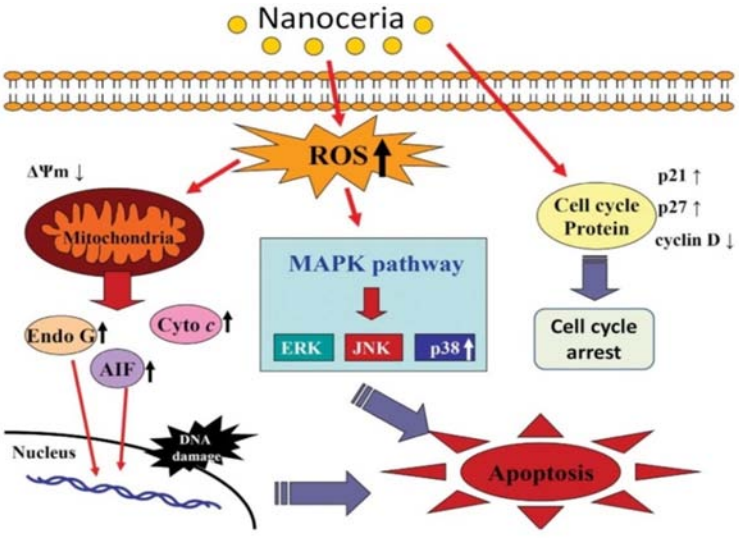

Figure 7. Proposed model of molecular toxicity pathways following exposure to nanoceria. (Adapted from Yu et al., 2012).

1.2.1.3 Parameters influencing the redox potential of nanoceria

Due to the controversial results found in literature, recent studies have been developed in order to deeply study the potential redox behaviour of nanoceria. In this context, several groups have proved that nanoceria redox potential can be affected by different factors such as particle size, synthesis method, shape, surface chemistry, pH or coating among others. However, not much is known about how exactly changes in these parameters could affect nanoceria behaviour in biological environments (Grulke et al., 2014).

Some authors have pointed out pH as one of the factors acting as an important modulator of nanoceria redox activity (Asati et al., 2010; Wason et al., 2013). Changes in this chemical parameter would lead to toxic pro-oxidative effects (Hardas et al., 2012; Tseng et al., 2012). In this direction, an acidic pH would diminish the catalase mimetic activity of nanoceria, while the SOD activity would be unaffected. As a result, SOD activity of nanoceria continues converting superoxide ($O_2^{\cdot -}$) to hydrogen peroxide, but catalase activity cannot detoxify hydrogen peroxide in the same extent than at neutral pH. Consequently, oscillations in intracellular pH would increase the concentration of this molecule inside the cell, producing toxicity (Alili et al, 2011) (See Figure 8).

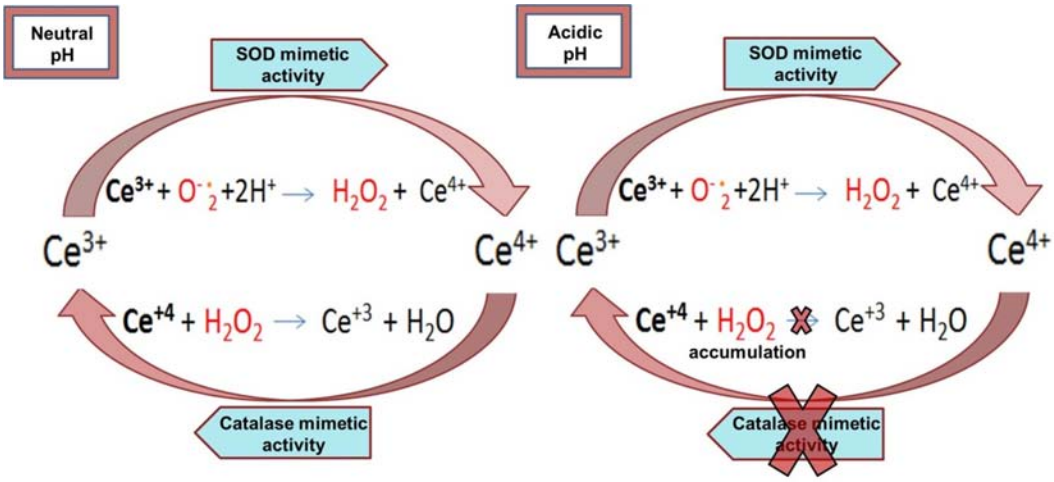

Figura 8. pH effect on enzyme mimetic activity of nanoceria.

As described by the Nobel Laureate Otto Warburg, cancer cells exhibit an acidic cytosolic pH due to the glucose consumption and lactic acid production (Vander et al., 2009). Thus, based on this phenomenon called “Warburg effect”, it is assumable that nanoceria could show a dual behaviour, on one side protecting normal cells by its antioxidant properties, while acting as oxidant in cancer cells on the other (Alili et al.,

2011). This hypothesis would set the basis for the study of the therapeutic application of nanoceria in cancer treatments (Gao et al., 2014). However, some authors have shown that distinct types of cancer cells may differ in intracellular pH and redox status and, eventually, in how nanoceria behaves into these cells (Pešic. et al., 2015). Therefore, the idea for selective killing of cancer cells by nanoceria needs to be further clarified.

1.2.1.4. Evaluation of nanoceria associated ROS production and oxidative DNA damage

In general, ROS induction has been considered as a common mechanism of cellular damage associated to NPs exposure (Wang et al*.,* 2011). Specifically, nanoceria as previously mentioned, has been related with ROS status showing both antioxidant and oxidant effects. Thus, studying the levels of these intracellular reactive molecules and their translation into oxidative DNA damage are highly recommended endpoints when studying the biological effects of nanoceria.

Several techniques exist for the determination and quantification of intracellular ROS. Among them, small-molecule fluorescent probes have been frequently used due to its fast and easy manipulation (Wang et al*.,* 2013). One of the most commonly performed techniques using small-molecule fluorescent probes is the 2',7'–dichloro-dihydro-fluorescein diacetate DCFH-DA assay (Dikalov, et al*.,* 2007). This technique allows the detection of a wide panel of oxygen-derived reactive molecules like H_2O_2, $ONOO^-$, lipid hydroperoxides, and, to a lesser extent, $O_2^{\bullet-}$. Once cell cultures are exposed to DCFH-DA, these molecules passively diffuse into the cells and are cleaved by intracellular esterases to 2′,7′-dichlorofluorescin (DCFH). Then, this compound is oxidized by intracellular ROS into 2', 7' –dichlorofluorescein (DCF). DCF is a highly fluorescent molecule which can be easily detected by fluorescence spectroscopy. On the other hand, dihydroethidium (DHE) is another small-molecule fluorescent ROS probe specific for $O_2^{\bullet-}$. The reaction between $O_2^{\bullet-}$ and DHE generates a highly specific red fluorescent product, 2-hydroxyethidium [2-OH-E(+)] which intercalates with DNA shifting its excitation and emission wavelengths, allowing its fluorescent identification and quantification (Wang et al., 2013). The combination of these two assays allows for the quantification of most of the existing reactive oxygen molecules. This approach provides a reliable evaluation of the effect of nanoceria in the cellular oxidative balance.

The protective/oxidant related effects of nanoceria at DNA level constitute another important endpoint to consider. Thus, among the techniques addressed to measure

genotoxicity, the comet assay allows the possibility to determine both oxidative DNA damage and the genotoxic DNA damage. This evaluation is carried out by using the alkaline comet assay with and without the use of formamidopyrimidine DNA glycosylase (FPG) enzyme. This classical method has been extensively used and validated for the genotoxicity assessment of a wide variety of compounds including NMs. This assay detects single- and double-stranded DNA breaks in naked supercoiled DNA. Strand breaks cause the supercoiled DNA to relax, allowing loops of DNA to migrate toward the anode upon electrophoresis, forming a 'comet tail'. The use of lesion-specific enzymes in the comet assay, specifically formamidopyrimidine DNA glycosylase (FPG), allows for the detection of 8-OH-dG, in addition to certain imidazole ring-opened purines and also causes breaks at apurinic/apyrimidinic sites (AP sites) (Collins, 2004).

1.2.1.5. Gaps, recommendations and initiatives in studies involving nanoceria

Despite the efforts devoted to understand the behaviour of nanoceria in biological models, the reality is that the high variability in the results obtained until now make difficult to stablish a general mode of action. Moreover, important variations in the experimental setups as well as in the nanoceria characteristics used by the different research groups makes these studies difficult to compare.

Considering these experimental pitfalls, several recommendations have been proposed to the research community in order to have a better understanding of the potential biological risks of this NM (Yokel et al., 2014). These are as follows:

1. To unravel why some studies report toxic effects of nanoceria, while others report that nanoceria is of low toxicity exhibiting antioxidant properties. It is necessary to determine if these differences are due to (i) the valence state or type of synthesis of nanoceria, (ii) the physicalchemical properties of the sample tested or (iii) the dose, exposure route, or experimental model used.
2. It is important to determine the potential interactions of nanoceria with different biological fluids (blood, lung lining fluid, etc.) with regard to agglomeration, surface reactivity and bioactivity.
3. It is necessary to compare the effects induced by short-term/high-dose exposures with those induced under long-term/low-dose exposure scenario.

4. It is necessary to characterize the effects of co-exposures (with common environmental compounds) on the pulmonary and cardiovascular systems, among other targets.

5. The new *in vitro* tests need to include (i) the use of relevant doses according to the *in vivo* expected exposures, (ii) the determination of mechanisms other than oxidant stress, and (iii) approaches evaluating genotoxicity, as well as the induction of cell proliferation/transformation.

Among these recommendations, the use of long-term/low-dose treatments entails an important progress mimicking real exposure situations. So far the majority of the *in vitro* studies conducted are far away from real scenarios as nanoceria exposures mostly involve acute concentrations several orders of magnitude above real exposures and exposure times no longer than 24 hours (Cheng et al., 2013; Benameur et al., 2015; Franchi et al., 2015) . Regarding this point, efforts have been made with different NMs and chemicals of other natures to reproduce realistic conditions of exposure using low concentrations for long periods of time (weeks-months). Importantly, these experimental approaches also allow for the carcinogenic evaluation of different compounds through the treatment (Thurnherr et al., 2011; Wang et al., 2011; Lohcharoenkal et al., 2013; Annangi et al., 2015, 2016; Vales et al., 2015, 2016; Bach et al., 2016).

1.3. Long-term exposures for *in vitro* carcinogenic evaluation of nanoceria

1.3.1. The adequateness of using *in vitro* models

Although *in vitro* studies have certain limitations to represent kinetics and biodistribution of nanoceria -and NMs in general- taking part in an *in vivo* exposure, they are useful to resolve some mechanisms underlying many of the unknown nanoceria's adverse effects. *In vitro* studies can be used for long-term exposure at low environmentally relevant doses, to analyse cell transformation, to characterize effects of long-term co-exposures, and to assess mechanisms of genotoxicity/carcinogenicity. All of these points being listed among the recommendations necessaries to clarify the safety and usefulness of nanoceria as a therapeutic antioxidant agent (Yokel et al., 2014).

Focusing in the study of the carcinogenic potential of chemicals, to date the two year rodent bioassays play the main role in the standard OECD regulation (OECD Guideline 451). However, in order to limit the use of animals as much as possible, the application

of 3Rs (replacement, refinement and reduction in animal studies) is desirable. Additionally, for large testing programs, *in vivo* carcinogenicity is impractical. Therefore, alternative approaches to *in vivo* carcinogenicity assessment are urgently required (Annys et al., 2014). In this context, the use of *in vitro* long treatment protocols could be presented as a partial solution to mitigate this problem.

In terms of standardization and validation, the most advanced *in vitro* tests for carcinogenicity are the cell transformation assays (CTAs). Although CTAs do not mimic the whole carcinogenesis process *in vivo*, they represent a valuable support in identifying transforming potential of chemicals. *In vitro* cell transformation is a process characterized by a series of progressive distinctive events that often emulate manifestations occurring *in vivo,* and which are associated with neoplasia. Cellular and sub-cellular alterations include, among others: cellular immortality, phenotypic changes, aneuploidy, genetic variability, cellular disarray, anchorage-independent growth, and the ability of tumorigenicity once injected in an *in vivo* organism (Corvi et al., 2012).

Several researchers have studied the carcinogenic potential of NMs through *in vitro* long-term exposure models. As an example, Wang et al. (2011) determined that chronic exposure to single-walled carbon nanotubes causes malignant transformation to human lung epithelial cells. The transformed cells induced tumorigenesis in mice and exhibit an apoptosis resistant phenotype characteristic of cancer cells. Also, in our group several NPs have been assessed from the carcinogenic point of view like TiO_2-NPs, ZnO-NPs, CNT or Co-NPs, and more recently nanoceria, being the focus of this Thesis dissertation, by analyzing the effects of a co-exposure with cigarette smoke condensate (CSC). These studies showed the ability of these assays to detect genotoxic and non-genotoxic mechanisms involved in the carcinogenic potential of NMs (Vales et al., 2015, 2016; Anangi et al., 2015, 2016).

1.3.2. The lung epithelial model BEAS-2B cell line

Different cell lines have been used to perform long-term treatment exposures. The election depends in many cases on the primary route of entry and the assumed target of the studied compound. The most likely route of human unintentional exposure to nanoceria, and to the majority of NPs, is through inhalation (Yang et al., 2008). Focussing on nanoceria, following inhalation exposure, this poorly-soluble NM deposits primarily in the alveolar and tracheal bronchial regions based on physical properties related to its size-distribution and agglomeration/aggregation state (Oberdörster et al.,

2005). Some of the deposited particles are cleared via the mucociliary escalator to the pharynx and ingested, while others are transported through the airway epithelium (Yokel et al., 2014). At this point, macrophages and epithelial cells compete for particle uptake. However, some studies have shown that small particles are more readily taken up by epithelial cells than by macrophages and show greater rates of transfer across the epithelium (Costantini et al., 2001).

Among all lung epithelial cell lines used in *in vitro* studies, BEAS-2B obtained at autopsy of a noncancerous individual, is considered a good bronchial cell-line model exhibiting similar characteristics and cellular responses to carcinogens as the primary lung cells (Liao et al., 2007; Sargent et al., 2009). BEAS-2B cells are reported to possess a mutated $p53^{Ser}47$ gene (Gerwin et al., 1992). However, the American Type Culture Collection (ATCC) indicates that although the BEAS-2B cell line forms colonies in a semisolid medium characteristic of transformed cells, is non-tumorigenic in immunosuppressed mice. Additionally, this cell line can grow continuously in culture, allowing for long-term exposure studies, which would not be possible using primary lung cells (Wang et al*.,* 2011). Moreover, these cells have also been widely used to define conditions under which various agents and oncogenes cause neoplastic transformation (Gerwin et al., 1992; Khatlani et al., 2007).

Based on the use and suitability of this model in different pioneering studies (Khatlani et al., 2007; Wang et al., 2011; Luanpitpong et al., 2014), BEAS-2B has been chosen for both acute and long-treatments exposures in many of the experiments conducted in this Thesis.

1.3.3. The transformed *in vitro* phenotype

Due to the increasing use of NMs, chronic exposure is likely to occur in occupational and daily situations. As already mentioned, the small dimensions of these particles make them able to penetrate and incorporate intracellularly, resulting in some cases in direct or indirect genotoxic effects (Haase and Luch, 2016). Considering chronic exposures where DNA damage could be generated, genetic instability and carcinogenesis assessment should be a priority (Rojanasakul et al., 2016). Thus, in our Group and specifically as a part of this Thesis we evaluated the transforming effects of long-term exposure to nanoceria in lung epithelial BEAS-2B cells, along with the effects associated to a common plausible tobacco co-exposure. For characterizing this process, an *in vitro* cancer phenotype acquisition was assessed through different carcinogenic markers such as morphology, proliferation rate, gene differentiation

status, migration capacity, anchorage-independent cell growth and secretome analysis, including levels of metalloproteinase-9 (MMP-9), and cell growth promoting capability. In addition, being Fos-related antigen 1 (*FRA-1)* and phosphatase and tensin homolog (*PTEN*) pivotal genes during respiratory epithelium carcinogenesis (Karamouzis et al*.,* 2007; Yanagi et al., 2007), its mRNA expression levels were used to determine their role in cell transformation.

1.3.3.1. Cell proliferation

Although carcinogenesis involves many other processes, deregulated cell proliferation and suppressed cell death together provide the underlying platform for neoplastic progression (Evan and Vousden, 2001). Thereby, regulation of cell cycle became a key factor due to its influence in controlling cell division. Normal growth requires a balance between the activity of those genes that promote cell proliferation and those that suppress it. During the G1 phase, cells respond to extracellular signals by advancing toward another division, withdrawing from the cycle into a resting state (G0), or underlying apoptosis (Sherr, 1996) . Consequently, specific gene mutations leading to an inadequate progression of G1 phase entail that cancer cells may no longer respond to many of the signals that control cellular growth and death, as a result remaining indefinitely in the cycle and therefore increasing proliferation (Sherr, 1996). Considering increased cell proliferation as an evidenced hallmark of cancer, many *in vitro* studies have evaluated this parameter as a biomarker of cell transformation (Wang et al., 2011; Annangi et al*.,* 2014; Luanpitpong et al., 2014; Bach et al., 2016; Rojanasakul et al., 2016). Thus, analysing the number of cell divisions produced in a period of time or estimating the time required for cells to duplicate (doubling time) through long exposures compared with non-treated cells is a common and useful approach to evaluate if the treatment is influencing the cell cycle and undergoing carcinogenesis. Therefore, the time necessary for a population doubling to occur is calculated according to the equation 1:

$$Doubling\ time = \frac{duration * \log(2)}{\log(final\ concentration) - \log(initial\ concentration)}$$

Equation 1: Doubling time calculation. Source: http://www.doublingtime.com/compute.php

1.3.3.2. Epithelial to mesenchymal transition (EMT)

EMT is a reversible physiological process involved in three different cellular programs. Type-1 EMT is highly regulated and essential during embryonic implantation and organ formation. Type-2 and type-3 are operative after birth and are concerned with fibrosis and malignant cellular transformation respectively due to downstream signalling pathways being constitutive activated (Kovacic et al., 2012). Type-3 EMT is the process by which epithelial cells acquire mesenchymal malignant transformation features during carcinogenesis. Thus, studying these sequential series of changes is an important approach when evaluating the carcinogenic effects occurring in an epithelial *in vitro* cell line like BEAS-2B.

Cell transformation through EMT process is regulated by a number of signalling pathways and transcriptional factors, eventually resulting in the loss of epithelial markers and acquisition of mesenchymal features (Kalluri and Weinberg, 2009). Among the signal factors able to induce EMT, the transforming growth factor beta (TGF-β) is the most extensively studied inducer, interacting with several related EMT pathways, such as PI3K, Wnt, Hedgehog, Notch, or Ras-MAPK (Xiao and He, 2010; Lamouille et al*.,* 2014).

Several EMT *in vitro* studies have endorsed this program to study early stages of lung carcinogenesis, allowing a clearer identification of the molecular mechanisms of EMT (Xiao and He, 2010; Zhao et al*.*, 2013; Sohal et al*.,* 2014; Vu et al*.,* 2016). Thus, a number of distinct molecular events have been associated to the signalling pathways already mentioned. These include activation of transcription factors, expression of specific cell-surface proteins, reorganization and expression of cytoskeletal proteins, production of extra cellular matrix (ECM)-degrading enzymes such as matrix metalloproteinases (MMPs), or changes in the expression of specific microRNAs.

One of the essential molecular characteristics of EMT is the “cadherin switch”. E-cadherin (CDH-1) form adherence junctions with adjacent epithelial cells and thereby helps assemble epithelial tissue, whilst N-cadherin (CDH-2) is normally expressed in migrating neurons and mesenchymal cells during embryogenesis. Thus, down-regulation of CDH-1 and up-regulation of CDH-2 is considered a molecular hallmark of EMT (Kalluri and Weinberg, 2009). However, other involved factors have also been used as molecular biomarkers to demonstrate the passage of a cell through EMT. Thus, as showed in Figure 9, decrease in epithelial markers like Zonula occludens-1 (ZO-1), Laminin-1 or Mucin-1 (MUC-1), and increase in mesenchymal markers like

Vimentin, Fibronectin or Actin alpha 2 smooth muscle aorta (Acta-2) among others, have also been associated to this intricate process.

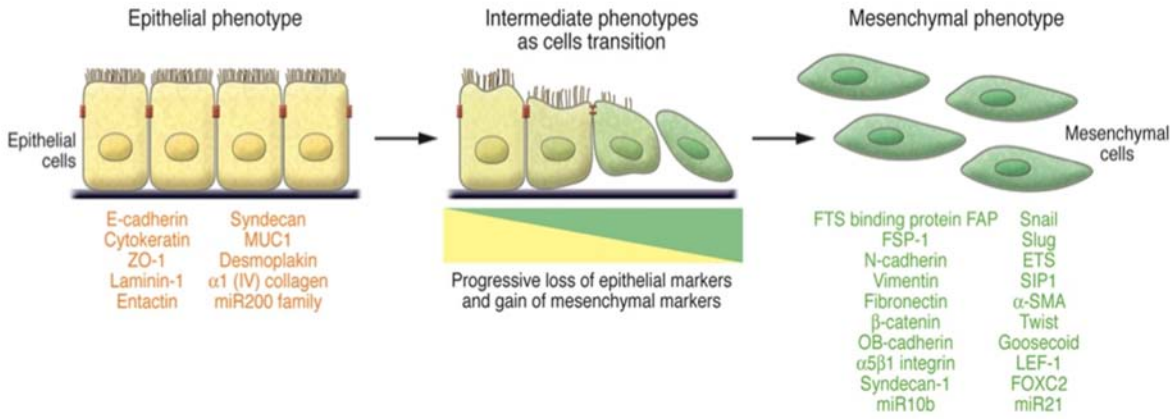

Figure 9. EMT process and some molecular biomarkers. (Adapted from Kalluri et al. 2009)

Gene expression studies are frequently used to determine the way a target gene changes its expression profile over time, as for example how much the expression changes over the course of a disease or after a treatment. In this case, the expression profile of some genes associated with the EMT process was analysed using real time reverse transcription polymerase chain reaction (real time RT-PCR) technique. Simply, total RNA is extracted and retrotranscribed to cDNA using TRIzol Reagent and the transcriptor first-strand cDNA synthesis kit respectively. The resulting cDNA is subjected to real-time PCR analysis on a Lightcycler 480 (Roche) to evaluate the relative expression levels of the mentioned genes.

The induction of this mesenchymal phenotype implies “spindle-like” morphology originated by the changes in the composition of cytoskeletal proteins. Moreover, these molecular changes prompt cells to increase the ability to migrate and invade other tissues, which are important characteristics during metastasis (Tse and Kalluri, 2007).

1.3.3.3. Migration and invasion

As above mentioned, during EMT cells change their structure and shape by cytoskeletal reorganization gaining in motility. At this point cells interact with the surrounding tissue structure, the ECM, which provides the substrate as well as a barrier towards the advancing cell body (Friedl and Wolf, 2003). Cancer-cell migration is typically regulated by integrins (transmembrane receptors connecting cells to ECM), MMPs, cell-to-cell adhesion and cell-to-cell communication molecules. Among the migration regulators, special attention is payed to MMPs. This prominent family of

proteinases is associated with tumorigenesis through different direct and indirect pathways (Kessenbrock et al., 2012). Focussing on cancer cell migration, MMPs are directly linked to the cleaving of cell-surface proteins as well as degrading components of the ECM, allowing migratory cells to invade neighbouring tissues and break through the basement membrane (Brinckerhoff and Matrisian, 2002).

To spread within the tissues, tumour cells use migration mechanisms that are the same as those that occur in normal, non-neoplastic cells during physiological processes such as embryonic morphogenesis, immune-cell trafficking and would healing (Friedl and Wolf, 2003). Thus, to study this process an easy and highly used *in vitro* assay is normally performed. The scratch assay mimics cell migration during wound healing *in vivo*. The basic steps involve creating a "wound" in a cell monolayer, capturing the images at the beginning and at regular intervals during cell migration to close the wound, and comparing the images to quantify the migration rate of the cells.

Mechanically, cell migration consists in a cycle of interdependent steps starting by the formation of a pseudopod attached to the ECM substrate and followed by contraction of regions of the leading edge or the entire cell body, thereby generating traction force that leads to the gradual forward gliding of the cell body (Lauffenburger and Horwitz, 1996). Thus, the migration of individual cells that detach from the primary tumor, enter lymphatic vessels or the bloodstream and seed in distant organs is how tumor cell invasion and metastasis is conventionally understood (Friedl and Wolf, 2003).

1.3.3.4. Tumor-stroma cross-talk

Intense cancer research has been developed to elucidate and understand the hallmarks of cancer cells. However, tumor cells do not act isolated, being surrounded by a highly rich microenvironment (del Pozo Martin et al., 2015). While normal cells turn into cancer cells, the surrounding microenvironment co-evolves into an activated state through continuous paracrine communication, thus creating a dynamic cross-talk signalling that promotes cancer initiation and growth, and ultimately leads to a fatal disease (Pietras and Östman, 2010). In the last years efforts have been dedicated to the study of these paracrine interactions, allowing a clearer identification of the regulators of this process.

The tumor microenvironment is formed by endothelial cells, pericytes, fibroblasts, various classes of leukocytes, and components of ECM (Xing et al., 2010). Among the changes detected in cell components, the trans-differenciation of fibroblasts into cancer-associated fibroblast (CAFs) is one of the most studied processes. Thus, CAF

directly stimulate tumor cell proliferation through provision of various growth factors, hormones and cytokines (Karagiannis et al., 2015). Interestingly, it has been shown that many of these factors acting in isolation are sufficient to induce transformation of epithelial cells, indicative of the CAFs capability to initiate carcinogenesis (Bhowmick et al., 2004).

On the other hand, within the components of ECM, MMPs represent key players in the molecular communication between tumor and stroma. Thus, in addition to their role in the degradation of ECM and cancer cell migration, MMPs regulate microenvironment signalling pathways controlling cell growth, inflammation and angiogenesis (Kessenbrock et al., 2012). Among more than 21 human MMPs, MMP-2 (gelatinase A) and MMP-9 (gelatinase B), are thought to play a key role in degradation of type IV collagen and gelatine, the two main components of ECM (Roomi et al., 2009). Additionally, increase in these MMPs secretion has been found in several types of human cancers and has been also associated with poor prognosis (Di Nezza et al., 2002). Due to the importance of these MMPs in carcinogenesis in our work we specifically focused in MMP-9 for the study of its activity using zymography technique. For this assay conditioned media (CM) taken from starved treated cells, containing secreted MMPs is resolved under denaturing conditions in precast gels containing its gelatine substrate by SDS-PAGE. Then, following a simple renaturing, developing, and staining; the areas of protease activity appeared as clear bands against a dark background. Comparisons between the MMP-9 protease activity of different treatments and controls can be consequently analysed.

As a consequence of the described paracrine interactions among microenvironment components, a dynamic cross-talk signalling is created leading to the activation of pathways favouring cancer growth and eventually leading to metastasis as shown in Figure 10.

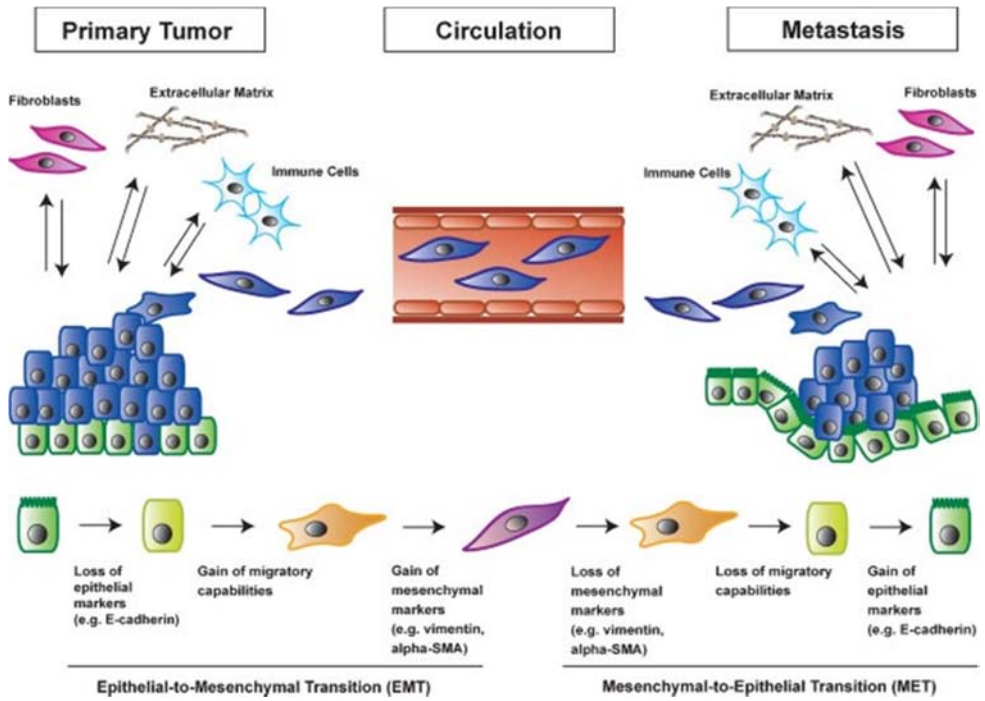

Figure 10. Mechanisms of metastasis: Epithelial-to-mesenchymal transition and contribution of tumor microenvironment (Tse and Kalluri, 2007).

Studying changes in cancer cell microenvironment has become an important focus of interest and a recent approach in cancer research. Regarding 2D *in vitro* cultures in which the complete microenvironment cannot be achieved, the use of CM taken from starved cancer cells could give us an idea about how this media, containing a wide variety of secreted factors (secretome) could affect the behaviour of other surrounding cells (Annangy et al., 2014). In this work the indirect soft agar has been chosen to analyse this process. Thus, the secretome of the long-term exposed cells is used to grow a cancer cell line (HCT-116) in a soft agar substrate, being this cell line prone to grow independently of anchorage. Thus, changes in the size of colonies indicate differences in the ability of CM in promoting surrounding cell growth.

1.3.3.5. Anchorage-independent cell growth

Cell anchorage-independent growth is the ability of transformed cells to grow independently of a solid surface, and it is a hallmark of carcinogenesis. The molecular mechanism underlying anchorage-independent growth has been linked to the activation of a mitochondrial biogenesis program also associated to potential for metastasis in primary breast and lung tumors (Mori et al., 2009). Therefore, this ability has been considered to be fundamental in cancer biology due to its connection with tumor cell aggressiveness *in vivo* such as tumorigenic and metastatic potentials, and

also utilized as a marker for *in vitro* transformation (Borowicz et al., 2014). Thus, the soft-agar assay is a well-established method considered to be one of the most stringent tests for *in vitro* malignant transformation (Borowicz et al., 2014). Thereby, the intrinsic property of transformed cells to anchorage-independent growth is evaluated as a hallmark of carcinogenesis as showed in Figure 11. Simply, long-term exposed cells are cultured in a semi-liquid substrate (soft-agar) for 21-28 days. Following this incubation period, formed colonies can be stained, quantified and the results compared with matched controls.

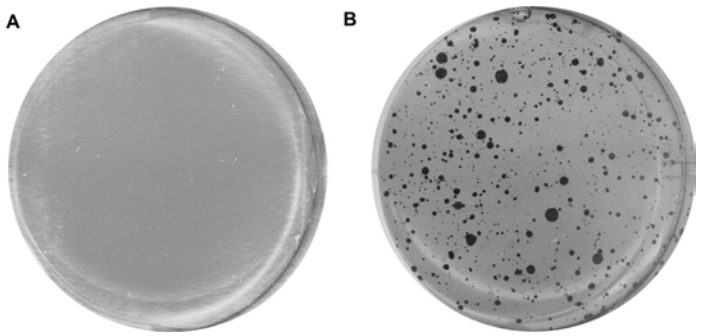

Figure 11. Soft-agar plates showing cell anchorage-independent growing in a non-transformed cell line (A) and in a cancer cell line (B).

1.3.3.6. Mechanisms of cell transformation

Normally in environmental carcinogenesis, the induced mechanism of cell transformation depends on how the compound directly or indirectly interacts with DNA. However, deregulation of specific genes could lead to the activation of common pathways. Thus, studying these gene expression levels light could be shed on the carcinogenic mechanism associated to a specific exposure. Among typical studied genes, *PTEN* and *FRA-1* constitute pivotal factors in cancer development of different cancer types including lung cancer (Karamouzis et al*.,* 2007; Yanagi et al., 2007).

1.3.3.6.1. *PTEN*

PTEN is a tumor suppressor gene involved in PI3K/AKT signaling pathway which expression has been altered at high frequency in a large number of cancers (Song et al*.,* 2012). Reduction and loss of *PTEN* protein expression has been noted often in transformed cell lines as well as in primary tumors; with frequencies to almost 70% of reduced expression in non–small-cell lung tumors (Soria et al., 2002). Thus, being *PTEN* involved in the PI3K/AKT signaling pathway, a decreased protein expression prevents the inhibition of several interactions inside the pathway, altering various

cellular functions associated to cancer features like apoptosis, growth, cell cycle, angiogenesis, invasion and autophagy (Arcaro and Guerreiro, 2007).

1.3.3.6.2. *FRA-1*

FRA-1 is one of the most common components of AP-1, a basic leucine zipper (bZIP) transcription factor involved in several cellular functions deregulated in cancer progression (Jochum et al*.,* 2001). Thus, deregulated FRA-1 mRNA and protein have been detected in multiple tumors as well as transformed cell lines, including breast, colon and lung (Young and Colburn, 2006). Although FRA-1 upregulation have been observed in several cancers, a decrease in its transcript have also been detected in lung cancer, correlated with advanced tumor stage and poor survival (Ma et al*.,* 2009). It seems that although FRA-1 deregulation is clearly linked to carcinogenesis, fluctuations in mRNA levels could be associated to carcinogenic stages.

1.3.4. Methodological limitations associated to long-term treatment studies in the NMs field

Carcinogenesis is a process that involves gene-environment interaction. The environmental factors involved in carcinogenesis are frequently long-term, rather than acute exposures. In order to study the role that NPs in general, and nanoceria in particular, play as an environmental factor in carcinogenesis, in vitro models must replicate this long-term contact. However, the reproduction *in vitro* of this exposure has several technical difficulties that challenge the validity and reliability of these experiments, and therefore the conclusions that can be drawn from them. For this reason we decided to investigate this further in this thesis dedicated to the biological aspects of nanoceria exposure.

When long-term treatment exposures are implemented *in vitro* in the nanotoxicology field, NP preparation and dispersion become crucial factors to assure validity and reliability. NPs are able to produce several biological effects by different mechanisms depending on their physico-chemical characteristics, including size, shape, surface area, chemical composition, solubility, surface charge, agglomeration/aggregation and/or crystal structure (Bai et al., 2010; Xu et al., 2010; Cho et al., 2010; Pujalté et al., 2011; Mcguinnes et al., 2011; Kermanizadeh et al., 2012). A consistent reproduction of the conditions of the exposure is crucial to assure reliability. The preparation and dispersion of NMs for cell treatments are determinant factors of their physico-chemical properties and of their toxicological properties (Murdock et al., 2008; Park et al., 2009; Jiang et al., 2009; Rocco et al., 2011). Consequently, the variability between every

process of dispersion through the long-term treatment is a threat to the reliability of the exposure and the validity of the whole experiment. We propose in this thesis an innovative strategy to overcome this limitation of long-term treatments, and to ultimately facilitate its implementation.

Our hypothesis in this thesis is that by preparing an aliquot of the NM stock dispersion, then freezing it immediately in liquid nitrogen and storing it at -80 ºC, and then using this preparation for each of the exposures in the long-term treatment, the reliability of the experiment would be at least as good as preparing serial fresh dispersions, while saving time and resources. In order to test this hypothesis, we validated the use of frozen dispersions by comparing fresh and frozen preparations of five different NMs (nanoceria, TiO_2-NPs, ZnO-NPs, Ag-NPs and CNT) regarding different physico-chemical and biological endpoints.

As preliminary information to predict possible NP-cell interactions primary sizes and morphologies were obtained using transmission electron microscopy (TEM). In order to determine the size of particles in solution (hydrodynamic size), which is directly linked with the aggregates size, values were obtained by dynamic light scattering (DLS). This is a highly used technique based on intensity fluctuations of laser light scattered by particles, moving in Brownian motion, the diffusion coefficient is determined and converted to particle size via the Stokes-Einstein equation. Additionally, this technique allows the measurement of “z potential” as a measure of surface charge and stability of the colloidal dispersion.

Dissolution of metallic NPs to ions is a mechanism by which NPs could induce cytotoxicity to mammalian cells. Thus, released ions have been linked to mitochondrial damage and consequent cellular redox imbalance (Sabella et al., 2014). The importance of released ions in the toxic profile of NMs make essential to consider this physico-chemical property when comparing fresh and frozen NP dispersions. The use of inductively coupled plasma mass spectrometry (ICP-MS) allows the detection of multi-element trace/ultratrace metal analysis of clinical and biological samples. Therefore, followed by NP dispersion ultracentrifugation, the technique detects and quantifies the presence of ions dissolved in the supernatant providing high-performance analysis with high sensitivity.

Intracellular uptake of NPs is also an important point to be considered since different percentage of cellular internalization could lead to different toxicological effects. Therefore, in addition to the determination of NP morphologies and primary sizes, TEM analyses are useful to determine cellular NP internalization. However, some problems

arise in the detection of very small particles that are prone to dissolve. In those cases complementary confocal microscopy could be used (Vila et al., 2016). This technique allows a better intracellular localization since 3D images with fluorescence-labeled NP are generated as showed in Figure 12.

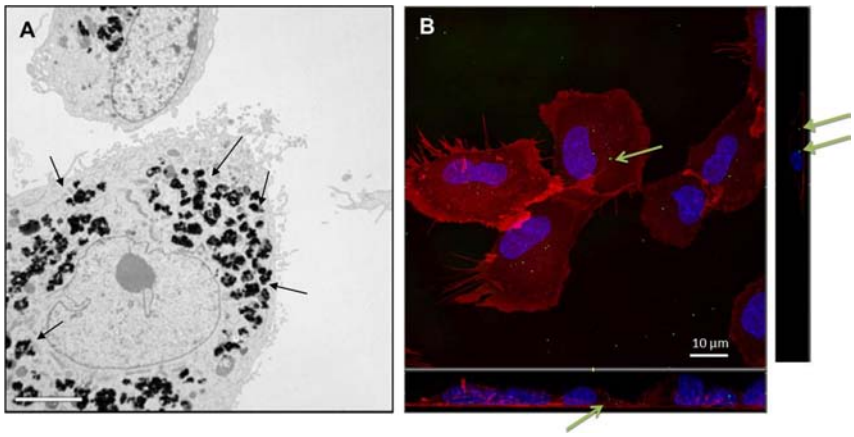

Figure 12. NP internalization by TEM (A) and confocal microscopy (B).

Apart from cellular uptake, differences in intracellular ROS generation between fresh and frozen NP dispersions could also be a cause of possible differences in NP associated-effects. As already mentioned, ROS is considered as a general mechanism causing cellular damage by NPs (Wang et al., 2011). Therefore, the common DCFH-DA assay for intracellular ROS detection was chosen to assess this endpoint. Finally, cellular viability is a basic parameter to be included in any study determining the biological effects of NMs. In this case, cell viability differences between dispersion protocols would show the final outcome produced by the physico-chemical NP properties and their interaction with the cellular model.

To our knowledge, this is the first study focused on the comparison between fresh and frozen dispersions. In our case of study involving long-term exposures to sub-toxic doses of NMs, the approach we proposed supposes advantages not only for the homogeneity of the sequential treatments, but also for the time consuming reduction in NMs dispersions tasks. Note that this type of experimental approach requires frequent preparation of newly NMs dispersions. Other than long-term exposures, the implementation of this methodology is an important consideration when homogenised treatments are highly required.

Furthermore, this procedure also can report advantages in other aspects of the nanotoxicology field. The potential use of high-throughput methodologies in NMs toxicity testing is another example. These approaches are currently limited by the

bottle-neck that supposes the time necessary to prepare different fresh concentrations of the NMs to be tested. Therefore, to prove the suitability of our proposal would help to extend the use of such high-throughput methodologies in the NMs field.

2. OBJECTIVES

2. OBJECTIVES

As mentioned in the Introduction section nanoceria is widely used in many industry and commercial products, mainly due to its interesting redox properties. However, no general agreement regarding its beneficial role in biological systems has been reached. The general objective of this Thesis is to evaluate the beneficial/harmful effects of nanoceria in an *in vitro* model to clarify the controversial data and gaps found in the literature.

To achieve these goals, we have set out the following four specific objectives:

1. To determine the antioxidant effects of nanoceria, after short exposure *in vitro,* using the lung epithelial cell line BEAS-2B as a model (study 1).

2. To evaluate the potential dual pro-/anti-oxidant properties of nanoceria depending on the tumoral and non-tumoral background of the exposed system (study 2).

3. To evaluate the transforming effects of long-term exposure to nanoceria in lung epithelial BEAS-2B cells, along with the effects associated to a common plausible tobacco co-exposure (study 3).

4. To establish a new NP dispersion method for the study of the in vitro long-term effects of NPs exposure (study 4).

3. RESULTS

3. RESULTS

Part of the obtained results derived from this Thesis has been published in different peer-review journals. Specifically, upon submission of this Thesis dissertation, two articles have been published already and two more manuscripts are currently in the process of submission. Consequently, the structure of this section is constituted by the content of the published articles being the rest positioned in the annexes section.

The four articles/manuscripts ordered according with the objectives of the Thesis, are as follows:

1. **Article 1:** Antioxidant and antigenotoxic properties of cerium oxide nanoparticles in a pulmonary like cell system.

2. **Annex 1:** Antioxidant potential of nanoceria in tumoral and transformed cells.

3. **Annex 2:** Nanoceria do not protect lung epithelial cells from the transforming effects of tobacco long-term exposure.

4. **Article 2:** Frozen dispersions of NMs are a useful operational procedure in nanotoxicology.

Article 1 (Study 1)

Antioxidant and antigenotoxic properties of cerium oxide nanoparticles in a pulmonary like cell system

Archives of Toxicology, 90: 269–278 (2016)

doi: 10.1007/s00204-015-1468-y

Impact factor: 6.637

3.1. Abstract of the first study (Article 1)

Antioxidant and anti-genotoxic properties of cerium oxide nanoparticles in a pulmonary-like cell system.

Nanoceria has been presented to the research community as a unique redox catalyst, based on the extended uses of this NM in different industrial applications. The presence of two oxidation states (Ce^{3+} and Ce^{4+}) on its surface, allows that many cerium atoms switch between both states. In this way, nanoceria acts catalyzing ROS-detoxifying reactions while simultaneously regenerates the reduced Ce^{3+} ions on its surface. Thereby, nanoceria has emerged as a promising therapeutic agent to be used in various diseases/disorders originated as a consequence of oxidative stress, such as neurodegenerative diseases, immune disorders, endocrine dysfunction, diabetes, osteoporosis, cancer and aging among others.

In this study we have used an epithelial lung cell line, BEAS-2B, as a model to study the possible antioxidant and antigenotoxic effect of nanoceria in a pulmonary-like system. For this aim, oxidative stress has been induced to cells by an acute treatment with a well-defined oxidative agent ($KBrO_3$) and the protective effect of nanoceria pre-treatment has been assessed through different biomarkers. Whereby, different endpoints like toxicity, intracellular ROS induction, genotoxicity and DNA oxidative damage (comet assay), and gene expression alterations associated to oxidative signaling pathways have been evaluated.

The obtained results confirmed the antioxidant properties of nanoceria in the epithelial BEAS-2B lung cell model. Thus, its pre-treatment significantly reduced the intracellular production of ROS induced by $KBrO_3$, as observed by using flow cytometry techniques. Similarly, a reduction in the levels of DNA oxidative damage, as measured with the comet assay complemented with formamidopyrimidine DNA glycosylase (FPG) enzyme, were also observed. Pre-treatment of BEAS-2B cells with nanoceria slightly increased the viability of cells treated with toxic concentrations of $KBrO_3$, as well as deregulated the expression of genes involved in the oxidative *Nrf2* pathway. Thus, the expression levels of HO-1 and SOD-2 were decreased with nanoceria pre-treatment in comparison with the levels induced by the oxidant treatment alone showing direct protective effects. Interestingly, SOD-2 transcript levels were up-regulated after nanoceria treatment which suggests an indirect protective effect of nanoceria stimulating the antioxidant cellular defence.

According to the results obtained in this study, nanoceria can be proposed as a promising pharmacological material with possible application in a very huge number of diseases caused by oxidative stresses, including those related with pulmonary system. However, further studies showing the absence of harmful secondary effects must be carried out to confirm its therapeutic usefulness.

Arch Toxicol (2016) 90:269–278
DOI 10.1007/s00204-015-1468-y

NANOTOXICOLOGY

Antioxidant and anti-genotoxic properties of cerium oxide nanoparticles in a pulmonary-like cell system

Laura Rubio · Balasubramanyam Annangi · Laura Vila · Alba Hernández · Ricard Marcos

Received: 6 October 2014 / Accepted: 13 January 2015 / Published online: 25 January 2015

Abstract Cerium oxide nanoparticles (CeO_2-NP) present two different oxidation states what can suppose an auto-regenerative redox cycle. Potential applications of CeO_2-NP to quench reactive oxygen species (ROS) in biological systems are currently being investigated. In this context, CeO_2-NP may represent a novel agent to protect cells and tissues against oxidative damage by its regenerative free radical-scavenging properties. In this study, we have used a human epithelial lung cell line, BEAS-2B, as a model to study the possible antioxidant and anti-genotoxic effect of CeO_2-NP in a pulmonary-like system. We have assessed the protective effect of CeO_2-NP pre-treatment in front of a well-defined oxidative stress-inducing agent ($KBrO_3$). Different endpoints like toxicity, intracellular ROS induction, genotoxicity and DNA oxidative damage (comet assay), and gene expression alterations have been evaluated. The obtained results confirmed the antioxidant properties of CeO_2-NP. Thus, its pre-treatment significantly reduced the intracellular production of ROS induced by $KBrO_3$. Similarly, a reduction in the levels of DNA oxidative damage, as measured with the comet assay complemented with formamidopyrimidine DNA glycosylase enzyme, was also observed. Pre-treatment of BEAS-2B cells with CeO_2-NP (at 2.5 µg/mL) slightly increased the viability of cells treated with $KBrO_3$ as well as down-regulated the expression of the *Ho1* and *Sod2* genes involved in the oxidative *Nrf2* pathway. Our finding would support the potential use-fulness of CeO_2-NP as a pharmacological agent to be used against diseases caused by oxidative stress.

Keywords Cerium oxide nanoparticles · Antioxidant · Antigenotoxic · Oxidative stress · BEAS-2B cells

Introduction

Reactive oxygen species (ROS) are generated by cells as by-products of their own aerobic metabolism, and they are essential to maintain the homeostasis of cells (Schieber and Chandel 2014). Since ROS react with lipids, proteins, and DNA (Cross et al. 1987), a range of different cytosolic antioxidant enzymes are responsible to counteract ROS production maintaining an oxidative redox balance. This balance between ROS production and antioxidant defences determines the degree of oxidative stress (Finkel and Holbrook 2000). Taking into account the relevance of the ROS effects and the possibility to counteract them by using antioxidant defences, a huge amount of literature has emerged looking for different ways to reduce oxidative stress and its undesired consequences (Saeidnia and Abdollahi 2013).

Nanoparticles possessing antioxidative properties have recently emerged as potent therapeutic agents (Narayanan and Park 2013). Among them cerium oxide nanoparticles (CeO_2-NP) have recently gained in popularity due to their well-known ability to switch between two oxidative states (III and IV) depending on the physiological environment (Karakoti et al. 2008). Its surface oxygen vacancies interact with ROS displaying antioxidant properties mimicking the

Electronic supplementary material The online version of this article (doi:10.1007/s00204-015-1468-y) contains supplementary material, which is available to authorized users.

L. Rubio · B. Annangi · L. Vila · A. Hernández · R. Marcos (*)
Grup de Mutagènesi, Departament de Genètica i de Microbiologia, Facultat de Biociències, Universitat Autònoma de Barcelona, Campus de Bellaterra, 08193 Cerdanyola Del Vallès, Barcelona, Spain
e-mail: ricard.marcos@uab.es

A. Hernández · R. Marcos
CIBER Epidemiología y Salud Pública, ISCIII, Madrid, Spain

activities of the cellular antioxidant enzymes such as super-oxide dismutase and catalase (Heckert et al. 2008; Pirmo-hamed et al. 2010). Therefore, CeO_2-NP enter into the cells promoting the removal of oxidative molecules and cell lon-gevity (Kong et al. 2011). This free radical-scavenging prop-erty has been described in different studies reporting gastro-intestinal (Colon et al. 2010), breast (Tarnuzzer et al. 2005), neuronal (Schubert et al. 2006), and endothelial (Chen et al. 2013) cell protection in in vitro and in vivo studies.

Different lung cell conditions like physiological and pathological hypoxia or exposure to different oxidant insults like cigarette smoke result in the disruption of the balance between ROS production and antioxidant defences determining a degree of oxidative stress (Fresquet et al. 2006; Tagawa et al. 2008) and establishing an inflammatory process where the pulmonary artery pressure increases epi-thelial malfunction and edema arises in an acute form. This chronic situation predisposes to a vascular proliferation, an increase in vascular reactivity, chronic pulmonary hyper-tension leading to heart failure (Halliwell 2012).

In this context, the use of CeO_2-NP would represent a novel approach for the protection of normal lung cells from different kind of oxidative insults (Niu et al. 2011). While previous studies reported this scavenging and protecting effect of CeO_2-NP in lung cells (Xia et al. 2008; Arya et al. 2013), little is known about the biological mechanism and the effect of the cytosolic ROS scavenging over DNA protection. With such aim in this work, we have corroborated the ability of CeO_2-NP to quench ROS insult induced by potassium bromate ($KBrO_3$) in the BEAS-2B lung cell line, evidencing the final effect on DNA protection which eventually leads to increase cell viability over the oxidative insult. It must be stated that $KBrO_3$ is a well-known oxidizing agent (Delker et al. 2006; Limonciel et al. 2012). In addition, we have also investigated the possible biological mechanism of action of CeO_2-NP by testing the expression of different genes involved in oxidative stress pathways.

Our results suggest that the internalization of CeO_2-NP in the BEAS-2B cells does not produce any toxic effect, at the tested concentrations, while protecting against general oxidative stress. Our results would reinforce the view supporting a possible pharmacological potential of CeO_2-NP.

Materials and methods

Culture cell lines

Human bronchial epithelial cells (BEAS-2B) were maintained in DMEM high glucose medium (LifeTechnologies, NY, USA) supplemented with 15 % fetal bovine serum (FBS; PAA®), 1 % of nonessential amino acids (NEAA; PAA®), and 2.5 μg/mL plasmocin (InvivoGen, CA, USA) at 37 °C in a humidified 5 % CO_2 incubator and subcultured at 80 % confluence.

Nanoparticles characterization and dispersion

CeO_2-NP were bought from Sigma-Aldrich (St Louis, MO, USA). According to the manufacturer, size and density of CeO_2-NP was <25 nm and 7.13 g/mL, respectively. To verify and expand the manufacturer's information, transmission electron microscopy (TEM; JEOL JEM-2011) was utilized to determine size and morphology of NP. Besides, characterization of hydrodynamic size and zeta potential of CeO_2-NP dispersed in cell culture medium by dynamic light scattering (DLS) and laser Doppler veloci-metry (LDV) methodologies, respectively, was performed on a Malvern Zetasizer Nano-ZS zen 3600 instrument. For these measures, CeO_2-NP were pre-wetted in 0.5 % absolute ethanol and dispersed at 2.56 mg/mL in 0.05 % bovine serum albumin (BSA) in double-distilled water by 16 min of sonication. This dispersion protocol follows the agreement reached in the UE Nanogenotox project (Nanogenotox 2011). Subsequently, the sonicated CeO_2-NP were dispersed in DMEM high glucose with 15 % FBS for the measurements.

Cell toxicity

Cell viability was determined by propidium iodide (PI) staining. BEAS-2B cells were plated in six-well plates in triplicate at a density of 1×10^5 cells/well and incubated overnight. Cells were then pre-treated with 2.5, 5 and 7.5 μg/mL CeO_2-NP for 24 h before addition of 50 mM $KBrO_3$ for just 3 h. Later on, PI (6.73 μM final concentra-tion) was added to culture medium with cells for 5 min, and viable or dead cells were manually counted in a Neubauer's chamber for cell viability measurement using fluorescence microscopy.

Intracellular localization of CeO_2-NP

BEAS-2B cells exposed to CeO_2-NP were fixed in 2 % (w/v) paraformaldehyde (Hatfield, PA, USA) and 2.5 % (v/v) glutaraldehyde (Merck, Darmstadt, Germany) in 0.1 M cacodylate buffer (Sigma-Aldrich, Steinheim, Germany) at pH 7.4. Cells were then processed as described in Mussá et al. (2012). Briefly, samples were post-fixed with osmium, dehydrated in acetone, embedded in Epon, polym-erized at 60 °C, and cut with an ultramicrotome. Finally, ultrathin sections placed in copper grids were contrasted with conventional uranyl acetate and Reynolds lead citrate solutions and observed using a Jeol 1400 (Jeol LTD, Tokyo, Japan) transmission electron microscope equipped with a CCD GATAN ES1000 W Erlangshen camera.

RNA extraction and real-time RT-PCR

Total RNA was extracted from treated and untreated BEAS-2B cells using TRIzol® Reagent (Invitrogen,USA). RNase-free DNase I (DNA-freeTM kit; Ambion, UK) was used to remove DNA contamination. The first-strand cDNA synthesis was performed using 1 µg of total RNA with the transcriptor first-strand cDNA synthesis kit (Roche, Basel, Switzerland) following the manufacturer's instructions. The resulting cDNA was subjected to real-time RT-PCR analysis on a Lightcycler 480 (Roche, Basel, Switzerland) to evaluate the relative expression levels of glutathione S-transferase pi (*Gstp1*), super oxide dismutase *(Sod2)*, and heme-oxygenase1 (*Ho1*) genes using *β-actin* as the housekeeping control. The primer sequences are given in supplementary material section (Table S1). Each 20 µL of reaction volume contained 5 µL of cDNA, 10 µL of 2X LightCycler 480 SYBR Green I Master (Roche, Germany), 3 µL of H_2O and 1 µL of each primer pairs (final concentra-tion 500 nM). The cycling parameters began with 95 °C for 5 min, then 45 cycles of 95 °C for 10 s, 61 °C for 15 s, and 72 °C for 25 s. Cycle threshold (Ct) values were calculated with the Lightcycler software package and then normalized with *β-actin* values.

Intracellular generation of ROS

The intracellular generation of ROS was measured by flow cytometry using the 6-carboxy-2,7′-dichlorodihydro-fluorescein diacetate (DCFH-DA) assay. Cells were seeded in triplicate in 24-well plates at a density of 5×10^4 cells/well and incubated overnight. Following day, cells were pre-treated with different concentrations of CeO_2-NP for 24 h before addition of 5 mM $KBrO_3$ for 30 min. Subsequently, cells were washed twice with PBS and incubated in the presence of 5 µM DCFH-DA in serum-free DMEM high glucose medium for 30 min at 37 °C. Cells exposed to 5 mM $KBrO_3$ alone for 30 min were considered as positive control. They were further analyzed by FACSCalibur. Data were evaluated using Flowjo Ver. 7.6.5. A minimum of three independent experiments were carried out. It must be indicated that flow cytometry methodology also permits to determine the uptake of CeO_2-NP by the BEAS-2B cells as a measure of the scattering of the laser light after interacting with the cell (complexity) (Suzuki et al. 2007).

Comet assay

The oxidative and genotoxic DNA damage in BEAS-2B cells pre-treated with CeO_2-NP for 24 h followed by treatment with 5 mM $KBrO_3$ for 30 min were evaluated by the alkaline comet assay with and without the use of formamidopyrimidine DNA glycosylase (FPG) enzyme, as previously described (Annangi et al. 2014). Briefly, cells were rinsed with ice-cold 0.2 % ethylene diamine tetraacetic acid (EDTA) in PBS, trypsinized, and centrifuged at 130 G for 8 min. The pellet was washed twice in PBS and resuspended to obtain 17,500 cells/25 µL. Cells were mixed with 0.75 % low melting point agarose at 37 °C (1:10) and dropped onto Gelbond film. Cells on Gelbond were lysed overnight in ice-cold lysis buffer at 4 °C and pH 10. Later, Gelbonds were gently washed twice (1 × 5 and 1 × 50 min) in enzyme buffer at pH 8.0 at 4 °C fol-lowed by 30 min incubation at 37 °C in only enzyme buffer (negative control) or in enzyme buffer containing FPG. Gelbond films were then rinsed with electrophoresis buffer for 5 min and left in the electrophoresis buffer for 25 min to allow for DNA unwinding and expression of alkali labile sites. Electrophoresis was carried out for 20 min at 0.8 V/ cm and 300 mA at 4 °C. Subsequently, the Gelbond films were rinsed in cold PBS for 15 min, fixed in absolute etha-nol for 2 h, air-dried overnight at room temperature, and stained for 20 min with 1:10,000 SYBR Gold in TE buffer. Finally, gels were visualized for comets using an epifluo-rescent microscope at 20× magnification. The quantifi-cation of DNA damage in cells as percentage of DNA in tail was analyzed by the Komet 5.5 Image analysis system (Kinetic Imaging Ltd, Liverpool, UK). One hundred ran-domly selected comet images were analyzed per sample. Three different samples were processed for each CeO_2-NP pre-treated, $KBrO_3$-treated, and control.

Statistical analysis

One-way ANOVA was performed to compare the means of treated versus controls, and multiple pair-wise comparisons were done using the Tukey's test. Group mean values of each experiment were also compared by unpaired Student's *t* test. In all cases, statistical significance was considered at $P < 0.05$.

Results

Characterization of cerium oxide NP

The morphology and mean size of CeO_2-NP in pristine form were measured by transmission electron microscopy (Fig. 1a). The shapes of CeO_2-NP were mostly cubic and triangular, and mean size distribution was 9.52 ± 0.66 nm diameter (Fig. 1b), calculated by measuring over 100 particles in random fields of view. The size of CeO_2-NP measured with TEM matched with the manufacturer's as specified <25 nm. The average hydrodynamic radius and zeta potential of CeO_2-NP were 93.17 ± 5.10 nm and −10.6 ± 1.3 mV, respectively (Fig. 1c). It could be inferred

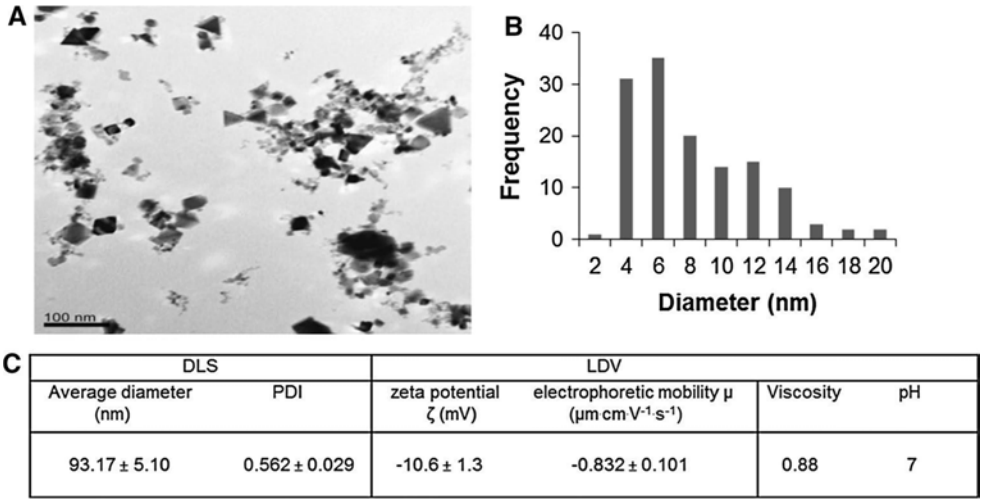

C

DLS		LDV			
Average diameter (nm)	PDI	zeta potential ζ (mV)	electrophoretic mobility μ (μm cm V^{-1} s^{-1})	Viscosity	pH
93.17 ± 5.10	0.562 ± 0.029	-10.6 ± 1.3	-0.832 ± 0.101	0.88	7

Fig. 1 **a** TEM image of CeO_2-NP in pristine form. **b** Size distribution of CeO_2-NP over 100 particles showing an aver-age of 9.52 ± 0.66 nm diameter. **c** CeO_2-NP average size and charge in exposure medium by pre-wetting with 0.5 % volume and steric stabilization using sterile-filtered 0.05 % w/v BSA. Data represented as mean ± SEM

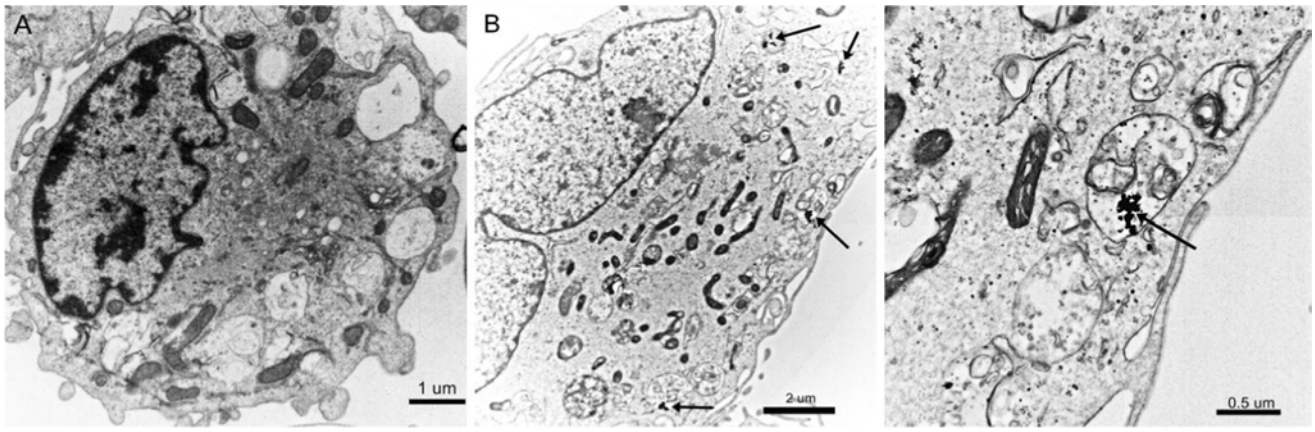

Fig. 2 Examples of TEM images showing internalization of CeO_2-NP in BEAS-2B cells after 24 h of treatment. image, **a** depicts untreated BEAS-2B cells without internalization of CeO_2-NP (magnifications 8,000×) whereas image, **b** shows localization of CeO_2-NP in vacuoles of BEAS-2B cells (magnification 8,000× and 12,000×) exposed to 7.5 μg/mL for 24 h. *Arrows* indicate nanoparticles or nanoaggregates.

from TEM and DLS data that CeO_2-NP showed some aggregation or agglomeration in dry and suspended forms possibly due to weak Van der Waals interactions or strong chemical bonds between individual particles.

Cellular uptake by TEM

To confirm the uptake of CeO_2-NP by BEAS-2B cells, we carried out TEM analysis of the cells exposed to 7.5 μg/mL CeO_2-NP. TEM images showed the internalization of CeO_2-NP when compared to untreated cells 24 h post-exposure (Fig. 2a, b). They were mainly confined to vacuoles as nanoaggregates, although they were also observed on the nuclear membrane. Internalization of CeO_2-NP was possibly occurred via passive diffusion or non-receptor-/receptor-mediated endocytosis.

It is interesting to remark that FACS methodology also permits to determine the uptake of CeO_2-NP by the BEAS-2B cells as a measure of complexity of cell (side scatter light). In this case, Fig. S1 clearly indicates that the levels of internalization increase with exposure concentrations. These results would confirm the data obtained by TEM.

Toxicity studies

Toxic and protective effects of CeO_2-NP after exposure to $KBrO_3$ were assessed by measuring the relative fluorescence intensity of PI uptake. A preliminary study on the toxicity induced by $KBrO_3$ indicates that after treatments lasting for 24 h, the obtained LC50 was 4.08 mM. For short-term treatments (50 mM and 3 h), induced toxicity was 75 %.

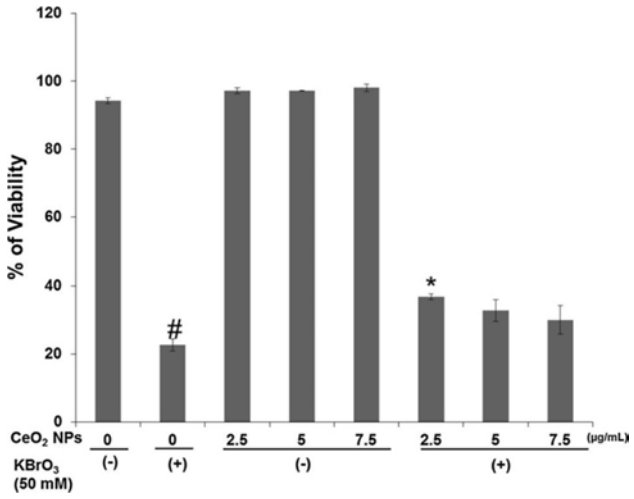

Fig. 3 Pre-treatment of BEAS-2B cells with CeO_2-NP for 24 h protect cells from $KBrO_3$-induced cell death. Histogram shows that $KBrO_3$-induced cell death is reduced due to pre-treatment with differ-ent non-toxic concentrations of CeO_2-NP for 24 h. This reduction in toxicity is indirectly related to CeO_2-NP dose, attaining statistical sig-nificance only at the dose of 2.5 µg/mL. One-way ANOVA for means of control versus exposed cells. $^{\#}P < 0.001$ for control versus $KBrO_3$-treated cells, $^{*}P < 0.05$ for $KBrO_3$-treated cells versus CeO_2-NP pre-treated cells

The results showed that pre-treatment of CeO_2-NP decreased cell mortality caused by addition of 50 mM of $KBrO_3$ for 3 h, although this decrease was statistically sig-nificant only at 2.5 µg/mL (Fig. 3; $P < 0.05$), compared to cell mortality induced by $KBrO_3$ in treated cells. Data also revealed that BEAS-2B cells exposed to CeO_2-NP concentra-tions ranging from 10 to 90 µg/mL were >90 % viable 24/48 h post-exposure compared to untreated cells (see Figure S2).

FACS measurement of intracellular reactive oxygen species (ROS) production

An important question to be elucidated was whether CeO_2-NP pre-treatment was able to diminish the intracellular ROS generated by $KBrO_3$. Thus, using FACS methodolo-gies, we determined the conversion of non-fluorescent DCFH-DA to fluorescent DCF in the cell mediated by oxi-dants. Our results demonstrated that CeO_2-NP pre-treated cells for 24 h were able to quench $KBrO_3$ (5 mM, 30 min) induced intracellular ROS (Fig. 4a, b). The percent of intra-cellular ROS in pre-treated cells with 2.5, 5 and 7.5 µg/ mL of CeO_2-NP were statistically significant at all the dose levels in comparison with $KBrO_3$ alone treated cells ($P < 0.01$), but there was no clear dose–effect relationship. Moreover, BEAS-2B cells pre-treated with same concen-trations of CeO_2-NP alone for 24 h did not show significant increase in intracellular ROS production compared with untreated cells.

In support of our previous data, we qualitatively ana-lyzed the ability of CeO_2-NP to quench the intracellu-lar ROS produced by $KBrO_3$ using fluorescence micros-copy. The data indicated highly fluorescent cells in 5 mM $KBrO_3$-treated cells due to ROS generation, whereas cells pre-treated with CeO_2-NP followed by 5 mM $KBrO_3$ for 30 min were non-fluorescent (Fig. 4c). This confirms our hypothesis that CeO_2-NP are potential intracellular ROS scavengers.

Gene expression data

The expression of antioxidant genes such as *Ho1, Sod2* and *Gstp1* was evaluated after 24 h of treatment with vary-ing doses of CeO_2-NP alone or followed by 5 mM $KBrO_3$ for 30 min (Fig. 5). Data revealed statistically significant increases in the expression of *Ho1* and *Sod2* genes in $KBrO_3$-treated cells compared to untreated cells ($P < 0.05$). On the other hand, pre-treatment of cells with CeO_2-NP mitigated the increased expression of *Ho1* and *Sod2* genes due to $KBrO_3$ treatment. Data did not show significant decrease in $KBrO_3$-induced *Gstp1* expression due to pre-treatment with CeO_2-NP.

Anti-genotoxicity activity of CeO_2-NP

The genotoxic and oxidative DNA damage (ODD) effects after 24 h of exposure with different concentrations of CeO_2-NP alone or followed by 5 mM $KBrO_3$ for 30 min are presented in Fig. 6. These results were obtained by using the comet assay. At the concentrations tested, $KBrO_3$-induced ODD was significantly decreased in CeO_2-NP pre-treated cells. A maximum effect was observed at 2.5 µg/ mL compared to $KBrO_3$-treated cells ($P < 0.01$) indicating anti-genotoxicity ability of CeO_2-NP at non-toxic dose lev-els. BEAS-2B cells treated with CeO_2-NP alone for 24 h showed neither genotoxic nor ODD compared to untreated cells. Considering these results, CeO_2-NP ought to be rel-evant for the decreased ODD levels observed.

Discussion

In our model of pulmonary-like system, using the epithelial lung cell line BEAS-2B, we have proven the antioxidant and anti-genotoxic potential of CeO_2-NP. This would indi-cate the potential usefulness of CeO_2-NP to fight against diseases associated to oxidative stress as already suggested (Niu et al. 2011).

Although the use of CeO_2-NP is increasing in differ-ent fields due to its use as a catalyst (Zheng et al. 2005), ultraviolet-absorbing compound in sunscreen (Zholobak et al. 2011), fuel additive (HEI 2001), or solar cells (Corma

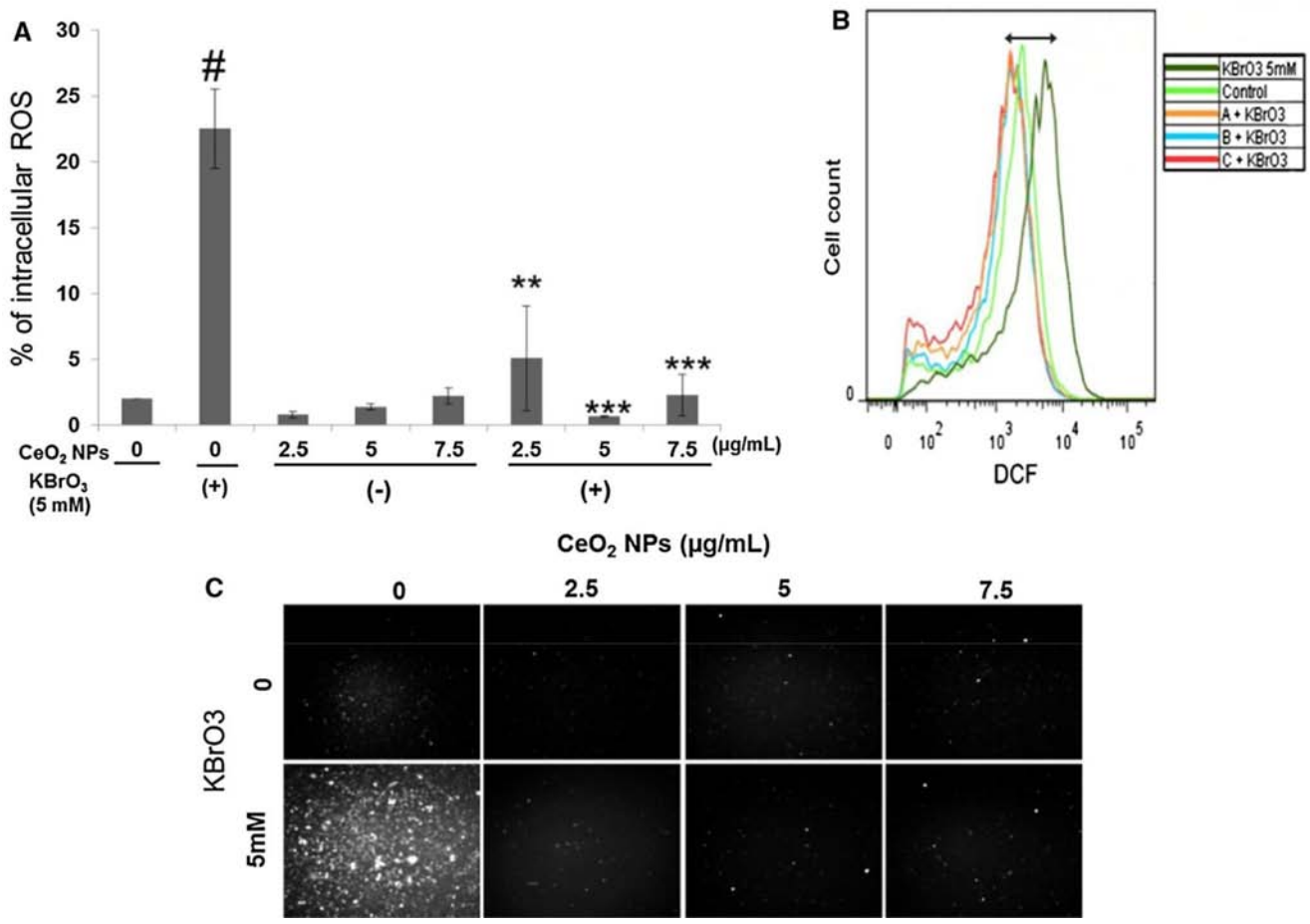

Fig. 4 Pre-treatment of BEAS-2B cells with CeO_2-NPs for 24 h mitigate $KBrO_3$-produced intracellular ROS. **a** The graph shows a signifi-cant decrease in $KBrO_3$ (5 mM, 30 min)-generated intracellular ROS because of pre-treatment with different non-toxic concentrations of CeO_2-NP for 24 h. **b** A representative histogram of ROS production for control, $KBrO_3$, CeO_2-NP pre-treated followed by 5 mM $KBrO_3$ exposure for 30 min. A decrease in relative fluorescence is reflected with a leftwards shift in x-axis in line histograms compared to $KBrO_3$-exposed cells. *Double-headed arrow* indicates the shift from right (fluorescent cells) to left (non-fluorescent cells). **c** Image shows BEAS-2B cells exhibiting DCF-DA fluorescence due to genera-tion of intracellular ROS in $KBrO_3$ cells whereas no fluorescence in CeO_2-NP pre-treated cells for 24 h. Data represented as mean ± SEM (n = 3). One-way ANOVA for means of control versus exposed cells. #$P < 0.001$ for control versus $KBrO_3$-treated cells, *$P < 0.05$ for $KBrO_3$-treated cells versus CeO $_2$-NP pre-treated cells. *Note* A, B and C in Fig. 4b indicate 2.5, 5 and 7.5 µg/mL CeO_2-NP, respectively

et al. 2004), we ought to expand its promising uses in the field of nanomedicine. The assumed antioxidant properties of CeO_2-NP have encouraged for its usage as a free radical scavenger that protects normal tissue from radiation damage due to radiotherapy (Colon et al. 2009, 2010; Baker 2013). In addition, it has also been proposed as antitumoral agent and to combat diseases characterized by ROS accumula-tion (Wason and Zhao 2013). Among such diseases, there are numerous lung disorders like respiratory distress syn-drome, emphysema, asthma, broncho-pulmonary dysplasia, and interstitial pulmonary fibrosis caused by oxidative stress (Choi and Alam 1996), and those could be presented as models for the pharmacological potential use of CeO_2-NP.

In our study we have demonstrated that CeO_2-NP are able to quench ROS produced in the BEAS-2B lung cell line, by a well-known oxidizing agent like $KBrO_3$ (Delker et al. 2006; Limonciel et al. 2012). In addition, other bio-markers like decreasing DNA damage, mimicking *Sod2* and *Ho1* activity, and reducing cell mortality have also been detected. Thus, it is likely that CeO_2-NP prevent lung epithelium oxidation and thereby inhibit the inflammatory process that otherwise in a chronic situation could lead to cell transformation processes (Tarnuzzer et al. 2005; Annangi et al. 2014).

CeO_2-NP internalization in BEAS-2B epithelial lung cells occurs without significant induction of cell mortal-ity, supporting their non-cytotoxic properties at the tested doses. It has already been demonstrated that CeO_2-NP uptake is carried out mediated endocytic pathways, and it is co-localized with mitochondria, lysosomes, and

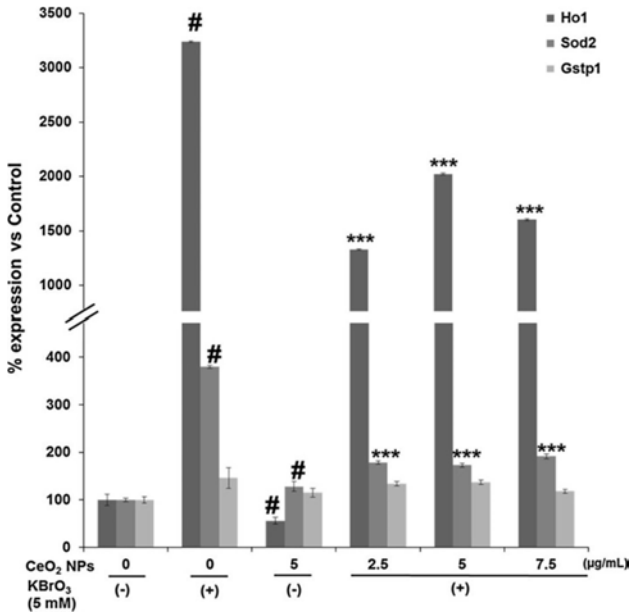

Fig. 5 Pre-treatment of BEAS-2B cells with CeO_2-NP for 24 h reduce $KBrO_3$-induced mRNA expression of antioxidant genes. The *graph* shows reduced mRNA expression of $KBrO_3$-induced *Ho1* and *Sod2* genes due to pre-treatment with different non-toxic concentrations of CeO_2-NP for 24 h. No effects were observed for the *Gstp1* gene. Data represented as mean ± SEM (n = 3). One-way ANOVA for means of control versus exposed cells. #$P < 0.01$ for control versus $KBrO_3$ or CeO_2-NP alone treated cells. ***$P < 0.001$ for $KBrO_3$ treated cells versus CeO_2-NP pre-treated cells

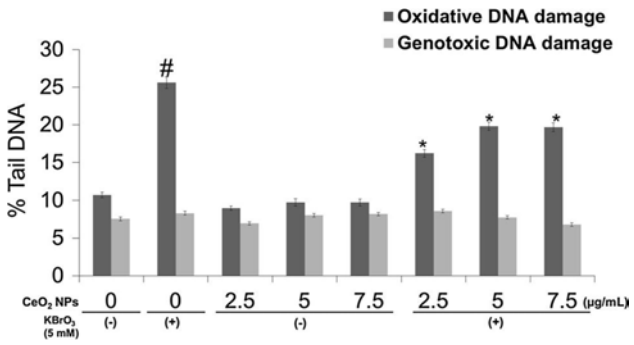

Fig. 6 Pre-treatment of BEAS-2B cells with CeO_2-NP for 24 h inhibit $KBrO_3$-induced ODD. The histogram shows a significant decrease in $KBrO_3$ (5 mM, 30 min) induced ODD due to pre-treatment with different non-toxic concentrations of CeO_2-NP for 24 h. Data represented as mean ± SEM (n = 3); one-way ANOVA for means of exposed versus control cells. #$P < 0.001$ for control versus $KBrO_3$-treated cells, *$P < 0.05$ for $KBrO_3$-treated cells versus CeO_2-NP pre-treated cells

endoplasmic reticulum as well as being abundant in the cytoplasm and the nucleus (Singh et al. 2010). Thus, it likely acts as cellular antioxidants in multiple compartments of the cell. The cytotoxicity of these nanoparticles is still controversial since although most of the studies stated no toxic effects of this nanomaterial (Xia et al. 2008; Hirst et al. 2009; Celardo et al. 2011), others indicated toxic effects mediated by ROS induction (Park et al. 2008; Kumari et al. 2014). These discrepancies may be attributed to different CeO_2-NP properties like size, crys-tal structure, or surface chemistry, although the protocol of nanomaterial dispersion can also affect the behavior of the nanoparticles (Ould-Moussa et al. 2014). Further-more, interaction between nanoparticles and proteins con-tained in cell-cultured media may also influence the uptake and consequently their biological effects (Maiorano et al. 2010). Finally, cell line characteristics such as *p53* status or tumoral origin can also influence the role of CeO_2-NP as cytotoxic (Wason et al. 2013) by accumulating hydroxyl ions over superoxide radicals in acidic pH potentiating cancer cell apoptosis, due to its valence-state oscillations (Asati et al. 2009). In this context, a recent study showed data in a tumoral lung cell line (A549) wherein apoptotic cell death via ROS-mediated DNA damage and cell cycle arrest, as well as morphological changes, were observed (Mittal and Pandey 2014). This would emphasize the importance of the cell line used to determine the toxicity of NP, including CeO_2-NP.

We have used CeO_2-NP to scavenge the enhanced ROS produced by $KBrO_3$. This chemical, considered by IARC as class II b carcinogen, passes easily into the cell thereby involving in depletion of GSH leading to oxidant damage (Crosby et al. 2000). Our results show that the levels of ROS generated by $KBrO_3$ were decreased close to the levels of untreated cells, due to 24-h pre-treatment of the cells with CeO_2-NP. The treatment of CeO_2-NP without oxidative stimulation does not produce any increase in ROS levels; by contrast, the basal intracellular levels of ROS were reduced which agrees with the possible role of CeO_2-NP to extend lifespan of cells (Strawn et al. 2006; Kong et al. 2011).

When we use the comet assay with FPG enzyme to look for possible effects arising from the quenching ROS properties of CeO_2-NP at DNA level, we detect that the oxidized purines resulting from $KBrO_3$ treatment decreased significantly when cells are pre-treated with CeO_2-NP. This result proves how efficiently the ROS-scavenging ability of the nanoparticles in cytoplasm would be counteract-ing the number of oxidant molecules that are able to reach and oxidize DNA. To our knowledge, this is the first study showing directly the connection between the cytoplasmic effects of CeO_2-NP scavenging ROS and preventing DNA from oxidative attack. Nevertheless, in most of the cases, no dose relationship was observed and the lower dose tested showing higher effect (viability, ROS scavenging, anti-genotoxicity).

Quenching ROS after an oxidative insult reduces chain reactions of self-propagating free radicals producing lipid peroxidation, DNA oxidation, and cell membrane structure

damage, thereby leading to cell death (Markovic and Trajkovic 2008; Hirst et al. 2009). It has been proposed that molecular mechanisms involved in oxidative stress follow a hierarchical expected response. Tier 1 is considered when low level of oxidative stress is induced. In this condition, more than 200 antioxidant and detoxification enzymes are activated to restore cellular redox homeostasis. At an intermediate level of oxidative stress (Tier 2), activation of MAPK and NF-κB cascades induces pro-inflammatory responses, e.g., cytokines and chemokines. Finally, at a high level of oxidative stress (established as Tier 3), perturbation of the mitochondrial permeability transition pore and disruption of electron transfer result in cellular apoptosis or necrosis (Xia et al. 2008; Li et al. 2008). The expression of two enzymes involved in tier 1 response (*Ho1* and *Sod2*) was evaluated in this study. Besides the role of *Ho1* in the catalysis of the heme ring, it is also considered to play a vital role in the maintenance of cellular homeostasis. Its induction has been extensively described after exposure to different agents causing oxidative stress such as heavy metals, endotoxin, heat shock, inflammatory cytokines, and prostaglandins among others (Choi and Alam 1996). In agreement with our results, up-regulation of the expression of *Ho1* after $KBrO_3$ exposure has also been described but using qPCR (Crosby et al. 2000; Limonciel et al. 2012), confirming again the role of this compound in the oxida-tive stress response. The statistically significant decrease in the expression of this gene after CeO_2-NP pre-treatment followed by oxidant exposure, in comparison with non-pre-treated cells, indicates how the scavenging of ROS is translated to the signaling pathways of oxidative stress. Our results show that 5 μg/mL of CeO_2-NP do not induce *Ho1* expression which differ from those reported by Eom and Choi (2009) in Beas-2B cells as they used Western blotting for demonstrating significant expression at a single dose only (1 μg/mL). This effect was directly related to the NP size (from 15 to 45 nm), and the authors proposed that this increase may be mediated through *p*38 MAP kinase. Since both dose and size are similar between studies, this dispar-ity may result from method (Western blot vs. RT-PCR) or from other unknown factors.

The increased expression of *Sod2* gene after CeO_2-NP pre-treatment agrees with the results reported by other authors (Colon et al. 2010). This would confirm that CeO_2-NP protect cells both directly by scavenging cellular ROS and indirectly by allowing cells to better respond to ROS insult (Wason and Zhao 2013). Thus, the pre-treatment with CeO_2-NP would activate an antioxidant gene pathway over-expressing *Sod2*. When the oxidant insult is produced, cells would be able to better counteract this stimulus acti-vating in turn the *Sod2* gene expression in a smoother way compared with the non-pre-treated cells.

No over-expression of the *Gstp1* was observed in our study, neither after CeO_2-NP pre-treatment nor after $KBrO_3$ stimulus. Although *Gstp1* is involved in the intermedi-ate level of oxidative stress response (Tier 2) and there are studies reporting positive induction (Limonciel et al. 2012), we fail to obtain such expression. Probably the oxi-dative insult caused was not enough to activate this tier 2 stage, and only the first level was reached or samples were obtained too soon to see it.

Finally, it should be stressed that the high scavenging efficiency of CeO_2-NP is consider to be much more effective than classical antioxidant enzymes and molecules (Colon et al. 2009, 2010). While well-known antioxidant molecules such as vitamin E, ascorbate, carotenes, melatonin, and lipoic acid present few active sites, the high ratio of surface area to volume of CeO_2-NP solves this problem and presents itself as unprecedented free radical-scaveng-ing agent (Tarnuzzer et al. 2005; Celardo et al. 2011). It has also been suggested that there is an auto-regenerative reac-tion cycle (not in the other antioxidants) occurring on the surface of CeO_2-NP due to its special structure with many oxygen vacancies allowing unique valence-state oscilla-tions, a prime factor for unparalleled antioxidant property (Tarnuzzer et al. 2005; Celardo et al. 2011).

As a summary, and according to the results obtained in this study, CeO_2-NP could be considered as a promising pharmacological compound with application in diseases caused by oxidative stresses, including those related with pulmonary system. Nevertheless, further studies showing the absence of harmful secondary effects must be carried out to confirm its therapeutic usefulness. These studies should take into account cell characteristics in the in vitro approaches and also include in vivo models.

Acknowledgments This investigation has been supported in part the Generalitat de Catalunya (CIRIT, 2014SGR-202), Barcelona (Spain). L. Rubio and L. Vila were supported by postgraduate fellow-ships from the Universidad Autònoma de Barcelona and Generalitat de Catalunya, respectively. B. Annangi was supported by a postdoc-toral fellowship from the Universitat Autònoma de Barcelona (UAB).

Conflict of interest The authors report no conflicts of interest. The authors alone are responsible for the content and writing of the paper.

References

Annangi B, Bach J, Vales G, Rubio L, Marcos R, Hernández A (2014) Long-term exposures to low doses of cobalt nanoparticles induce cell-transformation enhanced by oxidative damage. Nanotoxicol-ogy 2014:1–10. doi:10.3109/17435390.900582

Arya A, Sethy NK, Singh SK, Das M, Bhargava K (2013) Cerium oxide nanoparticles protect rodent lungs from hypobaric hypoxia-induced oxidative stress and inflammation. Int J Nanomed 8:4507–4520

Asati A, Santra S, Kaittanis C, Nath S, Perez JM (2009) Oxidase-like activity of polymer-coated cerium oxide nanoparticles. Angew Chem Int Ed Engl 48:2308–2312

Baker CH (2013) Harnessing cerium oxide nanoparticles to protect normal tissue from radiation damage. Transl Cancer Res 2:343–358

Celardo I, Pedersen JZ, Traversa E, Ghibelli L (2011) Pharmacological potential of cerium oxide nanoparticles. Nanoscale 3:1411–1420

Chen S, Hou Y, Cheng G, Zhang C, Wang S, Zhang J (2013) Cerium oxide nanoparticles protect endothelial cells from apoptosis induced by oxidative stress. Biol Trace Elem Res 154:156–166

Choi AM, Alam J (1996) Heme oxygenase-1: function, regulation, and implication of a novel stress-inducible protein in oxidant-induced lung injury. Am J Respir Cell Mol Biol 15:9–19

Colon J, Herrera L, Smith J, Patil S, Komanski C, Kupelian P, Seal S, Jenkins DW, Baker CH (2009) Protection from radiation-induced pneumonitis using cerium oxide nanoparticles. Nanomedicine 5:225–231

Colon J, Hsieh N, Ferguson A, Kupelian P, Seal S, Jenkins DW, Baker CH (2010) Cerium oxide nanoparticles protect gastrointestinal epithelium from radiation-induced damage by reduction of reac-tive oxygen species and up regulation of superoxide dismutase 2. Nanomedicine 6:698–705

Corma A, Atienzar P, García H, Chane-Ching JY (2004) Hierarchi-cally meso structured doped CeO_2 with potential for solar-cell use. Nat Mater 3:394–397

Crosby LM, Hyder KS, DeAngelo AB, Kepler TB, Gaskill B, Bena-vides GR, Yoon L, Morgan KT (2000) Morphologic analysis cor-relates with gene expression changes in cultured F344 rat meso-thelial cells. Toxicol Appl Pharmacol 169:205–221

Cross CE, Halliwell B, Borish ET, Pryor WA, Ames BN, Saul RL, McCord JM, Harman D (1987) Oxygen radicals and human dis-ease. Ann Intern Med 107:526–545

Delker D, Hatch G, Allen J, Crissman B, George M, Geter D, Kil-burn S, Moore T, Nelson G, Roop B, Slade R, Swank A, Ward W, DeAngelo A (2006) Molecular biomarkers of oxidative stress associated with bromate carcinogenicity. Toxicology 221:158–165

Eom HJ, Choi J (2009) Oxidative stress of CeO_2 nanoparticles via p38-Nrf-2 signaling pathway in human bronchial epithelial cell, Beas-2B. Toxicol Lett 187:77–83

Finkel T, Holbrook NJ (2000) Oxidants, oxidative stress and the biol-ogy of ageing. Nature 498:239–247

Fresquet F, Pourageaud F, Leblais V, Brandes RP, Savineau JP, Mar-than R, Muller B (2006) Role of reactive oxygen species and gp91phox in endothelial dysfunction of pulmonary arteries induced by chronic hypoxia. Br J Pharmacol 148:714–723

Halliwell B (2012) Free radicals and antioxidants: updating a per-sonal view. Nutr Rev 70:257–265

Health Effect Institute (HEI) (2001) Evaluation of human health risk for cerium added to diesel fuel. Comunication vol 9

Heckert EG, Karakoti AS, Seal S, Self WT (2008) The role of cerium redox state in the SOD mimetic activity of nanoceria. Biomateri-als 29:2705–2709

Hirst SM, Karakoti AS, Tyler RD, Sriranganathan N, Seal S, Reilly CM (2009) Anti-inflammatory properties of cerium oxide nano-particles. Small 5:2848–2856

Karakoti AS, Monteiro-Riviere NA, Aggarwal R, Davis JP, Narayan RJ, Self WT, McGinnis J, Seal S (2008) Nanoceria as antioxi-dant: synthesis and biomedical applications. JOM 60:33–37

Kong L, Cai X, Zhou X, Wong LL, Karakoti AS, Seal S, McGinnis JF (2011) Nanoceria extend photoreceptor cell lifespan in tubby mice by modulation of apoptosis/survival signaling pathways. Neurobiol Dis 42:514–523

Kumari M, Singh SP, Chinde S, Rahman MF, Mahboob M, Grover P (2014) Toxicity study of cerium oxide nanoparticles in human neuroblastoma cells. Int J Toxicol 33:86–97

Li N, Xia T, Nel AE (2008) The role of oxidative stress in ambient particulate matter-induced lung diseases and its implications in the toxicity of engineered nanoparticles. Free Radic Biol Med 44:1689–1699

Limonciel A, Wilmes A, Aschauer L, Radford R, Bloch KM, McMor-row T, Pfaller W, van Delft JH, Slattery C, Ryan MP, Lock EA, Jennings P (2012) Oxidative stress induced by potassium bromate exposure results in altered tight junction protein expression in renal proximal tubule cells. Arch Toxicol 86:1741–1751

Maiorano G, Sabella S, Sorce B, Brunetti V, Malvindi MA, Cingolani R, Pompa PP (2010) Effects of cell culture media on the dynamic formation of protein-nanoparticle complexes and influence on the cellular response. ACS Nano 4:7481–7491

Markovic Z, Trajkovic V (2008) Biomedical potential of the reactive oxygen species generation and quenching by fullerenes (C60). Biomaterials 29:3561–3573

Mittal S, Pandey AK (2014) Induced toxicity in human lung cells: role of ROS mediated DNA damage and apoptosis. BioMed Res Int 2014:ID891934

Mussá T, Rodríguez-Cariño C, Sánchez-Chardi A, Baratelli M, Costa-Hurtado M, Fraile L, Dominguez J, Aragon V, Montoya M (2012) Differential interactions of virulent and nonvirulent *H. parasuis* strains with naïve or swine influenza virus pre-infected dendritic cells. Vet Res 43:80

Nanogenotox (2011) http://www.nanogenotox.eu/files/PDF/Delivera-bles/nanogenotox%20deliverable%203_wp4_%20dispersion%20protocol.pdf

Narayanan KB, Park HH (2013) Pleiotropic functions of antioxidant nanoparticles for longevity and medicine. Adv Colloid Interface Sci 201–202:30–42

Niu J, Wang K, Kolattukudy PE (2011) Cerium oxide nanoparticles inhibit oxidative stress and nuclear factor-κB activation in H9c2 cardiomyocytes exposed to cigarette smoke extract. J Pharmacol Exp Ther 338:53–61

Ould-Moussa N, Safi M, Guedeau-Boudeville MA, Montero D, Con-jeaud H, Berret JF (2014) In vitro toxicity of nanoceria: effect of coating and stability in biofluids. Nanotoxicology 8:799–811

Park EJ, Choi J, Park YK, Park K (2008) Oxidative stress induced by cerium oxide nanoparticles in cultured BEAS-2B cells. Toxicol-ogy 245:90–100

Pirmohamed T, Dowding JM, Singh S, Wasserman B, Heckert E, Karakoti AS, King JE, Seal S, Self WT (2010) Nanoceria exhibit redox state-dependent catalase mimetic activity. Chem Commun (Camb) 46:2736–2738

Saeidnia S, Abdollahi M (2013) Toxicological and pharmacological concerns on oxidative stress and related diseases. Toxicol Appl Pharmacol 273:442–455

Schieber M, Chandel NS (2014) ROS function in redox signaling and oxidative stress. Curr Biol 24:R453–R462

Schubert D, Dargusch R, Raitano J, Chan SW (2006) Cerium and yttrium oxide nanoparticles are neuroprotective. Biochem Bio-phys Res Commun 342:86–91

Singh S, Kumar A, Karakoti A, Seal S, Self WT (2010) Unveiling the mechanism of uptake and sub-cellular distribution of cerium oxide nanoparticles. Mol Biosyst 6:1813–1820

Strawn ET, Cohen CA, Rzigalinski BA (2006) Cerium oxide nanopar-ticles increase lifespan and protect against free radical-mediated toxicity. FASEB 20:A1356

Suzuki H, Toyooka T, Ibuki Y (2007) Simple and easy method to evaluate uptake potential of nanoparticles in mammalian cells using a flow cytometric light scatter analysis. Environ Sci Tech-nol 41:3018–3024

Tagawa Y, Hiramatsu N, Kasai A, Hayakawa K, Okamura M, Yao J, Kitamura M (2008) Induction of apoptosis by cigarette smoke via ROS-dependent endoplasmic reticulum stress and CCAAT/ enhancer-binding protein-homologous protein (CHOP). Free Radic Biol Med 45:50–59

Tarnuzzer RW, Colon J, Patil S, Seal S (2005) Vacancy engineered ceria nanostructures for protection from radiation-induced cellu-lar damage. Nano Lett 5:2573–2577

Wason MS, Zhao J (2013) Cerium oxide nanoparticles: potential applications for cancer and other diseases. Am J Transl Res 5:126–131

Wason MS, Colon J, Das S, Seal S, Turkson J, Zhao J, Baker CH (2013) Sensitization of pancreatic cancer cells to radiation by cerium oxide nanoparticle-induced ROS production. Nanomedicine 9:558–569

Xia T, Kovochich M, Liong M, Mädler L, Gilbert B, Shi H, Yeh JI, Zink JI, Nel AE (2008) Comparison of the mechanism of toxicity of zinc oxide and cerium oxide nanoparticles based on dissolu-tion and oxidative stress properties. ACS Nano 2:2121–2134

Zheng X, Zhang X, Wang X, Wang S, Wu S (2005) Preparation and characterization of CuO/CeO_2 catalysts and their applications in low-temperature CO oxidation. Appl Catal A 295:142–149

Zholobak NM, Ivanov VK, Shcherbakov AB, Shaporev AS, Polezhaeva OS, Baranchikov AY, Spivak NY, Tretyakov YD (2011) UV-shielding property, photocatalytic activity and photocytotoxicity of ceria colloid solutions. J Photochem Photobiol B 102:32–38

Annex 1 (Study 2)

Antioxidant potential of nanoceria in tumoral and transformed cells

Submitted manuscript

3.2. Abstract of second study (Annex 1)

Antioxidant potential of nanoceria in tumoral and transformed cells

Despite the antioxidant nature already showed by nanoceria in different biological models, the intrinsic physico-chemical properties of this NM would make oxidative behavior feasible to occur. Thus, several factors have been proposed to explain the oxidative *in vivo* and *in vitro* effects shown by different groups. Among them, the pH has been one of the best factors studied. Thereby, although controversy exists regarding this aspect, some studies point out that in neutral environments nanoceria would act as an antioxidant while acidic environments would drive to pro-oxidant activity of nanoceria. As an extension of this hypothesis, nanoceria could be considered as an anticancer agent. Thus, cancer cells presenting an acidic microenvironment due to the Warburg effect would be damaged by nanoceria, whilst normal cells would be protected by its radical scavenging properties.

As contradictory results have been obtained regarding this point, the current situation challenges the use of nanoceria in the treatment of different oxidant diseases, including cancer. This is the reason why this work aims to study the relevance of cell type (tumoral *vs* non-tumoral) in the antioxidant nanoceria capacity. Thus, we have determined the ability of nanoceria to reduce the intracellular levels of ROS generated by cisplatin in five different human tumoral cells (A549, HCT116, Hep3B, Caco-2 and HeLa). Additionally, different tumoral conditions were forced in our models in order to deeper study the possible oxidant effect of nanoceria. Thus, using A549 cell line, a decrease of intracellular pH was forced by starving conditions (absence of serum in cell medium) and the use of 2-(N-morpholino) ethanesulfonic acid (MES) buffer. Finally, since the genetic background of cancer and normal cells studied so far differ considerably and may influence the final outcome, a normal mouse embryonic fibroblast cell line (MEF) and its arsenic-transformed isogenic counterpart (AsT-MEF) were also evaluated.

Results indicate that treatment with nanoceria was able to reduce the levels of cisplatin-induced intracellular ROS in practically all cell lines, being most of the changes significant. Although the extent of protection was different in each model, nanoceria behave generally as a ROS scavenger. The growth of A549 cell line in a forced acidic environment showed that the antioxidant properties of nanoceria were neither influenced by cell culture pH. Regarding the use of transformed and non-transformed isogenic cell lines, nanoceria elicited an antioxidant effect in both MEF and AsT-MEF as in the other cases.

Although the hypothesis of achieving differential cytotoxicity between tumoral and stromal cells is considered as one of the greatest challenges in chemotherapy, from our results we can conclude that the antioxidant properties of nanoceria are not affected by the tumoral condition in the tested cell lines. Therefore, the tumoral state of the cells is not a general argument to explain the non-protective role of nanoceria reported by different authors.

Annex 2 (Study 3)

Nanoceria do not protect lung epithelial cells from the transforming effects of tobacco long-term exposure

Submitted manuscript

3.3. Abstract of the third study (Annex 2)

Nanoceria do not protect lung epithelial cells from the transforming effects of tobacco long-term exposure

Nanoceria have been proposed as a new promising agent in the treatment of oxidant diseases based on several studies showing antioxidant properties. Conversely, other groups presented nanoceria as an oxidant compound affecting cellular functions in *in vitro* and *in vivo* models. This controversial information and the gaps found in nanoceria research make further studies highly required.

Among the existing gaps in nanoceria research, long-term exposures scenarios constitute an important area on the toxicological assessment of this NM, since chronic exposure is likely to occur in occupational and daily situations. Additionally, plausible nanoceria co-exposures are also relevant to study, since interactions with common environmental agents could influence the effects of this catalyst. Thus, this work aims to evaluate toxicological and carcinogenic potential of a long-term low-dose of nanoceria exposure in lung epithelial BEAS-2B cells, along with the effects associated to a common plausible tobacco co-exposure.

Lung epithelial BEAS-2B cells continuously exposed to 2.5 µg/mL of nanoceria, 1 and 5 µg/mL of tobacco smoke condensate (CSC), alone or in combination with nanoceria for up to 6 weeks, were monitored for the acquisition of an oncogenic phenotype. For characterizing this process, the *in vitro* cell transformation status was assessed through different carcinogenic markers such as cell morphology, proliferation rate, gene differentiation status, migration capacity, anchorage-independent cell growth and secretome analysis, including levels of metalloproteinase-9 (MMP-9), and cell growth promoting capability. In addition, being *FRA-1* and *PTEN* pivotal genes during respiratory epithelium carcinogenesis, its mRNA expression levels were used to determine their role in cell transformation.

Results evidenced no transforming ability of nanoceria in BEAS-2B cell line. However, results support a synergistic role on CSC transforming ability, as cells co-exposed to nanoceria-plus-CSC, when compared to cells exposed to CSC alone, showed a more noticeable spindle-like phenotype, an increased proliferation rate, higher degree of differentiation status dysregulation regarding EMT, higher migration capacity, increased anchorage-independent cell growth and a secretome with higher levels of MMP-9 and cell growth promoting capability, indicating potential tumor-stroma interactions. When mRNA expression of FRA-1 and *PTEN* was evaluated as a mechanism of tobacco-

induced transformation, nanoceria co-exposure was again found to exacerbate the observed expression changes.

According to the results obtained in this study, despite nanoceria did not show carcinogenic effects by itself, long-term nanoceria exposure cannot be considered safe as it may increase the oncogenic potential of other common environmental agents. Therefore, more attention needs to be paid to long-term approaches prior to an eventual application of nanoceria in biomedicine, as previously proposed.

Article 2 (Study 4)

Frozen dispersions of nanomaterials are a useful operational procedure in nanotoxicology

Nanotoxicology

doi: 10.1080/17435390.2016.1262918

Impact factor: 7.913

3.4. Abstract of the forth study (Article 2)

Frozen dispersions of nanomaterials are a useful operational procedure in nanotoxicology

NP treatments require accurate dispersion methodologies which imply high energy delivery to the sample. Small variability in the energy supplyed to nanoparticles in every process of dispersion is likely to occur and could lead to differences in physico-chemical properties between samples. Consequently, changes in some of these properties could affect how NPs interact with cellular models. Thus, variability in NP dispersions can affect the reliability of the results obtained in short-term exposure tests, and mainly in long-term experiments where several rounds of dispersion are required.

In order to overcome the limitations already mentioned, we propose to aliquot and freeze NMs stock dispersions. Thus, this work aims to compare fresh-prepared and frozen dispersion using five different model NMs dispersions (MWCNT, ZnO-, Ag-, TiO_2- and CeO_2-NP), as models. NP characterization was performed by the determination of primary size, morphology, hydrodynamic size, zeta potential and ion release. Biological endpoints were performed using BEAS-2B cell line. Thereby, viability, cellular uptake and induced ROS production was also assessed.

The obtained results show no significant differences between frozen and fresh NPs in their physico-chemical characteristics or their biological effects. Thus, regarding primary properties similarities were observed between freshly and frozen samples in regard to appearance, mean size or size distribution. The hydrodynamic behaviour directly linked with the size of formed aggregates showed increase of size in comparison with primary dimensions, but without significant differences between fresh and frozen samples. As anticipated, the obtained data revealed no significant differences in cell internalization when measured directly by TEM and confocal microscopy or indirectly by flow cytometry (FACS). Regarding viability, four out of the total five chosen NMs produced toxic effects in BEAS-2B. Following the trend observed in the rest of end-points studied, no differences in toxicity between fresh prepared dispersions and frozen dispersions were distinguished. Finally, ion release measured by inductively coupled plasma mass spectrometry (ICP-MS) showed some disparities between protocols. Among the four metallic NMs studied, high dissolution was observed in ZnO-NP and Ag-NP where no differences were obtained regarding the freezing protocol. However, significant variations were observed for those NPs with a poor dissolution rate (TiO_2-NP and CeO_2-NP) being the small obtained values and not the protocol the probable cause of such variability. In general, we consider that no

biological differences exist between the two methodology protocols regarding this endpoint.

This study is the first to demonstrate that there is no scientific evidence to dismiss the use of frozen NP dispersions, opening the door to the development of short and long-term experiments with higher consistency, accuracy and reproducibility in a much shorter time and using a simplified procedure.

NANOTOXICOLOGY, 2016
http://dx.doi.org/10.1080/17435390.2016.1262918

ORIGINAL ARTICLE

Frozen dispersions of nanomaterials are a useful operational procedure in nanotoxicology

Laura Vila[a] , Laura Rubio[a] , Balasubramanyam Annangi[a], Alba Garcıa-Rodrıguez[a], Ricard Marcos[a,b] and Alba Hernandez[a,b]

[a]Grup de Mutagenesi, Departament de Genetica i de Microbiologia, Facultat de Biociencies, Universitat Autonoma de Barcelona, Bellaterra, Spain; [b]CIBER Epidemiologıa y Salud Publica, ISCIII, Madrid, Spain

ABSTRACT

The variability observed in nanoparticle (NP) dispersions can affect the reliability of the results obtained in short-term tests, and mainly in long-term experiments. In addition, obtaining a good dispersion is time-consuming and acts as a bottleneck in the development of high-throughput screening methodologies. The freezing of different aliquots from a stock dispersion would overcome such limitations, but no studies have explored the impact of freezing thawing the samples on the physico-chemical and biological proper-ties of the nanomaterial (NM). This work aims to compare fresh-prepared and frozen MWCNT, ZnO-, Ag-, TiO_2- and CeO_2-NP dispersions, used as models. NP characterization (size and morphology by TEM), hydro-dynamic size and zeta potential were performed. Viability comparisons were determined in BEAS-2B cells. Cellular NP uptake and induced ROS production was assessed by TEM and flow cytometry, respectively. The obtained results show no important differences between frozen and fresh NP in their physicochemical characteristics or their biological effects. This study is the first to demonstrate that there is no scien-tific evidence to dismiss the use of frozen NP, opening the door to the development of short- and long-term experiments with higher consistency, accuracy and reproducibility in a much shorter time and using a simplified procedure.

ARTICLE HISTORY
Received 10 November 2015
Revised 28 September 2016
Accepted 20 October 2016

KEYWORDS
Fresh and frozen nanomaterials; biological properties; Ag-NP; MWCNT; ZnO-NP; TiO_2-NP; CeO_2-NP; BEAS-2B

Introduction

Nanotechnology is a relatively new area of materials science and engineering with an increasing number of applications due to its enormous potential benefits. The interest of nanomaterials (NMs) arises from the fact that their physico-chemical properties, such as mechanical, chemical, electrical, optical, magnetic, electro-optical and magneto-optical can be completely different from those of their bulk counterparts. These differences are due to their size in the range of the nanoscale (Steigerwald & Brus, 1990; Wang, 1991; Weller, 1993), and confer to the NM unique physico-chemical properties that make them interesting and desirable for industrial applications like electronics, biomedicine, cosmetics and food packaging (Epstein, 2011; Liu & Gu, 2009; Yang et al., 2009; Yen et al., 2011).

The rapid development of NM industry and the exponential production of NM of different nature have raised serious concerns about their potentially harmful effects in human health (Park & Grassian, 2010; Schmid & Riediker, 2008). In this context, different in vitro and in vivo studies have been performed in order to deter-mine the potential toxicity of NM in different biological scenarios (Brunner et al., 2006; Duffin et al., 2007). However, literature shows considerable disparities in the biological effects observed by dif-ferent laboratories. An important part of these differences can be attributed to differences in how the NM dispersions were pre-pared (Cho et al., 2011; Cohen et al., 2013). Although the mecha-nisms through which NM could interact with the cell components are not completely elucidated (Oberdorster et al., 2007), recent studies have observed that NM are able to produce several effects by different mechanisms depending on their physico-chemical characteristics – size, shape, surface area, chemical composition, solubility, surface charge, agglomeration/aggregation and/or crys-tal structure (Bai et al., 2010; Cho et al., 2010; Kermanizadeh et al., 2012; McGuinnes et al., 2011; Pujalte et al., 2011; Xu et al., 2010). Regarding in vitro studies, the dispersion of the NM is a determin-ant factor for their toxicological properties (Jiang et al., 2009; Murdock et al., 2008; Park et al., 2009; Roco et al., 2011). As small variations between dispersions may occur, an exhaustive charac-terization of the dispersion products is mandatory prior to each new experiment, and the resulting dispersion needs to be imme-diately used to avoid agglomeration/aggregation and precipitation (Stone et al., 2010). Despite of this, intrinsic variability between dispersion processes occurs both between and within laboratories. At this point, it should be pointed out that agglomeration, aggregation and precipitation occurs in real exposure scenarios.

Most of the in vitro studies addressed to assess the toxic and genotoxic effects of NM involve acute treatments with high doses of the compound (Chan et al., 2011). However, long-term expos-ure treatments with low doses are a more realistic approach in terms of human exposure, more if the carcinogenic potential of NM wants to be assessed (Annangi et al., 2015). The variability of every process of dispersion is of especial concern in this type of long-term experimental designs as the

CONTACT Ricard Marcos. ricard.marcos@uab.es. Grup de Mutagenesi, Departament de Genetica i de Microbiologia, Facultat de Biociencies, Universitat Autonoma de Barcelona, Bellaterra 08193, Cerdanyola del Valles (Barcelona), Spain; Alba Hernandez alba.hernandez@uab.es Grup de Mutagenesi, Departament de Genetica i de Microbiologia, Facultat de Biociencies, Universitat Autonoma de Barcelona, Bellaterra 08193, Cerdanyola del Valles (Barcelona), Spain Both persons contributed equally to the work.

NM-containing culture media needs to be changed every 2–3 days during weeks or months of continuous exposure. Thus, the slight variations between samples can generate substantial variations at the end of the exposure.

The rapid and constant production of new NM urges for the development of high-throughput screening methodologies. Those NM suspected to be more dangerous require priority for careful toxicological analysis. In this case, never mind the speed of the assay, the tedious preparation of fresh dispersions acts as a bottle-neck and prevents researchers from the application of these high-throughput methodologies.

In order to avoid the above-mentioned limitations, we propose to aliquot the NM stock dispersion, then freezing it immediately in liquid nitrogen and store it at 80 C until use. With this procedure, all the subsequent experiments would be performed with the exact same dispersion characteristics and, therefore, with the same NM biological properties. To test the adequateness of the procedure, in this study we analyzed some biological and physico-chemical properties of frozen NM and compared them with those of fresh samples to detect potential variations. Five NM have been selected as models, TiO_2-NP, ZnO-NP, CeO_2-NP, Ag-NP and MWCNT due to their extended use and large amount of collected information. Different endpoints were analyzed before and after the freezing procedure, such as NM characterization – dry size, size in dispersion and zeta potential – cell viability, induced react-ive oxygen species (ROS) production and NM cell internalization.

Material and methods

Nanomaterial dispersion and freezing

TiO_2-NP (NM102), Ag-NP (NM300K) and MWCNT (NM401) were obtained from the Joint Research Center (Ispra, Italy). ZnO-NP and CeO_2-NP were purchased from Sigma Chemical Co. (St. Louis, MO). For dispersion NMs were pre-wetted in 0.5% absolute ethanol and afterwards dispersed in 0.05% bovine serum albumin (BSA) in MilliQ water. The NMs in the dispersion medium were sonicated for 16 min to obtain a stock dispersion of 2.56 mg/mL according to the Nanogenotox protocol (Nanogenotox, 2011). Once soni-cated, part of the stock was used for the fresh measurements and the rest was immediately aliquoted, frozen in liquid nitrogen and stored at 80 C for at least one week before its use. In all cases, frozen NMs were thawed rapidly in a hot water bath prior to use.

Nanomaterials characterization

TiO_2-NP (NM102) is in anatase phase and the reported primary particle size was 21.7 ± 0.6 nm. ZnO-NP was reported as showing primary particle size less than 100 nm, whereas CeO_2-NP size was indicated as lower than 25 nm. The majority of the particles of Ag-NP (300K) presented a round shape and a typical particle size of around 20 nm. MWCNT (NM401) showed heterogeneous in nature, with rod-like shape in some cases (mostly straight or curved) and rounded or needle-like shape ends in other cases. The thickness of nanotubes was 67 ± 24 nm, and its length was 4048 ± 2371 nm. Except for CeO_2-NP and ZnO-NP purchased by Sigma Chemical Co. (St. Louis, MO), the rest of NMs were obtained and character-ized inside the European NanoReg project framework (http://www.nanoreg-materials.eu/Documentation/). For further character-ization, transmission electron microscopy (TEM) was utilized to obtain the nanoparticle (NP) size and their morphology on a JEOL JEM-2011 instrument (Tokyo, Japan). TEM sizes were calculated by measuring over 100 particles in random fields of view. Furthermore, characterization of the hydrodynamic size and zeta potential of NP by dynamic light scattering (DLS) and laser Doppler velocimetry (LDV) methodologies, respectively, was per-formed on a Malvern ZetasizerNano-ZS zen3600 instrument (Malvern, UK). The dispersions of NP used for these measures were prepared as indicated in the previous section.

All the measurements were performed in the two selected experimental conditions, one being just after dispersion (fresh) and the other after its freezing at 80 C for at least one week (frozen).

Cell culture

BEAS-2B cells were kindly provided by Dr. H. Norppa, from the Finnish Institute of Occupational Health. They were grown as a monolayer in 75 cm^2 culture flasks with DMEM High Glucose medium (Life Technologies, NY) supplemented with 10% fetal bovine serum (FBS), 1% of non-essential amino acids (NEAA) (PAA Laboratories GmbH, Pashing, Austria) and 2.5 mg/mL plasmocin (InvivoGen, San Diego, CA). Cells were maintained in a humidified atmosphere of 5% CO_2 and 95% air at 37 C. BEAS-2B cells were exposed to different concentrations of the five selected NMs – TiO_2-NP, ZnO-NP, CeO_2-NP, Ag-NP and MWCNT – for 24 h and then cells were collected to determine the different NP-induced biological effects.

Cell viability

Cell viability was determined by the Beckman counter method with a ZTM Series coulter-counter (Beckman coulter Inc., CA). About 1.5 10^5 BEAS-2B cells were plated in 6-well plates in tripli-cate and incubated overnight. Cells were then treated for 24 h with different doses of the five NM ranging from 10 to 300 lg/mL, depending on the NM. The IC_{50}, defined as the concentration of NM that reduces the cell viability by 50%, was calculated from averaging three independent survival curves.

Transmission electron microscopy

BEAS-2B cells were seeded in 6-well plates at a density of 1.75 10^5 cells/well. Cells were treated for 24 h with different concentration of NM (TiO_2-NP and CeO_2-NP: 10 and 100 lg/mL; ZnO-NP 10 and 20 lg/mL; Ag-NP: 1 and 5 lg/mL; MWCNT: 20 and 100 lg/mL). BEAS-2B cells were fixed in 2.5% (v/v) glutaraldehyde (EM grade, Merck, Darmstadt, Germany) and 2% (w/v) paraformal-dehyde (EMS, Hatfield, PA) in 0.1 M cacodylate buffer (PB, Sigma-Aldrich, Steinheim, Germany), pH 7.4 and processed following con-ventional procedures as previously described (Annangi et al., 2015). Samples were first post-fixed with osmium, dehydrated in acetone, later embedded in Epon, and finally polymerized at 60 C and cut with an ultramicrotome. Ultrathin sections were placed in copper grids and contrasted with uranyl acetate and Reynolds lead citrate solutions and then observed using a Jeol 1400 (Jeol LTD, Tokyo, Japan) TEM equipped with a CCD GATAN ES1000W Erlangshen camera.

Confocal microscopy

BEAS-2B cells were seeded in 35 mm petri dishes, 14 mm Microwell (MatTek Corporation, Ashland, MA) at a density of 1.5 10^5 cells/well. Cells were treated for 24 h with 10 lg/mL of Ag-NP. After, BEAS-2B cells were incubated with Cell Mask (Life Technologies, NY) – for cytoplasmic membrane staining – and Hoechst 33342 – for nucleus staining – at a concentration of 1/ 500 for 10 min. Cells were then immediately observed by confocal

microscopy Leica TCS SP5 with an objective of HC PLAPO Lambda blue 63x 1.40 oil UV. Ag-NPs were observed by reflection using an excitation wavelength of 488 nm and an emission wavelength of 480–495 nm. For image processing, Huygens essen-tial 4.4.0p6 (Scientific volume imaging, Netherlands) and Imaris 7.2.1 (Bitplane, AG) were used.

Cellular uptake and intracellular ROS production detected by FACS

Intracellular ROS production was assessed by flow cytometry (FC) using 6-carboxy-2,7^0-dichlorodihydro-fluorescein diacetate (DCFH-DA) staining. BEAS-2B cells were seeded in triplicate in 6-well plates at a density of 1.75 10^5 cells/well. Cells were treated for 24 h with different concentrations of NM (TiO_2-NP, CeO_2-NP and MWCNT: 0, 10, 50 and 100 lg/mL; ZnO-NP: 0, 10, 20 and 30 lg/ mL; Ag-NP: 0, 1, 5 and 10 lg/mL). After treatments, cells were washed twice with PBS and incubated in 5 lM DCFH-DA in serum-free DMEM medium for 30 min at 37 C. Potassium bromate ($KBrO_3$, 5 mM) was used as positive control and was added 15 min before trypsinization and collection of the cells. The conversion of non-fluorescent DCFH-DA to DCF by action of cellular esterases and its posterior oxidation to its fluorescent form by the presence of intracellular ROS was measured by fluorescence-activated cell sorting (FACS Calibur) as mean of fluorescence intensity. Data was analyzed with Flowjo.
FACS methodology also permits to determine the uptake of NP by the BEAS-2B cells. This is obtained by measuring the scattering of the laser light after interacting with the cell (complexity) (Suzuki et al., 2007). The percentage of fluorescent cells over the horizontal line marked by the controls gives us the value of internalization.

Quantification of the ions release using ICP-MS

Dissolution to the ionic form of freshly sonicated and 80 C frozen TiO_2-NP, ZnO-NP, Ag-NP and CeO_2-NP in DMEM þ 10% FBS medium was evaluated at different time intervals using ICP-MS. Initial concentration of 10 lg/mL TiO_2-NP, ZnO-NP, Ag-NP and CeO_2-NP of freshly prepared and frozen samples were dispersed in DMEM þ 10% FBS for 24, 48, 72 and 96 h. Subsequently, the supernatant from the respective samples was collected and ultra-centrifuged for 10 min at 10 000g to precipitate undissolved NP. After centrifugation, 0.25 mL of the resultant supernatant contain-ing Zn, Ce and Ag ions were carefully transferred to a new vial and digested with concentrated nitric acid (HNO_3; Merck) at 150 C for 30 min on a heating block. For Ti ions analysis, 0.5 mL of the resultant supernatant was digested with HNO_3 and hydro-fluoric acid (HF) under similar conditions. Digested samples were further diluted in 1% HNO_3 for quantitative analysis of Ti, Zn and Ce ions using ICP-MS. The quantity of released ions from freshly prepared and 80 C frozen NP (lg/mL) at different time intervals were determined by averaging at least three independent experiments.

Results and discussion

Nanoparticles characterization

In nanotoxicological studies, it is important to have control of the dispersion characteristics when NP are administered to cultured cells (Johnston et al., 2013). In our case, we have used the dispersion protocol generated in the frame of the Nanogenotox EU project (Nanogenotox, 2011). Results are indicated in Figure 1, where

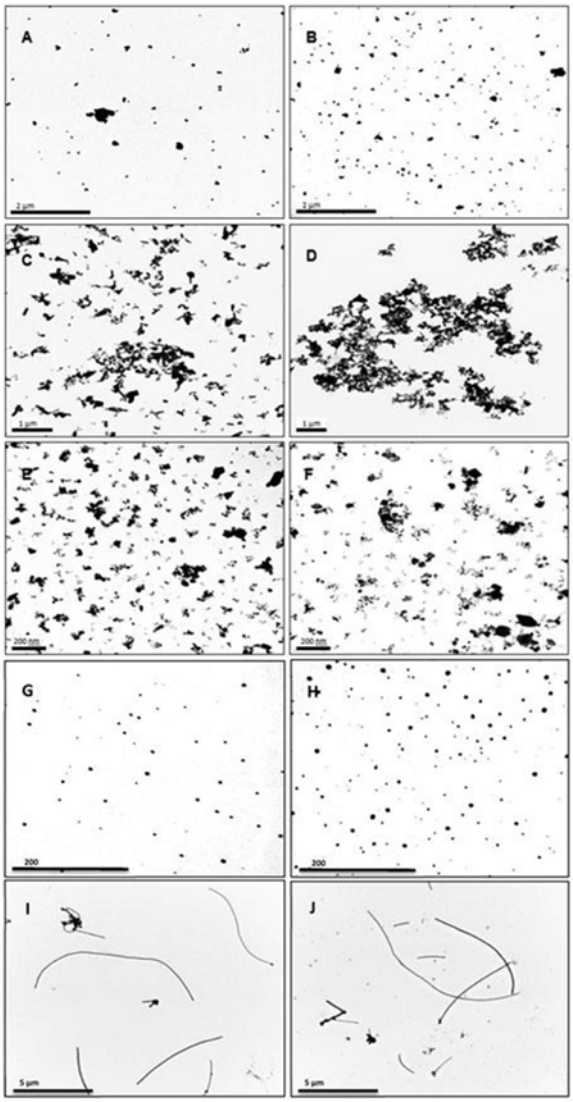

Figure 1. TEM images of TiO_2-NP (A, B), ZnO-NP (C, D), CeO_2-NP (E, F), Ag-NP (G, H) and MWCNT (I, J) in dried form. The left side (A, C, E, G and I) corresponds to the freshly prepared dispersions and the right side (B, D, F, H and J) to the thawed dispersions from frozen samples.

we show representative TEM images of TiO_2-NP, ZnO-NP, CeO_2-NP, Ag-NP and MWCNT. The mean sizes of NP and its size distri-bution obtained from TEM images are shown in Table 1 and Figure 2, respectively. These results show small differences between freshly and frozen samples regarding appearance, mean size or size distribution without any difference associated to the preparation method.

The values of hydrodynamic radius and zeta potential for fresh and frozen NP dispersions are also indicated in Table 1. These results obtained by DLS showed some aggregation or agglomer-ation of NPs in water suspension but without significant differen-ces between fresh and frozen samples. The differences in size observed between TEM and DLS are due to the fact that TEM selects isolated NP only, while the hydrodynamic size measured by DLS does not discriminate isolated NP from aggregates. In add-ition, DLS measurements also include the influence of the surfac-tant layer around the NP.

From the results reported above we conclude that the values observed between frozen dispersions do not differ from those

Table 1. NPs average size (by TEM and DLS) and charge by pre-wetting with 0.5% volume and steric stabilization using sterile-filtered 0.05% w/v BSA. Data repre-sented as mean ± SD.

	TEM	DLS		LDV	
NP	Mean sizes (nm)	Average diameter (nm)	PDI	Zeta potential, f (mV)	Electrophoretic mobility (lm cm V ^{1} s ^{1})
TiO_2-NP fresh	20.01 ± 0.75	575.9 ± 8.0	0.471 ± 0.021	19.5 ± 0.5	1.53 ± 0.04
TiO_2-NP 80 C	22.36 ± 0.94	612.4 ± 44.8	0.403 ± 0.041	25.4 ± 0.1	1.99 ± 0.07
ZnO-NP fresh	91.94 ± 4.89	241.2 ± 3.2	0.150 ± 0.031	22.4 ± 0.5	1.76 ± 0.04
ZnO-NP 80 C	81.58 ± 5.17	297.4 ± 8.3	0.175 ± 0.013	23.6 ± 0.7	1.85 ± 0.05
CeO_2-NP fresh	9.57 ± 0.67	163.6 ± 16.3	0.471 ± 0.021	28.5 ± 0.2	2.23 ± 0.01
CeO_2-NP 80 C	8.87 ± 0.61	154.6 ± 13.	0 0.471 ± 0.021	19.5 ± 1.2	1.53 ± 0.09
Ag-NP fresh	7.74 ± 2.48	80.81 ± 3.4	0.369 ± 0.054	6.84 ± 0.2	0.54 ± 0.01
Ag-NP 80 C	8.52 ± 1.82	83.52 ± 0.7	0.302 ± 0.003	12.4 ± 0.9	0.97 ± 0.07
MWCNT fresh	6.01 ± 4.09 lm	937 ± 19.2	0.263 ± 0.025	18.4 ± 3.4	1.46 ± 0.27
MWCNT 80 C	5.89 ± 4.63 lm	899 ± 2.7	0.237 ± 0.019	22.8 ± 0.8	1.78 ± 0.06

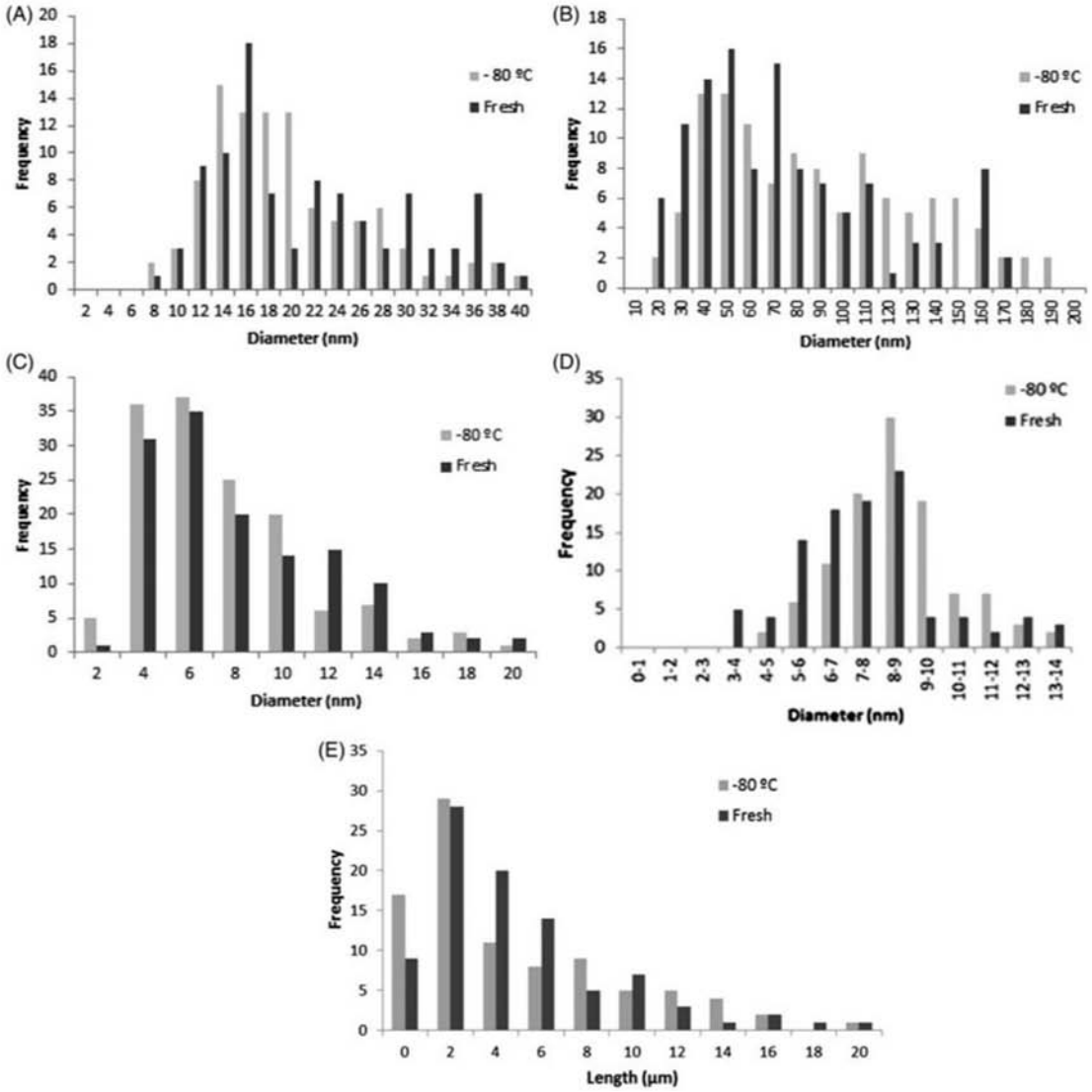

Figure 2. Size distribution of TiO_2-NP (A), ZnO-NP (B), CeO_2-NP (C), Ag-NP (D) and MWCNT (E) over 100 randomly selected particles for both the freshly prepared and the thawed dispersions from frozen samples.

observed for the fresh samples. This indicates that the main parameters used for NP characterization are not affected by the freezing protocol. NMs dispersion is an important step previous to their use. More than to avoid agglomerations the finality of this step is to provide a standardized method to be routinarily used when evaluating NP effects. Indeed, the UE project Nanogenotox dismissed the use of specific dispersion protocols due to the large differences and heterogeneity existing between NPs, and pro-posed a common standardized protocol that to be used for any kind of NP. The advantages of this method have promoted its use in a posterior UE project involved in regulatory aspects (NanoReg). Agglomeration size is an important factor modulating cell uptake

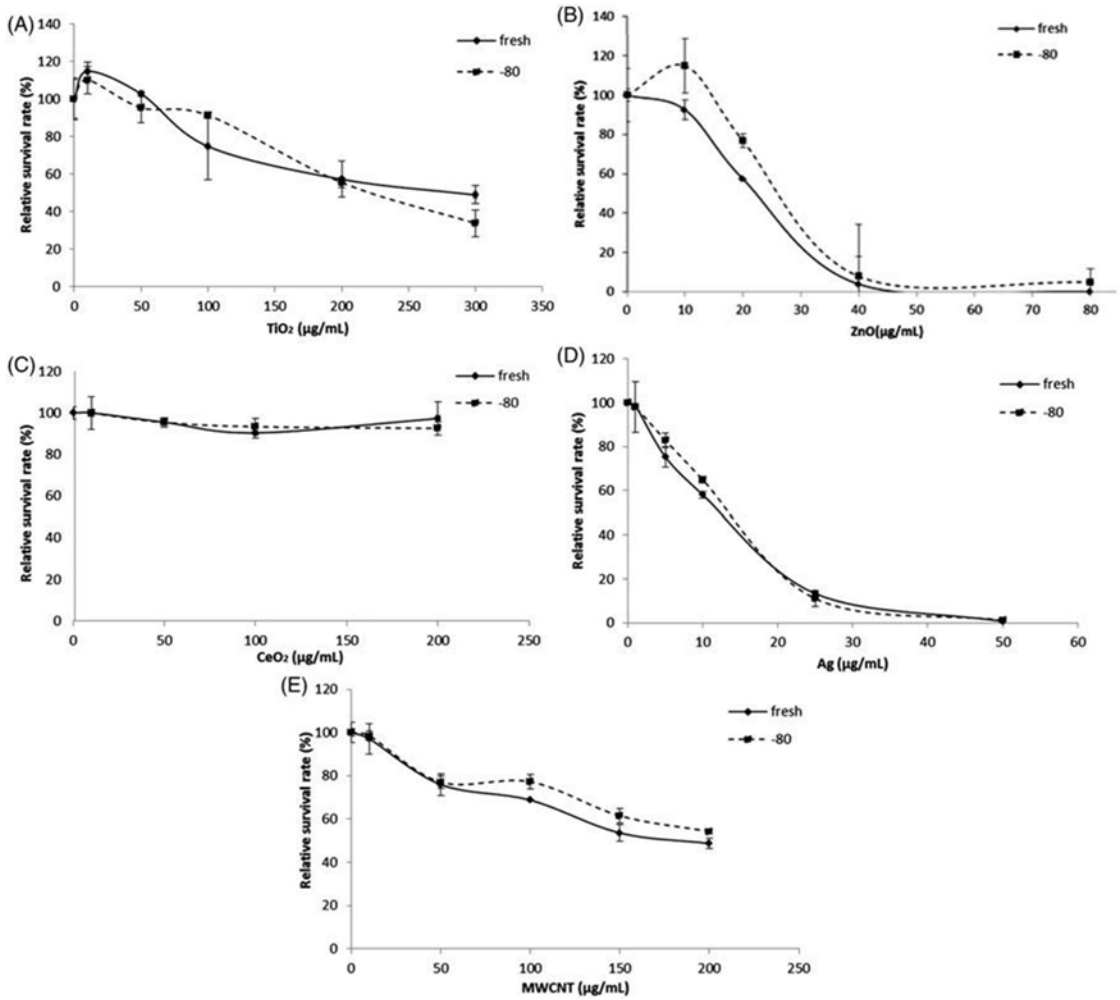

Figure 3. Cell viability of BEAS-2B cells treated with various concentrations of TiO_2-NP (A), ZnO-NP (B), CeO_2-NP (C), Ag-NP (D) and MWCNT (E) for 24 h. Data are pre-sented as percentage of viable cells with respect to controls. Data represented as mean ± SEM (n ¼ 3); $p < 0.05$, $p < 0.01$ and $p < 0.001$.

during the treatment period and, consequently, it can affect the NP-associated effects. Therefore, cell agglomeration needs to be considered when performing in vitro or in vivo studies (Bruinink et al., 2015). Our findings indicate that this important parameter is not affected by the followed experimental procedure. Nevertheless, other variables can influence cell uptake, such as the sedimentation and diffusion velocities. These parameters have been found to influence the intake of gold NPs, where higher sedimentation rates were found to result in higher cell uptake (Cho et al., 2011). In addition, particle kinetics and property trans-formations in physiological fluids can have important implications for in vitro dosimetry, which may explain some of the differences found between studies (Cohen et al., 2013).

Cell viability

Cell viability is a basic parameter to be included in any study determining the biological effects of NMs. There are different approaches to detect changes in cell viability, but many of them use reagents or reporter dyes that can potentially interfere with the NP of study. In fact, this type of interaction has been reported for different NMs (Kroll et al., 2012; Monteiro-Riviere et al., 2009). Also, the use of methods based in optical detection are not recommended here due to its known modulation by NP as it has been reported using 24 well-characterized NP (Kroll et al., 2012). To avoid this problem, we have determined cell viability by dir-ectly counting the number of living cells after different exposures.

Cell viability of BEAS-2B cells treated with several concentrations of fresh and 80 C frozen TiO_2-NP, ZnO-NP, CeO_2-NP, Ag-NP and MWCNT is shown in Figure 3. As indicated, after 24 h of TiO_2-NP exposure the IC_{50} found in BEAS-2B was 258.84 lg/mL for fresh NP and 235.73 lg/mL for frozen NP. The IC_{50} for ZnO-NP was 22.80 lg/mL for fresh NP and 24.11 lg/mL for frozen NP. The IC_{50} for Ag-NP was 11.88 lg/mL for fresh NP and 12.59 lg/mL for frozen NP. The IC_{50} for MWCNT was 225.71 lg/mL for fresh NP and 179.66 lg/mL for frozen NP. The exposure of BEAS-2B cells with CeO_2-NP showed no toxicity at neither of the tested concen-trations. The obtained data revealed no differences in toxicity between fresh prepared dispersions and frozen dispersions. Besides, our cell counter method has shown to be useful to test the potential toxic effects of different NMs (Annangi et al., 2015; Vales et al., 2015).

Since toxicity of NMs is associated to many of their physico-chemical properties (Oberdorster et al., 2005), it is not surprising that we did not find differences in toxicity between the two dis-persion protocols as no important differences were observed in the dispersion characteristics.

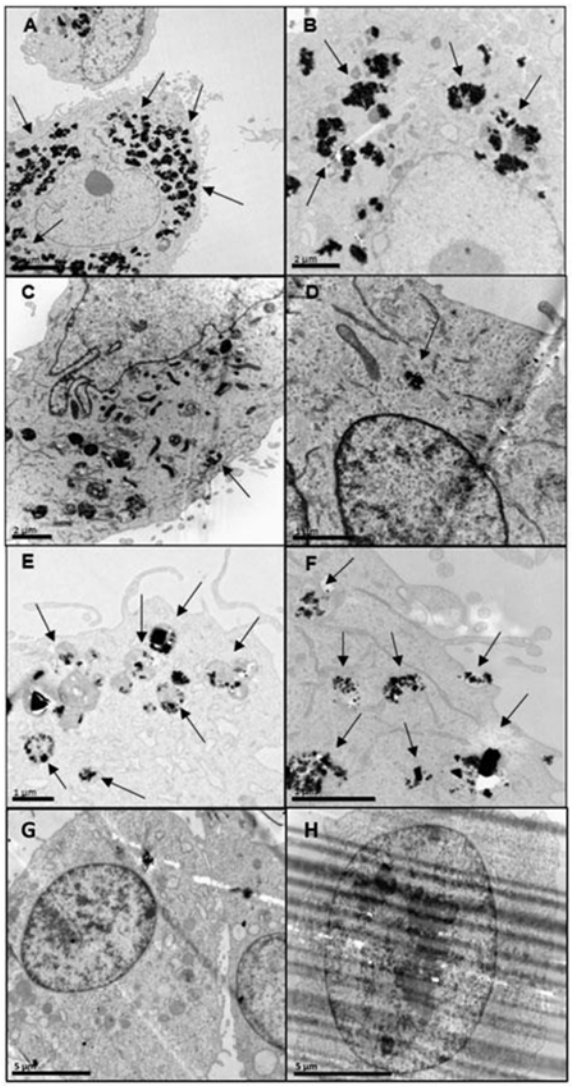

Figure 4. TEM images from BEAS-2B cells treated with fresh (left panel) or frozen (right panel), 100 lg/mL of TiO_2-NP (A, B), 20 lg/mL of ZnO-NP (C, D), 100 lg/mL of CeO_2-NP (E, F) and 100 lg/mL of MWCNT (G, H). Images show the NP cellular uptake after 24 h of treatment. Nano-agglomerates in vacuoles are observed. Arrows indicate some nanoparticles or nano-agglomerates. No uptake was observed for MWCNT.

Transmission electron microscopy

TEM analysis of cells exposed for 24 h at different doses of TiO_2-NP, ZnO-NP, CeO_2-NP and MWCNT were performed in order to confirm the uptake ability by BEAS-2B cells, as well as to detect possible differences of fresh and frozen NP. As observed in Figure 4, TEM images showed the internalization of TiO_2-NP, ZnO-NP and CeO_2-NP. ZnO-NP uptake was significantly lower than the uptake of TiO_2-NP and CeO_2-NP. We checked 10 cell images in each case to detect the presence/absence of NP. According to the observed, we classified the case as a high, medium or low uptake. From this point of view, this is a qualitative approach more than a quantitative one. No differences in uptake were observed between fresh and frozen samples. In addition, a dose-dependent cellular uptake was observed in BEAS-2B cells for the three types of NP, and they were mainly confined into vacuoles as nano-agglomerates. No cel-lular uptake was observed for MWCNT. As a conclusion, no quali-tative differences in cellular uptake were observed when fresh NPs were compared with their frozen-matched samples after analyzing 10 cells per case. There are different mechanisms of cell internal-ization according to the size of the NPs. Small NP can enter by dif-fusion, and medium sized NPs are internalized by endocytosis (Bruinink et al., 2015). Other characteristics of NP, such as the charge can also modulate NP uptake (Roy et al., 2014). Our find-ings indicating that there is no significant variations in NP cell uptake confirm that no important changes were induced in the selected NP by freezing procedures.

Confocal microscopy

Due to the differences observed when measuring the uptake of Ag-NP between TEM and FACS, we decided to use confocal microscopy with this type of NP to better characterize its uptake. Results show the advantages of this methodology over TEM, not only to detect NP but also to set its localization inside the cells and particularly inside the nucleus. Using this approach, we have been able to demonstrate a high uptake of Ag-NP by BEAS-2B cells, and no differences were detected when fresh and frozen NPs were compared. Figure 5 shows Ag-NP reaching the nucleus by confocal microscopy.

Cellular uptake and intracellular ROS production measured by FACS

In addition to using TEM to measure cellular uptake, FACS method-ology permits to determine the uptake of NP (Suzuki et al., 2007). FC analysis detects cell uptake by increases in the intensity of the side scatter. In this sense, the percentage of more complex cells indicates the internalization of NPs by those cells (Xia et al., 2015). In our study, FC data showed significant dose-dependent increase in the internalization of the selected NP, which reinforce the useful-ness of the methodology (Figure 6). From this figure, it must be indicated the little internalization of ZnO-NP by the BEAS-2B cells. To explain the discrepancy observed for MWCNT between TEM and FACs data, we assume that MWCNT exposure changes cell morph-ology which also changes cell complexity, making this technique not applicable for this kind of NP and cell type. Then, FACS data for MWCNT are not related with internalization.

Furthermore, FACS methodology permits to elucidate whether fresh and frozen NPs were able to generate intracellular ROS. The conversion of the non-fluorescent DCFH-DA to fluorescent oxi-dized DCF into the cells was determined after 24 h of treatment. As observed, BEAS-2B cells exposed to different NPs did not gen-erate differences in the levels of intracellular ROS between fresh and frozen NP (Figure 7). Moreover, our results showed that only nano-ZnO, both fresh and frozen were able to significantly increase the intracellular ROS production and only at the highest concentration evaluated (30 lg/mL). A high and significant increase in the percentage of ROS production (71.33%) was obtained for the positive control $KBrO_3$ (data not shown). The abil-ity of NP of inducing ROS is important as it has been proposed as a general toxic/genotoxic mechanism of NMs (Møller et al., 2013). Our results confirm that freezing procedures does not change NP ability to enter into the cell and trigger the cascade of events involved in ROS production.

Quantification of released ions using ICP-MS

NMs – and mainly metal NMs – are not completely stable and, as consequence, some release of ions is produced after suspension. To know the percentage of released ions is important to under-stand the toxicological profile of NMs due to the toxicity of most of the metallic ions. In humans, it has been

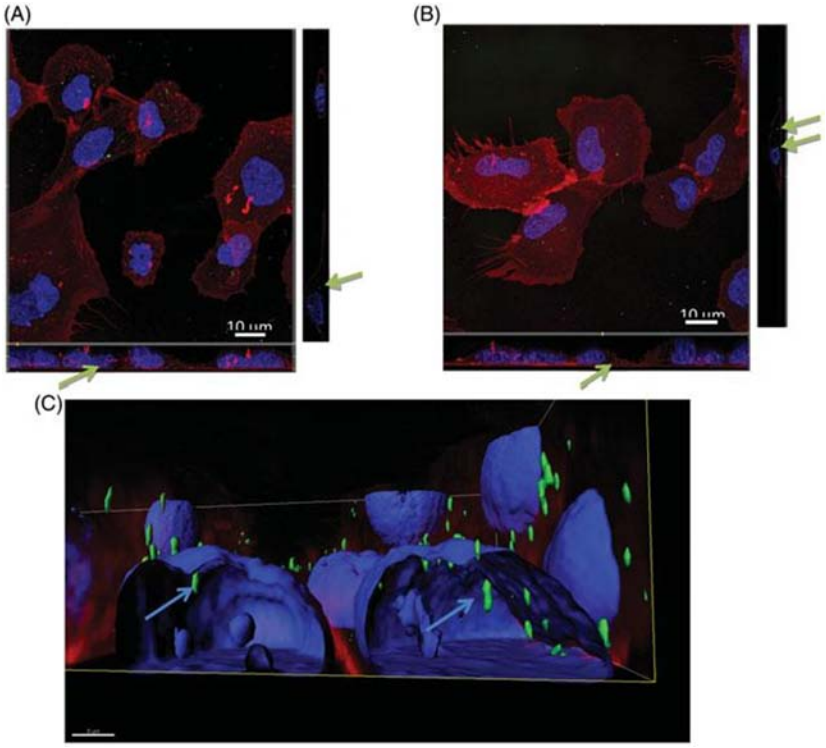

Figure 5. Confocal images from BEAS-2B cells treated with fresh or frozen 10 lg/mL of Ag-NP (A, B). Cellular uptake was measured after 24 h of treatment. Nucleuses are stained in blue, cell membranes in red and Ag-NP in green. Arrows indicate NPs inside the cells and inside the nucleus (C).

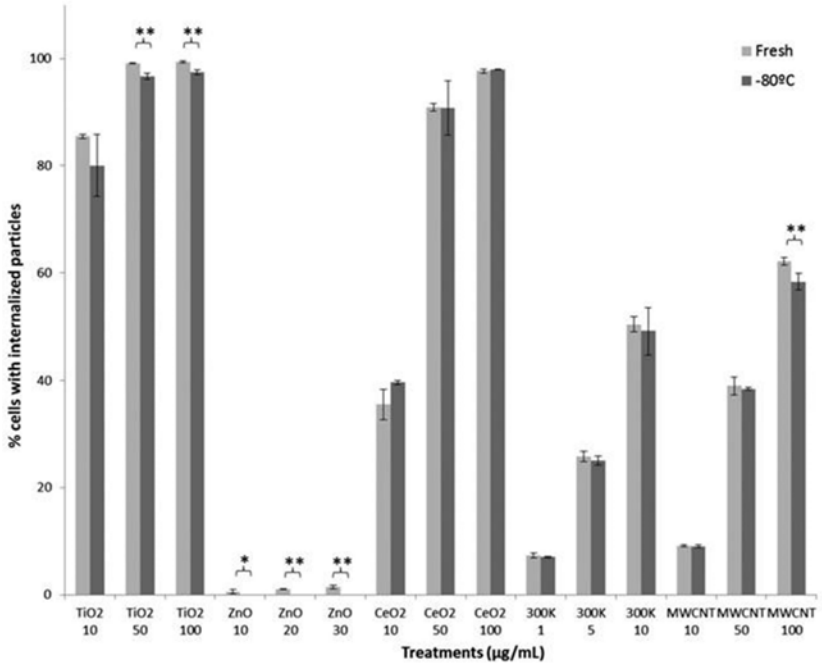

Figure 6. Percentages of cells with internalized NP after 24 h of treatment. The graphic shows a dose-dependent internalization of TiO_2-NP, CeO_2-NP, Ag-NP and MWCNT, and a very low internalization of ZnO-NP, without differences between the newly prepared dispersion and the thawed dispersion from frozen samples. $p < 0.05$ and $p < 0.01$ when compared to the control.

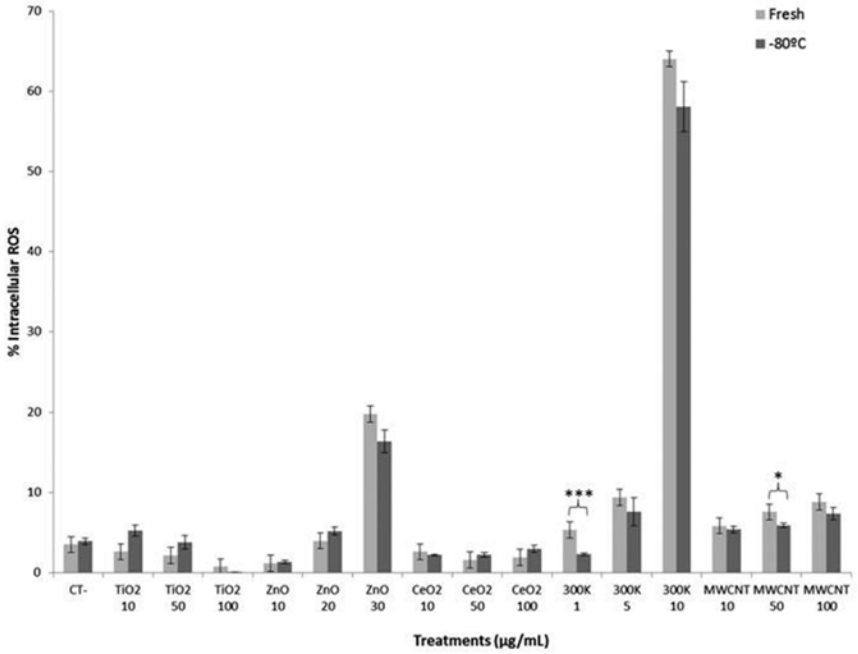

Figure 7. Percentage of intracellular reactive oxygen species (ROS) in BEAS-2B cells after 24 h of treatment with fresh or frozen TiO_2-NP, ZnO-NP, CeO_2-NP, Ag-NP and MWCNT. The graphic shows an increase in the levels of ROS in BEAS-2B exposed to ZnO-NP, Ag-NP and MWCNT, whereas no significant ROS production was detected in BEAS-2B exposed to TiO_2-NP, CeO_2-NP or low concentrations of ZnO-NP. In general, no differences are observed between the newly prepared dispersion and the thawed dispersion from frozen samples. $p < 0.05$ and $p < 0.001$ when compared to the control. Positive control ($KBrO_3$) induced a 71.33% of ROS (data not shown in the figure).

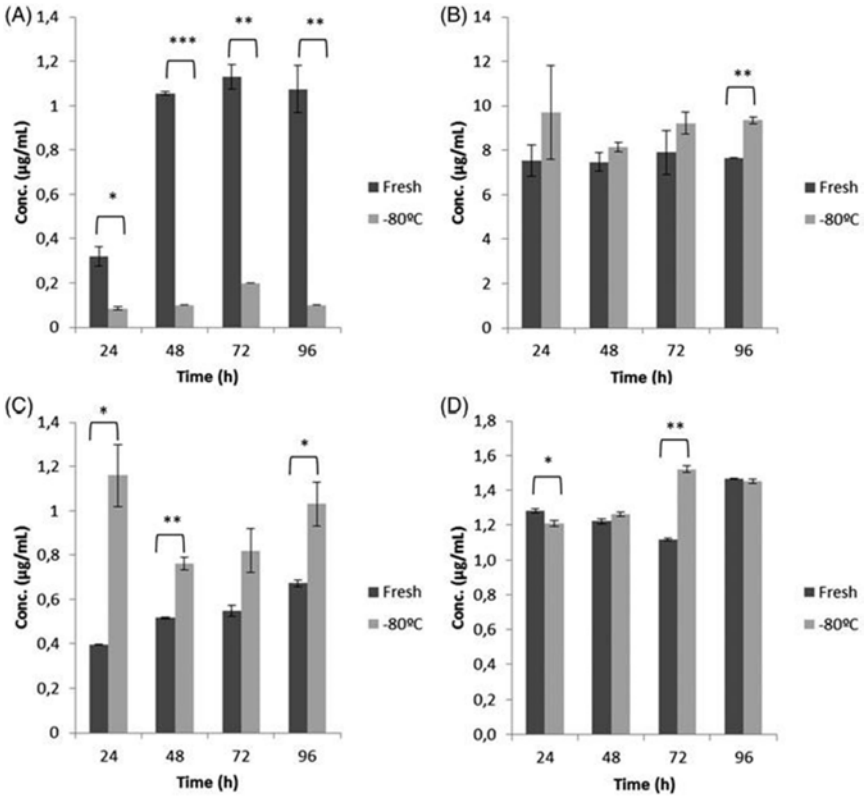

Figure 8. Dissolution of TiO_2-NP (A), ZnO-NP (B), CeO_2-NP (C) and Ag-NP (D) to their ionic forms in DMEM þ 10% FBS medium, evaluated at different time intervals (24, 48, 72 and 96 h) using ICP-MS. The initial concentration was 10 lg/mL. The reported data were determined by averaging at least three independent experimental values.

demonstrated that the presence of metals and metal alloys in orthopedic and dental implants supposes the release of metal NPs and metal ions due to the corrosive physiological in vivo environment (Matusiewicz, 2014). Indeed, Gebel et al. (2014) have defined three categories to determine the potential adverse health effects caused by NPs. One of them refers to the chemically mediated toxicity. In this cat-egory, toxicity of NMs may be mediated by the specific chemical properties of their components. In this context, a NM may release toxic ions which are responsible of the adverse induced effects. This has been described for different types of NMs, such as cad-mium-based quantum dots that may release cadmium ions (Chen et al., 2012), silver NPs that release silver ions (McShan et al., 2014) and zinc oxide NPs that are toxic mainly as a result of the release of zinc ions (Petrochenko et al., 2014).

The importance of released ions in the toxic profile of NMs make essential to consider this characteristic mode of action. In this context, it is important to demonstrate that frozen concentra-tions do not alter the stability of NMs and no variations in ions release are produced. In the detection of released ions, ICP-MS has emerged as the most promising technique for multi-element trace/ultratrace metal analysis of clinical and biological samples, providing high-performance analysis with high sensitivity (Matusiewicz, 2014). Since ICP-MS has limitations to distinguish between the particulate and ionic from, special care should be paid in the ultracentrifugation procedure and in obtaining the supernatant. We have determined the release of ions in a due time experiment lasting for 96 h and the obtained results are indi-cated in Figure 8. As observed, ZnO-NP is the most unstable NM and around 80% was dissolved into its ionic form after 24 h. No relevant changes were detected from that point on. The low uptake observed for ZnO-NP, when TEM and confocal methods were used can be due to the high solubility of this NP. Accordingly, the toxicity observed would be due to the Zn ions release as observed before (Sabella et al., 2014). Similar results were obtained for Ag-NP. On the other hand, significant variations were observed for those NPs with a poor dissolution rate (TiO_2-and CeO_2-NP), although changes were not found to follow a clear pattern; a higher release of ions was found for fresh TiO_2-NP, whereas it was higher in frozen CeO_2-NP. The small observed val-ues can be the cause of such observations. With regard to the TiO_2-NP, it should be stated that the observed value for frozen material agree with the reported data in the literature more than that obtained with fresh dispersions (Soto-Alvaredo et al., 2014).

Conclusions

The results obtained in this study support the advantages of using frozen dispersions of NMs in toxicology studies. Different end-points, such as NP characterization, solubility, cell viability, cellular uptake and intracellular ROS production have been evaluated and no differences between freshly prepared samples and frozen sam-ples were observed, supporting our proposal. Nevertheless, tox-icity not only depends on dispersion characteristics but also on dosimetry. Aspects, such as effective density, effective agglomer-ation density and delivered dose should be further considered to support the reliability of our proposal, as suggested in Pal et al. (2015).

Our approach supposes many advantages in nanotoxicological studies, not only for the time consuming reduction in NM disper-sions tasks but also for the repeatability between experiments. Our results will be especially beneficial in two different scenarios. Firstly, in studies involving long-term exposures to sub-toxic doses of NMs. There is an increasing interest toextend such type of studies as they represent a more realistic scenario of human exposure. Nevertheless, this type of approach requires freshly pre-pared NM dispersions every 3–4 days during weeks/months. The use of frozen samples would then represent an important reduc-tion of time and a potential increase in the homogeneity of the selected doses. Secondly, the extension of high-throughput meth-odologies in NMs toxicity testing is limited by the bottleneck that supposes the time necessary to prepare different concentrations of the different NMs to be tested. In this case, our proposal will help to extend the use of such high-throughput methodologies in the NM field.

Disclosure statement

The authors declare that there is no conflict of interest, and are responsible for the content and writing of the article.

Funding

This investigation has been partially supported by the Generalitat de Catalunya (CIRIT, 2014SGR-202), by the Ministry of Economy and Competition (SAF2015-63519-R) and by the EC FP7 NanoReg (Grant Agreement NMP4-LA-2013-310584). L. Rubio and L. Vila were funded by postgraduate fellowships from the Universitat Autonoma de Barcelona and the Generalitat de Catalunya, respectively. B. Annangi was supported by a postdoctoral fellow-ship from the Universitat Autonoma de Barcelona (UAB).

References

Annangi B, Bach J, Vales G, Rubio L, Marcos R, Hernandez A. 2015. Long-term exposures to low doses of cobalt nanoparticles induce cell transformation enhanced by oxidative damage. Nanotoxicology 9:138–47.

Bai W, Zhang Z, Tian W, He X, Ma Y, Zhao Y, Chai Z. 2010. Toxicity of zinc oxide nanoparticles to zebrafish embryo: a physicochemical study of toxicity mechanism. J Nanopart Res 12:1645–54.

Bruinink A, Wang J, Wick P. 2015. Effect of particle agglomeration in nanotoxicology. Arch Toxicol 89:659–75.

Brunner TJ, Wick P, Manser P, Spohn P, Grass RN, Limbach LK, et al. 2006. In vitro cytotoxicity of oxide nanoparticles: comparison to asbestos, silica, and the effect of particle solubility. Environ Sci Technol 40:4374–81.

Chan J, Ying T, Guang YF, Lin LX, Kai T, Fang ZY, et al. 2011. In vitro toxicity evaluation of 25-nm anatase TiO_2 nanoparticles in immortalized keratinocyte cells. Biol Trace Elem Res 144:183–96.

Chen N, He Y, Su Y, Li X, Huang Q, Wang H, et al. 2012. The cyto-toxicity of cadmium-based quantum dots. Biomaterials 33:1238–44.

Cho EC, Zhang Q, Xia Y. 2011. The effect of sedimentation and dif-fusion on cellular uptake of gold nanoparticles. Nat Nanotechnol 6:385–91.

Cho WS, Duffin R, Poland CA, Howie SE, MacNee W, Bradley M, et al. 2010. Metal oxide nanoparticles induce unique inflammatory footprints in the lung: important implications for nanoparticle testing. Environ Health Perspect 118:1699–706.

Cohen J, DeLoid G, Pyrgiotakis G, Demokritou P. 2013. Interactions of engineered nanomaterials in physiological media and impli-cations for in vitro dosimetry. Nanotoxicology 7:417–31.

Duffin R, Tran L, Brown D, Stone V, Donaldson K. 2007. Proinflammogenic effects of low-toxicity and metal nanopar-ticles in vivo and in vitro: highlighting the role of particle sur-face area and surface reactivity. Inhal Toxicol 19:849–56.

Epstein HA. 2011. Nanotechnology in cosmetic products. Skinmed 9:109–10.

Gebel T, Foth H, Damm G, Freyberger A, Kramer PJ, Lilienblum W, et al. 2014. Manufactured nanomaterials: categorization and approaches to hazard assessment. Arch Toxicol 88:2191–211.

Jiang J, Oberdorster€ G, Biswas P. 2009. Characterization of size, surface charge, and agglomeration sate of nanoparticle disper-sions for toxicological studies. J Nanopart Res 11:77–89.

Johnston H, Pojana G, Zuin S, Jacobsen NR, Møller P, Loft S, et al. 2013. Engineered nanomaterial risk. Lessons learnt from com-pleted nanotoxicology studies: potential solutions to current and future challenges. Crit Rev Toxicol 43:1–20.

Kermanizadeh A, Gaiser BK, Hutchison GR, Stone V. 2012. An in vitro liver model – assessing oxidative stress and genotoxicity following exposure of hepatocytes to a panel of engineered nanomaterials. Part Fibre Toxicol 9:28.

Kroll A, Pillukat MH, Hahn D, Schnekenburger J. 2012. Interference of engineered nanoparticles with in vitro toxicity assays. Arch Toxicol 86:1123–36.

Liu D, Gu N. 2009. Nanomaterials for fresh-keeping and steriliza-tion in food preservation. Recent Pat Food Nutr Agric 1:149–54.

Matusiewicz H. 2014. Potential release of in vivo trace metals from metallic medical implants in the human body: from ions to nanoparticles-a systematic analytical review. Acta Biomater 10:2379–403.

McGuinnes C, Duffin R, Brown SL, Mills N, Megson IL, Macnee W, et al. 2011. Surface derivatization state of polystyrene latex nanoparticles determines both their potency and their mechan-ism of causing human platelet aggregation in vitro. Toxicol Sci 119:359–68.

McShan D, Ray PC, Yu H. 2014. Molecular toxicity mechanism of nanosilver. J Food Drug Anal 22:116–27.

Monteiro-Riviere NA, Inman AO, Zhang LW. 2009. Limitations and relative utility of screening assays to assess engineered nano-particle toxicity in a human cell line. Toxicol Appl Pharmacol 234:222–3.

Møller P, Danielsen PH, Jantzen K, Roursgaard M, Loft S. 2013. Oxidatively damaged DNA in animals exposed to particles. Crit Rev Toxicol 43:96–118.

Murdock RC, Braydich-Stolle L, Schrand AM, Schlager JJ, Hussain SM. 2008. Characterization of nanomaterial dispersion in solu-tion prior to in vitro exposure using dynamic light scattering technique. Toxicol Sci 101:239–53.

Nanogenotox. 2011. http://www.nanogenotox.eu/files/PDF/Deliverables/nanogenotox%20deliverable%203_wp4_%20dispe-sion%20protocol.pdf.

Oberdorster G, Oberdorster E, Oberdorster J. 2005. Nanotoxicology: an emerging discipline evolving from studies of ultrafine particles. Environ Health Perspect 113:823–39.

Oberdorster G, Stone V, Donaldson K. 2007. Toxicology of nano-particles: a historical perspective. Nanotoxicology 1:2–25.

Pal AK, Bello D, Cohen J, Demokritou P. 2015. Implications of in vitro dosimetry on toxicological ranking of low aspect ratio engineered nanomaterials. Nanotoxicology 9:871–985.

Park M, Lankveld D, Van Loveren H, Jong W. 2009. The status of in vitro toxicity studies in the risk assessment of nanomaterials. Nanomedicine (Lond) 4:669–85.

Park H, Grassian VH. 2010. Commercially manufactured engineered nanomaterials for environmental and health studies: important insights provided by independent characterization. Environ Toxicol Chem 29:715–21.

Petrochenko PE, Zhang Q, Bayati MR, Skoog SA, Scott Phillips K, Kumar G, et al. 2014. Cytotoxic evaluation of nanostructured zinc oxide (ZnO) thin films and leachates. Toxicol in Vitro 28:1144–52.

Pujalte I, Passagne I, Brouillaud B, Treguer M, Durand E, Ohayon-Courtes C, LAzou B. 2011. Cytotoxicity and oxidative stress induced by different metallic nanoparticles on human kidney cells. Part Fibre Toxicol 8:10.

Roco MC, Hersam MC, Mirkin CA. 2011. Nanotechnology research directions for societal needs in 2020: summary of international study. J Nanoparticle Res 13:897–919.

Roy R, Kumar S, Tripathi A, Das M, Dwivedi PD. 2014. Interactive threats of nanoparticles to the biological system. Immunol Lett 158:79–87.

Sabella S, Carney RP, Brunetti V, Malvindi MA, Al-Juffali N, Vecchio G, et al. 2014. A general mechanism for intracellular toxicity of metal-containing nanoparticles. Nanoscale 6:7052–61.

Schmid K, Riediker M. 2008. Use of nanoparticles in Swiss industry: a targeted survey. Environ Sci Technol 42:2253–60.

Soto-Alvaredo J, Blanco E, Bettmer J, Hevia D, Sainz RM, Lopez Chaves C, et al. 2014. Evaluation of the biological effect of Ti generated debris from metal implants: ions and nanoparticles. Metallomics 6:1702–8.

Steigerwald ML, Brus LE. 1990. Semiconductor crystallites: a class of large molecules. ACC Chem Res 23:183–8.

Stone V, Nowack B, Baun A, van den Brink N, von der Kammer F, Dusinska M, et al. 2010. Nanomaterials for environmental stud-ies: classification, reference material

issues, and strategies for physico-chemical characterization. Sci Total Environ 408:1745–54.

Suzuki H, Toyooka T, Ibuki Y. 2007. Simple and easy method to evaluate uptake potential of nanoparticles in mammalian cells using a flow cytometric light scatter analysis. Environ Sci Technol 41:3018–24.

Vales G, Rubio L, Marcos R. 2015. Long-term exposures to low doses of titanium dioxide nanoparticles induce cell transformation, but not genotoxic damage in BEAS-2B cells. Nanotoxicology 9:568–78.

Wang Y. 1991. Nonlinear optical properties of nanometer-sized semiconductor clusters. ACC Chem Res 24:133–9.

Weller W. 1993. Quantized semiconductor particles: a novel state of matter for materials science. Adv Mater 5:88–95.

Xia B, Chen B, Sun X, Qu K, Ma F, Du M. 2015. Interaction of TiO2 nanoparticles with the marine microalga Nitzschia closterium: growth inhibition, oxidative stress and internalization. Sci Total Environ 508:525–33.

Xu M, Fujita D, Kajiwara S, Minowa T, Li X, Takemura T, et al. 2010. Contribution of physicochemical characteristics of nano-oxides to cytotoxicity. Biomaterials 31:8022–31.

Yang H, Liu C, Yang D, Zhang H, Xi Z. 2009. Comparative study of cytotoxicity, oxidative stress and genotoxicity induced by four typical nanomaterials: the role of particle size, shape and com-position. J Appl Toxicol 29:69–78.

Yen SJ, Hsu WL, Chen YC, Su HC, Chang YC, Chen H, et al. 2011. The enhancement of neural growth by amino-functionalization on carbon nanotubes as a neural electrode. Biosens Bioelectron 26:4124–32.

4. DISCUSSION

4. DISCUSSION

Nanotechnology industry has experienced an exponential increase regarding investment and production in the last two decades. This is mainly due to the interesting properties offered by NMs for many purposes. The possibility of designing and manipulating matter at the nanoscale with specific physic-chemical properties for its use in predefined applications has been the key factor for the strong impulse of this field.

The inclusion of these new materials in such a big number of daily life products has sparked as a social concern on the security and regulation linked to these small particles. However, due to the fast development of these nano-products, no extensive and conclusive toxicological experiments have been performed before its introduction into the market. Thus, no specific regulation for these NMs exists at the moment in Europe, being regulated by the guidelines associated to its macromolecular counterparts http://ec.europa.eu/environment/chemicals/nanotech/ index_en.htm).

Nevertheless, due to their small size of NMs, their ability to penetrate cellular membranes and the fact that they show completely different physic-chemical properties when compared with their macromolecular homologues, make this situation not acceptable (Nel et al., 2006). As a consequence, in 2008 the public Organization for Economic Cooperation and Development (OECD) developed a Working Party of Manufactured Nanomaterials (WPMN). Large and important projects were launched out of this initiative in order to study the potential health effects of these compounds (MARINA, NanoTEST or NanoGenotox, among others) and aiming to create a proper regulation background (NANoREG).

4.1. Potential properties of nanoceria

In the frame of the WPMN, thirteen priority representative NMs were listed as requiring immediate testing. Among them, nanoceria was chosen as one of those with higher growth projection (Ivanenko et al., 2013). These particles emerged as an outstanding catalytic material with interesting uses in several industrial applications (Kosynkin et al., 2000; Lawrence et al., 2011; Dao et al., 2011).

Regarding its biological applications, nanoceria was presented as a potent antioxidant agent due to its ability to reversibly bind oxygen and shift oxidation states (Ce^{3+}/Ce^{4+}) depending on environmental factors (Estevez and Erlichman, 2014). The interconversion of oxidation states gives rise to a large number of oxygen vacancies on

the surface of nanoceria and it is this key property that makes it a promising ROS scavenger, and an interesting candidate for the treatment of diseases characterized by increased oxidative stress levels.

The commercialization of this NM for industrial applications has been widely extended since 1999 (Li et al., 2016). However, its use as a ROS scavenger in therapeutics is still controversial due to both antioxidant and toxic effects observed in in vitro and in vivo models, as recently reviewed (Yokel et al., 2014). Considering the great potential presented by this NM in biomedicine and other fields in the near future, making a complete and conclusive evaluation is crucial for its safety use. Thus, in this Thesis we have evaluated both the beneficial and toxic potential effects of nanoceria in several biological in vitro models and treatment conditions.

4.1.1. Antioxidant properties

ROS are spontaneously generated during mitochondrial oxidative metabolism as well as in cellular response to xenobiotics, cytokines, and bacterial invasion (Ray et al., 2012). An excess of intracellular ROS causes oxidative stress, which results in an increased risk for atherosclerosis, diabetes, cancer, neurodegeneration, and other diseases. In order to prevent the undesirable effects of oxidative stress, cells have developed an antioxidant defence system based on enzymatic and non-enzymatic antioxidants molecules. However, this cellular system is sometimes overwhelmed by oxidant molecules generating cellular damage. Although antioxidant intakes contribute to the maintenance of adequate antioxidant status in the body, research on new potential molecules has been extensively developed to respond to situation where oxidative stress is generated (Firuzi et al., 2011).

Among the potential antioxidant molecules, nanoceria is presented as a well-known redox catalyst in acellular systems and has generally shown this ability in biological models as well (Grulke et al., 2014). Consequently, nanoceria has been able to scavenge oxidant molecules where unbalanced ROS situations in intracellular environments arise (Nelson et al., 2016). Following the described intrinsic redox properties of these NPs, in our first study we demonstrated that nanoceria was able to reduce the ROS produced by the well-known oxidizing agent $KBrO_3$ in the in vitro BEAS-2B lung cell line model.

In addition, other biomarkers analysed in our first study have given strength to the theoretically attributed antioxidant role of nanoceria. Thus, a decreased oxidative DNA damage was observed when cells were pre-treated with nanoceria before the oxidant

insult by the comet assay. In addition, downregulation in the expression of the HO1 gene, considered a marker of cellular homeostasis maintenance, also observed after nanoceria treatment when compared to the expression corresponding to the $KBrO_3$ treatment alone. Similarly, NP pre-treatment before the oxidant challenge also diminished the gene expression of the antioxidant SOD2 gene. Finally, reduced cell mortality was detected indicating nanoceria-related cellular protection and an extended lifespan. According to our results, nanoceria would enter easily into the cells -as visualized using transmission electron microscopy (TEM)- mediated by endocytic pathways as suggested by Singh et al. (2010) and co-localize in the cytoplasm, preconditioning the microenvironment for the oxidant insult. Once $KBrO_3$-induced ROS start spreading into the intracellular space, the oxygen defects and Ce^{3+}/Ce^{4+} interconversion associated to nanoceria would quench in some extent the existing oxidant molecules. By this action, nanoceria would eventually act preventing from the cascade of effects triggered by radicals, starting from lipid peroxidation, membrane structure damage in the cytoplasm, oxidative DNA damage (oxidised purine bases) in the nucleus and finally apoptosis and cell death (Ray et al., 2012).

The key to these observed beneficial effects has been generally agreed and related to the special characteristics of nanoceria. Thus, nanoceria mimics the mode of action of two important biological enzymes such as SOD and CAT. Korsvik et al. (2007) were the first investigators who demonstrate the SOD-mimetic activity of nanoceria. When a ROS unbalance occurs and there is an excess of superoxide radical ($O_2^{\cdot -}$) (the precursor of most other reactive oxygen species), the toxic effects are normally controlled and reduced through the activity of SOD enzymes (McCord et al., 1969). Therefore, these enzymes eradicate $O_2^{\cdot -}$ by converting it into H_2O_2 and O_2 through a two-step catalytic dismutation reaction as shown in Figure 13 (Nelson et al., 2016).

$$(1) \quad O_2^{\bullet -} + 2H^+ + (Cu^+)\text{-SOD} \rightarrow H_2O_2 + (Cu^{2+})\text{-SOD}$$

$$(2) \quad O_2^{\bullet -} + (Cu^{2+})\text{-SOD} \rightarrow O_2 + (Cu^+)\text{-SOD}$$

Figure 13. SOD catalytic dismutation reaction (Adapted from Nelson et al., 2016)

Similarly, the presumed catalytic mechanism whereby nanoceria scavenges $O_2^{\cdot -}$ was proved when the generation of H_2O_2 from the catalytic degradation of $O_2^{\cdot -}$ by nanoceria was detected (Korsvik et al., 2007). This reaction is reported as follows in Figure 14 (Ivanov et al., 2009; Reed et al., 2014).

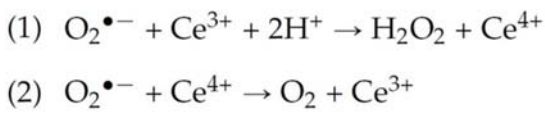

Figure 14. SOD mimetic catalysis of nanoceria (Adapted from Nelson *et al.*, 2016)

Interestingly, in our first study we found an upregulation expression of the SOD-2 gene after a single treatment with nanoceria. Similarly, pre-treatment of nanoceria for 24 hours before a single-dose of radiation was found to confer protection from radiation-induced cell death, presumably by reducing the amount of ROS and increasing the expression of SOD-2 in a dose-dependent manner, as showed previously in the study performed by Colon et al. (2010). Thus, apart from the direct SOD-mimetic scavenging effect observed by nanoceria, the increase in the expression levels of antioxidant genes confirms the indirect protective role of these NPs allowing the cells to rebound in response to ROS insult.

On the other hand, Rzigalinski et al. (2006) were one of the first groups demonstrating the CAT-mimetic activity of nanoceria. High levels of H_2O_2 generated as a product of SOD enzymes are actually considered more dangerous to cellular homeostasis than high levels of $O_2^{\cdot -}$. Among others, CAT is the most efficient antioxidant enzyme acting by reducing the disproportionate levels of H_2O_2 by reducing this compound into O_2 and H_2O (Karakoti et al., 2010; Nelson et al., 2016). The key findings from Rzigalinski and co-workers's study were, in the first place, that Ce^{4+} was required on the surface of nanoceria in order to decompose the added H_2O_2, as shown in Figure 15; and secondly, that the luminescence spectra of nanoceria surface reverted back to its original properties once the H_2O_2 was decomposed; thus showing the regenerative nature of the Ce^{3+}/Ce^{4+} redox couple on the nanoceria surface.

Figure 15. CAT mimetic catalysis of nanoceria (Adapted from Nelson *et al.*, 2016)

The proposed enzyme-mimetic activity would explain the results observed in our study -and many others- that show decreased intracellular ROS (Tarnuzzer et al., 2005; Schubert et al., 2006; Colon et al., 2010; Pagliari et al., 2012), diminished DNA damage (Caputo et al., 2015) and reduced cell mortality (Demokritou et al., 2013; Kwon et al., 2016). These beneficial effects are a direct consequence of the radical scavenging activity of nanoceria.

In addition to the biomarkers analysed in our experiments, other studies have shown that nanoceria cooperates to maintain cellular homeostasis through different mechanisms/endpoints. Apoptosis prevention is one example (Celardo et al., 2011; González-Flores et al., 2014). At this point, Celardo et al. (2011) found a direct relationship between nanoceria ROS scavenging properties and pro-survival effects. By characterizing apoptosis in two different leukocyte cell lines authors showed how nanoceria exerted strong anti-apoptotic effects only in redox-dependent apoptosis. In another interesting study focussed in an Alzheimer disease model, conjugated nanoceria was functionalized to be localized specifically into mitochondria. In this case, nanoceria treatment exhibited mitigation of reactive gliosis and mitochondrial damage, both considered key factors in the first stages of Alzheimer disease (Kwon et al., 2016). Moreover, Kong et al. (2011) found an integral role of nanoceria in up-regulating the expression of neuroprotection-associated genes, and in down-regulating apoptosis signalling pathways in retinal dysfunction. Nanoceria was also able to protect against inflammation. Thus, Niu et al. (2007) demonstrated that redox sensitive transcription of pro inflammatory factors such as tumor necrosis factor-a (TNF-α), interleukin-6 (IL-6), monocyte chemoattractant protein-1 (MCP-1) and interleukin-8 (IL-8) were significantly suppressed by injecting the animals with these NPs. In the same study, nanoceria was able to suppress endoplasmic reticulum (ER) stress and reduce the apoptotic cell death in the myocardium (Niu et al., 2007). Finally, an increase in wound-healing activity was detected after treatment with nanoceria (Davan et al., 2012). Authors showed that locally applied nanoceria to incised rats enhanced wound healing activity, wound tensile strength, and wound closure time relative to treatment with the well-known antiseptic povidone-iodine. These enhancements were attributed to the ROS-scavenging abilities of nanoceria at the site of injury and the protection of the native tissue by increased production of collagen and hydroxyproline, essential for wound healing activity.

Although specific cell lines could behave differently with regard to nanoceria biointeractions (as for example, interactions with specific membrane receptors), modulating in this way internalization and effects, a wide variety of different *in vitro* cell lines have shown similar antioxidant results. This occurs with neuronal (Schubert et al., 2006), endothelial (Chen et al., 2013) gastrointestinal epithelium (Colon et al., 2010), breast epithelium (Tarnuzzer et al., 2005), stem cells (Mandoli et al., 2010), cardiomyocytes (Niu et al., 2011), lung epithelium cells (Rubio et al., 2016) or human monocytes (Ting et al., 2013).

In relation with the promising results obtained from *in vitro* studies in the applicability of nanoceria as oxidative related disease treatment, *in vivo* studies have also shown favourable results for the treatment of endometriosis (Chaudhury et al., 2013), gastric ulcers (Prasad et al., 2013), retinitis pigmentosa (Kong et al., 2011; Cai et al., 2012; Wong et al., 2013, 2015), Alzheimer disease (Kwon et al., 2016), multiple sclerosis (Heckman et al., 2013), diabetes (Pourkhalili et al., 2012) or cancer (Alili et al., 2011; Sack et al., 2014).

Nowadays antioxidant therapy is the focus of enormous clinical interest and great emphasis is given to nutritional and pharmacological strategies to prevent or ameliorate human diseases by supplementing antioxidant molecules that enhance or mimic endogenous antiradical defence (Lobo et al., 2010). Although an extraordinary number of studies related with antioxidant treatments exist, only a few number of them have been approved in clinical trials. Thus, several are the parameters limiting the real effectiveness of an antioxidant like low bioavailability, high concentration requirement, low chemical stability, impossibility of recycling the active antioxidant, poor target specificity, or harmful side effects (Firuzi et al., 2011). Thus, considering the vast number of studies supporting the potential use of nanoceria in different oxidative related diseases and the limitations observed in classical antioxidant therapies, several are the experiments conducted by which the antioxidant ability of nanoceria has been compared with different well-known antioxidants (Celardo et al., 2011; Caputo et al., 2015). In these studies nanoceria presented even better ROS scavenge efficiency than trolox, pyruvate, ascorbate, cystathionine or NAC. These results, together with the high availability of this material in the environment, the large number of active sites exhibited due to the high surface to volume presented by NPs, and its auto regenerative reaction cycle ($Ce^{3+} \rightarrow Ce^{4+} \rightarrow Ce^{3+}$) make these nanoscale particles an ideal protectant cell agent candidate for the treatment of oxidative stress related diseases.

4.1.2. Pro-oxidant properties

As previously described, both SOD and CAT-mimetic activities are required for the antioxidant function of nanoceria. Therefore, unbalance activities of these enzymes could potentially lead to the accumulation of certain ROS like H_2O_2, producing oxidative stress and toxicity. Enzyme-mimetic activity of nanoceria is strongly correlated with the proportion of Ce^{3+}/Ce^{4+} states. Normally, nanoceria possess both SOD- and CAT-mimetic activity at varying degrees depending on this ratio of surface states. In general, nanoceria with high amounts of Ce^{3+} (40% to 60%) on the surface behave as SOD-mimetic (Korsvik et al., 2007; Dowding et al., 2013), while nanoceria with high amounts

of Ce^{4+} (70% to 80%) on the surface acts basically as CAT-mimetic (Pirmohamed et al., 2010; Das et al., 2013). However, several intrinsic and extrinsic parameters critically influence the overall catalytic efficiency of the mimetics. Whether or not nanoceria behaves predominantly as a SOD-mimetic or as a CAT-mimetic also depends on several factors like the starting reagents, the synthesis procedure, NP functionalization and a number of other parameters related to nanoceria preparation and structure (Walkey et al., 2015). Thus, some changes in some of these known or unknown factors could directly produce an unbalanced enzyme mimetic activity of nanoceria, leading to pro-oxidant behaviour.

One of the most studied factors related to an unbalanced mimetic activity of nanoceria is pH. However, some controversy exists since some studies show no clear effects (Singh et al., 2011; Xue et al., 2012) while other studies demonstrate pronounced effects on both the nanoceria Ce^{3+}/Ce^{4+} redox state and the catalytic antioxidant activity (Rzigalinski et al., 2006; Perez et al., 2008; Karakoti et al., 2010). Among the studies reporting a positive correlation, Perez et al. (2008) showed that the antioxidant activity of nanoceria depends directly on the pH of the surrounding medium. In this way nanoceria showed CAT-mimetic activity (degrading H_2O_2) in neutral and alkaline solutions, but were inactivated in acidic (pH 4) solutions (accumulating toxic H_2O_2). This behaviour was demonstrated in both acellular and cellular environments. A more recent study (Karakoti et al., 2012) appears to confirm these observations through fundamental XPS studies that demonstrate linear changes in Ce^{3+}/Ce^{4+} redox state with changes in pH. Thus, according to these studies, nanoceria could pose a dual role as an antioxidant or oxidant depending on the environmental pH conditions.

Assuming an acidic intracellular pH in tumoral cells due to the Warburg effect, some authors have proposed the use of nanoceria as a possible strategic treatment for oxidizing and killing cancer cells while protecting normal cells (Colon et al., 2009; Wason et al., 2013; Shcherbakov et al., 2014). To prove this potential mechanism we carried out *in vitro* studies using different cancer cell lines exposed to different concentrations of nanoceria. From our results we did not found enough data to support this theory. Thus, the treatments did not enhanced but reduced the levels of intracellular ROS induced by the potent pro-oxidant compound cisplatin. Although the magnitude of the protective antioxidant effect was dependent on the cancer cell line tested, in general ROS scavenge activity was observed in all cell lines and most importantly, no oxidant effects were encountered under any of the studied conditions. In addition, different cellular conditions were forced in our model to more deeply study the putative oxidant effect. Decreases in intracellular pH were achieved through

starving conditions (absence of serum in cell medium), based on the property of tumoral cells to increase the lactic acid production under starvation (Wu *et al*., 2013). According to that, no oxidant effects were detected under these scenarios either. Additionally, and in order to directly decrease the pH of the cell medium 2-(N-morpholino) ethanesulfonic acid (MES) was used, but again no increases in ROS production were detected.

The genetic background of the cancer and normal cells studied so far differ considerably and may influence the final outcome. Thus, to avoid the influence of genome characteristic in the observed effects of nanoceria in the tumoral and non-tumoral non isogenic cell lines used, a normal mouse embryonic fibroblast cell line (MEF) and its arsenic-transformed isogenic counterpart (AsT-MEF) were also evaluated. As in the other cases, nanoceria elicited an antioxidant effect in both MEF and AsT-MEF. Therefore, although mechanistic experiments have not been performed yet, our results do not indicate any oxidant role of nanoceria in different tumoral cell lines grown in different microenvironments and conditions. Thus, parameters other than the tumoral cell status may be playing part in the observed oxidant/antioxidant dual role of nanoceria.

Other authors have shown no oxidation but protection of different cancer cell lines by nanoceria, reinforcing our results. For example, Akhtar et al. (2015) using human breast cancer (MCF-7) and fibrosarcoma (HT-1080) cells observed no significant cell death in either cell model following treatment with nanoceria. On the contrary, the treatment significantly protected the cells, increasing the production of glutathione (GSH) in cellular defence against injury, and remarkably replenishing GSH depletion caused by H_2O_2. On the other side, De Marzi et al. (2013) using three tumoral cell lines (A549, Caco-2 and HepG2) did not find important toxicity after 24 hours of exposure in A549 and Caco-2 but acute toxicity was shown in HepG2 cells. Interestingly, in the three cell lines nanoceria acted as a protector in front of the oxidative stress induced by H_2O_2, as evaluated by using the comet assay. Other studies also verified the antioxidant effect of this NM by using different tumor cell lines like the human histiocytic lymphoma (U937) (González-Flores et al., 2014) or HeLa (Spulber et al., 2015). In these studies, authors showed that the protective role of nanoceria in these tumor cell lines was in some cases even more efficient than that induced by classical antioxidants as trolox or NAC, as mentioned before (González-Flores et al., 2014).

Contrary to our observations, differential results regarding the tumoral cell status have been obtained in other studies, where nanoceria was observed i.e. to protect normal cardiomyocytes (H9c2) and human dermal fibroblasts (BJ) against hydrogen peroxide

induced cytotoxicity, but no protection was observed in lung carcinoma cells (A-549) and breast carcinoma (BT-474) cells (Perez et al., 2008). Similar results have been reported by Das et al. (2007), showing that nanoceria protect immortalized normal breast epithelial cells (CRL8789) from cell toxicity and DNA damage against 10 Gy of radiation, while no protection was observed in breast cancer cells (MCF7) against the same radiation exposure. Alili et al. (2013) found non-toxic effects of nanoceria exposure for stromal fibroblast and endothelial cells while showing cytotoxic, pro-apoptotic, and anti-invasive effects on melanoma cells (A375). Differential behaviour have also been reported in pancreatic cells, where pre-treatment with nanoceria enhanced radiation-induced ROS production and cell death, preferentially in human pancreatic cancer cells (L3.6pl) when compared to normal pancreatic cells (hTERT-HPNE) (Wason et al., 2013).

It must be pointed out that the hypothesis of achieving differential cytotoxicity between tumoral and non-tumoral cells is considered as one of the greatest challenges in chemotherapy and high efforts are being conducted to identify anticancer drugs able to distinguish effectively between them (Gao et al., 2014). However, as noticed from the above mentioned studies, no consensus has been reached about the applicability of nanoceria in cancer treatments, since many are the factors (some known and others unknown) affecting the intracellular redox reactions of nanoceria. Although pH could play a role in the pro/antioxidant effects of this NM, all cancer cells do not present the same conditions, due to differences in their metabolisms. Thus, the efficacy of nanoceria treatment would vary depending on how notably the Warburg effect is affecting the intracellular pH.

Despite of the unclear pro/oxidant nanoceria effects preventing from the use of nanoceria in cancer treatment; also of importance is the fact that several studies have reported oxidative-dependent toxic effects of nanoceria in normal (non-tumoral) *in vitro* and *in vivo* models. Thus, among others; Park et al. (2008) reported cytotoxic effect of nanoceria using the BEAS-2B cell line, where cell viability and ROS generation were observed in a time- and dose-dependent manner. On the other hand, Eom and Choi (2009) also reported toxicity of these NPs in the same lung epithelial cell line. Such authors focused on the involvement of the oxidative stress generated by nanoceria in signal transduction pathways and transcription factors and, according to their results, nanoceria was found to behave as a pro-oxidant compound causing oxidative stress through strong induction of *HO-1* via the *p38-Nrf-2* signalling pathway. As noticed, discrepancies are found between laboratories when comparing the same cell line. These may be attributed to different nanoceria physicochemical properties given by

their synthesis process or by differences in crystal structure or surface chemistry, directly affecting to its redox activity. On the other side, some *in vivo* studies have shown pulmonary inflammation and alveolar interstitial fibrosis after nanoceria exposure. Thus, acute exposed Sprague Dawley rats by inhalation of 2 hours/day for 4 days to 2.7 mg/m^3 showed bronchoalveolar lavage fluid (BALF) levels of neutrophils increased six fold 24 hours post-exposure indicating inflammation, while BALF activity of LDH increased two fold indicating cytotoxicity (Demokritou et al., 2010). Another inhalation study, where sub-acute male CD1 mice were exposed to 2 mg/m^3 for 0, 7, 14, or 28 days of nanoceria also resulted in pulmonary and extrapulmonary toxicity. Therefore, BALF analysis revealed the induction of pulmonary inflammation, evident by an increase in the influx of neutrophils with a significant secretion of pro-inflammatory cytokines. This led to oxidative stress generation and cytotoxicity, evident by induction of lipid peroxidation, depletion of glutathione, and increased BALF LDH and proteins. Histopathological examination revealed that inhaled nanoceria was located throughout the pulmonary parenchyma, inducing a severe, chronic, active inflammatory response characterized by necrosis, proteinosis, fibrosis, and well-formed discrete granulomas in the pulmonary tissue and tubular degeneration leading to coagulative necrosis in kidneys (Aalapati et al., 2013). Finally, data from one sub-chronic inhalation exposure study using Sprague-Dawley rats exposed to microscale ceria at concentrations of 0, 5, 50.5, or 507.5 mg/m^3 for 6 hours/day, 5 days/week for 13 weeks is available. This study observed an increased incidence of alveolar epithelial hyperplasia. Histological examination revealed dose-related alveolar epithelial and lymphoid hyperplasia and pigment accumulation in the lungs, lymph nodes, and larynx of male and female rats at ≥ 5 mg/m^3 (EPA 2009). Despite the results obtained in these studies, it should be mentioned that the vast majority of published results classify nanoceria as a low toxic material (Yokel et al., 2014).

Apart from *in vitro* and *in vivo* studies, epidemiological studies are of great importance for risk assessment. However, the knowledge about occupational safety and health risk assessment of nanoceria is vague and no occupational exposure limits (OELs) and attendant action levels for nanoceria are available (Li et al., 2016). Nevertheless, from the information existing about occupational exposure to rare earth (RE) metals, of which cerium is the major component (80%), an induction of rare earth pneumoconiosis with pathologic conditions that include granulomas and interstitial fibrosis was observed (Sabbioni et al., 1982; Waring and Watling, 1990; McDonald et al., 1995). A common feature of rare earth pneumoconiosis is the presence of cerium particles in the alveoli and interstitial tissue even in patients, whose exposure to cerium had stopped for over

20 years, indicating the high biopersistence of these NPs in the lung (Pairon et al., 1994; Ma et al., 2011).

It is clear then that there exists a high disparity of results between studies carried out *in vitro* or *in vivo*, and also when epidemiologic studies are taken into consideration. It is however necessary to continue putting efforts in characterizing and controlling the factors affecting the redox coupled activities of nanoceria due to its applicability interest. Once its associated effects and modulating factors are well stablished, an efficient design of nanoceria properties would be possible, and would ensure a secure and predefined use of this NM in the extended list of its proposed therapeutic applications.

4.2. Long-term *in vitro* exposures

Due to the contradictory results and the gaps found in the literature regarding the toxicological evaluation of nanoceria, several recommendations have been proposed to the research community (Yokel et al., 2014). Among them, the study of long-term/low-concentration treatment supposes a very important challenge. Prolonged treatments at environmental relevant exposures reflect more accurately real scenarios, as long-term exposures into the workplace and in daily life are already occurring. In addition, since high biopersistence has been related to this NM, acute exposure treatments are far away from real scenarios and, consequently, it is feasible that they underestimate eventual adverse health effects associated to prolonged exposures (Yokel et al., 2012). Finally, it must be emphasized that this approach allows studying carcinogenic processes and its underlying mechanisms, which cannot be studied by common acute treatment endpoints.

Normally, *in vivo* models are used to study the effects produced by long-term treatments, as requested by OECD guidelines. However, during the last two decades, substantial efforts have been made towards the development and international acceptance of alternative *in vitro* methods to substitute as far as possible the use of laboratory animals. In continuation of this tendency, the European Chemicals Legislation (REACH) favours alternative methods to conventional *in vivo* testing, if validated and appropriated (Annys et al., 2014). Following Yokel's recommendation about studying long nanoceria exposures, our laboratory has created *in vitro* models to emulate a real scenario through long-term/low-concentration exposures. Despite *in vitro* models-associated limitations, its use for long-term approaches results fruitful since it allows to analysing cell transformation effects, a very relevant end-point poorly explored so far.

4.2.1. Hallmarks of carcinogenesis

Given the abilities of NMs to penetrate, biopersist, produce different types of damage, and initiate genotoxicity in exposed tissue, the possibility of NM to induce or promote tumorigenesis is a rising concern (Kumar and Dhawan, 2013). In fact, direct evidences exist regarding carcinogenicity of some produced NMs (Roller, 2009). This carcinogenic potential can be attributed to several mechanisms, such as direct interaction of NMs with the genetic material, indirect damage due to reactive oxygen species generation, release of toxic ions from soluble NPs, interaction with cytoplasmic/nuclear proteins, binding with mitotic spindle or its components, disturbance of cell cycle checkpoint functions, inhibition of antioxidant defences, as well as of many others processes (Kumar and Dhawan, 2013). Nevertheless, despite all the potential mechanisms underlying NM carcinogenesis, the number of studies assessing this potentiality is limited.

Only few studies have explored the importance of *in vitro* long-term exposures for assessing the carcinogenic potential of NPs. From our Group, efforts have been leaded to the standardization of different cellular models in order to study the transformation capacity of these new materials. Among them, a lung epithelial cell line like BEAS-2B has entailed an important model to work with, due to different reasons. First, lung cancer is the leading cause of cancer death (Siegel et al., 2015). Second, environmental and occupational exposure is the major cause of most cases of lung cancer (Samet, 2009). Third, inhalation is the first route by which NPs enter into the body (Hoet et al*.,* 2004). Thus several studies have been carried out to analyze the carcinogenicity of different NMs like TiO_2-NPs and CNT (Vales et al*.,* 2015, 2016) in this cellular model. In these studies, TiO_2-NPs induced cell transformation mediated by a non-genotoxic mechanism, while CNT induced chromosome instability as the leading cause of cellular transformation. In fact, based on different studies, both NMs have been categorized as possible carcinogens to humans (Group 2B) by IARC (Baan et al*.,* 2007).

Other strategic models have also been stablished in our Group, like the use of knock down cell lines for deeply study mechanisms associated to cell transformation. Considering that ROS induction has been established as a common mechanism of NMs-associated cell damage (Wang et al*.,* 2011), and taking into account that this mechanism is also a well-known promotor of cell transformation (Møller et al*.,* 2013; Bach et al*.,* 2016), oxidative DNA damage became a very relevant mechanism to be analysed when NP carcinogenesis is evaluated. For that, a wild-type mouse embryonic fibroblast cell line (MEF *Ogg1*$^{+/+}$) and its isogenic *Ogg1* knockout partner (MEF *Ogg1*$^{-/-}$)

unable to properly eliminate oxidative 8-oxo-2'-deoxyguanosine (8-OH-dG) lesions from DNA were selected (Annangi et al., 2015, 2016). In these studies, CoNP showed carcinogenic properties through oxidative stress mechanism after 12 weeks of exposure with low doses as showed by different carcinogenic markers. On the other hand ZnO-NPs in spite of causing high toxicity, did not present cell transforming ability after the same exposure time.

Out of the experiments above described, just a few more groups have used *in vitro* long treatment exposures for evaluating carcinogenic effects of NM. These include chronic exposures to sub-toxic doses of TiO_2-NPs which led to chromosomal instability and cell transformation in fibroblast cells (Huang et al*.,* 2009). Additionally, several studies also reported the carcinogenic potential of CNT after long-term exposure, showing that these NPs could cause malignant or neoplastic-like transformation in human lung epithelial cells (Wang et al*.,* 2011, Lohcharoenkal et al*.,* 2013; Luanpitpong et al*.,* 2014). In this case, due to the CNT fibre nature similar to other well-known carcinogens like asbestos, CNT have been the focus of many mechanistic studies. Thus, He et al. (2016) pointed out the association of mesothelin (MSLN) over-expression (over-expressed in many human tumours) with the malignant transformation of bronchial epithelial cells (BSW) using stably-transfected MSLN knockdown. Also, Luanpitpong et al. (2014) obtained new evidences supporting the role of cancer stem cells in CNT tumorigenesis. These studies indicate that, although some limitations could be linked to *in vitro* methodologies, faster and predictive results could be provided shedding light to possible unknown carcinogens and its mechanisms.

Focussing on nanoceria, to our knowledge only one very recently published study developed an *in vitro* long-term methodology for the evaluation of carcinogenic effects of these NPs. In such study, Rojanasakul et al. (2016) used a sub-chronic exposure to human primary small airway epithelial cells (pSAECs). Herein, cells continuously exposed to deposited concentrations of 0.18 μg/cm^2 or 0.06 μg/cm^2 of nanoceria were evaluated for changes in several cancer hallmarks, as evidence for neoplastic transformation. After ten weeks, nanoceria-exposed cells did not show any significant sign of cell transformation. Comparing with *in vivo* models, past research studies showed that pulmonary exposure to nanoceria resulted in no significant development of lung tumorigenesis. Thus, single inhalation exposure to nanoceria resulted in only 0.66% of rats developing alveolar papillary neoplasms, adenocarcinoma, or carcinoma across their lifespan compared to unexposed animals (Lundgren et al., 1996).

With the objective of covering some of the recommendations raised by the nanoceria community research, six weeks of sub-chronic exposure of the *in vitro* BEAS-2B model was performed by us. One important parameter to be considered when long-treatment exposures are conducted is the use of environmental relevant dose. Thus, the existing information about the worst-case exposure to nanoceria-containing diesel exhaust over a working lifetime exposure was used (Ma et al*.,* 2011). Several calculations were used to convert *in vivo* into *in vitro* exposures. Accordingly, 2.5 µg/mL would be closely equivalent to the occupational situation (10 mg/kg) (Ma et al*.*, 2011; Rojanasakul et al*.*, 2016). Being the model by which carcinogenesis was evaluated an epithelial cell-line, attention was payed to the analysis of some EMT molecular markers as well as cellular morphology, proliferation rate, migration ability, anchorage-independent cell growth capacity, secretome's MMP-9 content, and cell growth promoting capability, all of them considered as important indicators of carcinogenesis (Hanahan and Weinberg, 2000).

In addition to carcinogenic evaluation of nanoceria alone, co-exposure with other plausible compounds found in the environment is also an important factor to have into account since populations are rarely exposed to only one compound. Thus, in our study, with the intention of simulating a scenario were nanoceria coexists with tobacco, a well-known carcinogen targeting also mainly the lungs (Saha et al*.,* 2007), the interaction between these two compounds was studied. As reviewed, the mixture of chemicals contained in tobacco smoke condensate (CSC) is elevated and different mechanisms of action may be taking part in the CSC-induced malignant transformation (Hecht, 2002). Among them, ROS production and oxidative stress-induction are well-studied tobacco mechanisms of carcinogenesis (Valavanidis et al*.,* 2009). With this in mind, even though we did not find a direct application of nanoceria in cancer treatment as previously discussed, we evaluated the protective co-exposure effect as a possible indirect action mechanism. Therefore nanoceria could prevent ROS production due to its exhibited antioxidant properties in this cell line, delaying in this extent the cell transformation process.

Increases in the cell proliferation rate are one of the main hallmarks of cancer, as it has been extensively described in literature (Sherr, 1996). Focussing on this parameter we found that nanoceria did not alter cell proliferation rates, suggesting that these NPs do not interfere with cell cycle machinery and its regulation. Some other studies have evaluated the nanoceria potential in affecting cell time division. As with occurs with other biomarkers, conflictive results have been obtained. Thus, Rojanasakul et al*.* (2016) found increased rates for this parameter. In this case, the observed increases in cell growth were explained by a possible change in cerium state valences (Ce^{3+} and

Ce^{4+}). Thus, since moderate or high ROS generation can stimulate cell proliferation or cell death pathways, nanoceria redox cycling ability may determine ROS-associated impacts on growth. Inversely, Xiao et al. (2016) reported a decrease in cell division rate after acute treatment (10 µg/mL) of gastric cancer cells. In this situation authors found that nanoceria could promote the expression of putative ATP-dependent RNA helicase DEAH (Asp-Glu-Ala-His) and box helicase 15 (DHX15). Thus, as a mechanistic hypothesis, they suggested that increased expression of DHX15 in turn activates p38 MAPK signal pathway, leading to the inhibition of proliferation and migration in gastric cancer *in vitro* and *in vivo*. On the other hand, due to the well documented carcinogenic effects of CSC, high growth stimulation has been reported in previous studies (Jin et al*.,* 2004*)*. In agreement with these studies, after four weeks of treatment, decreased proliferation rates were observed in the highest concentration of CSC, as well as in the co-exposures. Interestingly, nanoceria seems to promote and enhance CSC growth effects.

EMT is a well-known process occurring in carcinoma-like lung cancer (Xiao et al*.,* 2010). As previously mentioned, the major characteristic of EMT is the conversion from epithelial cells to motile, invasive and migratory mesenchymal cells. In this dynamic process, epithelial cells lose cell polarity, cell-to-cell and cell-to-substrate adhesion decreasing the expression of epithelial molecular markers such as *CDH1*, while increasing the expression of mesenchymal markers such as *VIM*, Fibronectin or *CDH2*. In this process, also increased activity of some MMPs is observed and associated with the invasive phenotype. In this way, cancer cells acquire the capacity to migrate and invade the surrounding stroma and subsequently spread through the blood and lymphatic vessels to distant tissues (Kessenbrock et al., 2010).

Previous in *vitro* studies have indicated that various groups of active molecules found in cigarette smoke such as polycyclic aromatic hydrocarbons (PAH), nicotine-derived nitrosamine ketone (NNK), as well as the induction of ROS, can induce EMT through different signalling pathways (Zhao et al*.*, 2013; Wang et al*.*, 2014). Thus, higher levels of VIM and other mesenchymal markers, and a decrease in the expression of CDH1 was observed in smokers compared with normal non-smokers (Sohal et al*.*, 2010; Milara et al*.*, 2013). Partial similarities were found in our study where mesenchymal identity markers (*CDH2, VIM* and *ACTA2*) and epithelial markers (*CDH1* and *ZO1*) were analysed. Thus, treatments with both concentrations of CSC tended to maintain the level of expression of mesenchymal markers below controls, being this effect more pronounced in the case of co-exposed cells to nanoceria and CSC, where we observed a “U shape” behaviour described before in other cell transformation studies (Bach et

al., 2016). In addition, these markers experienced a progressive increased over time for cells exposed to nanoceria alone, indicating that in this case the treatment is affecting cells at the molecular level. It should be noticed that although gene expression patterns have been described in EMT, these changes do not occur at the same time and at the same level in all cell lines. In addition, modulations in mRNAs levels are continually occurring over time making difficult to observe stable expressions. Herein, the CSC associated "U shape" indicates deregulation of mesenchymal markers and a rising trend after 4 weeks of exposure. Extra analysis of transcripts for longer exposures could help us to understand this cell type specific EMT process. With regard to the epithelial markers *CDH1* and *ZO1*, we observed that treatment with nanonceria alone only produce very mild changes with respect to control cells. On the other hand, cells exposed to CSC alone or in combination with nanoceria evidenced a clear mRNA downregulation, being this trait considered as a hallmark of EMT that leads to destabilization of adherent junctions (Yilmaz and Christofori, 2009). Again the co-treatment produces a higher deregulation in all molecular markers analysed.

Change in cell morphology is a visual marker consequence of EMT. Coincident with the modification of cell-to-cell and cell-to-substrate adhesions, the epithelial cells adopt an extensively flattened and elongated mesenchymal morphology known as a "spindle like shape" (Nelson et al., 2008). At this time, also cytoskeletal intermediate filaments (IFs) undergo significant compositional change. Thus, epithelial cells, which normally express only keratin IFs (KIFs), initiate the expression of vimentin IFs (VIFs). Due to this change in IF composition, VIF expression has become a canonical molecular marker associated to EMT-associated morphology change (Mendez et al., 2010). Relating these concepts with our results, we observed clear changes in morphology after CSC5 exposure alone and in the co-exposures, in agreement with other carcinogenic markers. Regarding mesenchymal VIM transcript levels, conflicting results were observed since an initial decrease was observed. However, at week 4 when the morphological changes were visualized a rising trend was observed through a "U shape" expression. Also here, an extended time of exposure would help to relate morphological observed changes with molecular markers of EMT. On the other hand, nanoceria treatment did not induce changes in epithelial morphology of cells as also indicated by Asatis's work, where different cell lines such as cardiac myocytes (H9c2), human embryonic kidney (HEK293), lung (A549) and breast (MCF-7) carcinomas were studied (Asati et al., 2010).

Migration is an intrinsic cell ability that becomes dysregulated in early stages of cell transformation and, therefore, it is useful to study the initiation process. In our study nanoceria did not affect cell motility. However, other treatments promoted this process. CSC has shown to increase cell migration in several published studies. Thus, as reviewed by Akopyan and Bonavida (2006) the tobacco smoke carcinogen NNK, up-regulated cellular myelocytomatosis (c-Myc) and B cell leukemia/lymphoma 2 (Bcl2), two oncoproteins involved in the promotion of various cellular processes, including cell migration. In the same trend, higher migration rates were observed in our study at the higher concentration of CSC tested, as well as in the co-exposures. These findings show again how nanoceria could potentiate the effects of low dose CSC increasing and initiating migration capacity. In relation with this capacity, but contrary to our results, Xiao et al. (2016) found that nanoceria by itself inhibited the migration of gastric cancer cells. In their study, although the authors used similar concentrations (0.01–10 μg/mL) to that we used, they used acute 24 hours treatment.

Although the soft-agar assay (anchorage-independent colony formation assay) does not mimic the whole carcinogenesis process *in vivo*, the promotion of anchorage-independent cell growth is considered as one of the best *in vitro* mimicking biomarkers of cell transformation processes, linked to initiation stages in early tumorigenesis (Borowicz et al., 2014). Thus, different groups have used this technique to assay the carcinogenic effects of different compounds, including CSC (Veljkovic et al., 2011; Annangi et al., 2014; Bach et al., 2016). From our data, nanoceria treatment did not modulate the ability of cells to anchorage-independently growth. By the contrary, decreased number of colonies was observed when nanoceria treatment was compared with controls. In relation with this finding, Sighinolfi et al. (2016) investigated the potential initiator or promoter-like activity of different metallic NMs using the Balb/3T3 two-stage transformation assay. Among them nanoceria showed decreased number of foci by 65% in comparison to the positive control, suggesting a potential antagonism in the promotion of cell transformation. Apart from our study, only one more group has carried out the soft-agar assay using nanoceria in a long-term treatment study. In the already mentioned study, Rojanasakul et al. (2016) did not reported any significant increase in the number of colonies, evidencing one more time the low capability of this NM to induce cell transformation by itself. However, the significant increases in the number of colonies observed in CSC, and in nanoceria co-exposure treatments, clearly show positive results of an expected carcinogen, giving strength to the hypothesis of nanoceria as an enhancer of cell transformation induced by other carcinogens.

In cancer pathogenesis, one of the main concerns is the interaction between cancer cells with the surroundings stroma, because stroma is involved in tumor progression and invasion (Friedl and Wolf, 2003). This interaction takes place through the microenvironment provided by resident fibroblasts, endothelial cells, pericytes, leukocytes, and extra-cellular matrix (ECM) thanks to paracrine signalling (Pietras and Östman, 2010). Thus, these different cell types in the stromal environment are recruited by malignant cells to support tumor growth and facilitate metastatic dissemination. Among the changes produced in the stroma during the carcinogenesis process, the transdifferentiation of fibroblasts to CAFs plays a very important role in invasion and metastasis. Thus, in lung carcinoma Fromigué et al. (2003) reported the impact of the crosstalk between cancer cells and normal fibroblasts. Thus, in a co-culture model of lung tumor cells and normal pulmonary fibroblasts, exposure to cancer cells rendered the fibroblasts with a set of modulated genes, which potentially would affect the regulation of matrix degradation, angiogenesis, invasion, cell growth, and survival.

In our study, using the indirect soft-agar approach, the secretome of treated cells was evaluated in terms of extrinsic growth promotion ability. As occurs with the other biomarkers, the secretome of nanoceria treated cells did not modify the growth ability of other cell lines. This would indicate its unlikely carcinogenic potential and therefore the impossibility to generate changes in the tumor microenvironment. Interestingly, Alili et al. (2011) also studied tumor-stroma interactions addressing the effect of nanoceria in CAFs formation, and tumor invasion. Herein, they found that nanoceria down-regulate both the transdifferentiation of CAFs and the invasion of tumor cells. As a proposed mechanism they pointed out the redox ability of nanoceria to generate ROS and to induce CAFs transdifferentiation through transforming growth factor β1 (TGF-β1). Returning to our work, positive results were obtained regarding the ability of co-exposure's secretome to promote extrinsic cell growth. In these treatments, where tumoral behaviour was already observed, the effect of the nanoceria-CSC co-exposure seems to affect the tumor-stroma signalling crosstalk, increasing the aggressiveness of the tumoral status. Thus, the obtained results provide relevant information and highlight the importance of using the indirect soft-agar in the battery of assays used for the characterization of cell transformation processes. Further studies focusing on the characterization of these secretomes could give strength to the importance of co-exposures in cell transformation process of CSC, while shedding light to the relevance of specific molecules contained in the secretome (microRNAs, cytokines, exosomes etc) to unravel mechanisms associated to late stages of carcinogenesis.

MMPs have been implicated in cancer for more than 40 years. Specifically, these enzymes have been associated with cancer-cell invasion and metastasis. However, due to intense research effort during the last years in this field, new signalling functions between cancer cells and its microenvironment have been identified (Kessenbrock et al*.,* 2010). These proteases have an important role degrading and modifying ECM as well as cell-to-ECM and cell-to-cell contacts, therefore prompting detachment and migration of epithelial cells from the surrounding tissue (Radisky, 2005). MMPs are up-regulated in almost every type of human cancer, and their expression is often associated with poor survival (Di Nezza et al., 2002). Its abundance in the secretome of cancer cells is often representative of the amount of other tumor-related secreted factors (Egeblad, 2002). Therefore, the analysis of MMPs secretion is a common parameter studied in carcinogenesis. MMP-9 activity was examined in our study in chronically exposed BEAS-2B at the end of the exposure period. An increase was observed in CSC1, Ce+CSC1, CSC5 and Ce+CSC5-exposed cells, when compared to time-matched controls, evidencing a cancer-like feature. In this particular case, the co-exposure did not increase the effects of CSC alone, but reduced the levels. Considering the increased ability of co-exposures's secretome to potentiate tumor growth, as evaluated by the indirect soft-agar, it is assumable that MMP-9 does not represent the abundancy of other factors present in the microenvironment.

The potential underlying mechanisms of nanoceria co-carcinogenesis were studied here through the transcript levels of *FRA-1*. This gene is one of the most common components of AP-1, a basic leucine zipper (bZIP) transcription factor that regulates diverse genes and cellular processes such as cell proliferation, differentiation, invasion and apoptosis, among others; and it is considered to play an important role in tumorigenesis and progression (Young and Colburn, 2006). Interestingly, CSC's carcinogenesis mechanism has already been associated to *FRA-1* deregulation (Chu et al., 2005; Karamouzis et al., 2007). Thus, long-term exposure to cigarette smoke induces oxidative stress, leading to activation of stress-triggered kinases and potentiation of various important transcription factors, being AP-1 proteins an important target (Manna et al., 2006; Valko et al., 2006). Curiously, in our study the exposure to the lower dose (1 µg/mL CSC) significantly increase the mRNA levels of *FRA-1* in BEAS-2B cells with no signs of transformation. On the contrary, the exposure of 5 µg/mL reduced transcript levels in cells already exhibiting a transformed phenotype. Apparently, under our experimental conditions CSC stimulates *FRA-1* expression in non-transformed cells, but a downregulation is triggered once cells acquire a cancer-like phenotype. Thus, the role of *FRA-1* in malignancies is still controversial. Although it

is over-expressed in many human malignancies, including thyroid, oesophagus, colon, and breast (Young and Colburn, 2006), which would indicate an important role in tumorigenesis, other works revealed the contrary. Thus, Ma et al. found that *FRA-1* was down-regulated in NSCLC, compared with normal bronchial epithelium. Further, the low expression of *FRA-1* correlated with advanced tumor stage and poor survival (Ma et al*.,* 2009). In our study, when *FRA-1* was analyzed in cells co-treated with nanoceria and CSC that exhibit cancer-like phenotypic properties, *FRA-1* was also found to be significantly down-regulated. In the same direction, being *PTEN* a well-known tumor suppressor, altered *PTEN* gene expression have been associated with a wide range of human tumors (Salmena et al*.,* 2008). While mutation of the *PTEN* gene itself is an infrequent event in lung adenocarcinomas, loss of *PTEN* protein expression is seen in 39-77% of these tumors (Marsit et al*.*, 2005; Tang et al*.*, 2006). These observations support a profound involvement of *PTEN* down-regulation in the development of lung adenocarcinomas. Although *PTEN* has been studied extensively, its role in cigarette smoke induced carcinogenesis has not been deeply explored. However, Barbieri et al. (2008) proposed cigarette smoke to interact with the inflammatory cytokine IL-1B causing reduction of *PTEN* activity though the ROS/Src/EGFR-p38MAPK pathway. In our work *PTEN* transcripts appear to be moderately down-regulated in CSC treatment while high de-regulation was observed in co-treatments. Thus, the down-regulation found in our study may be of interest in terms of CSC+nanoceria carcinogenic mechanisms.

An important conclusion derived from our obtained results is that while low concentrations of CSC do not induce cell transformation, the interaction with nanoceria enhances its carcinogenic potential. Also, carcinogenic effects produced by higher effective concentrations of CSC are generally exacerbated by nanoceria. Therefore, nanoceria co-exposures should be taken into consideration requiring further detailed studies. It would be of interest to evaluate the effect of these interactions using other relatively common environmental toxicants, as the implications of the potential negative effects on human health would be of big importance. In this context, Snow et al*.* (2014) evaluated the interaction of nanoceria with diesel exhaust (DE), since this NM is frequently commercialized as a diesel additive for increasing fuel combustion efficiency while decreasing soot emissions. As in the case of CSC, DE exposure induces well-known adverse cardiopulmonary effects. Thus, nanoceria added to diesel fuel increases fuel burning efficiency but leads to altered emission characteristics and potentially altered health effects. Therefore, in close agreement with our results, after two day treatment of *in vivo* male Sprague Dawley rats several lung injury biomarkers

indicated that DE co-exposure induces more adverse pulmonary effects than DE alone (Snow et al., 2014). Also, Ma et al. (2014) focussed on the effects of the combined exposure to DE and nanoceria on the pulmonary system in the same rat model. In their study, although nanoceria and DE induced lung injury by themselves, pulmonary responses to the combined exposure could not be readily predicted by results from either single particle exposure. There is strong evidence, however, that these particles, through combined exposure, are co-localized in the lung tissues and are able to elicit multiple responses from lung cells, leading to the development of lung injury, granulomas, impairment of cell-mediated immunity, and pulmonary fibrosis. Thus, indicating that nanoceria generated in exhaust emission with DE from diesel may pose serious adverse health effects. These results reinforce the idea that studying the co-exposures of nanoceria with other environmental agents is essential given their oncogenic potential. It seems that although nanoceria by itself does not produce deleterious effects, the uncontrolled redox activity of this NM interacting with other compounds could lead to unexpected biological effects.

As a global assumption after the discussion of this part of the Thesis we can consider that although nanotechnology could provide important advances to society, responsible development will require adequate tiered toxicity screening workflows for human risk assessment (Nel et al., 2013). Thus, since a majority of NMs exposures of concern are likely chronic in nature, chronic exposure screening models should continue to be developed in order to better represent the carcinogenic process taking part *in vivo*. The use of this sub-chronic *in vitro* model for a neoplastic transformation testing strategy could help identifying genotoxic and non-genotoxic tumorigenic NMs, by capturing both initiation and promotion in early tumorigenesis (Creton et al., 2012; Rojanasakul et al., 2016).

4.2.2. Methodological approaches to overcome limitations associated to long-term treatment studies in the NM field.

When assessing NMs harmful effects, the use of environmental relevant exposures through *in vitro* long-term studies provides more reliable results than classical acute procedures (Annangi et al*.,* 2015; Vales et al*.,* 2015). However, considerations should be taken into account regarding NMs exposure procedures. It must be remembered that dispersion is a crucial step when working with NMs. Thus, NP long-term treatments require from repeated dispersion procedures each time the culture medium is changed or cells are sub-cultured, which is very time-consuming. In addition, small variability in the quality of each dispersion is likely to occur leading to differences in

different physico-chemical properties such as size distribution, surface area, solubility, surface charge, agglomeration/aggregation and/or crystal structure (Johnston et al., 2013). In close relation with this, several studies have shown that NMs induce different cellular mechanisms depending on their specific physico-chemical characteristics (Bai et al., 2010; Cho et al., 2010; Xu et al., 2010; McGuinnes et al., 2011; Pujalté et al., 2011; Kermanizadeh et al., 2012). Considering this fact, using different dispersions with eventually changing properties for long-term treatment exposures could generate accumulative modulatory effects through the exposure, which would generate data misinterpretations. The need of freshly prepared dispersions is also a bottleneck when different high-throughput techniques are meant to be used in the NM field. In this case, before any given assay different concentrations of different NMs are required at the same moment. This implies several hours of work previous to the assay, which is inconvenient in terms of organization, and at the end of the process the initial concentrations cannot be anymore considered as "fresh dispersions".

In front of these technical problems we proposed to aliquot and freeze NM dispersions in order to apply treatments with exactly the same physico-chemical properties. Then, we studied and proved that no difference exists between fresh and frozen dispersions of five different NMs regarding classical particle characterization parameters such as: primary and hydrodynamic size, zeta potential, cellular internalization, viability, generation of intracellular ROS, and ion release. To our knowledge, this is the first study focusing on the comparison between fresh and frozen dispersions. The implementation of this methodology is an important consideration when homogenised treatments are highly required.

One of the first steps when analysing the potential biological effects of NPs is their physico-chemical characterization. Information about primary size and morphology is important to predict possible NP-cell interactions (Albanese and Chan, 2011). In our study no significant differences were observed between freshly prepared and frozen samples regarding appearance, mean size or size distribution. However, it is important to study the hydrodynamically behaviour in suspension because it determines NP-cell interactions and cellular internalization (Albanese and Chan, 2011). Aggregation of NMs normally occurs in biological environments and takes place when “Van der Waals” attractive forces between particles are greater than the electrostatic repulsive forces produced by the nanostructure surface (Verwey et al., 1948; Derjaguin et al., 1993). The hydrodynamic size values obtained by DLS directly links with the ability to formed aggregates. In our case, although we showed some increase of size in comparison with

primary dimensions, no significant differences between fresh and frozen samples were observed.

Since no differences were observed regarding the physico-chemical properties of the selected NMs between fresh and frozen dispersions, no differences in their biological effects were expected. However, this is some that requires confirmation. Thus, to further validate our proposed approach (using frozen dispersions for long treatment studies), internalization, viability and intracellular ROS production parameters were evaluated in our BEAS-2B cell line.

As anticipated, the obtained data revealed no significant differences in cell internalization when measured directly by TEM and confocal microscopy, or indirectly by FACS. TEM images showed internalization of TiO_2-NP, ZnO-NP and CeO_2-NP being mainly confined into vacuoles as nano-agglomerates. On the other hand, no cellular uptake was observed for MWCNT, possibly due to difficulty of internalize long fibres of around 4 μm. Due to practical problems in the detection of Ag-NPs by TEM, confocal methodology was used for this specific case. Using this approach, we demonstrated high uptake of Ag-NP by BEAS-2B cells detected in the cytoplasm and reaching the nucleus, and no differences regarding the use of fresh or frozen dispersions were observed. In parallel, because of the possibility of using FACS technology as a measure of cellular uptake (Suzuki et al*.,* 2007), this technique was also used as an additional measure of NP internalization. Good correlations were observed between microscopic and cytometric techniques except for MWCNT. We assume that the observed differences were due to the toxicity exerted by these fibre-like NPs, intracellular structure and complexity changes. Being these parameters the base for FACS cell internalization analysis, results obtained from MWCNT lead to wrong interpretation. Then, FACS data obtained for MWCNT are not directly related with their internalization. Despite the assumed considerations, we conclude that no differences exist with regard to cellular uptake of the selected NMs according to the protocol used (fresh *vs* frozen).

Cellular viability is a basic parameter to be included in any study determining the biological effects of NMs. Four of the total five selected NMs produced toxic effects in BEAS-2B when fresh dispersions were used. Following with the trend observed in this study, when viability data was determined no differences in toxicity between fresh prepared dispersions and frozen dispersions were found, giving strength to our hypothesis.

Finally, due to the importance of ion release as a toxicity mechanism of some metallic NMs (Xia et al., 2008; Park et al., 2010), it is important to demonstrate that frozen concentrations do not alter the chemical stability of NMs and no variations in ions release are produced. Therefore, in order to analyse this parameter, inductively coupled plasma mass spectrometry (ICP-MS) was used. Among the four metallic NMs studied, ZnO-NP and Ag-NP are the ones that give off more ions, as reported by several groups (Fukui et al., 2012; Hsiao et al., 2015). In concordance, higher levels of dissolution were observed for these NPs in our study, although no biological differences were obtained regarding the fresh/freezing protocol. However, significant variations were observed for those NPs with a poor dissolution rate (TiO_2-NP and CeO_2-NP), although their total levels are barely significant. In these cases, no clear pattern was observed regarding the fresh/freezing protocol used, being the small ability to dissolve the possible cause of such a high variability. However, no cellular effects have been generally described related with the ion released from these particles (Griffitt et al., 2008; Xia et al., 2008). This, along with the insignificant values obtained, make us to assume that the observed differences in solubility do not induce biological differences between the two methodological protocols, regarding this endpoint.

The results obtained in this study support the implementation of this new methodology as an operative improvement in long-term *in vitro* studies. Therefore, the use of frozen samples would represent an important reduction of time, since two treatments and one cell passage are normally performed per week during several weeks or months. Additionally, and more importantly, a potential increase in the homogeneity of the results would be achieved. This strategy could also provide other benefits to the nanotoxicology field. Currently, the extension of high-throughput methodologies in NMs toxicity testing is limited by the bottleneck that supposes the time necessary to prepare different concentrations of different NMs to be tested. In this case, our proposal will help to extend the use of such high-throughput methodologies in the NM field.

5. CONCLUSIONS

5. CONCLUSIONS

According with the objectives raised in the frame of this Thesis with the aim of assessing the biological effects of nanoceria in an *in vitro* model, we conclude that:

1. Nanoceria exerts antioxidant and antigenotoxic properties in an epithelial lung cell line BEAS-2B following short-term treatments. Thus, cells pretreated with this NM are able to significantly quench the effects produced by a well-known oxidative compound.

2. Under our experimental conditions, no oxidative but antioxidant behavior of nanoceria was detected by the treatment of different cancer cell lines and forced tumor environments. This, rules out the use of this NM in cancer therapy as proposed by some authors.

3. The carcinogenic evaluation of *in vitro* long-term low-dose exposure of nanoceria in lung epithelial BEAS-2B cells, along with the effects associated to a common plausible tobacco (CSC) co-exposure, showed that although nanoceria did not induce cell transformation by its own, this NM exhibits a synergistic role on CSC transforming ability.

4. Equivalent physico-chemical properties and biological effects between fresh prepared and frozen NP dispersions indicated that a freezing NP dispersion procedure can be implemented as a solution for the methodological limitations associated to long-term treatment studies in the nanotoxicology field.

6. ANNEXES

6. ANNEXES

6.1. Annex 1: Study 2

Antioxidant potential of nanoceria in tumoral and transformed cells

Submitted paper

Antioxidant potential of nanoceria in tumoral and transformed cells

Laura Rubio[1], Ricard Marcos[1,2,*], Alba Hernández[1,2,*]

[1]Grup de Mutagènesi, Departament de Genètica i de Microbiologia, Facultat de Biociències, Universitat Autònoma de Barcelona, Cerdanyola del Vallès, Spain.
[2]CIBER Epidemiología y Salud Pública, ISCIII, Spain.

[*]Corresponding author at: Grup de Mutagènesi, Departament de Genètica i de Microbiologia, Facultat de Biociències, Universitat Autònoma de Barcelona, Campus de Bellaterra, 08193 Cerdanyola del Vallès (Barcelona), Spain. Phone: +34 93 581 20 52; Fax: +34 93 581 23 87;
E-mail address: ricard.marcos@uab.es (R. Marcos)
alba.hernandez@uab.es (A. Hernández)

Running Title: Nanoceria are antioxidant in cancer cells

ABSTRACT

In spite of the well demonstrated antioxidant properties of cerium oxide NPs (nanoceria; CeO_2NP) important controversy swirl over its use as a protective therapeutic agent. Among the different factors hypothesised as explanatory of the observed discrepancies, the cell-type variable is one of the most accepted. Our work aims to study the relevance of cell type (tumoral *vs* non-tumoral) in the antioxidant nanoceria capacity. We have determined the ability of nanoceria to reduce the levels of reactive oxygen species (ROS) generated by the antitumoral agent cisplatin in five different human tumoral cells. Results indicate that combined treatment with nanoceria was able to reduce the levels of induced ROS in practically all cases. Pro-oxidant effects were never observed. The growth of A549 cell line in a forced acidic environment showed that the antioxidant properties of nanoceria were not influenced by the culture pH. A normal mouse embryonic fibroblast cell line (MEF) and its arsenic-transformed isogenic counterpart (AsT-MEF) were also evaluated. As in the other cases, nanoceria elicited an antioxidant effect in both MEF and AsT-MEF. From our results we can conclude that the tumoral state of the cells is not a general argument to explain the non-protective role of nanoceria.

Key words: Nanoceria; ROS; tumoral cells; antioxidant; prooxidant; tumour microenvironment.

1. Introduction

Cerium oxide (CeO_2) is considered as a potent free radical scavenger due to its strong redox capacity. It exists in both trivalent (+3) and tetravalent (+4) state and may flip-flop between the two states in a redox reaction (Esch et al., 2005; Korsvik et al., 2007; Nelson et al., 2016). Alterations in this oxidation state results in oxygen vacancies or deficiencies in the lattice structure due to the loss of oxygen and/or its electrons. Interestingly, these changes are dynamic and may occur spontaneously or in response to different physical parameters (Esch et al., 2005) or physiological environments (Karakoti et al., 2008). Size is one of these important parameters as more oxygen vacancies are generated when size decreases (Deshpande et al., 2005; Reed et al., 2014). This finding has promoted the use of CeO_2 nanoparticles (CeO_2NP, nanoceria) as an antioxidant agent. Indeed, NPs such as nanoceria have emerged as potential therapeutic agents to be used in various oxidative stress diseases/disorders, including cancer (Celardo et al., 2011; Narayanan and Park, 2013; Walkey et al., 2015 Kwon et al., 2016). The potential antioxidant properties of nanoceria have been evaluated *in vitro* using different cellular types including human colon and lung fibroblasts (Colon et al., 2009, 2010) and breast epithelial cells (Tarnuzzer et al., 2005) exposed to radiation, neuronal rodent cells exposed to glutamate (Schubert et al., 2006), human umbilical vein cells submitted to H_2O_2 (Chen et al., 2013), and human bronchial epithelial cells exposed to potassium bromate (Rubio et al., 2016). In all the cases, the treatment of cells with nanoceria resulted in cell protection in front of the oxidative damage induced by the different pro-oxidant agents used.

These antioxidant properties have also been observed in *in vivo* models. Nude mice pre-treated with intraperitoneal injections of nanoceria showed a decrease in the levels of caspase 3-positive cells in the colonic crypt 4 hours after X-rays irradiation. In addition, significant increases in the expression of SOD2 protein were observed, suggesting that nanoceria is able to protect the gastrointestinal epithelium against radiation-induced damage by anti-oxidant mechanisms (Colon et al., 2010). In a study using a mice model of autoimmune encephalomyelitis of multiple sclerosis nanoceria treatment significantly reduced the free radical levels in the brain, alleviating the clinical symptoms and motor deficits associated with disease progression (Estevez and Erlichman, 2014). Furthermore, this antioxidant ability was also observed in *Drosophila* where nanoceria reduced the ROS levels induced by potassium bromate. At the same time, nanoceria elicited an anti-genotoxic effect by reducing the frequency of induced mutant clones (Alaraby et al., 2016).

Despite these well characterized antioxidants properties of nanoceria, some discrepant results have been published where nanoceria behaved as a pro-oxidant agent (Yokel et al., 2014). This has been reported in human neuroblastoma cells (Kumari et al., 2014), lung adenocarcinoma A549 cells (Mittal and Pandey, 2014), and in melanoma 518A2 and colorectal adenocarcinoma HT-29 cell lines (Pešić et al., 2015). Although some emphasis has been put in the physicochemical characteristics of the nanoceria used, more interesting is the approach pointing out on characteristics of the cell type used. Differences between normal and cancer cells have been observed (Perez et al., 2008) indicating that cancer cells would not be protected against H_2O_2-induced oxidative stress due to their acidic microenvironment. In fact, in the recent review carried out by Gagnon and Fromm (2015) authors reported more adverse effects when cancer cells were used, in comparison with those studies using non-cancer cells. Another important conclusion derived from this review is that the dose of the compound does not seem to be an important factor playing part in the observed effects, since adverse, null, and protective effects were found in different studies independently of the administered concentration. To help elucidate the adverse/ protective effects of nanoceria in cancer cells we have determined the nanoceria-associated changes in the levels of cisplatin-induced ROS in five different tumoral cells. Cisplatin has shown to induce ROS (Lee et al., 2016) and these effects are ameliorated by the use of antioxidant compounds as resveratrol and vitamin C (Lee et al., 2016; Leekha et al., 2016). In addition, the role of the acidic environment of cell culture medium was taken into account, as well as the genetic background of the normal *vs* tumoral set of cells. Thus, the effects of nanoceria in mouse embryonic fibroblasts transformed by 30 weeks of chronic arsenic exposure (AsT-MEF) -as indicated by morphological changes, increased proliferation, deregulated differentiation status, increased MMPs secretion, anchorage-independent cell growth and enhancement of tumor growth and invasiveness (Bach et al., 2016)- where compared to its isogenic normal counterparts.

Materials and methods

1.1. Cell lines and culture conditions

Five well known cancer cell lines namely A549, HCT116, Hep3B, Caco-2 and HeLa were used in this study. A549 is a human alveolar adenocarcinoma cell line provided by Dr. G. Linsel (BAUA, Germany). HCT116 is a human colon cancer cell line provided by Dr. M.A. Peinado (IRO, Spain). Hep3B is a human hepatoma cell line that was a generous gift from Dr. R. Depping (Universität Zu Lübeck, Germany). Caco-2 is a

human colorectal cancer cell line provided by Dr. V. Fessard (ANSES, France). HeLa is a human cervical cancer cell line provided by Prof. Collins (University of Oslo, Norway). We also used mouse embryonic fibroblasts (MEF) and their derived arsenic-transformed counterparts (AsT-MEF) generated in one of our previous studies (Bach et al., 2016).

A549, Caco-2, Hep3B and HeLa cell lines were maintained in DMEM high glucose medium (Life Technologies, NY, USA). HCT116 and MEF/AsT-MEF cell lines were maintained in DMEM/F12 (Life Technologies, NY, USA). All cell lines were supplemented with 10% foetal bovine serum (FBS; PAA®), 1% of non-essential amino acids (NEAA; PAA®, Pasching, Austria and 2.5 µg/mL plasmocin (InvivoGen, CA, USA) at 37 ºC in a humidified 5% CO_2 incubator.

The A549 cell line was also used to study possible changes in nanoceria-associated oxidant behaviour depending on cell culture characteristics. Two different cell culture conditions were assessed in this case; acidic extracellular pH and starving conditions. The compound 4-morpholineethanesulfonic acid hydrate (MES hydrate; Sigma-Aldrich, MO, USA) was used to decrease the medium pH from 8.31 to 6.58. Deprivation of FBS for 24 h in DMEM high glucose medium was used to starve A549 cells.

1.2. Nanoparticles characterization and dispersion

Nanoceria were purchased from Sigma-Aldrich (St Louis, MO, USA). According to the manufacturer, size and density were <25 nm and 7.13 g/mL, respectively. To ascertain the manufacturer´s information regarding size and morphology, transmission electron microscopy (TEM; JEOL JEM-2011) was utilized. Besides, characterization of hydrodynamic size and zeta potential of nanoceria dispersed cell culture medium by dynamic light scattering (DLS) and laser Doppler velocimetry (LDV) methodologies, respectively, was performed on a Malvern Zetasizer Nano-ZS zen3600 instrument. For these measurements, nanoceria were pre-wetted in 0.5% absolute ethanol and dispersed at 2.56 mg/mL in 0.05% bovine serum albumin (BSA) in double distilled water by 16 min of sonication, according to the Nanogenotox protocol (Nanogenotox, 2011). Subsequently, the sonicated nanoceria were dispersed in DMEM high glucose or DMEM/F12 with 10% FBS for the measurements.

1.3. Cell viability

Cell viability was determined by the Beckman counter method with a ZTM Series coulter-counter (Beckman Coulter, CA, USA). This device accurately counts cells (1-120 microns) with the Electrical Zone Method (EMZ) known as the Coulter Principle. The different cell lines were plated in 6 well plates in triplicate at a density of 1 x 10^5

cells/well and incubated overnight. Cells were then treated with 2.5, 5, 10, 50 and 100 µg/mL nanoceria for 24 h. Viability was determined comparing number of cells of treatments versus controls. Dead cells were removed washing two times with PBS (Bach et al., 2016). Cell toxicity was calculated from averaging three independent survival curves.

1.4. Assessment of intracellular generation of ROS by DCFH-DA and DHE assays

The intracellular generation of ROS was measured by flow cytometry using two different assays, the 6- carboxy-2,7´-dichlorodihydro-fluorescein diacetate **(**DCFH-DA) and the dihydroethidium (DHE) assays. All experiments performed with both protocols, with the different cell lines, and also with different cell culture conditions, were processed in the same way. Cells were seeded in triplicate in 24 well plates at a density of 5 x 10^4 cells/well and incubated overnight. Next day, cells were pre-treated with different concentrations of nanoceria for 2 h before the addition of 20 µM cisplatin (Sigma-Aldrich, MO, USA) in the same medium up to 24 h. Subsequently, cells were washed twice with PBS and incubated in the presence of 5 µM DCFH-DA or 10 µM DHE in serum free DMEM high glucose medium for 30 min at 37 ºC. Cells exposed to cisplatin alone were considered as positive control. After DCFH-DA and DHE exposure cells were trypsinized and immediately analysed by FACS Calibur. Data were evaluated using Flowjo Ver. 7.6.5 software. A minimum of three independent experiments were carried out.

2. Results

2.1. Characterization of nanoceria

Different experiments were carried out to certify that the nanoceria used in the study agreed with the specifications given by the supplier. In a first instance TEM images of nanoceria were used to determine both morphology and size (Figure 1A). As observed, they mostly showed cubic and triangular morphologies. Mean size distribution was calculated by measuring over 100 particles in random fields of view resulting in values of 9.52 ± 0.66 nm diameter (mean ± standard deviation) (Fig. 1B). This size matched well with manufacturer's indications (< 25 nm).

The average hydrodynamic radius and zeta potential values of nanoceria in suspension were 93.17 ± 5.10 nm and -10.6 ± 1.3mV, respectively (Figure 1C). From these values it could be inferred that nanoceria showed some aggregation or agglomeration.

2.2. Cell viability

Cell viability curves were carried out to determine the potential toxicity of nanoceria in all selected cell lines. Cells were exposed to a wide range of concentrations (from 2.5 to 100 µg/mL) for a 24 h period. As observed in Figure 2, no significant toxic effects were observed at the selected range of doses. The significant variations observed in Figure 2A are considered as marginal since no dose-effects were observed. Furthermore, the comparison between mouse embryonic fibroblasts transformed by 30 weeks of chronic arsenic exposure (AsT-MEF), with its concurrent control, did not show differences in cell viability in the range of doses evaluated (Figure 2B).

From these results, 2.5, 5 and 10 µg/mL nanoceria concentrations were selected to carry out the subsequent experiments evaluating the protective effects of nanoceria. Toxicity of cisplatin was determined using A549 cells and a LC50 of 50 µM was obtained (results not shown). Consequently, 20 µM was selected as a moderate toxic concentration. This concentration did not produced significant toxic effects in the different cell lines but produced a very clear increases in the levels of ROS.

3.3. Nanoceria effects on the levels of induced intracellular ROS

Flow cytometry was used to demonstrate intracellular ROS levels measured as DCFH-DA and DHE fluorescence intensity. As observed in all the experiments, exposure to cisplatin (20 µM, 24 h) produced high and significant increases of ROS in all the cell lines, supporting our view that it is a good positive control.

The DCFH-DA results showed that the treatment with nanoceria alone (2.5, 5 and 10 µg/mL; 24 h) produced significant decreases in the levels of basal endogenous ROS only in the HeLa cell line. The rest of cell types showed no significant variations in ROS production after nanoceria treatment when compared to their corresponding controls. For the combined exposures, cells were first treated with the different doses of nanoceria for 2 h (to preadapt cells) and cisplatin was subsequently added until the end of the 24 h-exposure period. Interestingly, all the combined treatments produced significant decreases in the levels of ROS when compared to the values induced by cisplatin alone as showed in figure 3. At this point it should be mentioned the results obtained with the HCT cell line where antioxidant effects were obtained only at 5 µg/mL of combined exposure; the effects observed at lower and higher concentrations (2.5 and 10 µg/mL) did not reach statistical significance. The results obtained by DHE assay confirmed the outcome previously observed with DCFH-DA. Thus, from the clear increase induced in intracellular ROS by cisplatin in all the cells lines, combined treatments with nanoceria produced significant scavenge of the oxidant molecules as showed in Figure 4. As in the case of DCFH-DA the antioxidant effect of nanoceria in

HCT cell line was weaker than in the other cell lines and although mild decreases were observed in comparison with cisplatin alone, no statistically differences were observed. From these results it is clear that nanoceria acts generally as an antioxidant agent on all the selected cell lines.

As comparisons on the effects of nanoceria between normal and cancer cells in all published studies have been done using cell lines with very distant genetic backgrounds, we used the isogenic cell lines MEF and AsT-MEF to avoid the influence of the genotype in the analysis. In our case MEF cells are non-tumorigenic whereas AsT-MEF exhibit a cancer-like phenotype induced by chronic exposure to the carcinogenic compound arsenic. As observed in Figure 5 and 6, the levels of ROS produced in transformed cells in both assays were higher than the observed in the non-transformed cells. Nevertheless, in both cell lines the antioxidant effect of the different doses of nanoceria was evident in the combined exposures. In both cases very significant decreases in the levels of ROS were observed.

Since cancer cells have an altered metabolism in comparison with normal cells, the effects of nanoceria on A549 cells cultured in two different conditions were assessed in this case using DFCH-DA. Acidic extracellular pH and starving conditions were evaluated and the results are indicated in Figure 7. As observed, cisplatin induced high levels of ROS regardless of the culture conditions, although the ROS levels obtained in standard conditions were much higher than those observed in acidic and starving conditions. On the other hand, treatment with nanoceria alone reduced significantly the levels of basal endogenous ROS in cells growing in starving conditions. When combined exposures were evaluated, all the combined treatments reduced significantly the levels of ROS induced by cisplatin alone. From these results it is clear that the antioxidant properties of nanoceria do not depend on the cell culture conditions.

3. Discussion

Our results do not support the idea of nanoceria behaving as a pro-oxidant compound in cancer cells. The treatment of several cancer cell lines with nanoceria did not enhance but reduces the levels of intracellular ROS induced by the potent pro-oxidant compound cisplatin. In this way, the reported data do not support the assumption that nanoceria acts either as an anti-oxidant or pro-oxidant compound depending on cell characteristics. The use of two different standard assays for the determination of the antioxidant potential of nanoceria gives strength to the obtained results. Thus, although both assays determine intracellular ROS each one reacts with different reactive molecules. While DCFH-DA penetrates cell membranes and reacts

with H_2O_2, $ONOO^-$, lipid hydroperoxides, and, to a lesser extent with superoxide, DHE reacts mainly with the latter. Therefore, these two assays cover the main panel of intracellular ROS and its combination is a good choice to analyse the effect of nanoceria in oxidative scenarios.

Different authors have supported the suggestive view that the higher sensitivity of tumour cells to nanoceria, in comparison with the normal surrounding cells, would reinforce the use of nanoceria as an antitumoral agent. This has been suggested for different cell lines such as human neuroblastoma (Kumari et al., 2014) and lung adenocarcinoma A549 (Mittal and Pandey, 2014) cell lines. Pešić et al. (2015) also observed a prooxidant behaviour in cancer cells by comparing a battery of four cancer and four normal cell lines. Authors assumed that antioxidant capacity was damaged in the cancer cells due to the prooxidant ability of nanoceria, and pointed out the idea that selective killing of cancer cells by nanoceria may be related to the difference of intracellular pH existing between cancer and normal cells. However, this hypothesis was not proved and authors encouraged for further clarification. In this context our results provide interesting data to help solving this controversy.

It must be pointed out that differential cytotoxicity is considered as one of the greatest challenges in chemotherapy and that high efforts are being put to identify anti-cancer drugs able to distinguish effectively between tumour and normal cells (Gao et al., 2014). Dextran coated nanoceria was observed to protect normal cardiomyocytes (H9c2) and human dermal fibroblasts (BJ) against hydrogen peroxide induced cytotoxicity. In contrast, no protection was observed in lung carcinoma cells (A-549) and breast carcinoma (BT-474) cells (Perez et al., 2008). Also, concentrations of nanoceria (polymer-coated) that were non-toxic for stromal cells showed cytotoxic, proapoptotic, and anti-invasive properties on melanoma cells (Alili et al., 2013). In this study, human dermal fibroblast (HDFs) and human microvascular endothelial cells (HMEC-1) were non-sensitive to 150 μM of dextran coated nanoceria, contrarily to what occurs with melanoma cells (A375). Similar results were reported in pancreatic cells, where pretreatment with nanoceria enhanced radiation-induced ROS production and cell death, preferentially in human pancreatic cancer cells (L3.6pl), when compared to normal pancreatic cells (hTERT-HPNE) (Wason et al., 2013).

On the other hand different studies showed that cancer cells were protected by nanoceria exposure, reinforcing our results. Thus, in the study of De Marzi et al. (2013) authors used three different human tumoral cell lines (A549, Caco-2 and HepG2). Non-important toxicity of nanoceria was observed after 24 h of exposure in A549 and Caco-2, but HepG2 showed significant acute toxic effects. Interestingly, long-term (10 days) exposures to nanoceria elicited toxic effects in all the used cell lines. In addition,

nanoceria acted as a protector in the three cell lines in front of the oxidative stress induced by H_2O_2, as evaluated using the comet assay. In the same direction, the induction of apoptosis and ROS generation by the tumour necrosis factor-alpha (TNFa) plus cycloheximide in the human histiocytic lymphoma cell line (U937) was significantly reduced by nanoceria. Noteworthy, this reduction was much more significant than that induced by classical antioxidants as trolox and N-acetyl cysteine (González-Flores et al., 2014). More recently nanoceria showed a protective effect on the oxidative stress induced by paraquat in HeLa cells. This effect was observed for both nanoceria and nanoceria containing nanoreactors, proving that both act as efficient ROS detoxification systems (Spulberg et al., 2015).

Besides of their cancerous origin the standard stablished tumoral cell lines usually present complex and unstable genomes prone to the accumulation of genetic changes. Thus, these cell lines can differ notably between laboratories, complicating the comparisons. On the other hand, the different genetic backgrounds existing between the normal and cancer cells used to compare the effects of nanoceria can suppose a limitation, as genome may influence the outcome. To avoid such uncertainties we have extend our study by using two recently generated isogenic normal and transformed cell lines (MEF and AsT-MEF). AsT-MEF was obtained by 30 weeks of chronic exposure to the carcinogenic compound arsenite, and showed all features of cancer cells such as spindle-like morphology, increased proliferation, de-regulated differentiation status, increased MMPs secretion, anchorage independent cell growth and enhancement of tumour growth and invasiveness (Bach et al., 2016). A protective effect of nanoceria was again observed in both MEF and AsT-MEF cells, reinforcing the idea that the tumoral origin or phenotype is not a sufficient strong cell characteristic to modulate the pro-oxidant/anti-oxidant attributes of nanoceria.

It is well stablished that tumours, and consequently tumour cells, have a different metabolism compared to normal cells (Vander Heiden et al., 2009). A common distinguishing feature of solid tumours is the presence of an acidic extracellular environment due to an upregulated glycolitic activity and production of lactic acid (Wu et al., 2007). In these conditions tumour cells show as extremely efficient in maintaining tumour cell pH in the alkaline range, despite the acidic surroundings (Parks et al., 2013). This acidic pH could affect the conversion of Ce^{4+} to Ce^{3+}, disrupting the reversibility of the redox system and consequently inhibiting the ability of nanoceria to scavenge more radicals (Perez et al., 2008). In this scenario, cancer cells would be only able of catalysing the conversion of highly unstable superoxide to far more stable H_2O_2, as acidic pH has been shown to inhibit the catalase activity of nanoceria (Alili et al., 2011; Wason and Zhao, 2013). To prove this hypothesis we acidified the medium of

our cancer cell line A549 by changing the pH from 8.31 to 6.58, and also by deprivation of FBS. We observed a significant decrease in the basal levels of ROS when treating with CeNPs in A549 cells and in starving conditions. No similar data have been found in the literature. We assume that this can be due to the ability of nanoceria of interacting and modulating free radicals, independently of the existing levels of ROS. Indeed, in the present study nanoceria behave as an antioxidant in almost all cell types analysed, but the strength of this ability is not equal in all of them, which can also explain the results obtained at the highest concentration of nanoceria in acidic conditions. Nevertheless, our results indicate that in neither of these culture conditions pro-oxidant behaviour of nanoceria was observed. At this point it should be indicated that the changes in the proportions of Ce^{4+}/Ce^{3+} observed by Perez et al. (2008) were done in acellular experiments where pH was acidified to 4.0, far away from the pH obtained in our experiment.

Summing up, our results do not support the general view that tumour cells present special sensitivity when compared to normal cells. Although cell characteristics could modulate in some way the observed outcome, physicochemical characteristics of nanoceria should be taken into account as more determinant modulators (Dowding et al., 2013; Grulke et al., 2014; Pulido-Reyes et al., 2015). Various factors, including synthetic routes, composition, purity, particle size, surface charge, and the use of non-stabilized nanoceria for *in vitro* studies have been proposed to explain the discrepancies between studies (Heckman et al., 2013). In fact, the efficiency of nanoceria particles has been associated with the decreasing particle size, which induces specific control of oxygen vacancies and determines their reactivity (Zhang et al., 2002). In addition, nanoceria aggregation in solution is supposed to be responsible for a decrease in their scavenging efficiency (Xue et al., 2011) and, furthermore, coating is also an important factor modulating nanoceria properties. Dextran coated nanoceria was demonstrated to show long-term stability in aqueous solutions without precipitation and without losing the protective effects towards agents inducing oxidative damage (Perez et al., 2008). In the same way, encapsulation of nanoceria in polymer vesicles reduced their toxicity, but preserving their antioxidant characteristics (Spulberg et al., 2015).

In conclusion, our results indicate that tumoral cell characteristics are not enough to explain the contradictory antioxidant/prooxidant activity reported for nanoceria. Other factors should be explored to completely understand the differential effects reported for nanoceria in different systems.

References

Alaraby, M., Hernandez, A., Annangi, B., Demir, E., Bach, J., Rubio, L., Creus, A., Marcos, R., 2015. Antioxidant and antigenotoxic properties of CeO_2 NPs and cerium sulphate: Studies with *Drosophila melanogaster* as a promising *in vivo* model. Nanotoxicology 9, 749-759.

Alili, L., Sack, M., Karakoti, A.S., Teuber, S., Puschmann, K., Hirst, S.M., Reilly, C.M., Zanger, K., Stahl, W., Das, S., Seal, S., Brenneisen, P., 2011. Combined cytotoxic and anti-invasive properties of redox-active nanoparticles in tumor-stroma interactions. Biomaterials 32, 2918-2929.

Alili, L., Sack, M., von Montfort, C., Giri, S., Das, S., Carroll, K.S., Zanger, K., Seal, S., Brenneisen, P., 2013. Downregulation of tumor growth and invasion by redox-active nanoparticles. Antioxid. Redox Signal. 19, 765-778.

Bach, J., Peremartí, J., Annangi, B., Marcos, R., Hernández, A., 2016. Oxidative DNA damage enhances the carcinogenic potential of chronic arsenic exposure. Arch. Toxicol. 90, 1893-1905.

Celardo, I., Pedersen, J.Z., Traversa, E., Ghibelli, L., 2011. Pharmacological potential of cerium oxide nanoparticles. Nanoscale 3, 1411-1420.

Chen, S., Hou, Y., Cheng, G., Zhang, C., Wang, S., Zhang, J., 2013. Cerium oxide nanoparticles protect endothelial cells from apoptosis induced by oxidative stress. Biol. Trace Elem. Res. 154, 156-166.

Colon, J., Herrera, L., Smith, J., Patil, S., Komanski, C., Kupelian, P., Seal, S., Jenkins, D.W., Baker, C.H., 2009. Protection from radiation-induced pneumonitis using cerium oxide nanoparticles. Nanomedicine 5, 225-231.

Colon, J., Hsieh, N., Ferguson, A., Kupelian, P., Seal, S., Jenkins, D.W., Baker, C.H., 2010. Cerium oxide nanoparticles protect gastrointestinal epithelium from radiation-induced damage by reduction of reactive oxygen species and upregulation of superoxide dismutase 2. Nanomedicine 6, 698-705.

Decan, N., Wu, D., Williams, A., Bernatchez, S., Johnston, M., Hill, M., Halappanavar, S., 2016. Characterization of *in vitro* genotoxic, cytotoxic and transcriptomic responses following exposures to amorphous silica of different sizes. Mutat. Res. Genet. Toxicol. Environ. Mutagen. 796, 8-22.

De Marzi, L., Monaco, A., De Lapuente, J., Ramos, D., Borras, M., Di Gioacchino, M., Santucci, S., Poma, A., 2013. Cytotoxicity and genotoxicity of ceria nanoparticles on different cell lines *in vitro*. Int. J. Mol. Sci. 14, 3065-3077.

Deshpande, S., Patil, S., Kuchibhatla, S., Seal, S., 2005. Size dependency variation in lattice parameter and valency states in nanocrystalline cerium oxide. Appl. Phys. Lett. 87, 133113.

Dowding, J.M., Das, S., Kumar, A., Dosani, T., McCormack, R., Gupta, A., Sayle, T.X.T., Sayle, D.C., von Kalm, L., Seal, S., Self., 2013. Cellular interaction and toxicity depend on physicochemical properties and surface modification of redox-active nanomaterials. ACS Nano 7, 4855-4868.

Esch, F., Fabris, S., Zhou, L., Montini, T., Africh, C., Fornasiero, P., Comelli, G., Rosei, R., 2005. Electron localization determines defect formation on ceria substrates. Science 309, 752-745.

Estevez, A.Y., Erlichman, J.S., 2014. The potential of cerium oxide nanoparticles (nanoceria) for neurodegenerative disease therapy. Nanomedicine 9: 1437-1440.

Gao, Y., Chen, K., Ma, J.L., Gao, F., 2014. Cerium oxide nanoparticles in cancer. Onco. Targets Ther. 7, 835-840.

Gagnon, J., Fromm, K.M., 2015. Toxicity and protective effects of cerium oxide nanoparticles (nanoceria) depending on their preparation method, particle size, cell type and exposure route. Eur. J. Inorg. Chem. 27, 4510-4517.

González-Flores, D., De Nicola, M., Bruni, E., Caputo, F., Rodríguez, A.B., Pariente, J.A., Ghibelli, L., 2014. Nanoceria protects from alterations in oxidative metabolism and calcium overloads induced by TNFα and cycloheximide in U937 cells: pharmacological potential of nanoparticles. Mol. Cell. Biochem. 397, 245-253.

Grulke, E., Reed, K., Beck, M., Huang, X., Cormack, A., Seal, S., 2014. Nanoceria: Factors affecting its pro- and anti-oxidant properties. Environ. Sci. Nano. 1, 429-444.

Heckman, K.L., DeCoteau, W., Estevez, A., Reed, K.J., Costanzo, W., Sanford, D., Leiter, J.C., Clauss, J., Knapp, K., Gomez, C., Mullen, P., Rathbun, E., Prime, K., Marini, J., Patchefsky, J., Patchefsky, A.S., Hailstone, R.K., Erlichman, J.S., 2013. Custom cerium oxide nanoparticles protect against a free radical mediated autoimmune degenerative disease in the brain. ACS Nano 7, 10582-10596.

Karakoti, A. S., Monteiro-Riviere, N. A., Aggarwal, R., Davis, J. P., Narayan, R. J., Self, W. T., McGinnis, J., Seal, S., 2008. Nanoceria as Antioxidant: Synthesis and Biomedical Applications. JOM. 60, 33-37.

Korsvik, C., Patil, S., Seal, S., Self, W.T., 2007. Superoxide dismutase mimetic

properties exhibited by vacancy engineered ceria nanoparticles. Chem. Commun. (Camb) 10, 1056-1058.

Kroll, A., Dierker, C., Rommel, C., Hahn, D., Wohlleben, W., Schulze-Isfort, C., Göbbert, C., Voetz, M., Hardinghaus, F., Schnekenburger, J., 2011. Cytotoxicity screening of 23 engineered nanomaterials using a test matrix of ten cell lines and three different assays. Part. Fibre Toxicol. 8: 9.

Kumari, M., Singh, S.P., Chinde, S., Rahman, M.F., Mahboob, M., Grover, P., 2014. Toxicity study of cerium oxide nanoparticles in human neuroblastoma cells. Int. J. Toxicol. 33, 86-97.

Kwon, H.J., Cha, M.-Y., Kim, D., Kim, D.K., Soh, M., Shin, K., Hyeon, T., Mook-Jung, I., 2016. Mitochondria-targeting ceria nanoparticles as antioxidants for Alzheimer's disease. ACS Nano 10, 2860-2870.

Lee, Y.J., Lee, G.J., Yi, S.S., Heo, S.H., Park, C.R., Nam, H.S., Cho, M.K., Lee, S.H., 2016. Cisplatin and resveratrol induce apoptosis and autophagy following oxidative stress in malignant mesothelioma cells. Food Chem. Toxicol. 9796-9807.

Leekha, A., Gurjar, B.S., Tyagi, A., Rizvi, M.A., Verma, A.K., 2016. Vitamin C in synergism with cisplatin induces cell death in cervical cancer cells through altered redox cycling and p53 upregulation. J. Cancer Res. Clin. Oncol. 142, 2503-2514.

Mittal, S., Pandey, A.K., 2014. Cerium oxide nanoparticles induced toxicity in human lung cells: role of ROS mediated DNA damage and apoptosis. Biomed. Res. Int. 2014, 891934

Nanogenotox, 2011 http://www.nanogenotox.eu/files/PDF/Deliverables/nanogenotox%20deliverable%203_wp4_%20dispersion%20protocol.pdf.

Narayanan, K.B., Park, H.H., 2013. Pleiotropic functions of antioxidant nanoparticles for longevity and medicine. Adv. Colloid Interface Sci. 201-202, 30-42.

Nelson, B,C., Johnson, M.E., Walker, M.L., Riley, K.R., Sims, C.M., 2016. Antioxidant cerium oxide nanoparticles in biology and medicine. Antioxidants (Basel) 5, 15.

Parks, S.K., Chiche, J., Pouyssegur, J., 2013. Disrupting proton dynamics and energy metabolism for cancer therapy. Nat. Rev. Cancer 13, 611-623.

Parks, S.K., Cormerais, Y., Marchiq, I., Pouyssegur, J., 2016. Hypoxia optimises tumour growth by controlling nutrient import and acidic metabolite export. Mol. Aspects Med. 47-48, 3-14.

Perez, J.M., Asati, A., Nath, S., Kaittanis, C., 2008. Synthesis of biocompatible dextran-coated nanoceria with pH-dependent antioxidant properties. Small 4, 552-556.

Pešić, M., Podolski-Renić, A., Stojković, S., Matović, B., Zmejkoski, D., Kojić, V., Bogdanović, G., Pavićević, A., Mojović, M., Savić, A., Milenković, I., Kalauzi, A., Radotić, K., 2015. Anti-cancer effects of cerium oxide nanoparticles and its intracellular redox activity. Chem. Biol. Interact. 232, 85-93.

Pulido-Reyes, G., Rodea-Palomares, I., Das, S., Sakthivel, T. S., Leganes, F., Rosal, R., Seal, S., Fernández-Piñas, F., 2015. Untangling the biological effects of cerium oxide nanoparticles: the role of surface valence states. Sci. Rep. 5, 15613.

Reed, K., Cormack, A., Kulkarni, A., Mayton, M., Sayle, D., Klaessig, F., Stadler, B., 2014. Exploring the properties and applications of nanoceria: Is there still plenty of room at the bottom? Environ. Sci. Nano 1, 390-405.

Rubio, L., Annangi, B., Vila, L., Hernandez, A., Marcos, R., 2016. Antioxidant and anti-genotoxic properties of cerium oxide nanoparticles in a pulmonary like cell system. Arch. Toxicol. 90, 269-278

Ruenraroengsak, P., Tetley, T.D., 2015. Differential bioreactivity of neutral, cationic and anionic polystyrene nanoparticles with cells from the human alveolar compartment: robust response of alveolar type 1 epithelial cells. Part. Fibre Toxicol. 12: 19

Schubert, D., Dargusch, R., Raitano, J., Chan, S.W., 2006. Cerium and yttrium oxide nanoparticles are neuroprotective. Biochem. Biophys. Res. Commun. 342, 86-91.

Spulber, M., Baumann, P., Liu, J., Palivan, C.G., 2015. Ceria loaded nanoreactors: a nontoxic superantioxidant system with high stability and efficacy. Nanoscale 2015 7, 1411-1423.

Tarnuzzer, R.W., Colon, J., Patil, S., Seal, S., 2005. Vacancy engineered ceria nanostructures for protection from radiation-induced cellular damage. Nano Lett. 5, 2573-2577.

Vander Heiden, M.G., Cantley, L.C., Thompson, C.B., 2009. Understanding the Warburg effect: the metabolic requirements of cell proliferation. Science 324, 1029-1033.

Walkey, C., Das, S., Seal, S., Erlichman, J., Heckman, K., Ghibelli, L., Traversa, E., McGinnis, J.F., Self, W.T., 2015. Catalytic properties and biomedical applications of cerium oxide nanoparticles. Environ. Sci. Nano 2, 33-53.

Wason, M.S., Zhao, J., 2013. Cerium oxide nanoparticles: potential applications for cancer and other diseases. Am. J. Transl. Res. 5, 126-131.

Wason, M.S., Colon, J., Das, S., Seal, S., Turkson, J., Zhao, J., Baker, C.H., 2013. Sensitization of pancreatic cancer cells to radiation by cerium oxide nanoparticle-induced ROS production. Nanomedicine 9, 558-569.

Wu, M., Neilson, A., Swift, A.L., Moran, R., Tamagnine, J., Parslow, D., Armistead, S., Lemire, K., Orrell, J., Teich, J., Chomicz, S., Ferrick, D.A., 2007. Multiparameter metabolic analysis reveals a close link between attenuated mitochondrial bioenergetic function and enhanced glycolysis dependency in human tumor cells. Am. J. Physiol. Cell Physiol. 292, C125-136.

Xue, Y., Luan, Q., Yang, D., Yao, X., Zhou, K., 2011. Direct evidence for hydroxyl radical scavenging activity of cerium oxide nanoparticles. J. Phys. Chem. C 115, 4433-4438.

Yokel, R.A., Hussain, S., Garantziotis, S., Demokritou, P., Castranova, V., Cassee, F.R., 2014. The yin: An adverse health perspective of nanoceria: Uptake, distribution, accumulation, and mechanisms of its toxicity. Environ. Sci. Nano 1, 406-428.

Zhang, F., Chan, S.W., Spanier, J.E., Apak, E., Jin, Q., Robinson, R.D., Herman, I. P., 2002. Cerium oxide nanoparticles: Size-selective formation and structure analysis. Appl. Phys. Lett. 80, 127-129.

FIGURE LEGENDS

Fig. 1. (A) Representative TEM image of nanoceria in pristine form. (B) Size distribution of nanoceria over 100 particles. (C) Values of average size and charge in culture medium by pre-wetting with 0.5% volume and steric stabilization using sterile-filtered 0.05% w/v BSA. Data represented as mean ± SEM.

Fig. 2. Cell viability data for the selected cell lines after nanoceria exposure. (A) Cell viability for standard cancer cell lines. (B) Cell viability for the isogenic normal (MEF) and transformed (AsT-MEF) cells. Cells were treated with a range of nanoceria concentrations in exposures lasting for 24 h. Viability data are plotted with respect to the control (untreated), which was set as 100%. *Statistically significant (P<0.05) differences.

Fig. 3. Levels of intracellular ROS measured by DCFH-DA in the different cancer cell lines. Cisplatin (20 μM, 24 h) was used as powerful agent inducing ROS (positive control). Cells were exposed to different concentrations (2.5, 5 and 10 μg/mL) of nanoceria for 24 h alone or in combination with cisplatin. Combined exposures supposed the addition of nanoceria for 2 h prior to the exposure to cisplatin until the end of the 24 h-period. Dotted line corresponds to 200% fold increase.Statistically significant differences ^{B}(P<0.01), ^{C}(P<0.001) versus the negative control, and ^{a}(P<0.05), ^{b}(P<0.01), ^{c}(P<0.001) versus the positive control (cisplatin).

Fig. 4. Levels of intracellular ROS measured by DHE in the different cancer cell lines. The information about this graph corresponds exactly with the described in Figure 3.

Fig 5. Intracellular ROS levels obtained by DCFH-DA observed in normal MEF cells and the transformed AsT-MEF cell lines. Cells were assessed for ROS intracellular production after cisplatin, nanoceria, and the combined exposures. In all cases exposures lasted for 24 h. Statistically significant differences ^{A}(P<0.05) versus the negative control, and ^{c}(P<0.001) versus the positive control (cisplatin).

Fig. 6. Intracellular ROS levels obtained by DHE observed in normal MEF cells and the transformed AsT-MEF cell lines. The information about this graph corresponds exactly with the described in Figure 5.

Fig 7. Intracellular ROS production of A549 cell line cultured in forced conditions measured by DCFH-DA. Different cell culture proceedings, being starving and acidic conditions. Cells were treated with cisplatin, different nanoceria concentrations, and the

combined exposures. In all cases exposures lasted for 24 h. Dotted line corresponds to 500% fold increase. Statistically significant differences ^{A}(P<0.05), ^{B}(P<0.01) versus the negative control, and ^{a}(P<0.05), ^{b}(P<0.01), ^{c}(P<0.001) versus the positive control (cisplatin).

FIGURES

Figure 1.

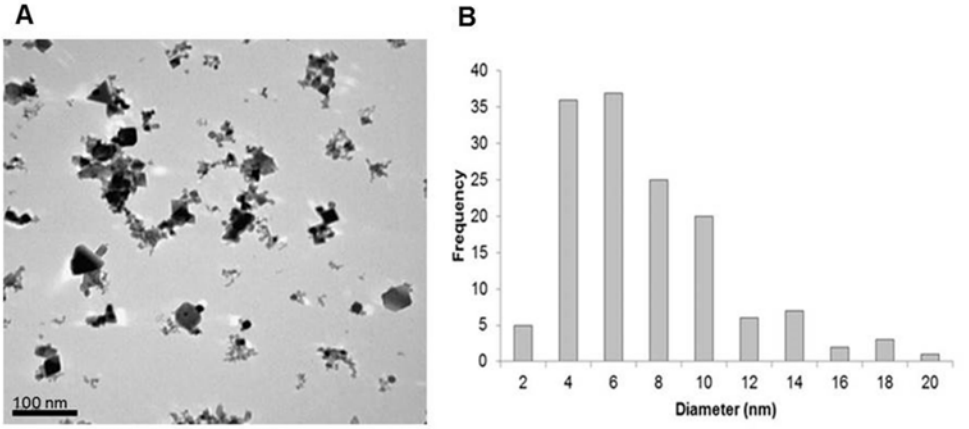

C

DLS		LDV			
Average diameter (nm)	PDI	Zeta potential ζ (mV)	Electrophoretic mobility (µm cm $V^{-1}s^{-1}$)	Viscosity (cP)	pH
95.74 ± 6.17	0.545 ± 0.031	-10.3 ± 1.9	-0.802 ± 0.149	0.88	7

Figure 2.

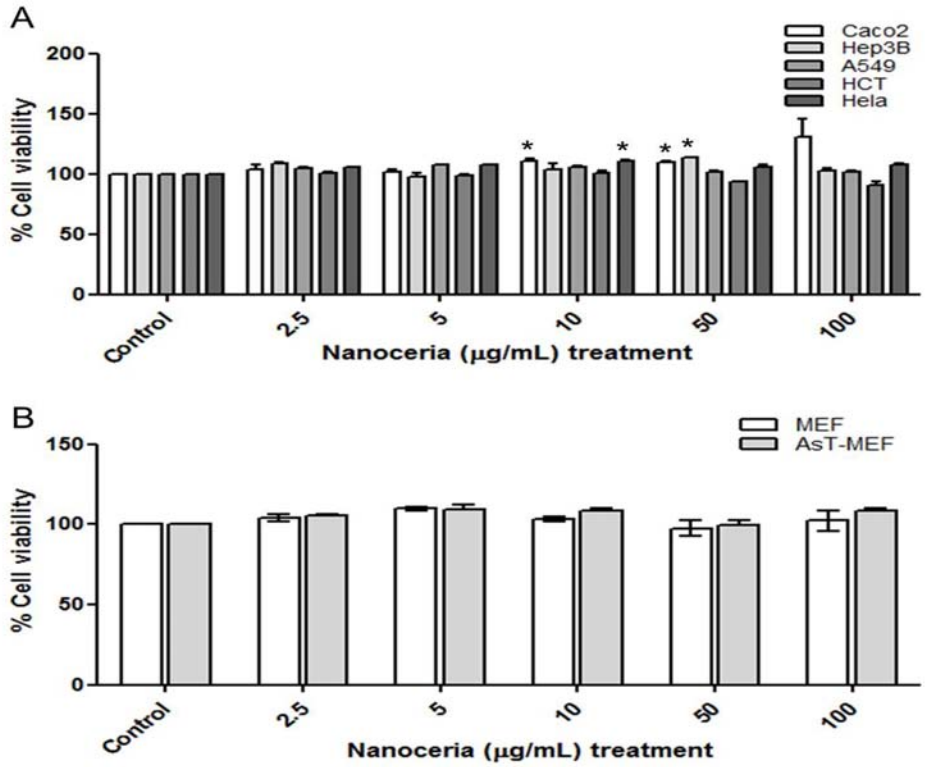

Figure 3.

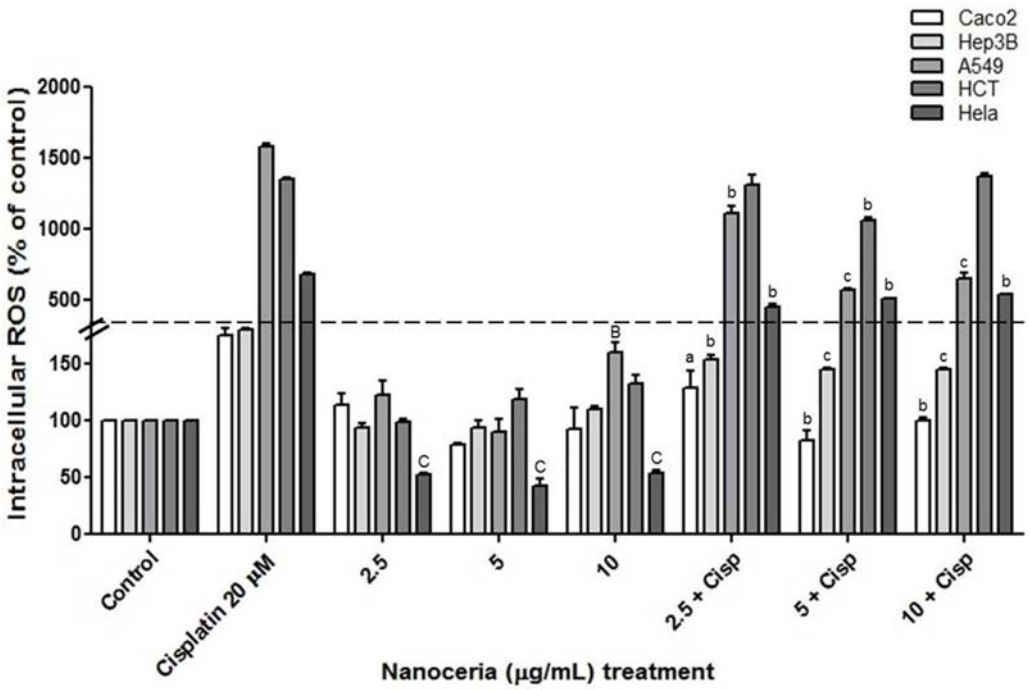

Figure 4.

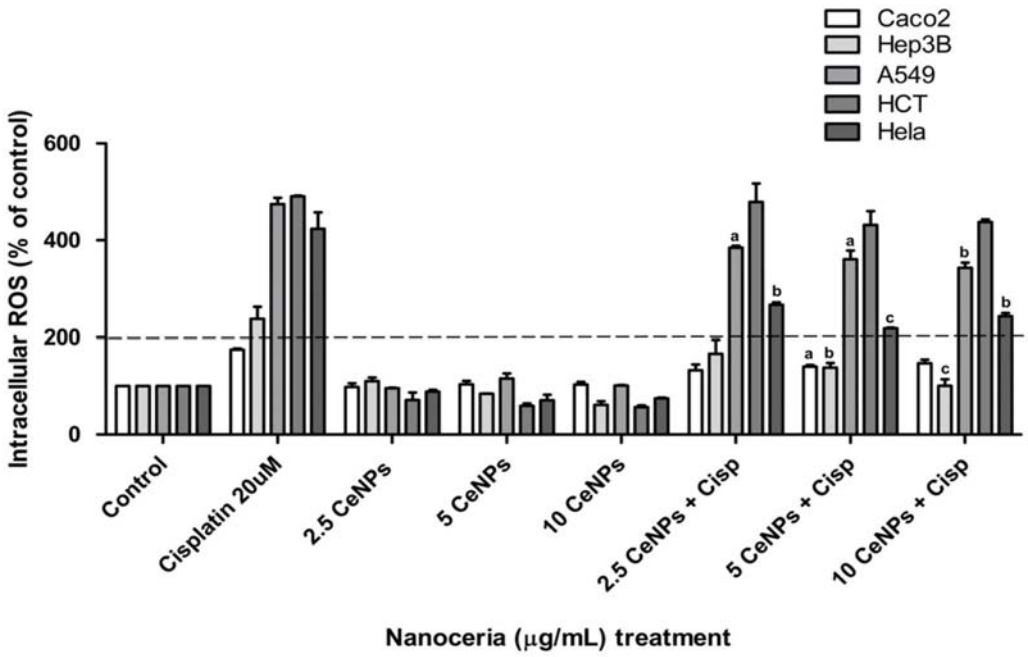

Figure 5.

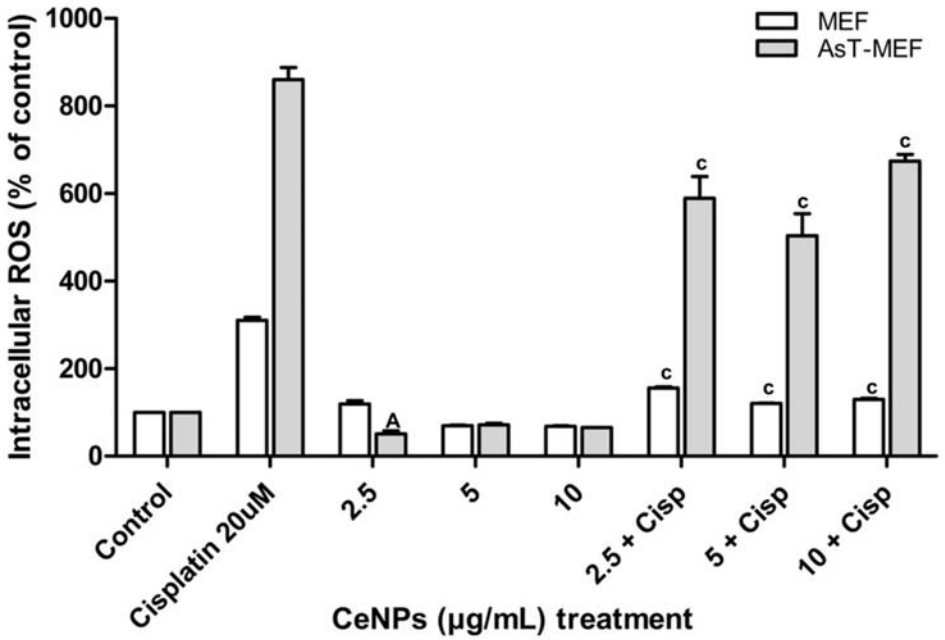

Figure 6.

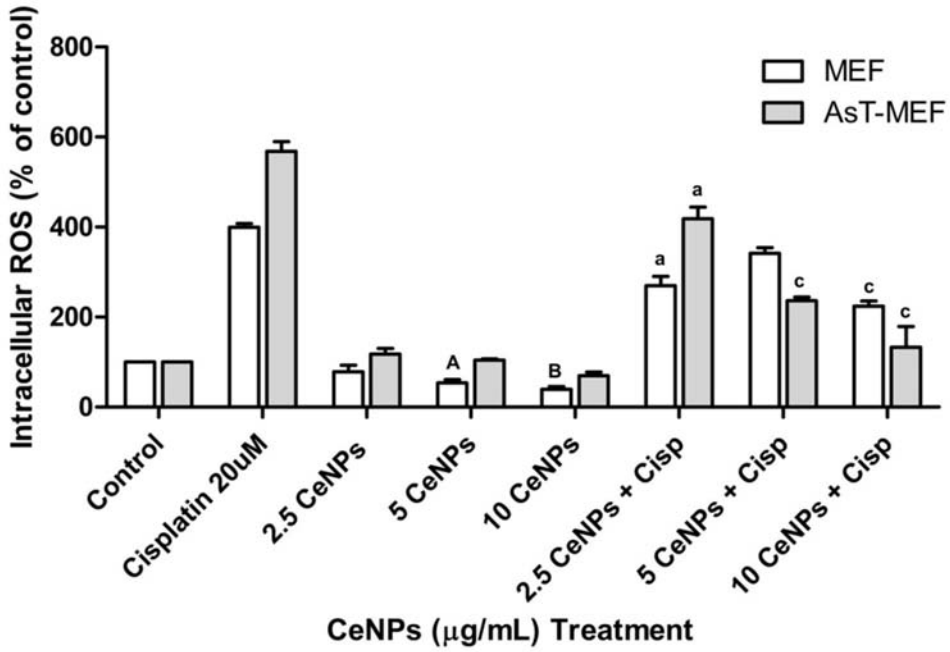

Figure 7.

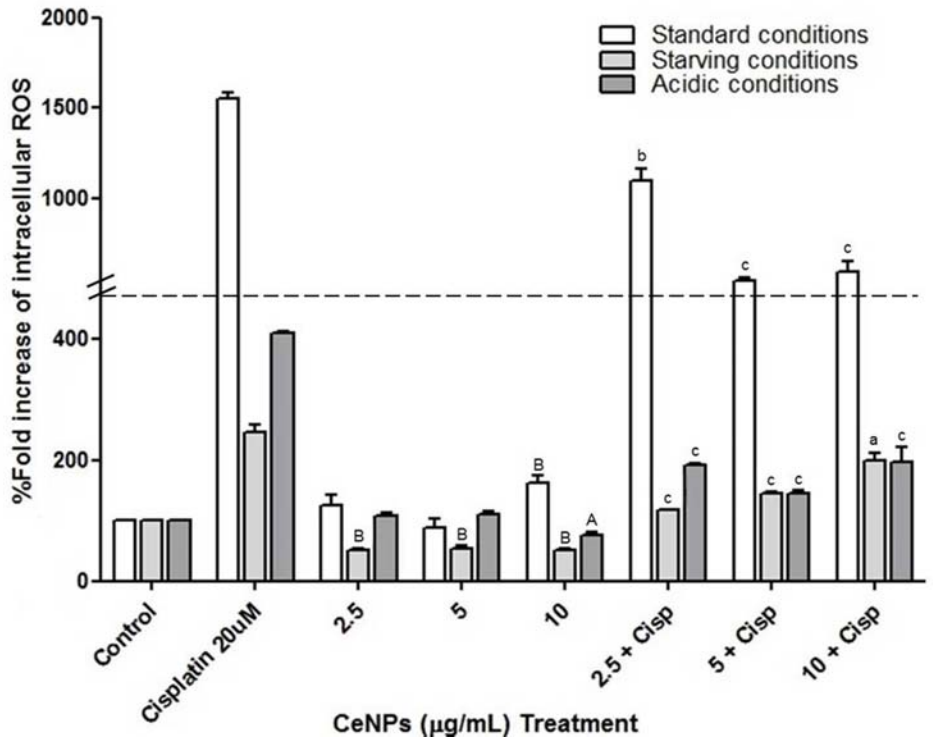

6.2. Annex 2: Study 3

Nanoceria do not protect lung epithelial cells from the transforming effects of tobacco long-term exposure

Submitted paper

Nanoceria do not protect lung epithelial cells from the transforming effects of tobacco long-term exposure

Laura Rubio[1], Jordi Bach[1], Ricard Marcos[1,2,§], Alba Hernández[1,2,§]

[1]Grup de Mutagènesi, Departament de Genètica i de Microbiologia, Facultat de Biociències, Universitat Autònoma de Barcelona, Bellaterra, Spain; [2]CIBER Epidemiología y Salud Pública, ISCIII, Spain.

[§]Corresponding authors at: Grup de Mutagènesi, Departament de Genètica i de Microbiologia, Universitat Autònoma de Barcelona, Edifici Cn, Campus de Bellaterra, 08193 Cerdanyola del Vallès (Barcelona), Spain.

E-mail: alba.hernandez@uab.es (A. Hernández)

ricard.marcos@uab.es (R. Marcos)

laura.rubio@uab.es (L. Rubio)

incubusboyd@hotmail.com (J. Bach)

Running title: Effects of tobacco and nanoceria long-term co-exposure.

Abstract

Background: Cerium oxide nanoparticles (nanoceria) have been proposed as a new promising agent in the treatment of different diseases, including cancer. However, several biosafety concerns need to be solved before its use in biomedical applications i.e. the lack of toxicological data under long-term exposure and co-exposure scenarios.

Methods: We evaluated the transforming effects of long-term exposure to nanoceria in lung epithelial BEAS-2B cells, along with the effects associated to a common plausible tobacco co-exposure. BEAS-2B cells continuously exposed to 2.5 μg/mL of nanoceria alone or in combination with 1 and 5 μg/mL of tobacco smoke condensate (CSC) for up to 6 weeks were monitored for changes associated with the acquisition of an oncogenic phenotype.

Results: Results evidence no transforming ability of nanoceria in BEAS-2B cells. However, results support a synergistic role on CSC transforming ability, as cells co-exposed to nanoceria-plus-CSC, when compared to cells exposed to CSC alone, showed a more noticeable spindle-like phenotype, an increased proliferation rate, higher degree of differentiation status dysregulation, higher migration capacity, increased anchorage-independent cell growth and a secretome with higher levels of MMP-9 and cell growth promoting capability. When mRNA expression of *FRA-1* was evaluated as a mechanism of tobacco-induced transformation, nanoceria co-exposure was again found to exacerbate the observed expression changes.

Conclusions: Long-term nanoceria exposure cannot be considered safe as it may increase the oncogenic potential of other environmental agents. More attention needs to be paid to long-term approaches prior to an eventual application of nanoceria in biomedicine.

Keywords: CeO_2NP, Nanoceria *in vitro* long-term exposure, Tobacco smoke condensate co-exposure, Cell transformation, Lung BEAS-2B cells.

Background

Hundreds of thousands of products containing nanomaterials (NM) have been settled in industry and in regular consumer products over the last years, due to the new and useful properties of materials at the nanometric scale. Several estimates suggest that the use of NM will continue experiencing an exponential increase, as substantial economic and technical resources are being dedicated to the study and design of new NM with industrial applicability. On the other side of the coin, the effects in occupationally and environmentally exposed population are uncertain, and the situation aggravates if we take into account that -precisely due to its small size- NM are able to strongly react with biologic material. The European Agency for Safety and Health at Work (EU-OSHA) has quantified in 20 years the discrepancy between the knowledge of the commercially available NM-associated effects and its impact on human health and environment [1]. We are facing a new scenario of exposure that needs the development of new aproaches to be used for a correct risk assessment, and to establish a regulatory framework where the exploitation of the new properties of NM is done guarantying the safety of the general population.

In the particular case of cerium dioxide nanoparticles (CeO_2NP, nanoceria), its availability as one of the most abundant rare earth oxides has prompted research on the synthesis and development of functional ceria nanoparticles. As a result, nanoceria is increasingly used in a variety of industrial and commercial applications, including catalysis [2] -as a diesel fuel additive to increase fuel combustion efficiency and decrease soot emissions [3]-, in chemical mechanical planarization/polishing [4], in semiconductors, in toner formulations [5], and as an additive in various nanocomposites, as reviewed [6]. The inevitable increase in consumer and occupational exposures raises the need for a comprehensive toxicological characterization of nanoceria [7]. Noteworthy, several companies and organizations have already identified nanoceria as a high priority material for toxicological evaluations [8, 9].

Nowadays, the medical and cancer applications of NP are considered as one of the most promising fields of nanotechnology [10]. Among the already implemented uses are drug delivery, gene therapy and cancer diagnosis and treatment [11]. In this sense, metal oxide NP are gaining interests in the scientific and medical communities [12]. Out of several metal oxide compounds with such potential applications, nanoceria have emerged as a promising therapeutic agent to be used in various oxidative stress diseases/disorders, including cancer [13]. From the chemical point of view, cerium can exist in two oxidation states, Ce^{3+} and Ce^{4+}. At the nanoscale, the structure of

nanoceria permits the coexistence of both oxidation states on the surface. This coexistence, along with its low reduction potential, allows nanoceria to switch between the two oxidation states, catalyzing ROS-detoxifying reactions while simultaneously regenerating reduced Ce^{3+} ions on the NP surface [14]. Thus, nanoceria is consistently shown to exhibit superoxide dismutase (SOD)-mimetic activity [15], as well as catalase-mimetic activity [16], supporting its applicability in the treatment against diseases related with increasing levels of reactive oxygen species (ROS), even as an antitumoral agent, since it is known that ROS contributes to cell transformation.

Previous studies in our Group corroborated the ability of nanoceria to quench ROS induced by potassium bromate, a well-known oxidant agent, in lung epithelial BEAS-2B cells [17]. In that work, several biological markers of damage and stress were found to be decreased by nanoceria, including cell mortality, genotoxic and oxidative DNA damage and expression of the oxidative stress-induced genes *SOD2* or *HO-1*, corroborating the beneficial effects of nanoceria as an antioxidant agent in lung epithelial cells under an acute regime of exposure. Other authors have been able to show the same protective effect *in vitro* using different cellular types including human colon, lung fibroblast and breast epithelial cells acutely exposed to radiation [18-20], neuronal rodent cells acutely exposed to glutamate [21], and human umbilical vein cells submitted to acute doses of hydrogen peroxide [22]. These antioxidant properties have also been observed in *in vivo* models. Mice pre-treated with nanoceria showed an amelioration of the gastrointestinal radiation-induced damage by anti-oxidant mechanisms [20]. Also, nanoceria treatment significantly reduced the free radical levels in the brain of mice with autoimmune encephalomyelitis of multiple sclerosis, preventing from disease progression [23], and it was able to reduce the ROS levels and the genotoxic effects induced by potassium bromate in *Drosophila* [24]. Despite these experimental evidences, several discrepant results have been published where nanoceria behaved as pro-oxidant agent [25] and/or exhibit signatures of toxicity/genotoxicity both *in vitro* and *in vivo,* as reviewed [26]. This controversy regarding its antioxidant behaviour along with its concerns of biosafety evidence the need of further research before this interesting catalytic material can be applied in biomedical applications with security. Although *in vitro* studies have certain limitations to represent kinetics and biodistribution of nanoceria -and NP in general- taking part in an *in vivo* exposure, they are useful to resolve some of the many unknowns of nanoceria's adverse effects. *In vitro* studies can be used for long-term exposure at low environmentally relevant doses, to analyse cell transformation, to compare short *vs* long-term effects, to characterize effects of long-term co-exposures, and to assess

mechanisms of genotoxicity/carcinogenicity, all of this points being recommendations necessary to clarify the safety and usefulness of nanoceria as a therapeutic antioxidant agent [26]. Taking this into account, in the present work we have used BEAS-2B cells as an *in vitro* pulmonary model of long-term exposure to nanoceria, as inhalation is the most likely route of human unintentional exposure to nanoceria. To evaluate the safety of the exposure (2.5 µg/mL of nanoceria for 6 weeks), several hallmarks of cancer were analysed through the exposure period. The same was done to evaluate nanoceria potential antioxidant protective effect, in this case in BEAS-2B cells co-exposed to nanoceria and tobacco smoke condensate. Cigarette smoke is the most important environmental risk factor for the development of lung cancer and it is known to have carcinogenic potential in the lung by oxidant mechanisms of action [27, 28].

Methods

Cigarette smoke condensate and cerium oxide nanoparticles

Cigarette smoke condensate (CSC) was purchased from Murty Pharmaceuticals (Lexington, KY, USA). As per the manufacturer's protocol, CSC was prepared by smoking University of Kentucky's 3R4F Standard Research Cigarettes on an FTC Smoke Machine. The condensate was extracted with DMSO by soaking and sonication to prepare a 4% (40 mg/mL) solution. Cerium dioxide nanoparticles (CeO_2NPs; nanoceria) were bought from Sigma-Aldrich (St Louis, MO, USA). According to previous studies in our lab, its size distribution averages 9.52 nm in diameter [17]. For the chronic treatment, CeO_2NPs were pre-wetted in 0.5% absolute ethanol and dispersed at 2.56 µg/mL in 0.05% bovine serum albumin (BSA) in sterilized Milli-Q water (Millipore, MA, USA) by 16 min of sonication.

Cell culture and in vitro long-term exposure

BEAS-2B lung epithelial cells were originally provided by Dr. H. Norppa (Finnish Institute of Occupational Health) and were grown as a monolayer with DMEM medium (Gibco, Paisley, UK) supplemented with 10% fetal bovine serum (FBS; PAA, Pasching, Austria), 1% non-essential amino acids (NEEA; PAA) and 2.5 µg/mL plasmocin (InvivoGen, CA, USA). Colorectal carcinoma HCT116 cells were cultured in DMEM/F12 medium (Gibco, Paisley, UK) containing 10% FBS, 1% NEEA and 2.5 µg/mL plasmocin. All cell lines were maintained in a humidified atmosphere of 5% CO_2 at 37 °C. BEAS-2B cells were continuously exposed for 6 weeks to 1 and 5 µg/mL sub-toxic concentrations of cigarette smoke condensate (CSC1 and CSC5), 2.5 µg/mL nanoceria or the combinations (Ce+CSC1 and Ce+CSC5). Concentrations of CSC were selected

based on 24 and 48 h toxicity data (data not shown). Nanoceria concentration was chosen according to previous data showing the highest antioxidant effects in BEAS-2B cells [17]. BEAS-2B cells were maintained in T-75 flasks and passaged weekly at a cell density of $0.5x10^5$ cells. Medium was replaced every 48 h and passage-matched controls were maintained for comparisons.

Cell morphology

Cell morphology was assessed throughout the exposure period by inverted microscopy. Images (20X objective) of the different treatments were taken at the end of the exposure period.

Cell proliferation

BEAS-2B cells treated with CSC and/or nanoceria were assessed for cell proliferation at the end of the exposure period. Treatments and passage-matched controls were plated in triplicates at $1x10^5$ in 6-well plates and grown for three days under normal conditions. At 24-h intervals, cells were collected by trypsinization and counted by Beckman Coulter® method. Proliferation was defined as time necessary for a population doubling to occur and was calculated according to the equations referred in http://www.doubling-time.com/compute.php.

Total RNA extraction and real-time RT-PCR

Expression changes associated with the differentiation cell status were assessed throughout the exposure by real-time RT-PCR. Total RNA from BEAS-2B cells was extracted using TRIzol® Reagent (Invitrogen, CA, USA) following the manufacturer's instructions. RNase-free DNase I (DNAfreeTM kit; Ambion, UK) was used to remove DNA contamination. The first-strand cDNA synthesis was performed using 1 µg of total RNA and the transcriptor first-strand cDNA synthesis kit (Roche, Basel, Switzerland). The resulting cDNAs were subjected to real-time 385 well plate PCR analysis on a LightCycler 480, to evaluate the relative expression of different genes. Epithelial to mesenchymal transition markers (*CDH2, Vimentin, Acta2, CDH1, ZO1, PTEN*) were analysed during week 0 (24 h treatment), 1, 2 and 4. *FRA-1* was analysed at week 6 of treatment as a CSC-related marker of carcinogenesis mechanism. The expression of *B2M* was used in all cases as the housekeeping control. The primers used are listed in supplementary Table 1. Each 20 µL of reaction volume contained 5 µL of cDNA, 10 µL of 2×LightCycler 480 SYBR Green I Master (Roche, Manheim, Germany), 3 µL of H2O and 1 µL of each primer pairs at a final concentration of 100 nM. The cycling parameters began with 95 °C for 5 min, then 45 cycles of 95 °C for 10 s, 61 °C for 15 s

and 72 °C for 25 s. Cycle time (Ct) values were calculated with the LightCycler software package and then normalized with B2M data.

Wound healing assay

The migration assay was performed to evaluate the effect of the different treatments in cell mobility at the end of the exposure period. Cells were seeded in a 24 well plates by triplicates at 0.8×10^5 cells per well and allowed to reach confluency. A scratch was made on the monolayer using a 200 µL pipette tip, and then washed with PBS twice to remove the floating cells and debris. DMEM 2% FBS was used to slow down the cell division. Three precise coordinates of each wound was photographed using an inverted microscopy at 4 h-intervals for 12 h. The wound area of each time point was measured using ImageJ software and the percentage of wound closing was calculated and compare to that of control cells.

Soft-agar assay

Colony formation in soft-agar was performed in long-term exposed BEAS-2B cells and passage-matched controls at the end of the exposure period, as previously described [29], to assess the cell's capacity for anchorage independent growth. BEAS-2B cells for the different treatments were collected and passed through a 30-µm mesh to obtain single cell suspensions. Subsequently, $6.5x10^4$ cells in 1.75 mL of DMEM containing 10% of FBS, 1% NEEA, 1% and 2.5 µg/ mL plasmocin were mixed in a 1:1:1 ratio with 2×DMEM containing 20% of FBS, 2% NEEA, 2% L-Glu 200 mM and 2% of penicillin–streptomycin and with 1.2% of bacto-agar (DIFCO, MD, USA). This mixture was enough to prepare triplicates containing $2x10^4$ cells each by dispensing 1.5 mL of the mixture over a 0.6% base agar (in supplemented 2×DMEM) in each well of a 6-well plate. Plates were allowed to sit for 45 min and then kept in the cell incubator for 30 days. Cells that were able to form colonies were stained by 24-h incubation with 1 mg/mL of (2-p-iodophenyl)-3-3(p-nitrophenyl)-5-phenyl tetrazolium chloride (INT; Sigma, MO, USA). Plates were scanned and colony counting was performed using the colony cell counter enumerator software OpenCFU (3.9.0) [30]. A modified version of the assay was performed using 72 h conditioned media (CM) from long-term exposed BEAS-2B and passage matched controls to assess its capacity of promoting the growth of surrounding tissue. HCT116 cells were collected and passed through a 30-µm mesh to obtain single cell suspensions. Subsequently, $3.5x10^4$ cells were suspended in 1.75 mL of BEAS-2B CM and mixed in a 1:1:1 ratio with supplemented 2×DMEM and 1.2% of bacto-agar. This mixture was enough to prepare triplicates containing $1x10^4$ cells in each well. The following remaining steps were performed as indicated above. HCT116

cells in top-agar mixture with and without FBS were used as positive and negative controls, respectively.

Secretion of MMP-9 by zymmography

The activity of secreted matrix metalloproteinase 9 (MMP-9) was examined in chronically exposed BEAS-2B and passage-matched controls at the end of the exposure period. Cells were cultured in basal medium (without serum or supplements) for 72 h, the CM was collected and secreted MMP-9 activity was measured by a standard zymographic method with reagents from Bio-Rad (Hercules, CA, USA) following the manufacturer's instructions. Briefly, samples were resolved in 10% precast gels with gelatine by SDS-PAGE at 100 V for 90 min and then incubated in 1x zymogram renaturing buffer for 30 min. Subsequently, gels were incubated overnight with 1x zymogram-developing buffer at 37 °C to achieve maximum sensitivity. Gels were then stained with 0.1% of Coomassie brilliant blue R-250 for 1 h and distained in methanol/acetic acid/dH2O solution (4:1:5) until the areas of protease activity appeared as clear bands against a dark blue background. The area of the bands was measured densitometrically using the ImageJ analysis program.

Statistics

Unpaired Student's *t*-test or analysis of variance followed by Dunnett's multiple comparison test was performed, as appropriate, to compare treated cells with untreated time-matched controls at respective time points. In all cases, a two-sided $P < 0.05$ was considered statistically significant.

Results

Cell morphology and proliferation of long-term exposed BEAS-2B cells

Evaluation of cell morphology and growth properties of CSC and/or nanoceria-exposed BEAS-2B cells through the exposure showed that at week 6 cells started to exhibit different morphology patterns, depending on the treatment. Control cells, cells exposed to nanoceria alone (Ce 2.5 µg/mL) and cells exposed to the lower dose of CSC (CSC1; 1µg/mL) showed no appreciable changes in cell morphology during the complete duration of the exposure (Figure 1A). Cells exposed to the higher dose of CSC (CSC5; 5 µg/mL) and co-exposed Ce+CSC1 and Ce+CSC5 cells exhibited spindle-like shape and tended to lose cell adhesion. Interestingly, at the same time-of-exposure, cells co-exposed to tobacco and nanoceria showed a clear increase in the proliferation rate when compared with time-matched controls or cells exposed to CSC alone (Figure 1B).

In fact, population doubling times of the above mentioned co-treatments decreased from 23.29±1.72 h of CSC1 to 16.46±0.31 h of Ce+CSC1, and from 18.55±0.09 h of CSC5 to 14.81±0.30 h of Ce+CSC5. Exposure to nanoceria alone showed no effects in the proliferation rate.

Differentiation status of long-term exposed BEAS-2B cells

The altered mRNA expression of *CDH2*, *VIM*, *ACTA2*, *CDH1*, *ZO1* and *PTEN* genes in BEAS-2B cells, long-term exposed to CSC and/or nanoceria, were studied as indicators of epithelial to mesenchymal transition and cellular differentiation status (Figure 2 and 3). Overall, all treatments showed a certain degree of dysregulation of gene signatures responsible for BEAS-2B's differentiation program, although with marked differences between them. Thus, the mesenchymal identity markers *CDH2*, *VIM* and *ACTA2* (Figure 2 A and 3A) experienced a progressive increased over time for cells exposed to nanoceria alone, indicating that in this case the treatment is affecting cells at the molecular level. Conversely, treatments with both doses of CSC tended to maintain the level of expression of this markers below controls, being this effect more pronounced in the case of co-exposed cells to nanoceria and CSC, where we can observe the "U shape" behaviour described before in other cell transformation studies [29]. When it comes to the epithelial markers *CDH1* and *ZO1* (Figure 2B and 3B), we observed that the treatment with nanonceria alone only produce very mild changes with respect to control cells, whereas cells exposed to CSC alone or in combination with nanoceria evidenced a clear mRNA downregulation. Finally, long-term exposure to nanoceria alone did not produce changes in the tumor suppressor gene *PTEN,* but a downregulation was observed in cells exposed to CSC, being more pronounced when combined with nanoceria (Figure 2C and 3C). As noticed in the figures, the week 4 of treatment is the time where higher differences were observed between CSC alone or in combination with nanoceria, suggesting that this is a relevant time-point in terms of regulation of differentiation status at the molecular level under the studied regime of exposure.

Migration ability of long-term exposed BEAS-2B cells

The migration process is an intrinsic cell ability that becomes dysregulated in early stages of cell transformation and, therefore, useful to study the initiation process. When cells were analysed after 6 weeks of treatment, a significant increase in the degree of migration capacity was evident only in cells exposed to the higher dose of CSC and cells co-exposed to nanoceria and CSC (Figure 4). No cellular migratory ability was observed before (data not shown). Results showed a faster wound closure in cells

exposed to Ce+CSC1, CSC5 µg/mL and Ce+CSC5 treatments, compared with its time-matched controls. No differences were observed in cells exposed to nanoceria alone or to the lowest dose of CSC.

Anchorage-independent growth ability of long-term exposed BEAS-2B cells

Although the soft-agar assay (anchorage-independent colony formation assay) does not mimic the whole carcinogenesis process *in vivo*, the promotion of anchorage-independent cell growth is considered a good biomarker of cell transformation processes, linked to the acquisition of cancer-like phenotype. We have analysed the effects, over the exposure time, and observed significant changes in this cancer features at week 6 (Figure 5). As shown in the figure, slight and non-biologically relevant changes are seen in cells exposed to nanoceria alone or CSC1 alone, but relevant increases were observed for Ce+CSC1, CSC5 and Ce+CSC5. Of special interest here is the comparison of CSC5 *vs* Ce+CSC5, as a significant increase in the ability to grow independent of anchorage of around 1.5-fold was observed in the co-treated cells, indicating again that nanoceria is exacerbating the effects induced by CSC.

Secretome of long-term exposed BEAS-2B cells

The extracellular matrix modulators matrix metalloproteinases (MMPs) are known to influence local cancer cell invasion and distant metastasis, and enhanced MMPs activities are often found in transformed cells. Its abundancy in the secretome of exposed cells is often representative of the amount of other tumor-related secreted factors present. When the secreted MMP-9 activity was evaluated in BEAS-2B cell's secretome during the course of the exposure, an increase was observed in CSC1, Ce+CSC1, CSC5 and Ce+CSC5-exposed cells, when compared to time-matched controls (Figure 6), evidencing a cancer-like feature. However, MMP-9 activity was lower in the co-exposed cells than in cells exposed to CSC alone, suggesting that co-treatment was, in this particular case, beneficial. No effect was observed in cells exposed to nanoceria alone.

To better test whether co-exposed cells present a secretome with lower cancer-related factors and thus with lower potential of influencing growth promotion, we evaluated the ability of the different secretomes to promote the expansion of cancer HCT116 cells by the modified colony-forming assay. As seen in Figure 7, co-exposed cells significantly increased the size of the HCT116 colonies, when compared to cells exposed to CSC alone, indicating that MMP-9 did not reflect the abundancy of other factors present, and demonstrating that nanoceria co-exposure negatively influences

the cell's secretome ability to promote tumoral cell growth. The colony sizes were 173.2±4.0 µm in controls, 225.9±2.5 µm in Ce+CSC1 and 265.7±4.6 µm in Ce+CSC5. Nanoceria treatment alone was not found to influence cell's secretome.

FRA-1 dysregulation as a mechanism of transformation in long-term exposed BEAS-2B cells

The dysregulation of *Fos-related antigen 1* (*FRA-1)* expression was studied here as it is known to play part in the carcinogenesis associated to CSC exposure. *FRA-1* mRNA levels were analysed through the exposure using qPCR. At week 6 of exposure, Ce+CSC1, CSC5 and Ce+CSC5-exposed cells showed a very drastic decrease in *FRA-1* expression, being in the Ce+CSC5 case 0.12-fold of controls. Conversely, Ce 2.5 µg/mL and CSC1 µg/mL evidenced a raise of expression over controls (Figure 8). Interesting here is the fact that cells that showed positive for most of the rest biomarkers of cell-transformation studied -Ce+CSC1, CSC5 and Ce+CSC5- were found here to exhibit a differential pattern of *FRA-1* dysregulation, supporting a role of *FRA-1* in the carcinogenesis process associated to CSC and Ce+CSC exposure.

Discussion

There has been a rapid growth in the nanotechnology field towards the development of nanomedicine products to improve therapeutic strategies against cancer [10]. These nanomedical agents have been shown to improve the pharmacokinetic and pharmacodynamic properties of conventional treatment agents and may enhance the efficacy of existing anticancer compounds with less toxicity [10].

Nanoceria particles can reversibly bind oxygen and shift oxidation states (Ce^{3+}/Ce^{4+}) depending on the environment [23]. This interconversion of oxidation states gives rise to a large number of oxygen vacancies on the surface of nanoceria and it is the key property that makes it a potent antioxidant agent, and an interesting candidate for the treatment of diseases characterized by increased ROS levels, including cancer. However, several issues need to be resolved before this interesting catalytic material can be applied in biomedical applications with security. One of them lies in the fact that literature evidences concerns regarding its biosafety using *in vitro* and *in vivo* models and different types of exposure. Although the acute effects of nanoceria are very low, toxic and genotoxic increases with exposure time have been reported, possibly due to nanoceria's biopersistence. In this way, accumulated doses produce granuloma in the lung and liver, and fibrosis in the lung, among other effects, as reviewed [26]. According with its biopersistence and increased toxicity with time, there is a risk that

long-term exposure to low nanoceria levels may eventually lead to adverse health effects. In this context, a correct evaluation of the nanoceria-associated health risk requires to consider a long-term or chronic scenario of exposure at environmentally relevant doses of the compound. Despite its limitations, the use of *in vitro* models in long-term scenarios can be in this sense adequate and useful, as they allow analyzing cell transformation effects, an end-point poorly explored so far. To date only few studies have explored the importance of long-term exposures for assessing the carcinogenic potential of NP. These include chronic exposures to sub-toxic doses of TiO_2NP which led to chromosomal instability and cell transformation in fibroblast cells [31], as well as in human lung epithelial cells (BEAS-2B) [32]. Similarly, CoNP were carcinogenic via oxidative stress mechanism in mouse embryonic fibroblasts after 12 weeks of exposures with low doses [33]. Additionally, a few studies reported the possible carcinogenic potential of carbon nanotubes (CNT) after long-term exposure showing that CNT could cause malignant or neoplastic-like transformation in human lung epithelial (MeT5A) cells [34-36], as well in BEAS-2B cells [37]. In the present study, 6 weeks of long-term exposure of BEAS-2B cells to 2.5 µg/mL of nanoceria did not produce any significant changes in cellular morphology, proliferation rate, migration ability, anchorage-independent cell growth capacity or secretome's MMP-9 content and cell growth promoting capability. Thus, according to our data, nanoceria alone showed secure in terms of carcinogenesis, at least taking into account the *in vitro* cancer-like phenotype characteristics evaluated here.

Another issue that faces nanoceria applicability in therapy is the fact that its antioxidant effects have not been observed by some authors, yet they observed the contrary pro-oxidant effect. Nanoceria physico-chemical characteristics such as shape or size have been proposed as the source of this variation, and also some characteristics of their surrounding environment such as the pH [38]. Thus, i.e., no protection was observed in lung carcinoma cells (A-549) and breast carcinoma (BT-474) cells against hydrogen peroxide [39], polymer-coated nanoceria at relatively low concentrations were found to be cytotoxic and pro-apoptotic on melanoma A375 cells [40], and pretreatment with nanoceria enhanced radiation-induced ROS production and cell death in human pancreatic L3.6pl cancer cells [41]. In the present work, the protective co-exposure effect of nanoceria was evaluated using a long-term *in vitro* approach. Thus, BEAS-2B cells were continuously exposed to 1 and 5 µg/mL of tobacco smoke condensate (CSC) alone. Active and second-hand exposures to tobacco are frequent in the population and it is believed that 80% to 90% of all respiratory cancers are related to active smoking. As occurs with nanoceria, CSC

targets mainly the lung [27]. The mixture of chemicals contained in CSC is elevated and thus different mechanisms of action may be taking part in the CSC-induced malignant transformation. Among them, ROS production and oxidative stress-induction are well-studied tobacco mechanisms of carcinogenesis [42]. In the present work, 6 weeks of treatment to CSC induced intrinsic and extrinsic cancer-like features in lung BEAS-2B cells, as indicated by the appearance of spindle-like cell morphology, increased proliferation rate, dysregulation of cellular differentiation status and down-regulation of the suppressor gene *PTEN*, increased migration ability and increased anchorage-independent cell growth capability. Interestingly, continuous co-exposure of CSC with 2.5 μg/mL of nanoceria was unable to protect from the above mentioned effects of tobacco. Contrary, co-exposure to nanoceria exacerbated the observed effects of one or the other dose of CSC in all analysed end-points and, moreover, induced important cancer-related changes in the secretome of co-exposed cells that were not observed when cells were exposed to CSC alone. Therefore, it would be of interest to evaluate the effect of nanoceria co-exposure using other relatively common environmental toxicants such as tobacco smoke, as the implications of the potential negative effects on human health would be of big importance. Of note also here is the fact that the duration of the exposure is something to take into account when examining nanoceria biological properties, as short-term nanoceria exposure using the same model system was found by us to be beneficial in one of our previous works [17].

As mutations in the *PTEN* gene and loss of PTEN expression have both been associated with a wide range of human tumors [43](Salmena et al. 2008), the transcript down-regulation found here may be of interest in terms of CSC+nanoceria carcinogenic mechanisms. In the same direction, FRA-1 is one of the most common components of AP-1, a basic leucine zipper (bZIP) transcription factor that regulates diverse genes and cellular processes such as cell proliferation, differentiation, invasion and apoptosis, among others [44](Young and Colburn 2006). Thus, FRA-1 is thought to play an important role in tumorigenesis and progression. *In vitro* acute exposure to cigarette smoke has been found before to increase the levels of *FRA-1* in lung cells [45](Zhang, Adiseshaiah and Reddy, 2005), so its regulation was studied herein as a mechanism of CSC-induced carcinogenesis. Interestingly, 6 weeks of exposure to the lower dose of 1 μg/mL CSC significantly increase the mRNA levels of *FRA-1* in BEAS-2B cells with no signs of transformation; while the same time of exposure at 5 μg/mL dose reduced transcript levels in BEAS-2B cells already exhibiting a transformed phenotype. Apparently, under our experimental conditions CSC stimulates *FRA-1* expression in non-transformed cells, but a downregulation is triggered once cells acquire a cancer-

like phenotype. It is important to consider here that previous studies positively associating cigarette smoke with *FRA-1* expression were conducted under acute regime of exposure, with poor relevance for carcinogenesis-related processes. Also, the roles of FRA-1 in malignancies are still controversial. It has been validated to be overexpressed in many human malignancies, including thyroid, esophagus, colon, and breast [44](Young and Colburn 2006), which would indicate an important role in tumorigenesis, but to be absent in invasive cervical cancer, revealing an anticarcinogenic role of FRA-1 [46](Prusty and Das, 2005). Accordingly, the work of Ma et al. (2009)[47] found that *FRA-1* was downregulated in NSCLC, compared with normal bronchial epithelium. Further, the low expression of *FRA-1* correlated with advanced tumor stage and poor survival [47](Ma et al., 2009). When *FRA-1* was analysed in cells co-treated with nanoceria and CSC that also exhibit cancer-like phenotypic properties, *FRA-1* was also found to be significantly down-regulated. In both Ce+CSC1 and Ce+CSC5 exposed cells the down-regulation is more pronounced than in cells exposed to CSC1 and CSC5 alone, being the difference highly significant in the case of CSC1 vs. Ce+CSC1, indicating that nanoceria exposure exacerbate the expression inhibition that was found here to be associated with the oncogenic phenotype.

Conclusions

In summary, we propose that long-term exposure to sub-toxic doses of nanoceria alone do not suppose a health concern in terms of lung carcinogenesis, although more research needs to be done using chronic approaches to better characterize the associated risk. However, long-term co-exposure of nanoceria and a common lung carcinogenic agent such as CSC evidenced that the NP potentiated most of the evaluated CSC-induced cancer-like phenotypic features. Thus, nanoceria was unable to protect from the carcinogenic effects of CSC long-term exposure in lung BEAS-2B cells but rather the contrary, dismissing its use as a protective agent in chronic oxidant-dependent pathologies.

References

1. UE-OSHA. Mananging nanomaterials at workplace. https://osha.europa.eu/en/themes/nanomaterials
2. Lawrence NJ, Brewer JR, Wang L, Wu T-S, Wells-Kingsbury J, Ihrig MM, et al. Defect engineering in cubic cerium oxide nanostructures for catalytic oxidation. Nano Lett. 2011;11:2666-71.
3. Park B, Donaldson K, Duffin R, Tran L, Kelly F, Mudway I, et al. Hazard and risk assessment of a nanoparticulate cerium oxide-based diesel fuel additive -a case study. Inhal Toxicol. 2008;20:547-66.
4. Kosynkin VD, Arzgatkina AA, Ivanov EN, Chtoutsa MG, Grabko AI, Kardapolov AV, et al. The study of process production of polishing powder based on cerium dioxide. J Alloys Compd. 2000;303-304:421-5.
5. Bello D, Martin J, Santeufemio C, Sun Q, Lee Bunker K, Shafer M, et al. Physicochemical and morphological characterisation of nanoparticles from photocopiers: implications for environmental health. Nanotoxicology. 2013;7:989-1003.
6. Reed K, Cormack A, Kulkarni A, Mayton M, Sayle D, Klaessig F, et al. Exploring the properties and applications of nanoceria: is there still plenty of room at the bottom? Environ Sci Nano. 2014;1:390-405.
7. Zhang H, He X, Zhang Z, Zhang P, Li Y, Ma Y, et al. Nano-CeO_2 exhibits adverse effects at environmental relevant concentrations. Environ Sci Technol. 2011;45:3725-30.
8. Integrated Laboratory Systems Inc. Chemical information profile for ceric oxide [CAS no. 1306-38-3]. Supporting Nomination for Toxicological Evaluation by the National Toxicology Program, Research Triangle Park, NC, 2006. p. 21
9. Organisation for Economic Co-operation and Development. List of manufactured nanomaterials and list of endpoints for phase one of the sponsorship programme for the testing of manufactured nanomaterials: Revision, in Series on the safety of manufactured nanomaterials, 2010, Number 27, ENV/JM/MONO(2010)46.
10. Wicki A, Witzigmann D, Balasubramanian V, Huwyler J. Nanomedicine in cancer therapy: Challenges, opportunities, and clinical applications. J Control Release. 2015;200:138-57.
11. Passeri D, Rinaldi F, Ingallina C, Carafa M, Rossi M, Terranova ML. Biomedical

applications of nanodiamonds: An overview. J Nanosci Nanotechnol. 2015;15:972-88.

12. Rasmussen JW, Martinez E, Louka P, Wingett DG. Zinc oxide nanoparticles for selective destruction of tumor cells and potential for drug delivery applications. Expert Opin Drug Deliv. 2010;7:1063-77.

13. Narayanan KB, Park HH. Pleiotropic functions of antioxidant nanoparticles for longevity and medicine. Adv Colloid Interface Sci. 2013;201-202:30-42.

14. Nelson BC, Johnson ME, Walker ML, Riley KR, Sims CM. Antioxidant cerium oxide nanoparticles in biology and medicine. Antioxidants (Basel). 2016;5:15.

15. Heckert EG, Seal S, Self WT. Fenton-like reaction catalyzed by the rare earth inner transition metal cerium. Environ Sci Technol. 2008;42:5014-9.

16. Pirmohamed T, Dowding JM, Singh S, Wasserman B, Heckert E, Karakoti AS, et al. Nanoceria exhibit redox state-dependent catalase mimetic activity. Chem Commun (Camb). 2010;46:2736-8.

17. Rubio L, Annangi B, Vila L, Hernández A, Marcos R. Antioxidant and anti-genotoxic properties of cerium oxide nanoparticles in a pulmonary-like cell system. Arch Toxicol. 2016;90:269-78.

18. Tarnuzzer RW, Colon J, Patil S, Seal S. Vacancy engineered ceria nanostructures for protection from radiation-induced cellular damage. Nano Lett. 2005;5:2573-7.

19. Colon J, Herrera L, Smith J, Patil S, Komanski C, Kupelian P, et al. Protection from radiation-induced pneumonitis using cerium oxide nanoparticles. Nanomedicine. 2009;5:225-31.

20. Colon J, Hsieh N, Ferguson A, Kupelian P, Seal S, Jenkins DW, et al. Cerium oxide nanoparticles protect gastrointestinal epithelium from radiation-induced damage by reduction of reactive oxygen species and upregulation of superoxide dismutase 2. Nanomedicine. 2010;6:698-705.

21. Schubert D, Dargusch R, Raitano J, Chan S-W. Cerium and yttrium oxide nanoparticles are neuroprotective. Biochem Biophys Res Commun. 2006;342:86-91.

22. Chen S, Hou Y, Cheng G, Zhang C, Wang S, Zhang J. Cerium oxide nanoparticles protect endothelial cells from apoptosis induced by oxidative stress. Biol Trace Elem Res. 2013;154:156-66.

23. Estevez AY, Erlichman JS. The potential of cerium oxide nanoparticles (nanoceria) for neurodegenerative disease therapy. Nanomedicine (Lond). 2014;9:1437-40.

24. Alaraby M, Hernández A, Annangi B, Demir E, Bach J, Rubio L, et al. Antioxidant and antigenotoxic properties of CeO_2 NPs and cerium sulphate: Studies with *Drosophila melanogaster* as a promising i*n vivo* model. Nanotoxicology. 2015;9:749-59.

25. Kumari M, Singh SP, Chinde S, Rahman MF, Mahboob M, Grover P. Toxicity study of cerium oxide nanoparticles in human neuroblastoma cells. Int J Toxicol. 2014;33:86-97.

26. Yokel RA, Hussain S, Garantziotis S, Demokritou P, Castranova V, Cassee FR. The Yin: An adverse health perspective of nanoceria: uptake, distribution, accumulation, and mechanisms of its toxicity. Environ Sci Nano. 2014;1:406-28.

27. Saha SP, Bhalla DK, Whayne TF, Gairola C. Cigarette smoke and adverse health effects: An overview of research trends and future needs. Int J Angiol. 2007;16:77-83.

28. Rao P, Ande A, Sinha N, Kumar A, Kumar S. Effects of cigarette smoke condensate on oxidative stress, apoptotic cell death, and HIV replication in human monocytic cells. PLoS One. 2016;11:e0155791.

29. Bach J, Peremartí J, Annangi B, Marcos R, Hernández A. Oxidative DNA damage enhances the carcinogenic potential of *in vitro* chronic arsenic exposures. Arch Toxicol. 2016;90:1893-905.

30. Geissmann Q. OpenCFU, a new free and open-source software to count cell colonies and other circular objects. PLoS One. 2013;8:e54072.

31. Huang S, Chueh PJ, Lin YW, Shih TS, Chuang SM. Disturbed mitotic progression and genome segregation are involved in cell transformation mediated by nano-TiO_2 long-term exposure. Toxicol Appl Pharmacol. 2009;241:182-94.

32. Vales G, Rubio L, Marcos R. Long-term exposures to low doses of titanium dioxide nanoparticles induce cell transformation, but not genotoxic damage in BEAS-2B cells. Nanotoxicology. 2015;9:568-78.

33, Annangi B, Bach J, Vales G, Rubio L, Marcos R, Hernández A. Long-term exposures to low doses of cobalt nanoparticles induce cell-transformation enhanced by oxidative damage. Nanotoxicology. 2015;9:138-47.

34. Wang L, Luanpitpong S, Castranova V, Tse W, Lu Y, Pongrakhananon V, et al. Carbon nanotubes induce malignant transformation and tumorigenesis of human lung epithelial cells. Nano Lett. 2011;11:2796-803.

35. Wang L, Stueckle TA, Mishra A, Derk R, Meighan T, Castranova V, et al. Neoplastic-like transformation effect of single-walled and multiwalled carbon nanotubes compared to asbestos on human lung small airway epithelial cells. Nanotoxicology, 2014;8:485-507.

36. Lohcharoenkal W, Wang L, Stueckle TA, Dinu CZ, Castranova V, Liu Y, et al. Chronic exposure to carbon nanotubes induces invasion of human mesothelial cells through matrix metalloproteinase-2. ACS Nano. 2013;7:7711-23.

37. Vales G, Rubio L, Marcos R. Genotoxic and cell-transformation effects of multi-walled carbon nanotubes (MWCNT) following *in vitro* long-term exposures**.** J Hazard Mat. 2016; 306:193-202**.**

38. Gagnon J, Fromm KM. Toxicity and protective effects of cerium oxide nanoparticles (nanoceria) depending on their preparation method, particle size, cell type, and exposure route. Eur J Inorg Chem. 2015;2015:4510-7.

39. Perez JM, Asati A, Nath S, Kaittanis C. Synthesis of biocompatible dextran-coated nanoceria with pH-dependent antioxidant properties. Small. 2008;4:552-6.

40. Alili L, Sack M, von Montfort C, Giri S, Das S, Carroll KS, et al. Downregulation of tumor growth and invasion by redox-active nanoparticles. Antioxid Redox Signal. 2013;19:765-78.

41. Wason MS, Colon J, Das S, Seal S, Turkson J, Zhao J, et al. Sensitization of pancreatic cancer cells to radiation by cerium oxide nanoparticle-induced ROS production. Nanomedicine. 2013;9:558-69.

42. Johnson MD, Schilz J, Djordjevic M V, Rice JR, Shields PG. Evaluation of *in vitro* assays for assessing the toxicity of cigarette smoke and smokeless tobacco. Cancer Epidemiol Biomark Prev. 2009;18:3263-304.

43. Salmena L, Carracedo A, Pandolfi PP. Tenets of *PTEN* tumor suppression. Cell. 2008;133:403-14.

44. Young MR, Colburn NH. Fra-1 a target for cancer prevention or intervention. Gene. 2006;379:1-11.

45. Zhang Q, Adiseshaiah P, Reddy SP. Matrix metalloproteinase/epidermal growth factor receptor/mitogen-activated protein kinase signaling regulate fra-1 induction

by cigarette smoke in lung epithelial cells. Am J Respir Cell Mol Biol. 2005;32:72-81.

46. Prusty BK, Das BC. Constitutive activation of transcription factor AP-1 in cervical cancer and suppression of human papillomavirus (HPV) transcription and AP-1 activity in HeLa cells by curcumin. Int J Cancer. 2005;113:951-60.

47. Ma K, Chang D, Gong M, Ding F, Luo A, Tian F, et al. Expression and significance of FRA-1 in non-small-cell lung cancer. Cancer Invest. 2009;27:353-9.

Legends to figures

Figure 1. Morphology (A) and proliferation changes (B) observed in BEAS-2B cells long-term exposed to environmentally relevant doses of nanoceria and/or CSC at week 6 of exposure. Cells exposed to Ce+CSC1, CSC5 and Ce+CSC5 showed spindle-like morphology and higher proliferation rates. Data are presented as mean values with time-matched controls set to 100% (n=3); error bars represent standard error of the mean; $^{a}P<0.05$, $^{b}P<0.01$, $^{c}P<0.001$ compared with time-matched controls or between treatments, as indicated.

Figure 2. Expression changes associated with BEAS-2B cell's differentiation program during long-term exposure to nanoceria and/or CSC 1 μg/mL. (A) Expression changes of the mesenchymal identity markers *CDH2*, *VIM* and *ACTA2*. (B) Expression changes of the epithelial markers *CDH1* and *ZO1*. (C) Expression changes of the tumor suppressor gene *PTEN*. Data are presented as mean values with time-matched controls set to 100% (n=3); error bars represent standard error of the mean; $^{a}P<0.05$, $^{b}P<0.01$, $^{c}P<0.001$ compared with time-matched controls.

Figure 3. Expression changes associated with BEAS-2B cell's differentiation program during long-term exposure to nanoceria and/or CSC 5 μg/mL. (A) Expression changes of the mesenchymal identity markers *CDH2*, *VIM* and *ACTA2*. (B) Expression changes of the epithelial markers *CDH1* and *ZO1*. (C) Expression changes of the tumor suppressor gene *PTEN*. Data are presented as mean values with time-matched controls set to 100% (n=3); error bars represent standard error of the mean; $^{a}P<0.05$, $^{b}P<0.01$, $^{c}P<0.001$ compared with time-matched controls.

Figure 4. Migration ability of BEAS-2B cells after 6 weeks of nanoceria and/or CSC exposure. Cells exposed to Ce+CSC1, CSC5 and Ce+CSC5 showed increased motility rates. Data are presented as mean percent of wound closing (n=3); error bars represent standard error of the mean; $^{a}P<0.05$, $^{b}P<0.01$, $^{c}P<0.001$ compared with time-matched controls or between treatments, as indicated.

Figure 5. Anchorage-independent cell growth capacity of BEAS-2B cells after 6 weeks of nanoceria and/or CSC exposure. Cells exposed to Ce+CSC1, CSC5 and Ce+CSC5 showed higher capacity to grow in soft-agar. Data are presented as mean values with time-matched controls set to 100% (n=3); error bars represent standard error of the mean; $^{a}P<0.05$, $^{b}P<0.01$, $^{c}P<0.001$ compared with time-matched controls or between treatments, as indicated.

Figure 6. MMP-9 secretion of BEAS-2B cells after 6 weeks of nanoceria and/or CSC exposure. Cells exposed to CSC1, Ce+CSC1, CSC5 and Ce+CSC5 showed increased

MMP-9 secretion when compared to control cells. Data are presented as mean values with time-matched controls set to 100% (n=3); error bars represent standard error of the mean; [a]*P*<0.05, [b]*P*<0.01, [c]*P*<0.001 compared with time-matched controls or between treatments, as indicated.

Figure 7. Ability of 6 weeks-exposed BEAS-2B cell's secretome to induce anchorage-independent cell growth of HCT-116 cells. Secretome of cells exposed to Ce+CSC1 and Ce+CSC5 for 6 weeks act as inducer of anchorage-independent growth in HCT116 cells. Data are presented as mean values (n=3); error bars represent standard error of the mean; [c]*P*<0.001 compared with time-matched controls or between treatments, as indicated.

Figure 8. *FRA-1* dysregulation as a mechanism of transformation in nanoceria and/or CSC long-term exposed BEAS-2B cells. Cells exposed to Ce+CSC1, CSC5 and Ce+CSC5 showed a clear *FRA-1* down-regulation that is not observed in the rest of the treatments. Data are presented as mean values with time-matched controls set to 100% (n=3); error bars represent standard error of the mean; [a]*P*<0.05, [b]*P*<0.01, [c]*P*<0.001 compared with time-matched controls or between treatments, as indicated.

Figures

Figure 1.

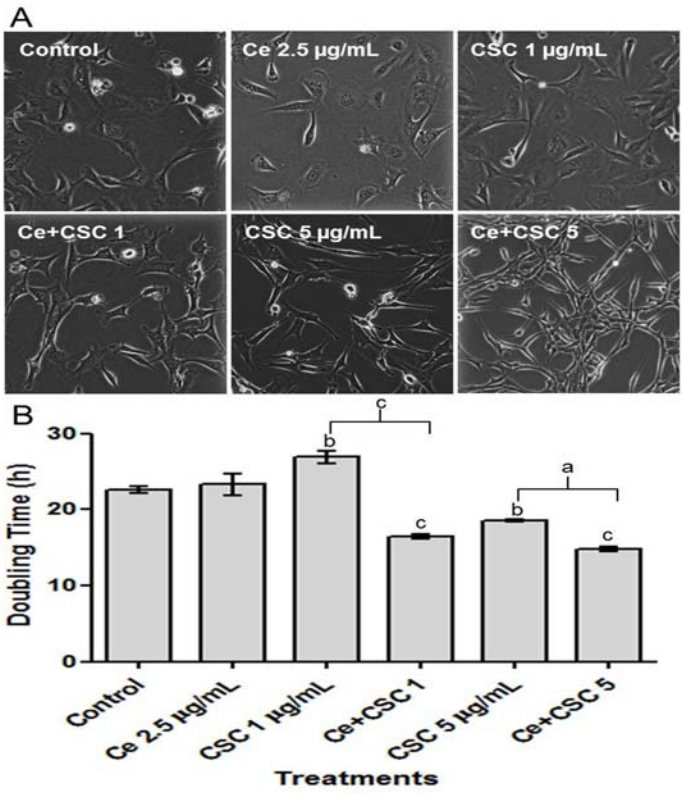

Figure 2.

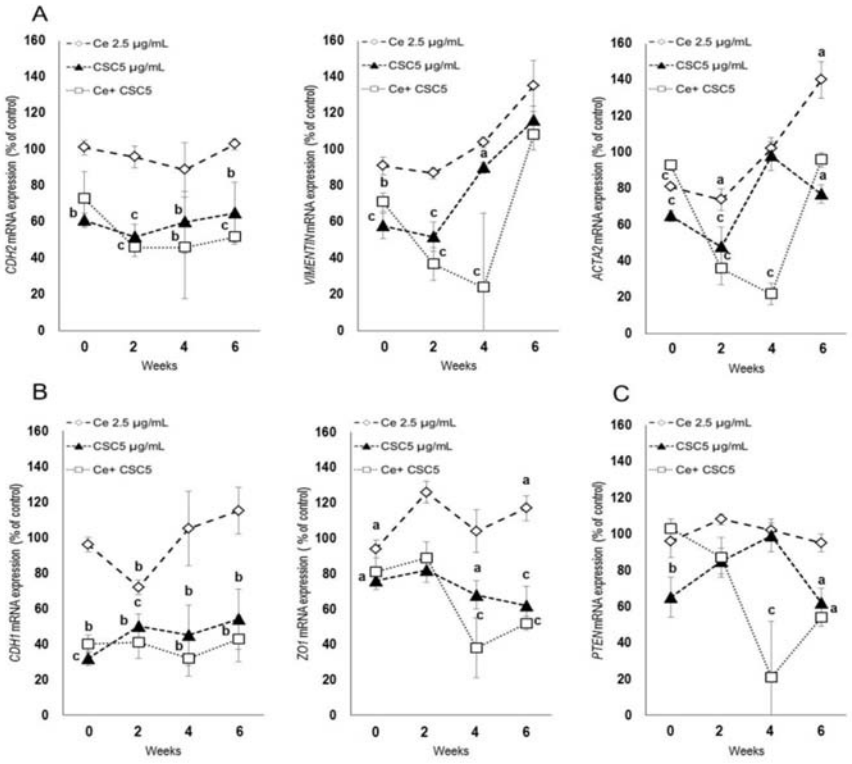

Figure 3.

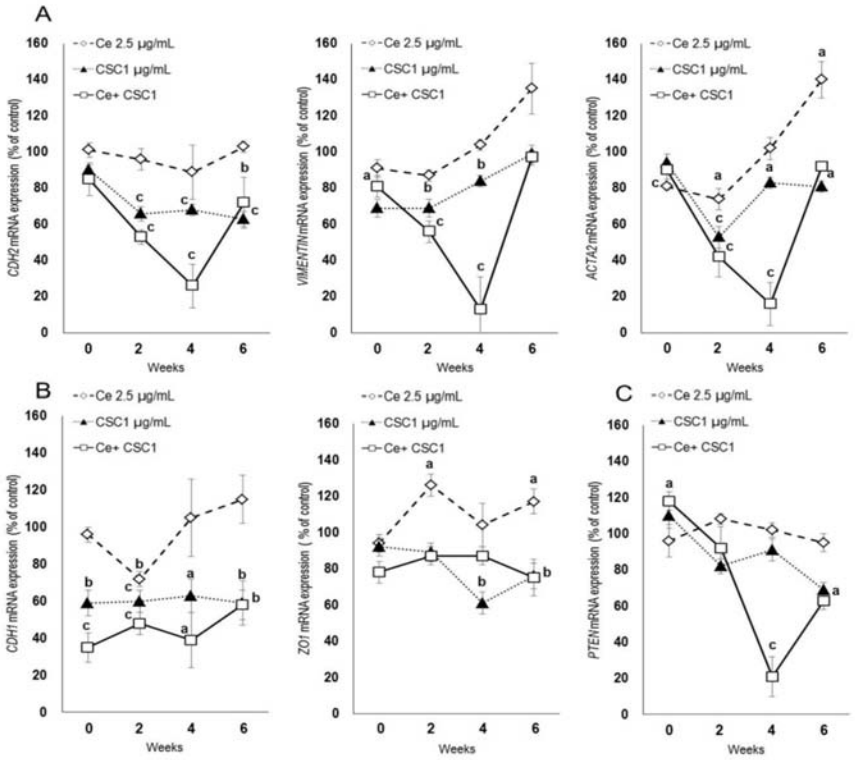

Figure 4.

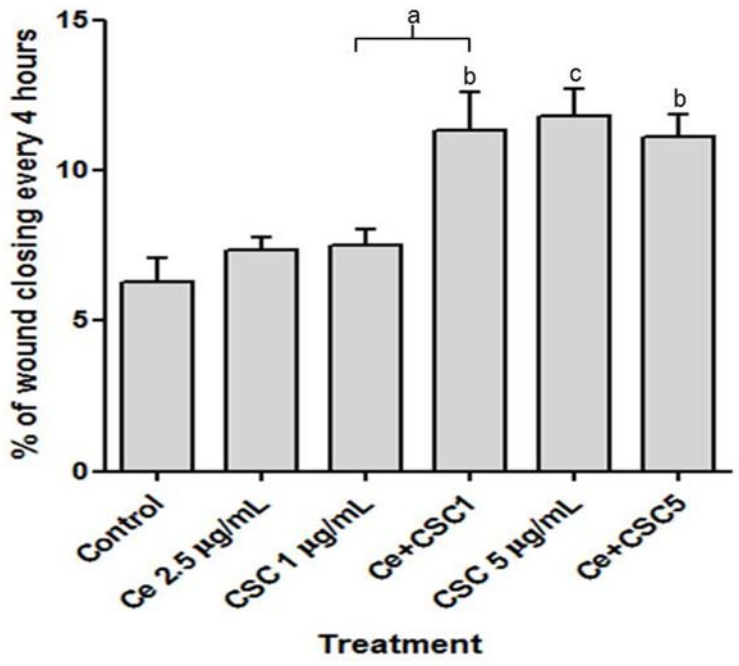

Figure 5.

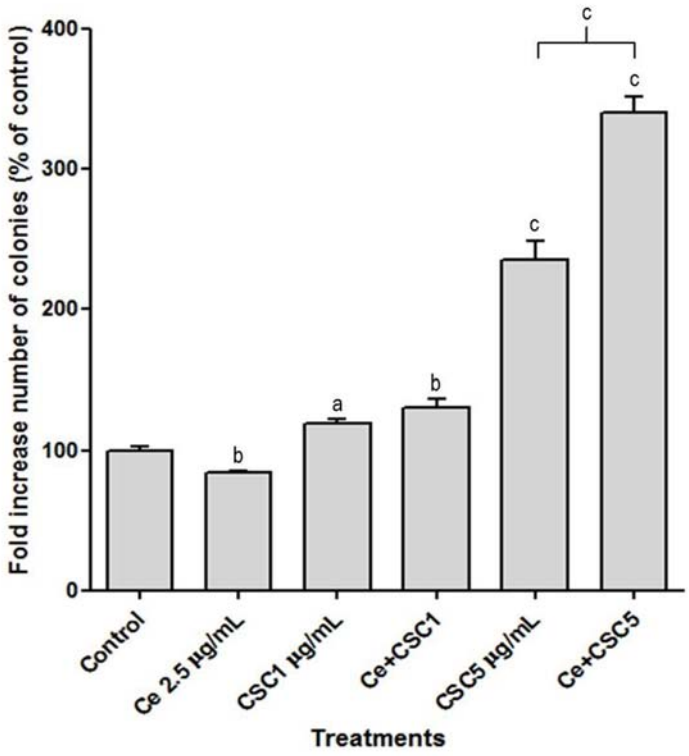

Figure 6.

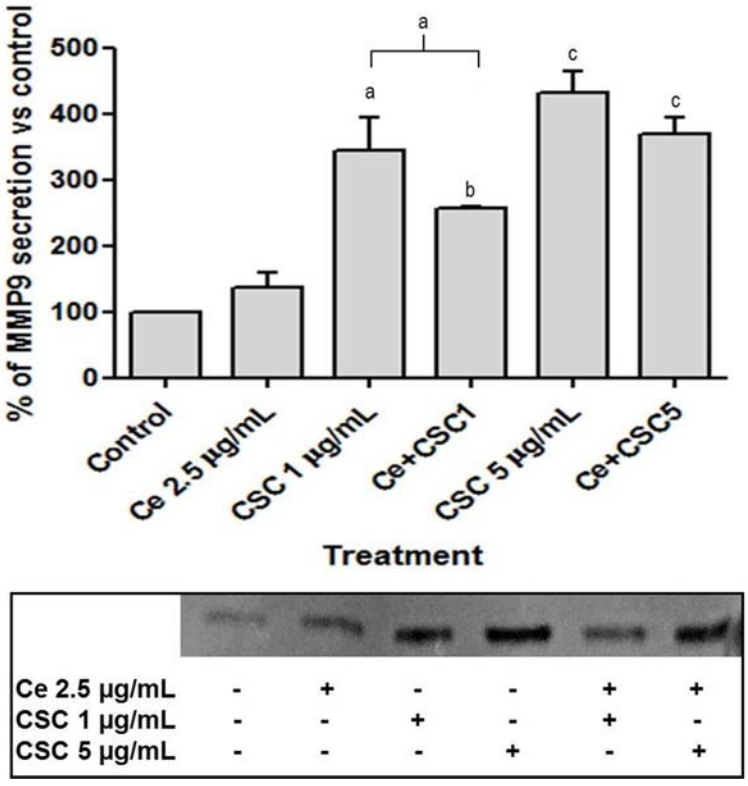

Figure 7.

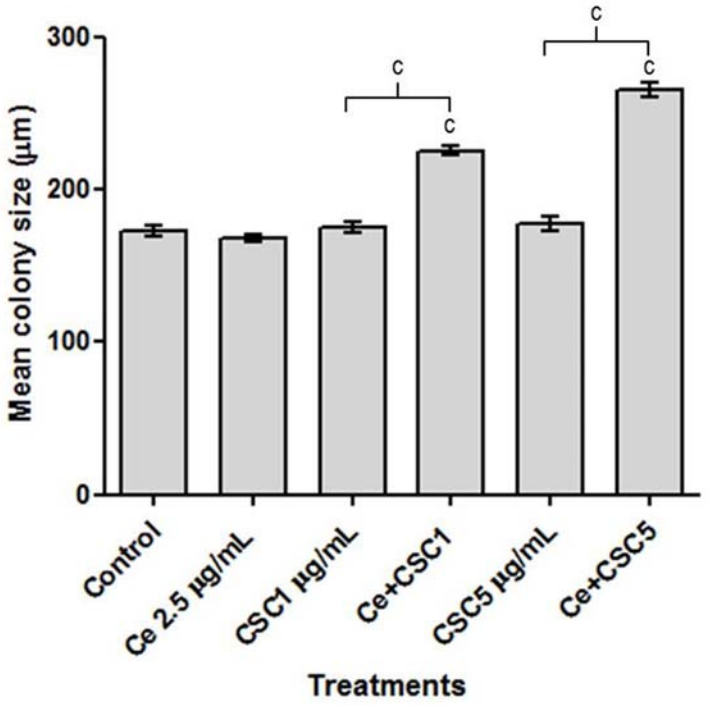

Figure 8.

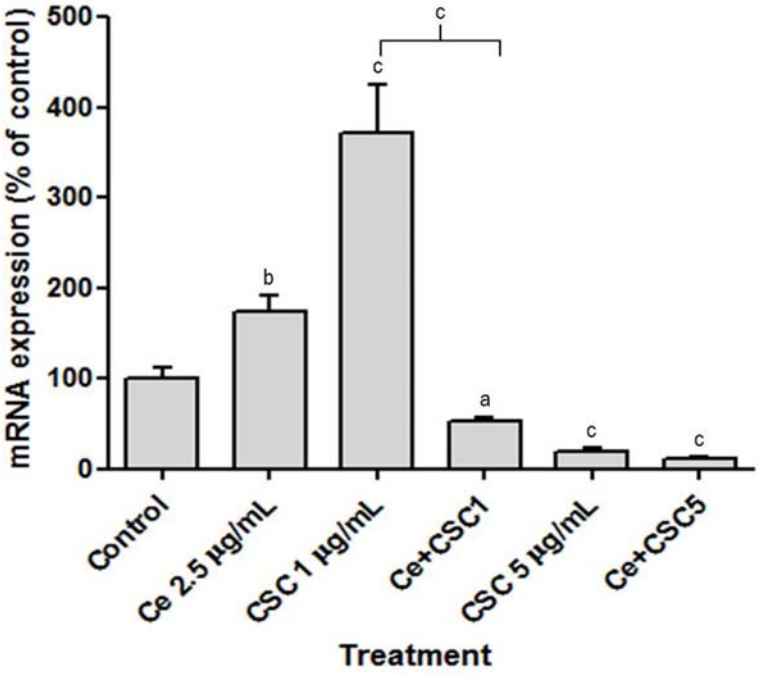

7. REFERENCES

7. REFERENCES

Aalapati S, Ganapathy S, Manapuram S, Anumolu G, Prakya BM. 2014. Toxicity and bio-accumulation of inhaled cerium oxide nanoparticles in CD1 mice. Nanotoxicology 8:786-798.

Akhtar MJ, Ahamed M, Alhadlaq HA, Khan MA, Alrokayan SA. 2015. Glutathione replenishing potential of CeO_2 nanoparticles in human breast and fibrosarcoma cells. J Colloid Interface Sci. 453:21-27.

Akopyan G, Bonavida B. 2006. Understanding tobacco smoke carcinogen NNK and lung tumorigenesis. Int J Oncol. 29:745-52.

Alaraby M, Hernández A, Annangi B, Demir E, Bach J, Rubio L, Creus A, Marcos R. 2015. Antioxidant and antigenotoxic properties of CeO_2 NPs and cerium sulphate: Studies with *Drosophila melanogaster* as a promising i*n vivo* model. Nanotoxicology 9:749-59.

Albanese A, Chan WC. 2011. Effect of gold nanoparticle aggregation on cell uptake and toxicity. ACS Nano 5:5478-89.

Alili L, Sack M, Karakoti AS, Teuber S, Puschmann K, Hirst SM, Reilly CM, Zanger K, Stahl W, Das S, Seal S, Brenneisen P. 2011. Combined cytotoxic and anti-invasive properties of redox active nanoparticles in tumor–stroma interactions. Biomaterials 32:2918–2929.

Alili L, Sack M, von Montfort C, Giri S, Das S, Carroll KS, Zanger K, Seal S, Brenneisen P. 2013. Downregulation of tumor growth and invasion by redox-active nanoparticles. Antioxid Redox Signal 19:765-778.

Annangi B, Bach J, Vales G, Rubio L, Marcos R, Hernández A. 2015. Long-term exposures to low doses of cobalt nanoparticles induce cell-transformation enhanced by oxidative damage. Nanotoxicology 9:138-47.

Annangi B, Rubio L, Alaraby M, Bach J, Marcos R, Hernández A. 2016. Acute and long-term in vitro effects of zinc oxide nanoparticles. Arch Toxicol 90:2201-13.

Annys E, Billington R, Clayton R, Bremm KD, Graziano M, McKelvie J, Ragan I, Schwarz M, van der Laan JW, Wood C, Öberg M, Wester P, Woodward KN. 2014.

Advancing the 3Rs in regulatory toxicology – Carcinogenicity testing: Scope for harmonisation and advancing the 3Rs in regulated sectors of the European Union. Regul Toxicol Pharmacol 69:234-242.

Arcaro A, Guerreiro AS. 2007. The phosphoinositide 3-kinase pathway in human cancer: genetic alterations and therapeutic implications. Curr Genomics 8:271-306.

Asati A, Santra S, Kaittanis C, Perez JM. 2010. Surface-charge-dependent cell localization and cytotoxicity of cerium oxide nanoparticles. ACS Nano 4:5321–5331.

Baan RA. 2007. Carcinogenic hazards from inhaled carbon black, titanium dioxide, and talc not containing asbestos or asbestiform fibers: Recent evaluations by an IARC Monographs working group. Inhal. Toxicol 19:213–228.

Bach J, Peremartí J, Annangi B, Marcos R, Hernández A. 2016. Oxidative DNA damage enhances the carcinogenic potential of in vitro chronic arsenic exposures. Arch Toxicol 90:1893–1905.

Bai W, Zhang Z, Tian W, He X, Ma Y, Zhao Y, Chai Z. 2010. Toxicity of zinc oxide nanoparticles to zebrafish embryo: a physicochem- ical study of toxicity mechanism. J Nanopart Res 12:1645–1654.

Barbieri SS, Ruggiero L, Tremoli E, Weksler BB. 2008. Suppressing *PTEN* activity by tobacco smoke plus interleukin-1beta modulates dissociation of VE-cadherin/beta-catenin complexes in endothelium. Arterioscler Thromb Vasc Biol 28:732-8.

Bello D, Martin J, Santeufemio C, Sun Q, Lee Bunker K, Shafer M, Demokritou P. 2013. Physicochemical and morphological characterisation of nanoparticles from photocopiers: implications for environmental health. Nanotoxicology 7:989–1003.

Benameur L, Auffan M, Cassien M, Liu W, Culcasi M, Rahmouni H, Stocker P, Tassistro V, Bottero JY, Rose J, Botta A, Pietri S. 2015. DNA damage and oxidative stress induced by CeO_2 nanoparticles in human dermal fibroblasts: Evidence of a clastogenic effect as a mechanism of genotoxicity. Nanotoxicology 9:696-705.

Bhowmick NA, Chytil A, Plieth D, Gorska AE, Dumont N, Shappell S, Washington MK, Neilson EG, Moses HL. 2004. TGF-beta signaling in fibroblasts modulates the oncogenic potential of adjacent epithelia. Science. 303:848-51.

Borowicz S, Van Scoyk M, Avasarala S, Karuppusamy Rathinam MK, Tauler J, Bikkavilli

RK, Winn RA. 1998. The soft agar colony formation assay. J Vis Exp 27:e51998. doi: 10.3791/51998.

Brinckerhoff CE, Matrisian LM. 2002. Matrix metalloproteinases: a tail of a frog that became a prince. Nat Rev Mol Cell Biol 3:207-214.

Buzea C, Pacheco II, Robbie K. 2007. Nanomaterials and nanoparticles: sources and toxicity. Biointerphases 2:17-71.

Cai X, Sezate SA, Seal S, McGinnis JF. 2012. Sustained protection against photoreceptor degeneration in tubby mice by intravitreal injection of nanoceria. Biomaterials 33:8771-81.

Caputo F, De Nicola M, Sienkiewicz A, Giovanetti A, Bejarano I, Licoccia S, Traversa E, Ghibelli L. 2015. Cerium oxide nanoparticles, combining antioxidant and UV shielding properties, prevent UV-induced cell damage and mutagenesis. Nanoscale 7:15643-15656.

Celardo I, De Nicola M, Mandoli C, Pedersen JZ, Traversa E, Ghibelli L. 2011. Ce^{3}+ ions determine redox-dependent anti-apoptotic effect of cerium oxide nanoparticles. ACS Nano 5:4537-4549.

Cohen CA, Kurnick MD, Rzigalinski BA. 2006. Cerium Oxide Nanoparticles Extend Lifespan and Protect Drosophila Melanogaster from Paraquat (Pq)-Induced Oxidative Stress (Os). Free Radical Biol. Med., 41:S20–S20.

Colon J, Herrera L, Smith J, Patil S, Komanski C, Kupelian P, Seal S, Jenkins DW, B. C. 2009. Protection from radiation-induced pneumonitis using cerium oxide nanoparticles. Nanomed. Nanotechnol 5:225–231.

Colon J, Hsieh N, Ferguson A, Kupelian P, Seal S, Jenkins DW, B. C. 2010. Cerium oxide nanoparticles protect gastrointestinal epithelium from radiation-induced damage by reduction of reactive oxygen species and upregulation of superoxide dismutase 2. Nanomedicine 6:698–705.

Collins AR. 2004. The comet assay for DNA damage and repair: principles, applications, and limitations. Mol Biotechnol 26:249-261.

Corvi R, Aardema MJ, Gribaldo L, Hayashi M, Hoffmann S, Schechtman L, Vanparys P. 2012. ECVAM prevalidation study on in vitro cell transformation assays: general

outline and conclusions of the study. Mutat. Res. 744:12–19.

Costantini MG. 2001. Evaluation of human health risk from cerium added to diesel fuel. Health Effects Institute. 9:1-64.

Creton S, Aardema MJ, Carmichael PL, Harvey JS, Martin FL, Newbold RF, O'Donovan MR, Pant K, Poth A, Sakai A, Sasaki K, Scott AD, Schechtman LM, Shen RR, Tanaka N, Yasaei H. 2012. Cell transformation assays for prediction of carcinogenic potential: state of the science and future research needs. Mutagenesis. 27:93-101.

Cross CE, Halliwell B, Borish ET, Pryor WA, Ames BN, Saul RL, McCord JM, Harman D. 1987. Oxygen radicals and human disease. Ann Intern Med 107:526-45.

Chaudhury K, Babu KN, Singh AK, Das S, Kumar A, Seal S. 2012. Mitigation of endometriosis using regenerative cerium oxide nanoparticles. Nanomedicine 9:439-48.

Chen J, Patil S, Seal S, McGinnis JF. 2006. Rare Earth Nano- particles Prevent Retinal Degeneration Induced by Intra- cellular Peroxides. Nat. Nanotechnol 1:142–150.

Chen S, Hou Y, Cheng G, Zhang C, Wang S, Zhang J. 2013. Cerium oxide nanoparticles protect endothelial cells from apoptosis induced by oxidative stress. *Biol* Trace Elem Res 154:156–66.

Cheng GL, Guo W, Han L, Chen EL, Kong LF, Wang LL, Ai WC, Song NN, Li HS, Chen HM. 2013. Cerium oxide nanoparticles induce cytotoxicity in human hepatoma SMMC-7721 cells via oxidative stress and the activation of MAPK signaling pathways. Toxicol In Vitro 27:1082–1088.

Cho WS, Duffin R, Poland CA, Howie SE, MacNee W, Bradley M, et al. 2010. Metal oxide nanoparticles induce unique inflammatory footprints in the lung: important implications for nanoparticle testing. Environ Health Perspect 118:1699–1706.

Chu M, Guo J, Chen CY. 2005. Long-term exposure to nicotine, via ras pathway, induces cyclin D1 to stimulate G1 cell cycle transition. J Biol Chem 280:6369-6379.

Dao NN, Dai Luu M, Nguyen QK, Kim BS. UV absorption by cerium oxide nanoparticles/epoxy composite thin films. Adv. Nat. Sci: Nanosci. Nanotechnol 2:1-4

Das M, Patil S, Bhargava N, Kang JF, Riedel LM, Seal S, Hickman JJ. 2007. Auto-catalytic ceria nanoparticles offer neuroprotection to adult rat spinal cord neurons. Biomaterials 28:1918-25.

Das S, Dowding JM, Klump KE, McGinnis JF, Self W, Seal S. 2013. Cerium oxide nanoparticles: applications and prospects in nanomedicine. Nanomedicine 8:1483-1508.

Davan R, Prasad RGSV, Jakka VS, Aparna RSL, Phani AR, Jacob B, Salins PC, Raju DB. 2012. Cerium oxide nanoparticles promotes wound healing activity in in-vivo animal model. Journal of Bionanoscience 6:78-83.

De Marzi L, Monaco A, De Lapuente J, Ramos D, Borras M, Di Gioacchino M, Santucci S, Poma A. 2013. Cytotoxicity and genotoxicity of ceria nanoparticles on different cell lines in vitro. International journal of molecular sciences 14:3065-3077.

Del Pozo Martin Y, Park D, Ramachandran A, Ombrato L, Calvo F, Chakravarty P, Spencer-Dene B, Derzsi S, Hill CS, Sahai E, Malanchi I. 2015. Mesenchymal Cancer Cell-Stroma Crosstalk Promotes Niche Activation, Epithelial Reversion, and Metastatic Colonization. Cell Rep 13:2456-69.

Demokritou P, Büchel R, Molina RM, Deloid GM, Brain JD, Pratsinis SE. 2010. Development and characterization of a Versatile Engineered Nanomaterial Generation System (VENGES) suitable for toxicological studies. Inhal Toxicol 2:107-116.

Demokritou P, Gass S, Pyrgiotakis G, Cohen JM, Goldsmith W, McKinney W, Frazer D, Ma J, Schwegler-Berry D, Brain J, Castranova V. 2013. An in vivo and in vitro toxicological characterisation of realistic nanoscale CeO_2 inhalation exposures. Nanotoxicology 7:1338-1350.

Derjaguin B, Landau L. 1993. Theory of the Stability of Strongly Charged Lyophobic Sols and of the Adhesion of Strongly Charged Particles in Solutions of Electrolytes. Prog. Surf. Sci 43:30–59.

Di Nezza LA, Misajon A, Zhang J, Jobling T, Quinn MA, Ostör AG, Nie G, Lopata A, Salamonsen LA. 2002. Presence of active gelatinases in endometrial carcinoma and correlation of matrix metalloproteinase expression with increasing tumor grade and invasion. Cancer 94:1466-75.

Dikalov S, Griendling KK, Harrison DG. 2007. Measurement of Reactive Oxygen Species in Cardiovascular Studies. Hypertension 49:717-727.

Dowding JM, Das S, Kumar A, Dosani T, McCormack R, Gupta A, Sayle TX, Sayle DC, von Kalm L, Seal S, Self WT. 2013. Cellular interaction and toxicity depend on physicochemical properties and surface modification of redox-active nanomaterials. ACS Nano 7:4855-68.

Egeblad M, Werb Z. 2002. New functions for the matrix metalloproteinases in cancer progression. Nat Rev Cancer 2:161-174.

Eom HJ, Choi J. 2009. Oxidative stress of CeO2 nanoparti- cles via p38-Nrf-2 signaling pathway in human bronchial ep- ithelial cell, BEAS-2B. Toxicol Lett 187:77–83.

Epstein HA. 2011. Nanotechnology in cosmetic products. Skinmed 9:109–10.

Estevez AY, Erlichman JS. 2014. The potential of cerium oxide nanoparticles (nanoceria) for neurodegenerative disease therapy. Nanomedicine 9:1437–1440.

Evan GI, Vousden KH. 2001. Proliferation, cell cycle and apoptosis in cancer. Nature 411:342–348.

Finkel T, Holbrook NJ. 2000. Oxidants, oxidative stress and the biology of ageing. Nature 498:239–247.

Firuzi O, Miri R, Tavakkoli M, Saso L. 2011. Antioxidant therapy: current status and future prospects. Curr Med Chem 18:3871-88.

Franchi LP, Manshian BB, de Souza TA, Soenen SJ, Matsubara EY, Rosolen JM, Takahashi CS. 2015. Cyto- and genotoxic effects of metallic nanoparticles in untransformed human fibroblast. Toxicol In Vitro 29:1319-1331.

Friedl P, Wolf K. 2003. Tumour-cell invasion and migration: diversity and escape mechanisms. Nat Rev Cancer 3:362-374.

Fromigué O, Louis K, Dayem M, Milanini J, Pages G, Tartare-Deckert S, Ponzio G, Hofman P, Barbry P, Auberger P, Mari B. 2003. Gene expression profiling of normal human pulmonary fibroblasts following coculture with non-small-cell lung cancer cells reveals alterations related to matrix degradation, angiogenesis, cell growth and survival. Oncogene 22:8487-8497.

Fukui H, Horie M, Endoh S, Kato H, Fujita K, Nishio K, Komaba LK, Maru J, Miyauhi A, Nakamura A, Kinugasa S, Yoshida Y, Hagihara Y, Iwahashi H. 2012. Association of zinc ion release and oxidative stress induced by intratracheal instillation of ZnO nanoparticles to rat lung. Chem Biol Interact 198:29-37.

Gao Y, Chen K, Ma JL, Gao F. 2014. Cerium oxide nanoparticles in cancer. Onco Targets Ther. 27:835-40.

Gerwin BI, Spillare E, Forrester K, Lehman TA, Kispert J, Welsh JA, Pfeifer AM, Lechner JF, Baker SJ, Vogelstein B, Harris CC. 1992. Mutant p53 can induce tumorigenic conversion of human bronchial epithelial cells and reduce their responsiveness to a negative growth factor, transforming growth factor beta 1.Proc. Natl. Acad. Sci. 89:2759–2763.

González-Flores D, De Nicola M, Bruni E, Caputo F, Rodríguez AB, Pariente JA, Ghibelli L. 2014. Nanoceria protects from alterations in oxidative metabolism and calcium overloads induced by TNFα and cycloheximide in U937 cells: pharmacological potential of nanoparticles. Mol Cell Biochem 397:245-253.

Griffitt RJ, Luo J, Gao J, Bonzongo JC, Barber DS. 2008. Effects of particle composition and species on toxicity of metallic nanomaterials in aquatic organisms. Environ Toxicol Chem 27:1972-1978.

Grulke E, Reed K, Beck M, Huang X, Cormack A, Seal S. 2014. Nanoceria: Factors affecting its pro- and anti-oxidant properties. Environ. Sci. Nano 1:429–444.

Haase A. Luch A. 2016. Genotoxicity of nanomaterials in vitro: treasure or trash? Archi of Toxicol 90:2827–2830.

Hailstone RK, Di Francesco AG, Leong JG, Allston TD, Reed K. 2009. A study of lattice expansion in CeO_2 nanoparticles by transmission electron microscopy. J Phys Chem 113:15155–15159.

Hanahan D, Weinberg RA. 2000. The hallmarks of cancer. Cell 100:57-70.

Hardas SS, Butterfield DA, Sultana R, Tseng MT, Dan M, Florence RL, Unrine JM, Graham UM, Wu P, Grulke EA, Yokel RA. 2010. Brain Distribution and Toxicological Evaluation of a Systemically Delivered Engineered Nano- scale Ceria. Toxicol Sci 116:562–576.

Harper T. 2011. Global funding of Nanotechnologies and its impact. Cientifica Ltd. http://cientifica.com/wp-content/uploads/downloads/2011/07/Global-Nanotechnology-Funding-Report-2011.pdf.

He X, Despeaux E, Stueckle TA, Chi A, Castranova V, Dinu CZ, Wang L, Rojanasakul Y. 2016. Role of mesothelin in carbon nanotube-induced carcinogenic transformation of human bronchial epithelial cells. Am J Physiol Lung Cell Mol Physiol 311:538-549.

Heckert EG, Seal S, Self WT. 2008. Fenton-like reaction catalyzed by the rare earth inner transition metal cerium. Environ Sci Technol 42:5014-5019.

Heckman KL, DeCoteau W, Estevez A, Reed KJ, Costanzo W, Sanford D, Leiter JC, Clauss J, Knapp K, Gomez C, Mullen P, Rathbun E, Prime K, Marini J, Patchefsky J, Patchefsky AS, Hailstone RK, Erlichman JS. 2013. Custom cerium oxide nanoparticles protect against a free radical mediated autoimmune degenerative disease in the brain. ACS Nano 7:10582-96.

Hecht SS. 2002. Cigarette smoking and lung cancer: chemical mechanisms and approaches to prevention. Lancet Oncol 3:461-469.

Hoet PH, Brüske-Hohlfeld I, Salata OV. 2004. Nanoparticles - known and unknown health risks. J Nanobiotechnology 2:12.

Hsiao IL, Hsieh YK, Wang CF, Chen IC, Huang YJ. 2015. Trojan-horse mechanism in the cellular uptake of silver nanoparticles verified by direct intra- and extracellular silver speciation analysis. Environ Sci Technol 49:3813-3821.

http://ec.europa.eu/environment/chemicals/nanotech/index_en.htm

http://www.doublingtime.com/compute.php

Huang S, Chueh PJ, Lin YW, Shih TS, Chuang SM. 2009. Disturbed mitotic progression and genome segregation are involved in cell transformation mediated by nano-TiO_2 long-term exposure. Toxicol Appl Pharmacol 241:182–194.

Hussain SM, Hess KL, Gearhart JM, Geiss KT, Schlager JJ. 2005. In vitro toxicity of nanoparticles in BRL 3A rat liver cells. Toxicol In Vitro 19:975–983.

Integrated Laboratory Systems Inc. Chemical information profile for ceric oxide [CAS no. 1306-38-3]. Supporting Nomination for Toxicological Evaluation by the National

Toxicology Program, Research Triangle Park, NC, 2006. p. 21

Ivanenko NB, Ivanenko AA, Solovyev ND, Zeimal' AE, Navolotskii DV, Drobyshev EJ. 2013. Biomonitoring of 20 trace elements in blood and urine of occupationally exposed workers by sector field inductively coupled plasma mass spectrometry. Talanta 116:764-769.

Ivanov VK, Shcherbakov B, Usatenko V. 2009. Structure-sensitive properties and biomedical applications of nanodispersed cerium dioxide. Russ. Chem. Rev. 78, 855–871.

Jiang J, Oberdorster G, Biswas P. 2009. Characterization of size, surface charge, and agglomeration sate of nanoparticle dispersions for toxicological studies. J Nanopart Res 11:77–89.

Jin Z, Gao F, Flagg T, Deng X. 2004. Tobacco-specific nitrosamine 4-(methylnitrosamino)-1-(3-pyridyl)-1-butanone promotes functional cooperation of Bcl2 and c-Myc through phosphorylation in regulating cell survival and proliferation. J Biol Chem 279:40209-19.

Jochum W, Passegué E, Wagner EF. 2001. AP-1 in mouse development and tumorigenesis. Oncogene 20:2401-2412.

Kalluri R, Weinberg RA. 2009. The basics of epithelial-mesenchymal transition. J Clin Invest 119:1420-1428.

Karagiannis GS, Poutahidis T, Erdman SE, Kirsch R, Riddell RH, Diamandis EP. 2012. Cancer-associated fibroblasts drive the progression of metastasis through both paracrine and mechanical pressure on cancer tissue. Mol Cancer Res 10:1403-18.

Karakoti A, Singh S, Dowding JM, Seal S, Self WT. 2010. Redox-active radical scavenging nanomaterials. Chem Soc Rev 39:4422-4432

Karakoti AS, Munusamy P, Hostetler K, Kodali V, Kuchibhatla S, Orr G, Pounds JG, Teeguarden JG, Thrall BD, Baer DR. 2012. Preparation and Characterization Challenges to Understanding Environmental and Biological Impacts of Nanoparticles. Surf Interface Anal 44:882–889.

Karamouzis MV, Konstantinopoulos PA, Papavassiliou AG. 2007. The Activator Protein-1 Transcription Factor in Respiratory Epithelium Carcinogenesis. Mol Cancer Res

5:109–20.

Keller J, Wohlleben W, Ma-Hock L, Strauss V, Gröters S, Küttler K, Wiench K, Herden C, Oberdörster G, van Ravenzwaay B, Landsiedel R. 2014. Time course of lung retention and toxicity of inhaled particles: short-term exposure to nano-Ceria. Arch Toxicol 88:2033-59.

Kermanizadeh A, Gaiser BK, Hutchison GR, Stone V. 2012. An in vitro liver model – assessing oxidative stress and genotoxicity following exposure of hepatocytes to a panel of engineered nanomaterials. Part Fibre Toxicol 9:28.

Kessenbrock K, Plaks V, Werb Z. 2010. Matrix metalloproteinases: regulators of the tumor microenvironment. Cell 141:52-67.

Khatlani TS, Wislez M, Sun M, Srinivas H, Iwanaga K, Ma L, Hanna AE, Liu D, Girard L, Kim YH, Pollack JR, Minna JD, Wistuba II, Kurie JM. 2007. c-Jun N-terminal kinase is activated in non-small-cell lung cancer and promotes neoplastic transformation in human bronchial epithelial cells. Oncogene 26:2658–2666.

Kong L, Cai X, Zhou X, Wong LL, Karakoti AS, Seal S, McGinnis JF. 2011. Nanoceria extend photoreceptor cell lifespan in tubby mice by modulation of apoptosis/survival signaling pathways. Neurobiol Dis 42:514-523.

Korsvik C, Patil S, Seal S, Self WT. 2007. Superoxide dismutase mimetic properties exhibited by vacancy engineered ceria nanoparticles. Chem Commun 14:1056-1058.

Kosynkin VD, Arzgatkina AA, Ivanov EN, Chtoutsa MG, Grabko AI, Kardapolov AV, Sysina NA. 2000. The study of process production of polishing powder based on cerium dioxide. J Alloys Compd: 303:421–425.

Kovacic JC, Mercader N, Torres M, Boehm M, Fuster V. 2012. Epithelial-to-mesenchymal and endothelial-to-mesenchymal transition from cardiovascular development to disease. Circulation 125:1795-808.

Kumar A, Dhawan A. 2013. Genotoxic and carcinogenic potential of engineered nanoparticles: An update. Arch Toxicol 87:1883-1900.

Kumari M, Singh SP, Chinde S, Rahman MF, Mahboob M, Grover P. 2014. Toxicity study of cerium oxide nanoparticles in human neuroblastoma cells. Int. J. Toxicol 33:86–

97.

Kwon HJ, Cha MY, Kim D, Kim DK, Soh M, Shin K, Hyeon T, Mook-Jung I. 2016. Mitochondria-Targeting Ceria Nanoparticles as Antioxidants for Alzheimer's Disease. ACS Nano 10:2860-2870.

Lamouille S, Xu J, Derynck R. 2014. Molecular mechanisms of epithelial-mesenchymal transition. Nat Rev Mol Cell Biol 15:178-96.

Lauffenburger DA, Horwitz AF. 1996. Cell migration: A physically integrated molecular process. Cell 84:359–369.

Lawrence NJ, Brewer JR, Wang L, Wu TS, Wells-Kingsbury J, Ihrig MM, Wang G, Soo YL, Mei WN, Cheung CL. 2011. Defect engineering in cubic cerium oxide nanostructures for catalytic oxidation. Nano Lett 11:2666–2671.

Lawton J. 2008. Novel Materials in the Environment: The case of nanotechnology" (twenty-seventh report). Royal commision on enviromental pollution, p.30.

Li Y, Li P, Yu H, Bian Y. 2016. Recent advances (2010-2015) in studies of cerium oxide nanoparticles' health effects. Environ Toxicol Pharmacol 44:25-29.

Liao WT, Lin P, Cheng TS, Yu HS, Chang LW. 2007. Arsenic promotes centrosome abnormalities and cell colony formation in p53 compromised human lung cells. Toxicol Appl Pharmacol. 225:162-70.

Liu D, Gu N. 2009. Nanomaterials for fresh-keeping and sterilization in food preservation. Recent Pat Food Nutr Agric 1:149–54.

Lobo V, Patil A, Phatak A, Chandra N. 2010. Free radicals, antioxidants and functional foods: Impact on human health. Pharmacogn Rev 48:118-126.

Lohcharoenkal W, Wang L, Stueckle TA, Dinu CZ, Castranova V, Liu Y, Rojanasakul Y. 2013. Chronic exposure to carbon nanotubes induces invasion of human mesothelial cells through matrix metalloproteinase-2. ACS Nano 7:7711–7723.

Luanpitpong S, Wang L, Castranova V, Rojanasakul Y. 2014. Induction of stem-like cells with malignant properties by chronic exposure of human lung epithelial cells to single-walled carbon nanotubes. Part Fibre Toxicol 11:1–17.

Luanpitpong S, Wang L, Manke A, Martin KH, Ammer AG, Castranova V, Yang Y, Rojansakul Y. 2014. Induction of stem-like cells with fibrogenic properties by carbon nanotubes and its role in fibrogenesis. Nano Lett 14:3110–3116.

Lundgren DL, Hahn FF, Griffith WC, Hubbs AF, Nikula KJ, Newton GJ, Cuddihy RG, Boecker BB. 1996. Pulmonary carcinogenicity of relatively low doses of beta-particle radiation from inhaled $144CeO_2$ in rats. Radiat Res 146:525-35.

Ma JY, Mercer RR, Barger M, Schwegler-Berry D, Scabilloni J, Ma JK, Castranova V. 2012. Toxicol Appl Pharmacol 262:255–264.

Ma JY, Zhao H, Mercer RR, Barger M, Rao M, Meighan T, Schwegler-Berry D, Castranova V, Ma JK. 2011. Cerium oxide nanoparticle-induced pulmonary inflammation and alveolar macrophage functional change in rats. Nanotoxicology 5:312-325.

Ma K, Chang D, Gong M, Ding F, Luo A, Tian F, Liu Z, Wang T. 2009. Expression and significance of FRA-1 in non-small-cell lung cancer. Cancer Invest 27:353-359.

Mandoli C, Pagliari F, Pagliari S, Forte G, Di Nardo P, Licoccia S, Traversa E. 2010. Stem cell aligned growth induced by CeO2 nanoparticles in PLGA scaffolds with improved bioactivity for regenerative medicine. Advanced Functional Materials 20:1617-1624.

Manna SK, Rangasamy T, Wise K, Sarkar S, Shishodia S, Biswal S, Ramesh GT. 2006. Long-term environmental tobacco smoke activates nuclear transcription factor-kappa B, activator protein-1, and stress responsive kinases in mouse brain. Biochem Pharmacol 71:1602-1609.

Marsit CJ, Zheng S, Aldape K, Hinds PW, Nelson HH, Wiencke JK, Kelsey KT. 2005. *PTEN* expression in non-small-cell lung cancer: evaluating its relation to tumor characteristics, allelic loss, and epigenetic alteration. Hum Pathol 36:768-776.

McCord JM, Fridovich I. 1969. Superoxide dismutase. An enzymic function for erythrocuprein (hemocuprein). J Biol Chem 244:6049-55.

McDonald JW, Ghio AJ, Sheehan CE, Bernhardt PF, Roggli VL. 1995. Rare earth (cerium oxide) pneumoconiosis: Analytical scanning electron microscopy and literature review. Mod Pathol 8:859–865.

McGuinnes C, Duffin R, Brown SL, Mills N, Megson IL, Macnee W, et al. 2011. Surface

derivatization state of polystyrene latex nanoparticles determines both their potency and their mechan- ism of causing human platelet aggregation in vitro. Toxicol Sci 119:359–68.

Mendez MG, Kojima S, Goldman RD. 2010. Vimentin induces changes in cell shape, motility, and adhesion during the epithelial to mesenchymal transition. FASEB J 24:1838-51.

Milara J, Peiró T, Serrano A, Cortijo J. 2013. Epithelial to mesenchymal transition is increased in patients with COPD and induced by cigarette smoke. Thorax 68:410-20.

Mittal S, Pandey AK. 2014. Cerium oxide nanoparticles induced toxicity in human lung cells:Role of ROS mediated DNA damage and apoptosis. Biomed Res Int 2014:891-934.

Møller P, Danielsen PH, Jantzen K, Roursgaard M, Loft S. 2013. Oxidatively damaged DNA in animals exposed to particles. Crit Rev Toxicol 43:96–118.

Mori S, Chang JT, Andrechek ER, Matsumura N, Baba T, Yao G, Kim JW, Gatza M, Murphy S, Nevins JR. 2009. Anchorage-independent cell growth signature identifies tumors with metastatic potential. Oncogene 28:2796-2805.

Murdock RC, Braydich-Stolle L, Schrand AM, Schlager JJ, Hussain SM. 2008. Characterization of nanomaterial dispersion in solution prior to in vitro exposure using dynamic light scattering technique. Toxicol Sci 101:239–53.

Narayanan KB, Park HH. 2013. Pleiotropic functions of antioxidant nanoparticles for longevity and medicine. Adv. Colloid Interface Sci 201:30–42.

Nel A, Xia T, Mädler L, Li N. 2006. Toxic potential of materials at the nanolevel. Science 311:622-7.

Nel AE, Madler L, Velegol D, Xia T, Hoek EM, Somasundaran P, Klaessig F, Castranova V, Thompson M. 2009. Understanding biophysicochemical interactions at the nano-bio interface. Nat Mater 8:543–57.

Nel AE, Nasser E, Godwin H, Avery D, Bahadori T, Bergeson L, Beryt E, Bonner JC, Boverhof D, Carter J, Castranova V, Deshazo JR, Hussain SM, Kane AB, Klaessig F, Kuempel E, Lafranconi M, Landsiedel R, Malloy T, Miller MB, Morris J, Moss K,

Oberdorster G, Pinkerton K, Pleus RC, Shatkin JA, Thomas R, Tolaymat T, Wang A, Wong J. 2013. A multi-stakeholder perspective on the use of alternative test strategies for nanomaterial safety assessment. ACS Nano 7:6422-33.

Nelson BC, Johnson ME, Walker ML, Riley KR, Sims CM. 2016. Antioxidant cerium oxide nanoparticles in biology and medicine. Antioxidants (Basel) 5:15.

Nelson CM, Khauv D, Bissell MJ, Radisky DC. 2008. Change in cell shape is required for matrix metalloproteinase-induced epithelial-mesenchymal transition of mammary epithelial cells. J Cell Biochem 105:25-33.

Niu J, Azfer A, Rogers LM, Wang X, Kolattukudy PE. 2007. Cardioprotective effects of cerium oxide nanoparticles in a transgenic murine model of cardiomyopathy. Cardiovasc Res 73:549-59.

Niu J, Wang K, Kolattukudy PE. 2011. Cerium oxide nanoparticles inhibit oxidative stress and nuclear factor-κB activation in H9c2 cardiomyocytes exposed to cigarette smoke extract. J Pharmacol Exp Ther 338:53-61.

Oberdörster G, Oberdörster E, Oberdörster J. 2005. Nanotoxicology: An Emerging Discipline Evolving from Studies of Ultrafine Particles. Environ.Health Perspect 113: 823-839.

Pagliari F, Mandoli C, Forte G, Magnani E, Pagliari S, Nardone G, Licoccia S, Minieri M, Di Nardo P, Traversa E. 2012. Cerium oxide nanoparticles protect cardiac progenitor cells from oxidative stress. ACS Nano 6:3767-3775.

Pairon JC, Roos F, Iwatsubo Y, Janson X, Billon-Galland MA, Bignon J, Brochard P. 1994. Lung retention of cerium in humans. Occup Environ Med 51:195–199.

Palmero C. 2014. Nanoblog: Nanoceria in our bodies. http://blogs.rsc.org/en/2014/12/01/nanoceria-in-our-bodies.

Park B, Donaldson K, Duffin R, Tran L, Kelly F, Mudway I, Morin J, Guest R, Jenkinson P, Samaras Z, Giannouli M, Kouridis H, Martin P. 2008. Hazard and risk assessment of a nanoparticulate cerium oxide-based diesel fuel additive - a case study. Inhal Toxicol 20:547–566.

Park EJ, Choi J, Park YK, Park K. 2008. Oxidative stress induced by cerium oxide nanoparticles in cultured BEAS-2B cells. Toxicology. 245:90–100.

Park EJ, Yi J, Kim Y, Choi K, Park K. 2010. Silver nanoparticles induce cytotoxicity by a Trojan-horse type mechanism. Toxicol In Vitro 24:872-878.

Park H, Grassian VH. 2010. Commercially manufactured engineered nanomaterials for environmental and health studies: important insights provided by independent characterization. Environ Toxicol Chem 29:715–21.

Park M, Lankveld D, Van Loveren H, Jong W. 2009. The status of in vitro toxicity studies in the risk assessment of nanomaterials. Nanomedicine 4:669–685.

Perez JM, Asati A, Nath S, Kaittanis C. 2008. Synthesis of biocompatible dextran-coated nanoceria with pH-dependent antioxidant properties. Small 4:552-556.

Pesic M, Podolski-Renic A, Stojkovic S, Matovic B, Zmejkoski D, Kojic V, Bogdanovic G, Pavicevic A, Mojovic M, Savic A, Milenkovic I, Kalauzi A, Radotic K. 2015. Anti-cancer effects of cerium oxide nanoparticles and its intracellular redox activity. Chem Biol Interact 232:85–93.

Pietras K, Ostman A. 2010. Hallmarks of cancer: interactions with the tumor stroma. Exp Cell Res 316:1324-31.

Pirmohamed T, Dowding JM, Singh S, Wasserman B, Heckert E, Karakoti AS, King S, Seal, Self WT. 2010. Nanoceria exhibit redox state-dependent catalase mimetic activity. Chem Commun (Camb) 46:2736-8.

Poland CA, Duffin R, Kinloch I, Maynard A, Wallace WA, Seaton A, Stone V, Brown S, Macnee W, Donaldson K. 2008. Carbon nanotubes introduced into the abdominal cavity of mice show asbestos-like pathogenicity in a pilot study. Nature Nanotech 3:423–428.

Pourkhalili N, Hosseini A, Nili-Ahmadabadi A, Rahimifard M, Navaei-Nigjeh M, Hassani S, Baeeri M, Abdollahi M. 2012. Improvement of isolated rat pancreatic islets function by combination of cerium oxide nanoparticles/sodium selenite through reduction of oxidative stress. Toxicol Mech Methods 22:476-482.

Prasad RGSV, Davan R, Jothi S, Phani AR, Raju DB. 2013. Cerium Oxide Nanoparticles Protects Gastrointestinal Mucosa From Ethanol induced Gastric Ulcers in In-vivo Animal Model. Nano Biomed. Eng 5:46-49.

Pujalté I, Passagne I, Brouillaud B, Tréguer M, Durand E, Ohayon-Courtès C, L'Azou B.

2011. Cytotoxicity and oxidative stress induced by different metallic nanoparticles on human kidney cells. Part Fibre Toxicol 8:10.

Radisky ES, Radisky DC. 2010. Matrix metalloproteinase-induced epithelial-mesenchymal transition in breast cancer. J Mammary Gland Biol Neoplasia 15:201-12.

Ray PD, Huang BW, Tsuji Y. 2012. Reactive oxygen species (ROS) homeostasis and redox regulation in cellular signaling. Cell Signal 24:981-990.

Reed K, Cormack A, Kulkarni A, Mayton M, Sayle D, Klaessig F, Stadler B. 2014. Exploring the properties and applications of nanoceria: is there still plenty of room at the bottom? Environ. Sci.: Nano 1:390-405.

Rocco C. 2011. The long view of nanotechnology development: the National Nanotechnology Initiative at 10 years. J Nanopart Res 13:427–445.

Rojanasakul L, Kornberg T, Davidson D, Demokritou P, Pirela S, Rojanasakul Y, Lua S, Deloid G, Schwegler-Berry D, Stueckle T. 2016. Evaluation of tumorigenic potential of CeO_2 and Fe_2O_3 engineered nanoparticles by a human cell in vitro screening model. NanoImpact. doi: 10.1016/j.impact.2016.11.001.

Roller M. 2009. Carcinogenicity of inhaled nanoparticles. Inhal Toxicol 1:144-157.

Roomi MW, Monterrey JC, Kalinovsky T, Rath M, Niedzwiecki A. 2009. Patterns of MMP-2 and MMP-9 expression in human cancer cell lines. Oncol Rep 21:1323-1333.

Rothen-Rutishauser B, Grass RN, Blank F, Limbach LK, Muhlfeld C, Brandenberger C, Raemy DO, Gehr P, Stark WJ. Direct combination of nanoparticle fabrication and exposure to lung cell cultures in a closed setup as a method to simulate accidental nanoparticle exposure of humans.Environ Sci Technol 43:2634–2640.

Rubio L, Annangi B, Vila L, Hernández A, Marcos R. 2016. Antioxidant and anti-genotoxic properties of cerium oxide nanoparticles in a pulmonary-like cell system. Arch Toxicol 90:269-78.

Rzigalinski B, Danelisen I, Strawn E, Cohen C, Liang C. 2006. Nanoparticles for Cell Engineering – A Radical Concept. In: Tissue, Cell and Organ Engineering Nanotechnologies for the Life Sciences. Kumar C (Ed.). Wiley & Sons, MA, USA.

Rzigalinski BA, Carfagna CS, Ehrich M. 2016. Cerium oxide nanoparticles in neuroprotection and considerations for efficacy and safety. WIREs Nanomed

Nanobiotechnol. doi: 10.1002/wnan.1444.

Sabbioni E, Pietra R, Gaglione P, Vocaturo G, Colombo F, Zanoni M, Rodi F. 1982. Long-term occupational risk of rare-earth pneumoconiosis. A case report as investigated by neutron activation analysis. Sci Total Environ 26:19–32.

Sabella S, Carney RP, Brunetti V, Malvindi MA, Al-Juffali N, Vecchio G, Janes SM, Bakr OM, Cingolani R, Stellacci F, Pompa PP. 2014. A general mechanism for intracellular toxicity of metal-containing nanoparticles. Nanoscale 6:7052-7061.

Sack M, Alili L, Karaman E, Das S, Gupta A, Seal S, Brenneisen P. 2014. Combination of conventional chemotherapeutics with redox-active cerium oxide nanoparticles: a novel aspect in cancer therapy. Mol Cancer Ther 13:1740-1749.

Saha SP, Bhalla DK, Whayne TF, Gairola CG. 2007. Cigarette smoke and adverse health effects: An overview of research trends and future needs. Int J Angiol 16: 77–83.

Salmena L, Carracedo A. Pandolfi PP. 2008. Tenets of *PTEN* tumor suppression. Cell 133:403–414.

Samet JM, Avila-Tang E, Boffetta P, Hannan LM, Olivo-Marston S, Thun MJ, Rudin CM: Lung cancer in never smokers: clinical epidemiology and environmental risk factors. Clin Cancer Res 2009, 15:5625–5645.

Sargent LM, Shvedova AA, Hubbs AF, Salisbury JL, Benkovic SA, Kashon ML, Lowry DT, Murray AR, Kisin ER, Friend S, McKinstry KT, Battelli L, Reynolds SH. 2009. Induction of aneuploidy by single-walled carbon nanotubes. Environ Mol Mutagen 50:708–717.

Schieber M, Chandel NS. 2014. ROS function in redox signaling and oxidative stress. Curr Biol 24:453-462.

Schmid K, Riediker M. 2008. Use of nanoparticles in Swiss industry: a targeted survey. Environ Sci Technol 42:2253–60.

Schubert D, Dargusch R, Raitano J, Chan S. 2006. Cerium and yttrium oxide nanoparticles are neuroprotective. Biochem. Biophys. Res. Commun. 342:86–91.

Shcherbakov AB, Zholobak NM, Spivak NY, Ivanov VK. 2014. Advances and prospects of using nanocrystalline ceria in cancer theranostics. Russion J Inorg Chem 59:1556–1575.

Sherr CJ. 1996. Cancer cell cycles. Science 274:1672–1677.

Siegel RL, Miller KD, Jemal A. 2016. Cancer statistics, 2016. CA Cancer J Clin 66:7-30.

Sighinolfi GL, Artoni E, Gatti AM, Corsi L. 2016. Carcinogenic potential of metal nanoparticles in BALB/3T3 cell transformation assay. Environ Toxicol. 31:509-519.

Singh S, Dosani T, Karakoti AS, Kumar A, Seal S, Self WT. 2011. A phosphate-dependent shift in redox state of cerium oxide nanoparticles and its effects on catalytic properties. Biomaterials 32:6745-6753.

Singh S, Kumar A, Karakoti A, Seal S, Self WT. 2010. Unveiling the mechanism of uptake and sub-cellular distribution of cerium oxide nanoparticles. Mol Biosyst 6:1813-1820.

Snow SJ, McGee J, Miller DB, Bass V, Schladweiler MC, Thomas RF, Krantz T, King C, Ledbetter AD, Richards J, Weinstein JP, Conner T, Willis R, Linak WP, Nash D, Wood CE, Elmore SA, Morrison JP, Johnson CL, Gilmour MI, Kodavanti UP. 2014. Inhaled diesel emissions generated with cerium oxide nanoparticle fuel additive induce adverse pulmonary and systemic effects. Toxicol Sci 142:403-17.

Sohal SS, Mahmood MQ, Walters EH. 2014. Clinical significance of epithelial mesenchymal transition (EMT) in chronic obstructive pulmonary disease (COPD): potential target for prevention of airway fibrosis and lung cancer. Clin Transl Med 3:33.

Sohal SS, Reid D, Soltani A, Ward C, Weston S, Muller HK, Wood-Baker R, Walters EH. 2010. Reticular basement membrane fragmentation and potential epithelial mesenchymal transition is exaggerated in the airways of smokers with chronic obstructive pulmonary disease. Respirology 15:930-938.

Song MS, Salmena L, Pandolfi PP. 2012. The functions and regulation of the *PTEN* tumour suppressor. Nat Rev Mol Cell Biol 13:283-96.

Soria JC, Lee HY, Lee JI, Wang L, Issa JP, Kemp BL, Liu DD, Kurie JM, Mao L, Khuri FR. 2002. Lack of *PTEN* expression in non-small cell lung cancer could be related to promoter methylation. Clin Cancer Res 8:1178-1184.

Spulber M, Baumann P, Liu J, Palivan CG. 2015. Ceria loaded nanoreactors: a nontoxic superantioxidant system with high stability and efficacy. Nanoscale 7:1411-1423.

Srinivas A, Rao PJ, Selvam G, Murthy PB, Reddy PN. 2011. Acute inhalation toxicity of cerium oxide nanoparticles in rats. Toxicol Lett 205:105–115.

Staal Y, Ma-Hock L, Muijser H, Treumann S, Strauss V, Landsiedel R. 2010. Inhaled multiwalled carbon nanotubes modulate the immune response of trimellitic anhydride-induced chemical respiratory allergy in brown Norway rats. Toxicol. Pathol. 42: 1130-1142.

Stankic S, Suman S, Haque F, Vidic J. 2016. Pure and multi metal oxide nanoparticles: synthesis, antibacterial and cytotoxic properties. J Nanobiotechnology. 14(1):73.

Steigerwald ML, Brus LE. 1990. Semiconductor crystallites: a class of large molecules. ACC Chem Res 23:183–8.

Suzuki H, Toyooka T, Ibuki Y. 2007. Simple and easy method to evaluate uptake potential of nanoparticles in mammalian cells using a flow cytometric light scatter analysis. Environ Sci Technol 41:3018–24.

Tang Z, Sahu SN, Khadeer MA, Bai G, Franklin RB, Gupta A. 2006. Overexpression of the ZIP1 zinc transporter induces an osteogenic phenotype in mesenchymal stem cells. Bone 38:181-98.

Tarnuzzer RW, Colon J, Patil S, Seal S. 2005. Vacancy Engineered Ceria Nanostructures for Protection from Radiation-Induced Cellular Damage. Nano Lett 5:2573–2577.

Thurnherr T, Brandenberger C, Fischer K, Diener L, Manser P, Maeder-Althaus X, Kaiser JP, Krug HF, Rothen-Rutishauser B, Wick P. 2011. A comparison of acute and long-term effects of industrial multiwalled carbon nanotubes on human lung and immune cells in vitro, Toxicol Lett 200:176–186.

Ting SR, Whitelock JM, Tomic R, Gunawan C, Teoh WY, Amal R, Lord MS. 2013. Cellular uptake and activity of heparin functionalised cerium oxide nanoparticles in monocytes. Biomaterials 34:4377-86.

Tiwari AK. 2001. Imbalance in antioxidant defense and human disease: Multiple approach of natural antioxidant therapy. Curr. Sci 81:1179-1187.

Trovarelli A. 1999. Structural and Oxygen Storage/Release Properties of CeO_2-Based Solid Solutions. Comments Inorg. Chem 20:263–284.

Tse JC, Kalluri R. 2007. Mechanisms of metastasis: epithelial-to-mesenchymal transition

and contribution of tumor microenvironment. J Cell Biochem 101:816-829.

Tseng MT, Lu X, Duan X, Hardas SS, Sultana R, Wu P, Unrine JM, Graham U, Butterfield DA, Grulke EA, Yokel RA. 2012. Alteration of Hepatic Structure and Oxidative Stress Induced by Intravenous Nanoceria. Toxicol Appl Pharmacol 260:173–182.

U. EPA. Toxicological Review of cerium oxide and cerium compounds (CAS No. 1306-38-3) In support of summary information on the integrated risk information system (IRIS). U.S. Environmental Protection Agency; 2009.

Valavanidis A, Vlachogianni T, Fiotakis K. Tobacco smoke: involvement of reactive oxygen species and stable free radicals in mechanisms of oxidative damage, carcinogenesis and synergistic effects with other respirable particles. Int J Environ Res Public Health 6:445-62.

Vales G, Rubio L, Marcos R. 2015. Long-term exposures to low doses of titanium dioxide nanoparticles induce cell transformation, but not genotoxic damage in BEAS-2B cells. Nanotoxicology 9:568-78.

Vales G, Rubio L, Marcos R. 2016. Genotoxic and cell-transformation effects of multi-walled carbon nanotubes (MWCNT) following in vitro sub-chronic exposures. J Hazard Mater. 306:193-202.

Valko M, Rhodes CJ, Moncol J, Izakovic M, Mazur M. 2006. Free radicals, metals and antioxidants in oxidative stress-induced cancer. Chem Biol Interact 160:1-40.

Vance ME, Kuiken T, Vejerano EP, McGinnis SP, Hochella MF, Rejeski D, Hull MS. (2015). Nanotechnology in the real world: Redeveloping the nanomaterial consumer products inventory. Beilstein J Nanotechnol. 6:1769-1780.

Vander Heiden MG, Cantley LC, Thompson CB. 2009. Understanding the Warburg effect: the metabolic requirements of cell proliferation. Science 324:1029–1033

Veljkovic E, Jiricny J, Menigatti M, Rehrauer H, Han W. 2011. Chronic exposure to cigarette smoke condensate in vitro induces epithelial to mesenchymal transition-like changes in human bronchial epithelial cells, BEAS-2B. Toxicol In Vitro. 25:446-53.

Verwey EOJ. 1948. Theory of the Stability of Lyophobic Colloids: The Interaction of Sol Particles Having an Electric Double Layer; Elsevier: Amsterdam.

Vevers WF, Jha AN. 2008. Genotoxic and cytotoxic potential of titanium dioxide (TiO2) nanoparticles on fish cells in vitro. Ecotoxicology 17:410–420.

Vila L, Rubio L, Annangi B, García-Rodríguez A, Marcos R, Hernández A. 2016. Frozen dispersions of nanomaterials are a useful operational procedure in nanotoxicology. Nanotoxicology 1:1-10.

Vu T, Jin L, Datta PK. 2016. Effect of Cigarette Smoking on Epithelial to Mesenchymal Transition (EMT) in Lung Cancer. J Clin Med. doi: 10.3390/jcm5040044.

Walkey C, Das S, Seal S, Erlichman J, Heckman K, Ghibelli L, Traversa E, McGinnis JF, Self WT. 2015. Catalytic Properties and Biomedical Applications of Cerium Oxide Nanoparticles. Environ Sci Nano 2:33-53.

Wang J, Chen Y, Lin C, Jia J, Tian L, Yang K, Zhao L, Lai N, Jiang Q, Sun Y, Zhong N, Ran P, Lu W. 2014. Effects of chronic exposure to cigarette smoke on canonical transient receptor potential expression in rat pulmonary arterial smooth muscle. Am J Physiol Cell Physiol 306:364-373.

Wang L, Luanpitpong S, Castranova V, Tse W, Lu Y, Pongrakhananon V, Rojanasakul Y. 2011. Carbon Nanotubes Induce Malignant Transformation and Tumorigenesis of Human Lung Epithelial Cells. Nano Lett. 11:2796-2803

Wang X, Fang H, Huang Z, Shang W, Hou T, Cheng A, Cheng H. 2013. Imaging ROS signaling in cells and animals. J Mol Med 91:917–927.

Wang Y, Aker WG, Hwang HM, Yedjou CG, Yu H, Tchounwou PB. 2011. A study of the mechanism of in vitro cytotoxicity of metal oxide nanoparticles using catfish primary hepatocytes and human HepG2 cells. Sci Total Environ 409:4753-62.

Wang Y. 1991. Nonlinear optical properties of nanometer-sized semiconductor clusters. ACC Chem Res 24:133–9.

Waring PM, Watling RJ. 1990. Rare earth deposits in a deceased movie projectionist. A new case of rare earth pneumoconiosis? Med J Aust 153:726–730.

Wason MS, Colon J, Das S, Seal S, Turkson J, Zhao J, Baker CH. 2013. Sensitization of pancreatic cancer cells to radiation by cerium oxide nanoparticle-induced ROS production. Nanomedicine 9:558–569.

Weller W. 1993. Quantized semiconductor particles: a novel state of matter for materials science. Adv Mater. 5:88–95.

Wong LL, Hirst SM, Pye QN, Reilly CM, Seal S, McGinnis JF. 2013. Catalytic nanoceria are preferentially retained in the rat retina and are not cytotoxic after intravitreal injection. PLoS One 8:e58431.

Wong LL, Pye QN, Chen L, Seal S, McGinnis JF. 2015. Defining the catalytic activity of nanoceria in the P23H-1 rat, a photoreceptor degeneration model. PLoS One 10:e0121977.

Wu CA, Chao Y, Shiah SG, Lin WW. 2013. Nutrient deprivation induces the Warburg effect through ROS/AMPK-dependent activation of pyruvate dehydrogenase kinase. Biochim Biophys Acta. 1833:1147-1156.

Xia T, Kovochich M, Liong M, Mädler L, Gilbert B, Shi H, Yeh JI, Zink JI, Nel AE. 2008. Comparison of the mechanism of toxicity of zinc oxide and cerium oxide nanoparticles based on dissolution and oxidative stress properties. ACS Nano. 2:2121-2134.

Xiao D, He J. 2010. Epithelial mesenchymal transition and lung cancer. J Thorac Dis 2:154-159.

Xiao YF, Li JM, Wang SM, Yong X, Tang B, Jie MM, Dong H, Yang XC, Yang SM. 2016. Cerium oxide nanoparticles inhibit the migration and proliferation of gastric cancer by increasing DHX15 expression. Int J Nanomedicine 11:3023-3034.

Xing F, Saidou J, Watabe K. 2010. Cancer associated fibroblasts (CAFs) in tumor microenvironment. Front Biosci 15:166-79.

Xu C, Qu X. 2014. Cerium oxide nanoparticle: a remarkably versatile rare earth nanomaterial for biological applications. NPG Asia Mater 6:1-16.

Xu M, Fujita D, Kajiwara S, Minowa T, Li X, Takemura T, et al. 2010. Contribution of physicochemical characteristics of nano-oxides to cytotoxicity. Biomaterials 31:8022–8031.

Xue Y, Zhai Y, Zhou K, Wang L, Tan H, Luan Q, Yao X. 2012. The vital role of buffer anions in the antioxidant activity of CeO_2 nanoparticles. Chemistry 18:11115-11122.

Yanagi S, Kishimoto H, Kawahara K, Sasaki T, Sasaki M, Nishio M, Yajima N, Hamada K, Horie Y, Kubo H, Whitsett JA, Mak TW, Nakano T, Nakazato M, Suzuki A. 2007. *Pten* controls lung morphogenesis, bronchioalveolar stem cells, and onset of lung adenocarcinomas in mice. J Clin Invest 117:2929-2940.

Yang W, Peters JI, Williams RO 3rd. 2008. Inhaled nanoparticles--a current review. Int J Pharm 356:239-47.

Yang W, Thordarson P, Gooding JJ, Ringer SP, Braet F. 2007. Carbon nanotubes for biological and biomedical applications. Nanotechnol. 18:1-13.

Yen SJ, Hsu WL, Chen YC, Su HC, Chang YC, Chen H, Yeh SR, Yew TR. 2011. The enhancement of neural growth by amino-functionalization on carbon nanotubes as a neural electrode. Biosens Bioelectron 26:4124–32.

Yilmaz M, Christofori G. 2009. EMT, the cytoskeleton, and cancer cell invasion. Cancer Metastasis Rev 28:15-33.

Yokel RA, Au TC, MacPhail R, Hardas SS, Butterfield DA, Sultana R, Goodman M, Tseng MT, Dan M, Haghnazar H, Unrine JM, Graham UM, Wu P, Grulke EA. 2012. Distribution, elimination, and biopersistence to 90 days of a systemically introduced 30 nm ceria-engineered nanomaterial in rats. Toxicol Sci 127:256-68.

Yokel RA, Hussain S, Garantziotis S, Demokritou P, Castranova V, Cassee FR. 2014. The yin: An adverse health perspective of nanoceria: Uptake, distribution, accumulation, and mechanisms of its toxicity. Environ. Sci. Nano 1:406–428.

Young MR, Colburn NH. 2006. Fra-1 a target for cancer prevention or intervention. Gene 379:1-11.

Yu CC, Ko FY, Yu CS, Lin CC, Huang YP, Yang JS, Lin JP, Chung JG. 2012. Norcantharidin triggers cell death and DNA damage through S-phase arrest and ROS-modulated apoptotic pathways in TSGH 8301 human urinary bladder carcinoma cells. Int J Oncol 41:1050-60.

Zhang H, He X, Zhang Z, Zhang P, Li Y, Ma Y, Kuang Y, Zhao Y, Chai Z. 2011. Nano-CeO_2 exhibits adverse effects at environmental relevant concentrations. Environ. Sci. Technol 45:3725–3730.

Zhao Y, Xu Y, Li Y, Xu W, Luo F, Wang B, Pang Y, Xiang Q, Zhou J, Wang X, Liu Q. 2013.

NF-κB-mediated inflammation leading to EMT via miR-200c is involved in cell transformation induced by cigarette smoke extract. Toxicol Sci 135:265-76.